# University of Alberta

The effect of long-term interleukin-1beta exposure on sensory neuron electrical membrane properties: implications for neuropathic pain

by

Patrick Lester Stemkowski

A thesis submitted to the Faculty of Graduate Studies and Research
in partial fulfillment of the requirements for the degree of

Doctor of Philosophy

Centre for Neuroscience



Spring 2011
Edmonton, Alberta

**To my wonderful family: Vlad and Ruby, your love and support keep me grounded and serve as a constant reminder of the beauty in life.**

**And to my Mom for pushing me to achieve when I thought I couldn't…to my Dad for relating it 'all back to farming'…to my Sister for putting up with her older brother and being a great friend!**

## ABSTRACT

The effect of interleukin-1 beta (IL-1β) on the electrical properties of sensory neurons was assessed at comparable levels and exposure times to those found in animal models of neuropathic pain. Experiments involved whole cell current- or voltage-clamp recordings from rat dorsal root ganglion (DRG) neurons in defined medium, neuron enriched cultures.

5-6 days exposure to 100 pM IL-1β produced neuron specific effects. These included an increase in the excitability of medium diameter and small diameter isolectin B4 (IB4)-positive neurons that was comparable to that found after peripheral nerve injury. By contrast, a reduction in excitability was observed in large diameter neurons, while no effect was found in small diameter IB4-negative neurons.

Further characterization of changes in medium and small IB4-positive neurons revealed that some, but not all, effects of IL-1β were mediated through its receptor, IL-1RI. Using appropriate voltage protocols and/or ion substitutions, it was found that neuron specific changes in several ionic currents, including alterations in hyperpolarization activated inward current ($I_H$) and decreases in various $K^+$ currents contribute to the increased excitability produced by IL-1β.

Overall, these studies revealed that:

1. The effects of long-term exposure of DRG neurons to IL-1β are reflective of the enduring increase in primary afferent excitability reported after peripheral

nerve injury. This expands the recognized role of IL-1β in acute inflammatory pain to neuropathic pain.

2. Hyperexcitability in medium neurons exposed to IL-1β likely includes mixed populations of neurons corresponding to nociceptive and non-nociceptive primary afferent fibres and, therefore, has relevance to hyperalgesia and allodynia, respectively.

3. The responsiveness of small IB4-positive neurons, but not IB4-negative, to prolonged IL-1β exposure is consistent with the suggestion that small IB4-negative afferents are involved in inflammatory pain, while small IB4-positive afferents are involved neuropathic pain.

4. The identification of receptor mediated effects and several contributing ionic mechanisms, may have relevance to the development of new therapeutic approaches to neuropathic pain.

5. IL-1β can contribute to increased neuronal excitability by mechanisms that are independent of IL-1RI signalling. This should be taken into account when targeting IL-1β, or more specifically IL-1RI, in the management of neuropathic pain.

## ACKNOWLEDGEMENTS

This academic journey took everything I had in me and more, therefore, I have many people to thank for their help along the way.

First and foremost, I would like to thank my supervisor Dr. Peter Smith for seeing my potential when few would. Your light-heartedness always made the laboratory a pleasant working environment. Your enthusiasm inspired me to work harder. I would also like to thank my supervisory committee members, Drs. Bill Dryden and Fred Tse for sharing their expertise and knowledge. More specifically, to Bill for allowing me to pick his brain on almost any subject and Fred for the trippy calcium-imaging experiments back in the day. In addition, I would like to thank the other members of my thesis defense examining committee, Dr. Michael Gold from the University of Pittsburgh, USA and Dr. Brad Kerr from the Department of Anaesthiology at the University of Alberta, for taking time out of their busy schedules to read and review this thesis. I appreciate their expert advice and comments on my thesis.

I would also like to thank the Centre for Neuroscience for all their support and for offering an excellent graduate student training program. This includes Drs. Elena Posse de Chaves, Lucila Saavedra, Aaron Lai and Kathryn Todd for their help in establishing DRG cell cultures and ELISA experiments. This thank-you also includes Mrs. Carol Anne Johnson and Ms. Judy Duel (Department of Pharmacology) for their kindness and administrative support.

Finally, I would like to thank all my friends in the Smith Lab and extended family. This includes past labmates: Drs. Chris Ford and Tim Moran for all of their assistance in my training. To Mr. Ken Wong, Miss Camille Olechowski and Drs. Kwai Alier, James Biggs, Chris Carter, Shaona Acharjee, Van Lu and even that guy Sridhar Balasubramanyan for the good times at TGIFs, conferences and beyond! To Misses Briana Napier and Julie Lowe for their contributions to countless hours of data analysis and overall technical support. To Mr. Phillip Colmers for his inquisitive nature and help with the acute IL-1β application study. To Mes Dames Sabrina Gustafson-Vickers and Yishen Chen for their support and kindness. Last, but not least, to the Boss's Boss, Mrs. Anne Smith, for her warm hospitality and awesome meals!

**TABLE OF CONTENTS**

## LIST OF TABLES

## LIST OF FIGURES

## LIST OF ABBREVIATIONS

**4-AP:** 4-aminopyridine

**A:** 'afterhyperpolarization' neurons

**A-type:** 4-AP sensitive, rapidly activating potassium current

**ASICs:** acid sensing ion channels

**ACG:** anterior cingulate gyrus

**ADP:** afterdepolarizing potentials

**AHP:** afterhyperpolarzation

**ANOVA:** analysis of variance

**AP:** action potential

**AP1:** activator protein-1

**ASIC:** acid sensing ion channel

**B2:** bradykinin-2

**BDNF:** brain-derived neurotrophic factor

**$BK_{Ca}$:** 'large or big' conductance calcium-activated potassium channel

**BSA:** bovine serum albumin

**cAMP:** adenosine 3', 5' –cyclic monophosphate

**$C_{in}$:** input capacitance

**CCD:** chronic compression of the dorsal root ganglion

**CCI:** chronic constriction nerve injury

**CCL2:** chemokine ( C-C motif) ligand 2

**CCL3:** chemokine ( C-C motif) ligand 3

**CGRP:** calcitonin gene-related peptide

**COX-1:** cyclo -oxygenase- 1

**COX-2:** cyclo-oxygenase-2

**CNS:** central nervous system

**CPA:** conditioned place aversion

**CSF:** cerebrospinal fluid

**CXCL1:** chemokine (Cysteine-X-Cysteine motif) ligand 1

**D-hair:** down hair

**DMEM:** Dulbecco's Modified Eagle Medium

**DMEMHS:** DMEM supplemeted with 10% horse serum

**DRG:** dorsal root ganglion

**E-selectin:** endothelial-cell selectin

**ELISA:** enzyme-linked immunosorbent assay

**epsc:** excitatory post synaptic current

**F:** 'fast' neurons

**Fast $I_{AHP}$:** fast afterhyperpolarization current

**fMRI:** functional magnetic resonance imaging

**FNE:** free nerve ending

**FRAP:** fluoride-resistant acid phosphatase

**GABA:** gamma-aminobutyric acid

**GAD:** glutamic acid decarboxylase

**GDNF:** glial cell line-derived neurotrophic factor

**GFR$\alpha$-1:** GDNF family receptor alpha-1

**G-hair:** guard hair

**GPCR:** G-protein coupled receptor

**GSA-IB4:** α-D-galactose-specific *Griffonia simplicifolia* - isolectin B4

**H:** 'hump' neurons

**HCN:** hyperpolarization-activated cyclic nucleotide-gated cation channel

**hIK1:** human intermediate conductance calcium-activated potassium channel 1

**HTMRs:** high-threshold mechanoreceptors

**HVA:** high voltage activated calcium channel

**HVA-$I_{Ba}$:** high voltage activated calcium channel barium current

**$I_A$:** A-current

**$I_{Af}$:** fast transient A-current

**$I_{AHP}$:** afterhyperpolarization current

**$I_{Aht}$:** high threshold A-current

**$I_{As}$:** slow A-current

**IASP:** International Association for the Study of Pain

**IB4:** isolectin B4

**$I_{Ba}$:** barium current

**IC:** insular cortex

**$I_{Ca}$:** calcium channel currents

**ICAM1:** intracellular adhesion molecule-1

**ICE** interleukin-1β converting enzyme or caspase-1

**$I_D$:** dendrotoxin-sensitive potassium current

**$I_F$:** funny current

**IFM motif:** isoleucine-phenylalanine-methionine motif

**$I_H$:** hyperpolarization-activated current

**$I_K$:** steady state (delayed rectifier) potassium current

**$IK_{Ca}$:** intermediate conductance calcium-activated potassium channel

**IL-1β**: interleukin-1β

**IL-1Ra:** interleukin-1 receptor antagonist

**IL-1RAcP:** interleukin-1 receptor accessory protein

**IL-1RI:** type I interleukin-1 receptor

**IL-1RII:** type II interleukin-1 receptor

**$I_{NA}$:** sodium current

**iNOS:** inducible NO synthase

**IRAK:** IL-1RI receptor-associated kinase

**$K_{2P}$:** two-pore potassium channel

**$K_{Ca}$:** calcium-activated potassium channel

**$K_{IR}$:** inwardly- rectifying potassium channel

**$K_V$:** voltage-gated potassium channel

**L:** large, 'light' neurons with myelinated axons

**L-type:** long lasting calcium current

**L5:** 5$^{th}$ lumbar segment

**LI:** lamina I or the marginal layer

**LIF:** leukemia inhibitory factor

**LIIid:** dorsal inner lamina II

**LIIo:** outer lamina II or

**LPS:** lipopolysaccharide

**LTMRs:** low-threshold mechanoreceptors

**LVA:** low voltage activated channel

**MAPK:** mitogen activated protein kinase

**MHC II:** major histocompatibility factor II

**MMP:** matrix metalloprotease

**MyD88:** myeloid differentiation protein

**N-type:** neuronal calcium current

**NaN:** novel voltage-gated $Na^+$ channel

**NF:** neurofilament

**NF-κB:** nuclear factor-κB

**NGF:** nerve growth factor

**NK1:** neurokinin-1

**NMDA:** N-methyl-d-aspartate

**NMG:** *N*-methyl-D-glucamine

**NR2B:** N-methyl D-aspartate receptor subtype 2B

**NRM:** nucleus raphe magnus

**NSAID:** non-steroidal anti-inflammatory drug

**NT-3:** neurotrophin-3

**NT-4:** neurotrophin-4

**$P2X_4R$:** $P2X_4$ purinergic receptor

**p38 MAP kinase:** p38 mitogen-activated protein kinase

**$p75^{ntr}$:** p75 neurotrophin receptor

**PAG:** periaqueductal grey

**PAR-2:** protease-activated receptors 2

**PBS:** phosphate buffer solution

**PET:** positron emission tomography

**PFC:** prefrontal cortex

**$PGE_2$:** prostaglandin $E_2$

**$PGI_2$:** prostaglandin $I_2$ or prostacyclin

**PI3K:** phosphatidyl inositol-3 kinase

**PKA:** protein kinase A

**PKC:** protein kinase C

**PKC Gamma:** protein kinase C gamma

**$PLA_2$(II):** type II phospholipase $A_2$

**PMA:** premotor area

**PN3:** peripheral nerve sodium channel type 3

**PNL:** partial nerve ligation

**P/Q-type:** 'Purkinje' cell calcium channel

**pro-IL-1β**: IL-1β precursor protein

**$RAG1^{-/-}$:** immunodeficient rat

**RB:** rheobase

**RET:** rearranged during transfection

**RMP:** resting membrane potential

**R-type:** toxin 'resistant' calcium current

**RVM:** rostral ventral medulla

**S1:** 1st sacral segment

**SA1:** slowly adapting type I

**SD:** 'small dark' neurons with unmyelinated axons

**s.e.m.:** standard error of the mean

**SG:** *substantia gelatinosa*

**SI:** somatosensory cortex I

**SII:** somatosensory cortex II

**sIL- 1RII:** soluble type II interleukin-1 receptor

**$SK_{Ca}$:** small conductance calcium-activated potassium channel

**SNL:** spinal nerve ligation

**SNS:** sensory neuron specific

**SOM:** somatostatin

**SP:** substance P

**STZ:** streptozotocin

**T-type:** transient calcium current

**Tak1:** transforming growth factor β – activated kinase-1

**TBS-T:** tris-buffered saline-tween

**TDR:** time-dependent rectification

**TEA:** tetraethyl ammonium

**TENS:** transcutaneous electrical nerve stimulation

**TIR:** Toll-interleukin-1 receptor

**TLR:** Toll-like receptor

**TNF-α:** tumor necrosis factor-α

**TNFR:** tumor necrosis factor receptor

**TRAF6:** tumor necrosis factor receptor-associated factor-6

**TREK-1:** 2-pore potassium channel

**TrkA:** tropomyosin receptor kinase A

**TrkB:** tropomyosin receptor kinase B

**TrkC:** tropomyosin receptor kinase C

**TRP:** transient receptor potential

**TRPA:** ankyrin transmembrane protein channel

**TRPC1:** canonical-1 transient receptor potential channel

**TRPM:** melastatin or long transient receptor potential channel

**TRPV:** vanilloid transient receptor potential channel

**TTX:** tetrodotoxin

**TTX-R:** tetrodotoxin -resistant

**TTX-S:** tetrodotoxin -sensitive

**$V_{cmd}$:** command voltage

**VGC:** voltage-gated channel

**VGCC:** voltage-gated calcium channel

**VGSCs:** voltage-gated sodium channel

**vGLUT2:** vesicular glutamate transporter 2

**VGSC:** voltage-gated sodium channel

**$V_h$:** holding potential

**$V_p$:** conditioning prepulse

***$V_{Peak}$*:** peak voltage response

**VPL:** ventroposterolateral thalamic nucleus

**Vpr:** viral protein R

$V_{SS}$**:** steady state voltage

# CHAPTER 1

General Introduction

### *1.1 What is Pain?*

Pain can be defined as 'an unpleasant sensory and emotional experience associated with actual or potential tissue damage, or described in terms of such damage' (Merskey and Bogduk, 1994) To give functional meaning to this definition, I will provide a personal illustration. It was a cool and cloudy day in San Diego, but, for a Canadian, it was the perfect day to attempt surfing. Without hesitation, I ran into the Pacific Ocean and poised myself to 'catch' the perfect wave. That's when my right leg jerked and a sharp pain shot-up from my submerged foot. 'This is not good', I thought to myself. 'I need to get to shore immediately!' By the time I reached the sandy beach, the pain had transformed into a throbbing, burning, and almost unbearable pain. My foot was now swollen with, yes, blood. My friends looked on with empathy and concern. Local surfers suspected a stingray which was 'uncommon in November waters'. I was a survivor and my foot made a full recovery. I look forward to surfing again, but I'll never again enter the ocean with such naivety.

#### *1.1.1 Pain is necessary for survival*

Pain minimizes contact with the injurious stimulus; thus, promoting a protective response (Wang and Woolf, 2005). This protective response evokes both a reflex withdrawal from the stimulus and, as an unpleasant sensation, results in complex behavioural strategies to avoid further contact with such stimuli (Latremoliere and Woolf, 2009). Despite the unpleasant nature of pain, it would be difficult to imagine any organism surviving without it. For instance, what

would motivate an organism to limit use of an injured limb and allow healing? How would an organism learn from its surrounding environment? In the case of the stingray, how would an organism deter and defend against imposing threats? Cox and colleagues (2006) studied several families from Northern Pakistan that contained members with a congenital inability to experience pain and illustrated the following: 'The index case was a ten-year-old child, well known to the medical service after regularly performing 'street theatre'(Cox et al., 2006). He placed knives through his arms and walked on burning coals, but experienced no pain. He died before being seen on his fourteenth birthday, after jumping off a house roof'. Clearly, without the protection elicited by the pain response, the survival of a species is compromised. So long as pain reflects an injury, in space and time, then the benefits of pain outweigh costs.

### *1.1.2 The two dimensions of pain*

An important consideration, from the above definition, is that pain has sensory and emotional (affective) dimensions. The sensory dimension corresponds to nociception which is defined as the neural process of encoding and processing noxious or harmful stimuli (Lee et al., 2009). Through this process the nature (chemical, mechanical or thermal), location, intensity and temporal aspects of the stimulus become experienced (Wall, 1999). Although this specialized detection system (discussed below) is often the cause of pain, it is not synonymous with pain, which is a conscious experience that can occur in the absence of nociception (Lee et al., 2009). The affective dimension is the moment-

by-moment unpleasantness of pain, made up of emotional feelings associated with future implications, including distress, fear and suffering (Price, 2000). These concerns are the result of pain-related activity in limbic structures, such as the amygdala which elicits complex behaviours leading to escape and avoidance (Price, 2000).

The affective dimension suggests psychosocial aspects can influence the perception of pain such that 'pain is whatever the person says it is' (McCaffery and Pasero, 1999). Therefore, what is painful, yet tolerable to one individual or in one circumstance, can be unbearable to or in another. For instance, Rainville and colleagues (1999) demonstrated that hypnosis can manipulate the unpleasantness of a given noxious stimulus to individual human subjects. Further, while somatosensory regions of the brain always became active in response to the noxious stimulus, activity in affective regions varied with the degree of unpleasantness (Rainville et al., 1999;Rainville et al., 1997).

Relative to the physiological contribution of nociception to the pain experience, psychosocial aspects have been poorly addressed in pain research. This disparity is, in part, a consequence of animal models and measures of pain behaviour (Mogil, 2009). While reflexive measures, such as paw withdrawal, provide quantitative meaning to nociception, they give little insight about the psychological state of the animal and, thus, under-represent the pain experience (Price, 2000). Until recently, measures which include the monitoring of pain affect, such as conditioned place aversion (CPA), have been uncommon (Hummel et al., 2008). The focus on nociception in pain research has been associated with

the clinical failure of several potential pain medicines (Mogil, 2009). Thus, an understanding of both sensory and affective dimensions of pain may improve translational research.

*1.1.3 Pain symptoms*

Pain can result in hyperalgesia, allodynia and spontaneous pain. These symptoms are the consequence of a heightened state of sensitivity in response to tissue damage. The IASP (International Association for the Study of Pain) defines hyperalgesia as "an increased response to a stimulus which is normally painful" (Merskey and Bogduk, 1994) (Figure 1-1A). It is thought that hyperalgesia is the consequence of sensitized nociceptive nerve endings and, therefore, stimulus modality is harmful and response is painful (Sandkuhler, 2009). In contrast, allodynia is defined as 'pain due to a stimulus which does not normally provoke pain' (Merskey and Bogduk, 1994) (Figure 1-1B). Allodynia is determined by a different mechanism than hyperalgesia, where the original stimulus modality is non-harmful but the response has become painful. Therefore, the 'quality' of the sensation has changed. For example, allodynia is observed in patients with lesions of the nervous system where touch, light pressure, or moderate cold or warmth evokes pain when applied to apparently normal skin.

The difference between allodynia and hyperalgesia is not always straightforward. For instance, allodynia is often compared to the 'experience of pain in response to a warm shower after a sunburn'. Recently, such descriptions have come under scrutiny since it is unknown whether nociceptors are involved.

In 2008, the IASP task force suggested that sensitization of nociceptors can involve both a decrease in threshold and an increase in suprathreshold response. Thus, with a possible decrease in nociceptor threshold in the sunburn analogy, it would become difficult to distinguish hyperalgesia from allodynia. In cases of uncertainty, the IASP advises that hyperalgesia be the preferred term and, therefore, has adapted the definition of hyperalgesia with the following umbrella term: 'Increased pain sensitivity'. The term allodynia is reserved for situations where it is known that the stimulus is incapable of activating nociceptors (Sandkuhler, 2009).

Paroxysmal spontaneous pain is a common symptom of tissue injury resulting in chronic pain (Mogil, 2009). Unlike allodynia and hyperalgesia, spontaneous pain is non-evoked and is the most universal clinical symptom in chronic pain states, such as neuropathic pain (Backonja and Stacey, 2004). In addition, spontaneous pain appears to be a much better predictor of 'average' and 'worst' pain ratings than evoked pain hypersensitivities. Paradoxically, research has focussed on behavioural measures of hyperalgesia and allodynia in chronic pain animal models. For instance, in a 10 year period, 90% of the papers published in *Pain* reported evoked hypersensitivity data, whereas the remaining 10% reported spontaneous behaviour measurements (Mogil and Crager, 2004). The reluctance to study spontaneous pain experimentally has been attributed to the uncertainty of corresponding animal behaviours and, therefore, represents another important challenge in translational pain research (Mogil, 2009) .

*1.1.4 Pain as a disease*

As discussed above, nociceptive pain is critical to the survival of an organism and can be considered 'good pain'. Nociceptive pain is acute in duration, lasting long enough to respond to the noxious stimulus. In response to tissue damage, the protective function of pain is further enhanced by allodynia and hyperalgesia (Latremoliere and Woolf, 2009). Inflammation is critical to this process, whereby, a complex cascade of events (discussed below) leads to the activation and sensitization of sensory nerve fibres (Richardson and Vasko, 2002). This heightened state of sensitivity subsides in the absence of further tissue damage and once the wound has healed (Latremoliere and Woolf, 2009).

Pain symptoms persisting long after an initial insult suggest that the pain response has become maladaptive and thus can be considered a disease (Sandkuhler, 2009). These chronic pain states can be neuropathic or inflammatory in aetiology (Sandkuhler, 2009;Mogil, 2009). The IASP defines neuropathic pain as 'pain initiated or caused by a primary lesion or dysfunction in the nervous system' (Merskey and Bogduk, 1994). Neuropathic pain can be triggered by various insults including direct nerve and spinal cord trauma; viral infections including *Herpes zoster* and HIV; or metabolic diseases including diabetes (Irving, 2005). Chronic inflammatory pain is thought to be the consequence of an underlying inflammatory disorder related to tissue pathology such as arthritis, gastritis, colitis or dermatitis (Aley et al., 2000). Chronic inflammatory pain is also associated with post traumatic and repetitive strain injuries. Although distinct features between neuropathic- and chronic inflammatory pain states have been

reported, including neurochemical changes and responses to analgesics (Honore et al., 2000), both pain states are thought to involve nervous system plasticity (Latremoliere and Woolf, 2009). Further understanding of these pain states at a molecular and cellular level and how they relate to one another, is, therefore, required.

### *1.1.5 The price of pain*

The stakes are enormous, it is estimated that the price of pain in developed countries is US$ 1 trillion per year (Stewart et al., 2003). Contributing to this huge economic cost are low work productivity and absenteeism. Chronic pain, including neuropathic-, post-traumatic- and arthritic pain, has an estimated prevalence of 15-40% in industrialized nations (Gilron and Johnson, 2010). Healthcare expenses for the year 2000 in a large US health insurance study were three-fold higher for patients with neuropathic disorders (US$ 17,355/patient) than for non-neuropathic disorder patients (US$ 5,715/patient) (Berger et al., 2004). Further, neuropathic pain was associated with other chronic co-morbidities including poor sleep quality, anxiety and depression (Berger et al., 2004). In a Canadian neuropathic pain study, almost half the patients were retired, while 55.7% of total costs associated with neuropathic pain were attributed to time lost from work (Tarride et al., 2006). Therefore, chronic pain appears to be an economic burden in at least two ways: On one hand, it reduces taxable income which, in turn, jeopardizes funding for public healthcare systems, such as in Canada. On the other, chronic pain diseases, such as neuropathic pain, have a late

age of onset and, thereby, place demands on the healthcare system from the retired population. Taken together, more effective therapies would be expected to increase productivity, reduce healthcare demands and ease personal suffering.

### *1.2 Cutaneous Primary Afferents*

In the early nineteenth century, Charles Bell and Francois Magendie proposed that dorsal and ventral roots of the spinal cord have different functions (Perl, 1992). While ventral roots serve as the conduits for efferents to exit the spinal cord and carry motor commands to muscles for movement, dorsal roots are the conduits for afferents to enter the spinal cord and convey sensory information to higher centres where sensations are experienced. This proposal provided a crucial step towards the modern understanding of the mammalian nervous system. Since then, it is has become known that sensory neurons are the cellular correlates responsible for the transduction and transmission of sensory information. They are pseudo-unipolar in arrangement and are composed of cell bodies in the dorsal root ganglion (DRG) with associated dorsal roots leading to intraspinal terminations, as well as peripheral nerve fibres leading to afferent terminals in peripheral tissues, such as the skin. Beyond this basic arrangement, cutaneous sensory neurons are functionally, morphologically and neurochemically diverse, where no single parameter completely defines a given subpopulation (for visceral and muscle afferents, see the following book and articles: Scott (1992); Robinson and Gebhart (2008); and Perry and Lawson (1998)).

*1.2.1 Diverse morphology and neurochemistry*

Primary afferents can be classified according to size, extent of myelination, conduction velocity and neurochemical phenotype. Erlanger and Gasser's seminal studies established that the compound action potential of whole peripheral nerves consisted of a series of voltage peaks as the result of summing of impulses from groups of fibres whose conduction velocities centred around certain modal values (Gasser, 1937). These differences in conduction velocity were positively correlated with fibre cross-sectional diameter (Perl, 1992). The "A" deflection represents the most rapidly conducting, large diameter fibres, whereas, the "C" deflection represents the slowest conducting, small diameter fibres. The A-fibres are myelinated and have readily definable subgroups based on conduction velocities and related fibre diameters. From fastest to slowest, the A- fibre subgroups have been designated the Greek letters: α, β and δ. There is considerable variability in conduction velocity values between species and even between nerves of the same species (Perl, 1992), however, it is known that mammalian A-fibres can conduct up to 100 metres per second while C-fibres can conduct at less than 1 metre per second (Gasser, 1937). The majority of afferents that transmit painful information are Aδ or C, while the majority of afferents that convey innocuous thermal or mechanical information are Aβ–fibres. However, thinly myelinated and, possibly, some unmyelinated small afferents are associated with the transmission of innocuous sensations (Light and Perl, 2003). For instance, a woman with selective loss of large diameter, myelinated sensory fibres provided an opportunity to study C-fibres in isolation (Olausson et al., 2002).

Light touch to the back of the hand was felt as very diffuse and faint, yet pleasant. Thus, some C-fibres may be associated with sensations resulting from innocuous stimuli.

Light microscopy studies determined that fibre diameter is also positively correlated to cell body diameter and, therefore, Aβ–fibres are associated with the largest cell body diameters, typically greater than 40 micrometres, whereas, Aδ– and C-fibres are associated with medium (30-40 μm)- and small (< 30 μm)-sized cell bodies, respectively (Harper and Lawson, 1985a;Caffrey et al., 1992;Scroggs and Fox, 1992) (Table 1-1). Further, most early cytological and ultrastructural studies of DRG sensory neurons distinguished two types: large, 'light' (L) neurons with myelinated axons or 'small dark' (SD) neurons with unmyelinated axons (Lawson et al., 1974;Duce and Keen, 1977;Sommer et al., 1985). The cytoplasm of L neurons is characterized by uneven staining because of clumps of Nissl substance interspersed with lightly stained regions of the cytoplasm that contain microtubules and abundant amounts of neurofilament (NF). In contrast, SD neuron cytoplasms are more densely packed with organelles and have few NFs. Therefore, L and SD neurons can be further distinguished based on cytoplasmic protein phentotype. For instance, RT97, a monoclonal antibody against the phosphorylated form of the 200 kDa NF subunit, was shown to label L but not SD neurons in rat DRG (Lawson et al., 1984). In contrast, antibodies against the intermediate filament protein, peripherin, revealed labelling of mainly SD neurons in rat DRG (Ferri et al., 1990). Double immunofluroescence labelling has revealed considerable overlap between markers of NFs and intermediate

filaments and, therefore, reflects limitations in the initial cytochemical efforts to classify DRG neurons (Goldstein et al., 1991).

Many neurochemical studies have continued to distinguish sensory neuron subpopulations, which has led to the discovery and use of several cell surface and cytoplasmic markers (Aoki et al., 2004). For instance, small DRG neurons can be divided into two major subpopulations, the peptidergic and non-peptidergic. The peptidergic express substance P (SP) and calcitonin gene-related peptide (CGRP), while the non-peptidergic possess fluoride-resistant acid phosphatase (FRAP) activity (Knyihar-Csillik and Csillik, 1981;Hokfelt et al., 1975;Lee et al., 1985b). However, FRAP labelling had several technical disadvantages and, therefore, interest grew in alternate techniques, such as the use of cell-surface carbohydrate markers (Silverman and Kruger, 1990;Lawson et al., 1985). In 1990, Silverman and Kruger demonstrated that non-peptidergic neurons with FRAP activity had selective binding to the plant lectin α-D-galactose-specific *Griffonia* (or *Bandeiraea*) *simplicifolia* isolectin B4 (GSA-IB4) (Silverman and Kruger, 1990). Therefore, non-peptidergic small, cutaneous sensory neurons can be readily distinguished from the peptidergic subpopulation by the binding of IB4 (Aoki et al., 2004) (Table 1-1). More recently, it was determined that IB4-positive rat DRG neurons also highly co-localize with ATP-activated purinergic $P2X_3$ receptors (Bradbury et al., 1998) and, therefore, serves as another defining neurochemical and, perhaps, functional feature of non-peptidergic small DRG neurons. On the other hand, immunoreactivity for CGRP is commonly used to define peptidergic, small sensory neurons since CGRP reactivity (40% of all

sensory neurons) includes SP populations (20% of all sensory neurons) as well as other, SP exclusive, sensory neurons populations, such as somatostatin (SOM) expressing DRG neurons (Lee et al., 1985b;Lee et al., 1985a;Hokfelt et al., 1976;Aoki et al., 2004). In DRG, vanilloid transient receptor potential channel 1(TRPV1) immunoreactivity is restricted to small and medium -sized neurons with reactivity in both petidergic and non-petidergic sensory neurons (Caterina et al., 1997;Guo et al., 1999). Since TRPV1 is s a transducer of noxious thermal stimuli, its presence is commonly used to distinguish small, nociceptive sensory neurons from larger, presumed non-nociceptive, neurons.

Taken together, sensory neurons are neurochemically diverse, while large neurons are neurofilament rich, small neurons express many molecules commonly associated with nociceptive modalities, such as TRPV1, $P2X_3$ receptors and CGRP. Further, the identification of peptidergic and non-peptidergic small sensory neurons is suggestive of dual pain pathways with functionally distinct features. The presence of these molecules, along with others, is of pathophysiological relevance and will be discussed below. It is also important to consider that, while many of these cell surface and cytoplasmic molecules are useful as markers of phenotypes associated with distinct sensory neuron subpopulations, their presence varies between species, between innervated tissues, with animal age and after tissue injury (Aoki et al., 2005;Bennett et al., 1998;Bennett et al., 1996;Robinson and Gebhart, 2008).

*1.2.2 Diverse trophic support*

Neurotrophic factors of the nerve growth factor (NGF) family exert biological responses through the binding of their respective high affinity receptors: tropomyosin receptor kinase A (TrkA), TrkB and TrkC (Stephens et al., 2005). Additionally, all neurotrophins are capable of binding the p75 neurotrophin receptor ($p75^{ntr}$), which is unrelated to Trk receptors and belongs to the tumor necrosis factor receptor (TNFR) family. Neurotrophins exist as dimers and, upon receptor binding, Trk receptors become paired together inducing autophosphorylation and phosphorylation of other proteins through a cytoplasmic tyrosine kinase catalytic domain. Phosphorylation induces intracellular signalling pathways promoting precursor cell proliferation and differentiation, as well as neuronal survival (Stephens et al., 2005). Although adult sensory neurons do not require neurotrophic factors for their survival, the presence of several target-derived neurotrophins has been associated with the maintenance of differentiated sensory neuron phenotypes (Lindsay, 1992). For instance, peptidergic and non-peptidergic adult DRG neurons differ in neurotrophic support: the nerve growth factor (NGF) dependent and the glial cell line-derived neurotrophic factor (GDNF) dependent neurons, respectively (Bennett et al., 1998;Averill et al., 1995;Molliver et al., 1997). Consistent with neurotrophin dependence, peptidergic neurons express TrkA, whereas the non-peptidergic express receptor components for GDNF signalling, including the GDNF family receptor alpha-1 (GFRα-1) and the transmembrane tyrosine kinase receptor, rearranged during tranfection (RET) (Molliver et al., 1997;Bennett et al., 1998;Airaksinen and Saarma, 2002). Upon

removal of NGF or GDNF, respective cultured sensory neuron subpopulations are diminished or phenotypically switched (Fjell et al., 1999). The NGF-dependent population (CGRP-positive) represents roughly 40% of DRG neurons, whereas the GDNF-dependent population (IB4-positive) represents roughly 30% (Silverman and Kruger, 1990; Averill et al., 1995) with minimal overlap between the two population. More recently, the role of RET signalling in the postnatal development of sensory neurons has been analyzed in mice carrying a specific deletion of the Ret gene in DRG neurons (Valdés-Sánchez et al., 2010;Luo et al., 2007). The phenotype of this conditional knockout has indicated that RET signalling is not required for DRG neuron survival but is necessary for the proper differentiation of the non-peptidergic nociceptive subtype, as it appears to promote the expression of several markers that are characteristic of these sensory neurons and to support the normal extent of their peripheral projections in the skin (Luo et al., 2007).

Another member of the neurotrophin family, neurotrophin-3 (NT-3), also interacts with mature sensory neurons. In cutaneous afferents, mRNA for the NT-3 receptor, TrkC, is detected in larger sized adult sensory neurons, which show little size overlap with neurons expressing TrkA (McMahon et al., 1994). Further, *in situ* hybridization reveals that TrkC has minimal co-localization with TrkA expressing adult rat DRG (Wright and Snider, 1995). Thus, NT-3 responsive neurons may be functionally distinct from NGF responsive neurons. In support, Airaksinen and colleagues' (1996) work, involving single unit recordings from mice with null mutations of the NT-3 gene, showed that two mechanoreceptive

subsets of cutaneous afferents, D-hair receptors and slowly adapting mechanoreceptors, require this factor (Airaksinen et al., 1996). Other cutaneous receptors were unaffected. In adult NT-3 heterozygous animals, slowly adapting afferents had the greatest reduction in incidence with corresponding morphological losses of Aβ−fibre axons. Merkel cells, which are the end organs of slowly adapting mechanoreceptors, were severely reduced. This loss of Merkel cells, together with their innervating Aβ−fibres, happens in the first postnatal weeks of life, in contrast to muscle spindles and afferents, which are never formed in the absence of NT-3. Thus, NT-3 is essential for the maintenance, but not the establishment, of specific cutaneous afferents known to subserve fine tactile discrimination in humans.

Distinct sensory neuron populations responsive to BDNF may be more difficult to interpret. For instance, TrkB receptor expression has extensive overlap in size classification with both TrkA and TrkC expressing adult sensory neuron populations, suggesting BDNF may interact with a variety of sensory neuron populations. In contrast, other studies suggest that TrkB is found in a distinct class of medium-sized sensory neurons with minimal mRNA co-localization in TrkA and TrkC expressing sensory neurons (Wright and Snider, 1995). Another source of confusion, is that TrkB is also the high affinity receptor for neurotrophin-4 (NT-4) and, therefore, would obscure results in studies where BDNF is disrupted. Despite potential complications, several studies have examined the consequences of NT-4, BDNF and TrkB genetic perturbations in postnatal mice. For instance, immunohistochemistry and ultrastructural analysis

of cutaneous afferents in TrkB null mutant mice revealed a selective loss of the Meissner's corpuscle rapidly adapting mechanoreceptors (González-Martínez et al., 2004). In addition, only homozygous mutants for BDNF, and not NT-4, disrupted the development of Meissner's corpuscles in murine glabrous skin (González-Martínez et al., 2005). NT-4, however, is responsible for the maintenance of the down hair (D-hair) mechanoreceptors, which innervate a subpopulation of hair follicles (Stucky et al., 1998). Consistent with a role in the support of other cutaneous mechanoreceptors, Carroll and colleagues (1998) observed, electrophysiologically, slow-adapting mechanoreceptors, but not other types of cutaneous afferents, require BDNF in postnatal life (Carroll et al., 1998). In addition, Merkel cell numbers increase in the foot pad skin of mice overexpressing BDNF, suggesting some overlap with TrkC responsive afferents (Botchkarev VA et al., 1999). Last, Valdez-Sanchez and colleagues (2010) reported that BDNF is required for the survival of a significant fraction of postnatal peptidergic and non-peptidergic nociceptors in the DRG, suggesting overlap with TrkA expressing- and, even, GDNF responsive small sensory neurons. Further, *Bdnf* homozygous mutant mice lose approximately half of all nociceptive neurons during the first 2 weeks of life and adult heterozygotes exhibit hypoalgesia and a loss of 25% of all nociceptive neurons. Thus, depending on the study TrkB signalling may support distinct sensory neuron populations, such as rapidly adapting mechanoreceptors, or share a role in the support of slowly adapting mechanoreceptors and nociceptors.

Taken together, sensory neuron dependence on neurotrophic factors is a very complex phenomenon. The dependence is dynamic, altering with nervous system development and after tissue injury. In addition, sensory neuron responsiveness may be dependent on target tissue, sensory ganglia (DRG or trigemininal ganglia), species and the presence of one or multiple neurotrophic factor receptors, including $p75^{ntr}$ co-expression. Last, it is not clear which neurotrophic responses are direct or indirect; or if the primary effect is on mechanoreceptive cells, such as Merkel cells, or the innervating afferent fibres. Despite these complexities, it can be suggested that mechanoreceptive populations tend to depend on NT-3, whereas, nociceptive populations depend on NGF and GDNF. BDNF is likely involved in the maintenance of several sensory neuron populations (Table 1-1).

### *1.2.3 Diverse transduction mechanisms*

Seminal studies in the late nineteenth century examining the functional diversity of the sensory nerve endings included Max Von Frey's discovery that cutaneous sensitivity consisted of discrete points at which sensations could be elicited by mechanical, thermal or noxious stimuli (Perl, 1992). Von Frey then correlated, from independent histological studies, each discrete point to a specific structural entity. Thus, each of the sensory experiences begins with the activation of specific sensory afferents with specific nerve terminations in the skin. Cutaneous sensory neurons can be classified according to sensory modality

(Martin, 1985a). For example, thermoreceptors respond to warming or cooling, whereas mechanoreceptors respond to stretch, pressure and hair movement. In addition, nociceptors respond to harmful stimuli, many of which are polymodal and respond to various types of sensory stimuli. The transduction of stimulus modality into action potentials involves a variety of complex cellular and molecular processes (Lumpkin and Caterina, 2007).

Over the past decade, the molecular correlates of sensory transduction, whose activities depend on specific stimuli in the surrounding environment, have been identified (Voets et al., 2004). Cation channels, known as the transient receptor potential (TRP) channels, represent the first illustration that sensory ion channels can be gated by a physical stimulus (Dhaka et al., 2006;Caterina et al., 1997). TRP channels get their name from a *Drosphilia* phototransduction mutant that shows a transient instead of a sustained response to bright light (Cosens and Manning, 1969;Montell, 2005). These channels are divided into seven subfamilies, typically have six transmembrane domains, a pore region, cytoplasmic amino and carboxy termini and assemble as functional tetramers (Ramsey et al., 2006). Members of 3 families, the vanilloid TRP channels (TRPV), the melastatin or long TRP channels (TRPM), and the ankyrin transmembrane protein channels (TRPA) are of particular interest as thermoreceptors (Schepers and Ringkamp, 2009). In mammals, temperature sensitive TRPs are each tuned to distinct temperature ranges and, collectively, permit discrimination of temperature ranging from noxious cold to noxious heat (Lumpkin and Caterina, 2007). Four TRP channels belonging to the TRPV

subfamily are activated by heating, with characteristic activation temperatures ranging from warm temperatures (> 25 °C for TRPV4; >31 °C for TRPV3), to heat (> 43 °C for TRPV1) and noxious heat (> 52 °C for TRPV2) (Voets et al., 2004). In contrast, TRPM8 and TRPA1 are activated by cooling, (< 28 °C for TRPM8; <18 °C for TRPA1).

Many thermal TRPs are also chemo-, mechano- and /or osmo-sensitive. For instance, TRPV1 responds to protons and capsaicin, the pungent component of spicy peppers (Caterina and Julius, 2001;Caterina et al., 1997). In contrast, TRPM8 is activated by menthol (mint), while TRPA1 responds to a variety of pungent compounds, including cinnamaldehyde (cinnamon), allicin (garlic) and isothiocyanates (wasabe) (Bandell et al., 2004;Peier et al., 2002). TRPA1 and TRPV4 have been associated with mechanosensitivity (Kwan et al., 2006;Suzuki et al., 2003a). In addition, TRPV4 mediates animal behaviours in response to hypotonic stimuli and maybe of particular interest in hypersensitive states (Alessandri-Haber et al., 2005).

There are many other possible molecular correlates for sensory neuron transduction. For example, two pore potassium channels, such as TREK-1, close upon cooling and may allow depolarization of cold-sensitive neurons (Alloui et al., 2006;Maingret et al., 2000). Additionally, TREK-1 channels are stretch-sensitive and knockout mice have increased sensitivity to low-threshold mechanical stimuli (Patel et al., 1998;Alloui et al., 2006). Acid sensing ion channels (ASICs) respond to protons and membrane stretch, however, a role in mechanoception has been unsubstantiated with animal models (Lumpkin and

Bautista, 2005). Several *in vitro* and invertebrate studies suggest other molecules may be involved in sensory neuron transduction, including canonical-1 TRP channels (TRPC1), $P2X_3$ ATP-gated cation channels and voltage-gated channels (VGCs), including voltage-gated sodium channels (VGSCs) (Lumpkin and Caterina, 2007;Dhaka et al., 2006;Morris and Juranka, 2007).

The mechanisms by which stimuli interact with these molecular entities are still unresolved. Three gating models have been proposed for mechanosensitive channels (Lumpkin and Caterina, 2007):

1. Stretch-activated ion channels could open when forces in the lipid bilayer change. Experimentally, these channels can be activated by applying pressure to a membrane patch in order to alter membrane tension or curvature.

2. An alternate gating model proposes mechanosensitive channels are tethered to the cytoskeleton or extracellular matrix and tension, between these linkages, controls channel gating.

3. Channel opening could be indirect, involving the release of signalling intermediates from mechanosensitive proteins. One limitation of indirect gating mechanisms is that they are intrinsically slower than direct mechanisms and, therefore, may not be consistent with the kinetics expected for mechanoreceptors.

Indirect and direct mechanisms have also been proposed for temperature gating (Dhaka et al., 2006). For instance, the absence of TRPV4 thermosensitivity in excised membrane patches suggests that soluble factors indirectly gate, at least some, thermosensitive channels. Temperature activation could also occur indirectly via membrane bound factors or phase transitions in the lipid bilayer

(Dhaka et al., 2006). Alternatively, a thermodynamic model for a direct effect of temperature on thermosensitive channels has been proposed. The model is based on experimental evidence where changes in temperature produced leftward shifts in the voltage-dependent activation curves towards physiological voltages for a subset of TRPs, including TRPV1 and TRPM8 (Voets et al., 2004). A two-state (closed-opened) model was used to explain TRPM8 and TRPV1 channel activation in cold and heat, respectively. Essentially, TRPV1 channel opening rate increases with elevating temperatures, whereas, channel closing rate is relatively temperature independent. In contrast, TRPM8 channel closing rate increases with elevating temperatures, whereas, channel opening rate is temperature independent. Thus, TRPV1 channels open upon heating while TRPM8 channels close.

Taken together, the diverse sensory modalities of primary afferents may be associated with the expression pattern of transduction molecules, such as TRP channels, in cutaneous tissues. For instance, noxious heat sensations could be explained by the high expression of TRPV1 and TRPV2 in nociceptive Aδ– and C-fibres (Caterina and Julius, 2001;Lumpkin and Caterina, 2007). Though TRPM8 and TRPA1 are both expressed in small diameter sensory neurons, only TRPA1 expression co-localizes with putative nociceptive neuron markers, such as SP and CGRP, thereby, rationalizing noxious cold as distinct from cool thermo-sensations (Dhaka et al., 2006). Consistent with polymodal nociceptors, TRPA1 is expressed in a subset of TRPV1 expressing nociceptive neurons responding to noxious mechanical and thermal stimuli (Dhaka et al., 2006). The close apposition

between free nerve endings and keratinocytes, as well as the synaptic junctions between Merkel cells and Aβ–fibres suggest skin cells can act as first-line transducers of physical stimuli (Lumpkin and Caterina, 2007). In support, Merkel cells express TRPV4 and keratinocytes express TRPV3 and TRPV4 (Dhaka et al., 2006;Lumpkin and Caterina, 2007). In a manner analogous to auditory and taste transduction, skin cells could respond to innocuous heat and mechanical stimuli and, then, chemically transmit the signal to sensory neurons, such as Aβ–fibres (Lumpkin and Caterina, 2007).

### *1.2.4 Diverse connectivity*

Sensory neuron connectivity, both peripherally and centrally, is vital to the discriminative task of the somatosensory system. Connectivity in the skin forms one of five exteroceptive systems, which provides the body with information concerning the external environment (Munger and Ide, 1988). The remaining systems are devoted to the special senses: smell, taste, sight and hearing. Within the skin, there are several morphologically distinct nerve endings which can be classified according to afferent threshold, size of receptive field, adaptation and, ultimately, sensory modality (Tables 1-2, 1-3 and 1-4) (Martin, 1985b;Perl, 1992;Koerber and Mendell, 1992). For instance, Kruger and colleagues' careful physiological and cytological examination of the hairy skin in cats led to the discovery that free nerve endings (FNEs) are the nerve terminals of Aδ– and C-fibres, subserving the modalities of pain and temperature (Kruger et al., 1981).

The Aδ–fibres pass through the papillary dermis and penetrate the basement epidermal layer where they lose their myelin sheath, while peptidergic and non-peptidergic C-fibres terminate in different epidermal layers of glabrous and hairy skin (Lumpkin and Caterina, 2007;Kruger et al., 1981). Many FNEs are considered nociceptors. Certain nociceptors, whose afferent conduction velocities correspond to those of Aδ– and C-fibres, are high threshold mechanoreceptors and respond vigorously to only intense (tissue damaging) mechanical stimuli (Burgess and Perl, 1967;Bessou and Perl, 1969). Other nociceptors are polymodal, whose afferent conduction velocities are reflective of C-fibres, and respond vigorously to noxious mechanical and thermal stimuli and to chemical substances relevant to tissue damage (Burgess and Perl, 1967;Bessou and Perl, 1969). Still, some nociceptors, in deep subcutaneous tissue, have such high thresholds that they are unresponsive or "silent" in acute events, but become active after chronic tissue damage (Handwerker et al., 1991;Michaelis et al., 1996;Bessou and Perl, 1969). FNEs of Aδ– and C-fibres have also been associated with innocuous stimuli where some are considered thermoreceptors or low threshold mechanoreceptors (Munger and Ide, 1988;Bessou and Perl, 1969;Suzuki et al., 2003b;Alvarez and Fyffe, 2000;Light and Perl, 2003). Recently and as noted above, evidence is accumulating that many of the FNEs form *en passant* synapses with epidermal cells, such as keratinocytes (Denda et al., 2007;Lumpkin and Caterina, 2007). Further, epidermal cells are known to express stimulus transduction molecules and, therefore, FNEs may not always be the first-line transducers of pain and temperature.

Sensory corpuscles are capsulated low threshold mechanoreceptors formed by a central axon surrounded by variably arranged differentiated Schwann-related and perineurial-derived cells (Munger and Ide, 1988;González-Martínez et al., 2004). Two main subtypes of sensory corpuscles can be considered: the extensively capsulated, Pacinian corpuscles and the poorly capsulated, Meissner corpuscles (Tables 1-2 and 1-3). Meissner corpuscles lie just beneath the epidermis, while Pacinian corpuscles reside in the dermis and deeper tissues and, in both cases, the capsulated arrangements appears to act as a filter that protects the sensory endings from irrelevant stimuli (Johnson, 2001). Corpuscles can have Aα-, Aβ- or Aδ-sensory nerve fibres and upon static, mechanical skin displacement, only a few action potentials are recorded from sensory units and, therefore, corpuscle are defined as rapidly adapting. However, adaptation terminology is misleading since static displacement does not factor derivatives of displacement, such as velocity and direction (Perl, 1992). Thus, many rapidly adapting mechanoreceptors do not adapt rapidly when presented their most effective stimulus, such as dynamic mechanical displacements. Therefore, Pacinian and Meissner corpuscles are vibration detectors, which are ideally tuned to detect high (> 100 Hz) and low (< 100 Hz) frequencies, respectively (Johnson, 2001).

The Ruffini endings and Merkel cell–neurite complexes are slow adapting, low threshold mechanoreceptors of glabrous- and hairy skin (Perl, 1992;Johnson, 2001) (Tables 1-2 and 1-3). Ruffini endings are located in the connective tissue of the dermis and are relatively large spindle shaped structure tied into the local

collagen matrix (Johnson, 2001). Ruffini ending structure is considered analogous to that of the Golgi tendon organ in muscle and, therefore, suggests that Ruffini endings function as stretch receptors (Munger and Ide, 1988). Aα/β sensory axons branch between the fibrils and stretching of the skin tightens the fibrils which, in turn, leads to deformation and depolarization of the axonal ramifications (Brodal, 2010;Perl, 1992). The Merkel cell is a special cell type in the basal layer of the epidermis that enfolds the unmyelinated ending of the Aα/β afferent fibre (Perl, 1992;Johnson, 2001). The Merkel cell–neurite complex is selectively sensitive to a particular component of local displacement, which makes it sensitive to edges, corners and curvature. However, it is not known whether this selectivity is due to the Merkel cell or to the transducer mechanism within the afferent terminal (Boulais and Misery, 2007).

Afferent fibres innvervating hairs are additional low threshold mechanoreceptors of hairy skin. There are two main types of hair follicles (Munger and Ide, 1988): 1) guard hairs have thick diameter shafts, such as that found on the human scalp or outer coat of furred mammals; and 2) vellus hairs have thin diameter shafts, such as that found on the human eyelid or the down hairs of furred animals. Aα–, Aβ– or Aδ–nerve fibre endings wrap around the hair follicle, collectively termed the piloneural complex, and become activated upon the slightest bending of the hair (Alvarez and Fyffe, 2000;Lumpkin and Caterina, 2007;Munger and Ide, 1988). Ultrastructural analysis has revealed that axons innervate from the base of guard- and vellus hair follicles and split into

fork-like projections known as lanceolate terminals. Further, lanceolate terminals have been associated with rapidly adapting afferents and, thereby, enable hairs with movement detecting capabilities (Munger and Ide, 1988;Perl, 1992).

*1.2.5 Diverse electrophysiology*

Over the past thirty years the electrical membrane properties of sensory neuron cell bodies, within the mammalian DRG, have been extensively characterized (Koerber and Mendell, 1992). It has become clear from, a series of *in vivo, ex vivo* and *in vitro* studies, that DRG neurons have non-uniform electrical properties which loosely correlate to receptor- and afferent-type and, ultimately, sensory function. Matsuda and colleagues' intracellular recordings from somata in intact, but isolated, adult mouse DRG led to discovery of three distinct cell types on the basis of action potential (AP) shape, sensitivity to the puffer fish poison, tetrodotoxin (TTX) and ionic dependence (Matsuda et al., 1978;Yoshida et al., 1978;Koerber et al., 1988):

1. 'Fast' (F)-neurons, exhibiting brief APs which were mediated by tetrodotoxin (TTX)-sensitive $Na^+$ channels.

2. 'Afterhyperpolarization' (A)-neurons, exhibiting large and prolonged afterhyperpolarzations (AHPs) which were dependent on TTX-resistant $Na^+$ channels.

3. 'Hump' (H)-neurons, exhibiting broader spikes that were mediated by TTX-resistant $Na^+$ and $Ca^{2+}$ channels with the later producing a characteristic 'hump'or shoulder on the descending limb of the AP.

Similar AP shapes were described by Lawson's group where broad somatic APs tend to have slow C– ,as well as, some fast Aβ–conducting fibres, while narrow APs tend to have faster conducting fibres, including Aα–, Aβ– and Aδ-fibres (Harper and Lawson, 1985b). In addition, the shoulder on the repolarization phase was more often associated with broader somatic APs with C-fibre neurons also having the most prolonged AHPs. Studies in intact preparations, where the peripheral receptor could also be characterized, have associated sensory function with the heterogeneous electrical properties of DRG somatic membranes (Nicholls and Baylor, 1968;Rose et al., 1986;Koerber et al., 1988;Koerber and Mendell, 1992). From leech to cat, the major trend reported is that somatic spikes in nociceptors are characterized by broad APs with shoulders on the descending limb, while receptors responding to innocuous stimuli are characterized by narrower spikes. It was also discovered that Aδ–fibres innervating high-threshold mechanoreceptors (HTMRs) exhibit broader APs than Aδ–fibres innervating D-hairs (Rose et al., 1986;Koerber et al., 1988). Aβ HTMRs differ from Aβ low-threshold mechanoreceptors (LTMRs) in the same general way, however, Aβ LTMRs supplying different receptor types (e.g., slowly adapting type I (SA1), Pacinian corpuscles, etc.) exhibit no correlation between receptor type and electrophysiology of the soma. The relationship between AP shape and receptor threshold in C-fibres appears to be species dependent. For instance, C-fibre AP duration is longer for high threshold (nociceptive) afferents than for low threshold afferents in rat and guinea pig (Djouhri et al., 1998;Fang et al., 2005), however, no such relationship was found in cats (Traub and Mendell,

1988). Taken together, the variability of AP shapes in A-fibres and, possibly, C-fibres suggests AP duration is more related to receptor threshold than to conduction velocity.

*1.2.5.1 Voltage-gated sodium channels (VGSCs)*

The differential ionic dependencies and TTX sensitivities described in the seminal work of Matsuda and colleagues, suggest non-uniform ion channel composition among DRG cell types. Through several electrophysiological, pharmacological and molecular studies, it is now known that DRG neurons express a variety of voltage-gated ion channels (Nowycky, 1992). VGSCs are responsible for the fast upstroke of action potentials in electrically excitable cells (Catterall, 2000a). Kostyuk and colleagues' seminal voltage-clamp studies of sodium currents in the somata of isolated rat DRG demonstrated the existence of TTX-sensitive (TTX-S) sodium current in all cells measured (Kostyuk et al., 1981b). Consistent with properties reported by Hodgkin and Huxley in squid axon, DRG TTX-S sodium currents displayed voltage-dependent activation, rapid inactivation and selective ion conductance (Kostyuk et al., 1981b;Hodgkin and Huxley, 1952). However, some cells, as predicted from Matsuda and co-worker's (1978) study of DRG APs, revealed TTX-resistant (TTX-R) currents which displayed slower activation and inactivation kinetics, as well as, a depolarized voltage dependence for activation.

VGSCs channels form heteromultimeric proteins consisting of a large pore-forming $\alpha$-subunit and small extracellular accessory β-subunits which modulate channel membrane insertion and channel gating (Catterall, 2000a).

The α–subunit contains 4 internally homologous domains each with 6 α helical transmembrane segments (S1-S6) where S4 is the voltage sensor, S5 and S6 line the inner channel pore and the negatively charged amino acid residues of the S5-S6 linker (outer pore) form the ion selectivity filter, as well as, the TTX binding site (Catterall et al., 2005a;Catterall, 2000a). In addition, the intracellular loop, connecting domains 3 and 4, contains a hydrophobic triad of isoleucine, phenylalanine and methionine (the IFM motif) that is critical for fast inactivation. Further, the intracellular loop, connecting domains 1 and 2, contains several proposed sites for phosphorylation and modulation by protein kinases A and C (PKA and PKC). Since the discovery of the sodium channel protein by Catterall's group in 1980, nine mammalian sodium channel isoforms have been identified and functionally expressed (Beneski and Catterall, 1980). Similar to potassium channels and voltage-gated calcium channels, a standardized nomenclature has been developed for VGSCs where the name of an individual channel consists of the chemical symbol of the principal permeating ion ($Na^+$) with the principal physiological regulator (voltage) indicated as a subscript ($Na_V$) (Goldin et al., 2000). The number following the subscript indicates the gene subfamily (currently only $Na_V1$), and the number following the full point identifies the specific channel isoform (e.g., $Na_V1.1$). In this nomenclature, TTX-S isoforms, conferred by a pair of amino acid residues in the selectivity filter of the outer pore in all four domains, include $Na_V1.1$, $Na_V1.2$, $Na_V1.3$, $Na_V1.4$, $Na_V1.6$ and $Na_V1.7$, whereas, TTX-R isoforms include $Na_V1.5$, $Na_V1.8$ (formerly peripheral nerve sodium channel type 3 (PN3) and sensory neuron specific (SNS)) and $Na_V1.9$

(formerly novel voltage-gated Na+ channel (NaN)) (Catterall et al., 2005a;Catterall, 2000a;Terlau et al., 1991).

Since Kostyuk and colleagues' (1981) initial findings, several studies have reported variations in sodium current parameters in DRG neurons which have been associated with a heterogeneous sodium channel population. For instance, electrophysiological studies in DRG somata have demonstrated the presence of kinetically slow TTX-R sodium current in small, but not large sized neurons (Caffrey et al., 1992;Rizzo et al., 1994). Cloning studies identified sodium channel α-subunits $Na_V1.8$ and $Na_V1.9$, which produce TTX-R currents when heterologously expressed (Akopian et al., 1996;Sangameswaran et al., 1996;Dib-Hajj et al., 1998b). Further, *in situ* hybridization has revealed that transcripts for the two TTX-R sodium channels are preferentially expressed in small diameter sensory neurons which include nociceptive (C-type) neurons. Waxman's group demonstrated differential maintenance of the two DRG TTX-R isoforms, where $Na_V1.9$ is preferentially expressed in IB4-positive small DRG neurons while, both, small IB4-positive and negative neurons express $Na_V1.8$ (Fjell et al., 1999). The differential expression was also associated with alterations in sodium channel properties expected to influence excitability, such as a hyperpolarized voltage-dependency for activation and inactivation in IB4-positive neurons. The persistent nature of $Na_V1.9$ was further predicted to underscore the longer AP durations observed in small IB4-positive neurons (Fang et al., 2006). In a similar manner, many other isoforms have been characterized each with unique biophysical properties that influence AP generation, such as the rapidly repriming, resurgent

$Na_V1.6$ sodium current and the maintenance of high frequency firing (Rush et al., 2007). Taken together, heterogeneous expression of VGSC isoforms may be of importance in tuning electrical behaviour in different sensory neuron subpopulations and their altered expression or modulation by mediators may be of consequence after tissue damage (Rush et al., 2007;Cummins et al., 1999;Abdulla and Smith, 2002).

A series of immunocytochemical studies have determined the distribution of VGSC isoforms in sensory neurons and it is now known that large DRG neurons predominantly express TTX-S channels, such as $Na_V1.1$, $Na_V1.6$ and $Na_V1.7$, with some TTX-R $Na_V1.8$ expression, while small cells express TTX-S channels, in conjunction with TTX-R $Na_V1.8$ and $Na_V1.9$ channels (see review Rush et al., 2007). These findings have been further substantiated using intracellular recording, together with immunohistochemistry, to show the distribution of channels in DRG neurons that give rise to particular fibre types, such as the association of nociceptive C-fibres and broad APs with IB4-positive cell bodies immunoreactive for the $Na_V1.9$ isoform (Fang et al., 2006;Rush et al., 2007). Last, it is known that expression of multiple sodium channels, including TTX-R VGSCs, is not limited to the cell body and extends along the fibres, thereby, suggesting the likely importance of these channels in conduction and fibre characteristics (Rush et al., 2007).

*1.2.5.2 Voltage-gated calcium channels (VGCCs)*

VGCCs are the critical link between membrane depolarization and calcium entry and represent of one of several ways calcium can influence

membrane excitability and physiological processes, including neurotransmitter release (Catterall et al., 2005b;Gover et al., 2009). Biochemical characterization of VGCCs has revealed a complex protein structure composed of four or five distinct subunits that are encoded by multiple genes (Catterall et al., 2005b;Catterall, 2000b). The $\alpha_1$ subunit of 190 to 250 kDa is the largest subunit and, like the α-subunits of sodium channels, the $\alpha_1$ subunit of VGCCs is organized in four homologous domains (I-IV), each with six transmembrane segments (S1-S6). The S4 segment serves as the voltage sensor, while the pore loop between S5 and S6 in each domain determines ion conductance and selectivity. An intracellular β-subunit and a transmembrane, disulfide-linked $\alpha_2\delta$ subunit complex are components of most types of calcium channels. A γ-subunit has also been found in skeletal muscle calcium channels and related subunits are expressed in heart and brain. Although these auxiliary subunits modulate the level of expression and gating properties of the channel complex, the pharmacological and electrophysiological diversity of calcium channels arises primarily from the existence of multiple $\alpha_1$ subunits (Hofmann et al., 1994). In addition, the genes of the $\alpha_1$ subunits belong to the same gene superfamily that includes voltage-gated sodium and potassium channels, thus, the same channel nomenclature applies and includes gene subfamilies: $Ca_V1$ to 3 (Gover et al., 2009).

The calcium dependence for AP properties in the H-neurons of the DRG described by Matsuda and colleagues provided some of the initial clues for the contribution of an active calcium process in DRG neurons (Yoshida et al., 1978;Matsuda et al., 1978). It is now known that sensory neurons express several

biophysically and pharmacologically distinct VGCCs (Gover et al., 2009). The VGCCs include:

1. Low voltage activated (LVA) channels encoded by the gene subfamily $Ca_V3$, which have 'low' gating thresholds from -60 to -50 mV evoking rapidly inactivating 'transient' (T-type) currents, which are sensitive to changes in holding potential and which are non-selectively inhibited by amiloride and $Ni^{2+}$(Gover et al., 2009;Scroggs and Fox, 1992;Catterall et al., 2005b).

2. High voltage activated (HVA) channels encoded by gene subfamilies $Ca_V1$ and 2, which have 'high' gating thresholds from -30 to -20 mV. Further, HVA $Ca^{2+}$ currents include 'long-lasting' (L-type, $Ca_V1$) currents, 'Purkinje cell' (P/Q-type, $Ca_V2.1$) currents and 'neuronal' (N-type, $Ca_V2.2$) currents which are sensitive to blockade by most dihydropyridines, omega-agatoxin IVA and by omega-conotoxin GVIA, respectively (Gover et al., 2009;Scroggs and Fox, 1992;Catterall et al., 2005b;Fuchs et al., 2007;Acosta and Lopez, 1999).

3. Last, there are the intermediate voltage activated calcium channels which have 'intermediate' gating thresholds, evoking currents that are 'resistant' (R-type, $Ca_V2.3$) to most toxins.

Using electrophysiology and pharmacology, Scroggs and Fox examined the relative contribution of L-, N- and T-type currents among different sized DRG neurons (Scroggs and Fox, 1992). While N-type currents were found to be equally proportionate in small, medium and large cells, T-type currents had their greatest proportion in medium cells and L-type currents had their greatest contribution in small cells. This heterogeneous distribution of calcium current species among

DRG neurons, in particular T-type current, has been consistently observed (Schroeder et al., 1990;Lu et al., 2006;Abdulla and Smith, 2001b) and supported by the higher level of expression level for the $\alpha_{1I}$ ($Ca_v3.3$) T-type conducting subunit in smaller sized DRG neurons (Yusaf et al., 2001). Coupled to these findings, LVA and HVA channels are associated with different physiological roles. For instance, N-type VGCCs are highly expressed at presynaptic nerve terminals where they are involved in fast synaptic transmission (Zamponi et al., 2009;Todorovic and Jevtovic-Todorovic, 2006). On the other hand, T-type VGCCs are expressed in cell bodies and nerve endings of afferent fibres where they partake in regulating neuronal excitability by contributing to the initiation of repetitive discharge. Specifically, the unique biophysical properties attributed to T-type VGCCs permit them to lower AP threshold, promote bursting activity and generate subthreshold membrane oscillations.

*1.2.5.3 Potassium channels*

Potassium channels are the most diverse class of ion channels owing to numerous encoding genes, alternative mRNA splicing, α-subunit assemblies into dimeric or tetrameric channels, as well as, associations with β-subunits (Gutman et al., 2005). Potassium ion channels play important roles in the maintenance of resting membrane potential (RMP), the repolarization phase of the AP and the regulation AP firing frequency (Pischalnikova and Sokolova, 2009). The variation in AHP duration, observed by Matsuda and colleagues (1978), suggests that potassium conductances are another defining feature among sensory neurons. It is now known that DRG cells contain a wide variety of potassium channels of all

four families: voltage-gated ($K_V$), calcium-activated ($K_{Ca}$), inwardly- rectifying ($K_{IR}$) and two-pore ($K_{2P}$) channels. Although all four families have been associated with pain hypersensitivity (Ocaña et al., 2004), $K_V$ and $K_{Ca}$ channels and their relation to sensory neuron physiology will be the topic of further discussion. For more information on $K_{IR}$ and $K_{2P}$, see the following review articles: Bayliss and Barrett (2008); Lesage and Lazdunski (2000); Hibino et al. (2010); and Ocaña et al. (2004).

$K_V$ and $K_{Ca}$ constitute the six to seven transmembrane group of potassium-selective ion channels (Gutman et al., 2005). Each channel exists as a tetramer composed of four α-subunits either alone or in association with regulatory β-subunits (Pischalnikova and Sokolova, 2009;Ghatta et al., 2006). Similar to sodium and calcium channels, the α-subunit membrane-spanning domains include a positively charged S4 segment which endows many of these channels with voltage sensitivity. The α-subunit also contains the pore forming motif which consists of the P-loop (ion selectivity filter) and the S5 and S6 segments (Maylie et al., 2004;Gutman et al., 2005;Ghatta et al., 2006). The N and C-terminal domains of α-subunits differ in structure and function between families and subfamilies of potassium channels. For instance, the C-terminals of $K_{Ca}$ channels confer sensitivity to calcium, however, 'large or big' conductance $K_{Ca}$ ($BK_{Ca}$) channels, unlike small conductance $K_{Ca}$ ($SK_{Ca}$) and $K_V$ channels, have an extra membrane-spanning segment (S0) which leads to an extracellular terminus that binds regulatory β-subunits (Maylie et al., 2004;Ghatta et al., 2006).

The voltage-dependent delayed rectifier and fast transient potassium currents were first described in DRG neurons by Kostyuk's group (1981) where the two outward currents were separated by their differential presence at holding potentials of -90 mV versus -50 mV (Kostyuk et al., 1981a;Nowycky, 1992). Consistent with the potassium currents described by Hodgkin and Huxley in squid giant axon (Hodgkin and Huxley, 1952;Kostyuk et al., 1981a), the delayed rectifier current was characterized by its slow activation kinetics and lack of inactivation during maintained membrane depolarization. In contrast, the fast transient current or A-current ($I_A$) had, relatively, 'fast' activation kinetics and was almost completely inactivated at -50 mV. In addition, the fast transient current required a, relatively, small depolarization for activation when compared to the delayed rectifier current. Though both can be blocked by tetraethyl ammonium (TEA), fast transient potassium currents can also be pharmacologically separated from delayed rectifier currents by their susceptibility to the convulsant, 4-aminopyridine (4-AP), acting on the intracellular side of the membrane (Kostyuk et al., 1981a;Kameyama, 1983;Kasai et al., 1986). The existence of delayed rectifier- and fast transient potassium currents in DRG neurons was confirmed in subsequent studies, however, a third component was identified based on sensitivity to the Eastern green mamba venom, dendrotoxin, and greater susceptibility (<100 micromolar), relative to $I_A$ (>100 micromolar), to 4-AP block (Penner et al., 1986;Stansfeld et al., 1986). When isolated, the dendrotoxin-sensitive current ($I_D$) was calcium insensitive and displayed slow, incomplete inactivation relative to $I_A$ (Stansfeld and Feltz, 1988;Stansfeld et al.,

1986). Biophysically, potassium currents could be divided into non-inactivating and transient A-type currents with the later subdivided divided into fast ($I_{Af}$) and slow ($I_{As}$) components where $I_{Af}$ had, relatively, faster kinetics and more negative voltage dependencies than $I_{As}$ (McFarlane and Cooper, 1991). Thus, pharmacological and biophysical studies agree that at least three voltage-gated potassium currents can be readily identified in sensory neurons: sustained or non-inactivating, $I_A$ or $I_{Af}$ and $I_D$ or $I_{As}$ (but see also Gold et al., 1996b).

There is a complex distribution of the voltage-gated potassium currents among sensory neurons. While most sensory neuron subtypes have a non-inactivating or sustained potassium current, the distribution of transient components is less understood. For instance, A-type currents have been identified in subpopulations of large and small sensory neurons, including those associated with mechanoreceptors and nociceptors, respectively (Yoshida and Matsumoto, 2005;Everill et al., 1998;Gold et al., 1996b;Vydyanathan et al., 2005). However, it has been reported that the proportion of neurons with A-type current is greatest in small sensory neurons or C-fibres and least in large sensory neurons or Aα/β-fibres (Villiere and McLachlan, 1996;Pearce and Duchen, 1994), whereas, Abdulla and Smith (2001b) reported that A-type current is more frequently observed in large DRG neurons. Under thorough pharmacological and biophysical analysis, Gold and colleagues (1996) characterized six voltage-gated potassium currents in rat DRG neurons, three transient and three sustained, and that there is differential distribution among rat DRG neuron subpopulations (Gold et al., 1996b). Thus, it remains possible that most sensory neuron subtypes have at least

one transient and one sustained current. Regardless of the sensory neuron subtype, most studies agree sustained potassium currents shape APs, while transient currents are involved in the latency of firing, low firing frequency, spike adaptation and that there may be an inverse relationship in the proportion of these two broad classes of potassium current in any given sensory neuron (Connor and Stevens, 1971;Catacuzzeno et al., 2008;Yoshida and Matsumoto, 2005;Vydyanathan et al., 2005;McFarlane and Cooper, 1991).

Three classes of $K_{Ca}$ channels can be distinguished upon biophysical and pharamacological properties (Gover et al., 2009). Large conductance $BK_{Ca}$ channels are voltage-gated and sensitive to the scorpion-derived neurotoxins, iberiotoxin and charybdotoxin. In contrast, small conductance ($SK_{Ca}$) and intermediate conductance ($IK_{Ca}$) channels are voltage-insensitive and can be blocked by apamin and clotrimazole, respectively. Modulation of $K_{Ca}$ channels allows intracellular calcium elevations to regulate membrane excitability, whereby, the three $K_{Ca}$ channels are thought to have distinct functional roles. For instance, $BK_{Ca}$ channels are involved in AP repolarization and conduct the current underlying the fast AHP (fast $I_{AHP}$), whereas, $SK_{Ca}$ channels convey the $I_{AHP}$ that mediates intermediate or, possibly, slow AHPs in small nociceptive DRG neurons (Gold et al., 1996c;Gover et al., 2009;Scholz et al., 1998;Zhang et al., 2010;Vogalis et al., 2003b). In contrast, the physiological role of $IK_{Ca}$ in DRG neurons remains to be determined (Gover et al., 2009), however, they are thought to underlie slow AHP in enteric neurons (Vogalis et al., 2003a). Although the functions of $SK_{Ca}$ and $BK_{Ca}$ channels are well recognized in small diameter DRG

neurons, as wells as, nodose ganglion (visceral) neurons (Christian et al., 1994;Morita and Katayama, 1989), the expression of all three $K_{Ca}$ channels in the DRG including co-localization of $SK_{Ca}$ channels with small and large diameter neurons suggests that $K_{Ca}$ channels also have physiological importance in non-nociceptive neurons (Mongan et al., 2005;Li et al., 2007;Zhang et al., 2003;Bahia et al., 2005).

*1.2.5.4 Hyperpolarization-activated cyclic nucleotide-gated cation (HCN) channels*

HCN channels have significant homology with 6-transmembrane-domain potassium channels and possess an intracellular cyclic nucleotide-binding domain located in the C-terminus (Kaupp and Seifert, 2001;Santoro et al., 1998). The four presently known family members (HCN1-4) share substantial homology where individual HCN subunits assemble as homotetramers and, when expressed, homomers differ in two main respects: 1) rates of activation are in the order of HCN1>HCN2>HCN3>HCN4; and 2) HCN2 and 4 are strongly modulated by adenosine 3', 5' –cyclic monophosphate (cAMP) elevations which shifts the midpoint of activation in the positive direction by 12 to 20 mV. Similar to potassium channels, heteromers may also form functional HCN channels which have intermediate properties related to subunit composition (Ulens and Tytgat, 2001;Orio et al., 2009).

The HCN channels give rise to hyperpolarization-activated current ($I_H$) which consists of a slowly activating, non-selective cation current during a step hyperpolarization (Mayer and Westbrook, 1983). $I_H$ was first identified in the

cardiac sino-atrial node (DiFrancesco and Ojeda, 1980;Brown et al., 1979) as 'funny' current ($I_F$), but, subsequently, in the DRG where it acts to induce a slow depolarization or 'voltage sag' after a hyperpolarizing event (Mayer and Westbrook, 1983;Scroggs et al., 1994). Since then, $I_H$ has been found to be involved in a number of neuronal functions, including setting resting membrane potential, participating in pacemaker activity and modulating synaptic activity (Pape, 1996). HCN channels 1 to 3, but not likely HCN4, are present in the somata and axons of DRG neurons (Jiang et al., 2008;Tu et al., 2004;Kouranova et al., 2008). Further, HCN1 and fast $I_H$ are predominately found in larger DRG neurons, while slower $I_H$ currents are more variably expressed in small neurons (Tu et al., 2004;Momin et al., 2008;Kouranova et al., 2008). Last, knockout mutations or block with ZD7288 are associated with suppression of sensory neuron hyperexcitability and pain-related behaviours and, therefore, $I_H$ has attracted recent interest in pain research (Viana and Belmonte, 2008).

### *1.3 The Pain Pathway*

Once a stimulus has been translated into an action potential (transduction), various levels of the central nervous system (CNS) become involved in the processing of this sensory information. Although it remains uncertain how neurons function together to accomplish sensory processing, much progress has been made in identifying anatomical, physiological and neurochemical features of relevant cells and systems in the pain pathway.

*1.3.1 Primary afferent terminations*

Nociceptive information entering the spinal cord is initially processed in the dorsal horn and involves specific spatial terminations for primary afferents. For instance, the rostro-caudal and medio-lateral terminations of primary afferents encode the location of their individual peripheral receptive fields, thus, generating a somatotopic map of the body's surface onto the dorsal horn (Doubell et al., 1999). On the other hand, primary afferent terminations in the dorso-ventral plane of the dorsal horn encode different functional classes of sensory neurons. Based on Rexed's seminal work, the dorso-ventral plane of the dorsal horn can be subdivided into six horizontal laminae (LI to LVI) where neurons of common morphological features define each lamina (REXED, 1952;REXED, 1954) (Figure 1-2). The identities of primary afferents that terminate and release neurotransmitters, such as glutamate, within the marginal layer (LI), the *substantia gelatinosa* (LII), the *nucleus proprius* (LIII to LIV) and LV have been determined. For instance, large myelinated fibres, innervating low threshold mechanoreceptors that were characterized electrophysiologically and subsequently filled intracellularly with horseradish peroxidase, were shown to enter the cat spinal cord and send collaterals into the dorsal horn as they ascend and, sometimes, descend the dorsal column (Brown et al., 1977;Brown et al., 1978;Brown et al., 1980;Brown et al., 1981). These collaterals terminate ipsilaterally in laminae ventral to the outer lamina II (LIIo) and include extensive terminations in laminae III and IV. Similar patterns of termination were reported in the rat dorsal horn (Woolf, 1987). In contrast, identified C-fibres, including

nociceptive and thermoreceptive fibres, terminate ipsilaterally in laminae I, II and V (Light et al., 1979;Sugiura et al., 1989). Further, CGRP immunoreactivity revealed that peptidergic C-fibres, many of which co-localize SP or SOM, terminate in laminae I, IIo and V, whereas, IB4 labelling and/or $P2X_3$ immunoreactivity has revealed that non-peptidergic C-fibres terminate dorsally within inner lamina II (LIIid) (Bradbury et al., 1998;Traub et al., 1989;Ribeiro-da-Silva and Cuello, 1995). Although both classes of C-fibres transmit nociceptive information to the spinal cord, the function of non-peptidergic C-fibres remains poorly understood (Guo et al., 1999;Gerke and Plenderleith, 2001). Nociceptive, high threshold mechanoreceptive Aδ-fibres were shown to terminate ipsilaterally in laminae I and V, whereas, innocuous Aδ-fibres, innervating D-hairs terminate ipsilaterally in the deeper part of lamina II and lamina III (Light and Perl, 1979).Taken together, the superficial layers of the dorsal horn (LI and LIIo) receive heavy nociceptive input, while deeper laminae, with the exception of L5, receive non-nociceptive input.

*1.3.2 Spinal cord and central processes*

Since the pioneering efforts of Ramon Cajal, several attempts have been made to distinguish superficial dorsal horn neurons morphologically (Maxwell et al., 2007). Using dye filled microelectrodes and whole-cell recordings, a correlation between cell morphology (in particular dendritic orientation) and electrical behaviour has been recognized where four different neuron phenotypes can readily be identified within the *substantia gelatinosa* (Balasubramanyan et al.,

2006;Grudt and Perl, 2002;Prescott and De Koninck, 2002). The 'islet cells' have rostro-caudal extending dendrites where a large percentage fire continuously ('tonic' pattern) in response to depolarizing current commands. 'Central cells' also possess dendrites which extend rostro-caudally, but are less extensive than islet cells and fire an initial burst of APs before accommodation ('phasic'or 'transient' pattern). 'Vertical cells' or 'stalked cells' have a dorso-ventral orientation with sparse wide dendrites and tend to fire tonically, but some fire after an initial pause ('delay' pattern). Finally, 'radial cells' or 'multipolar cells' which possess a dendritic tree that radiates in all directions and typically have a delay firing pattern.

Recent advances have been made in the understanding the functional connectivity of SG neurons. For instance, dorsal root stimulation in horizontally sliced spinal cord preparations has revealed that islet- and central cells receive monosynaptic excitatory input from C-fibres, while the majority of vertical- and radial cells receive monosynaptic excitatory input from Aδ- and C-fibres (Yasaka et al., 2007). Further, immunoreactivity of dorsal horn neurons for the main inhibitory neurotransmitter in the CNS, gamma-aminobutyric acid (GABA), or the rate- limiting enzyme in the synthesis of GABA, glutamic acid decarboxylase (GAD), have been identified in islet cells (Maxwell et al., 2007;Todd and McKenzie, 1989;Mackie et al., 2003). Whereas, the majority of vertical cells are immunoreactive for excitatory markers, such as the vesicular glutamate transporter 2 (vGLUT2) and, possibly, protein kinase C gamma (PKC gamma) (Maxwell et al., 2007;Polgar et al., 1999;Todd et al., 2003). Finally,

simultaneously paired recordings from synaptically connected neurons have demonstrated that LII islet tonic cells can make monosynaptic inhibitory connections with LII central phasic cells, while central phasic cells monosynaptically excite LII vertical delay cells. In turn, LIIo vertical delay cells, with their dorsal extensions into LI, can monosynaptically excite LI projection neurons which possess SP receptor immunoreactivity (Lu and Perl, 2003;Lu and Perl, 2005). Thus, it appears nociceptive processing circuitry within the SG involves coordinated cross talk between excitatory and inhibitory synapses which serve to regulate the transfer of sensory information onto the pain projecting neurons of LI.

LI contains the highest density of projection neurons in the dorsal horn and it has become widely accepted that LI is a major site of nociceptive output to higher centres where pain can be experienced (Todd, 2002). In support, retrograde tracers applied to targets in the thalamus have revealed that many LI projection neurons are spinothalamic tract neurons (Trevino and Carstens, 1975). The axons of these projection neurons cross the midline and ascend through the anterolateral quadrant of the spinal cord, transmitting pain relevant information to the thalamus and brainstem (Christensen and Perl, 1970). Spinothalamic neurons terminate somatotopically in the ventroposterolateral (VPL) thalamic nucleus which then conveys nociceptive information to the somatosensory cortex, thus, permitting the accurate localization of acute pain. The anterolateral system also contains projection neurons, such as spinoreticular and spinotectal tract neurons, which have brainstem terminations in the recticular formation and the periaqueductal

gray region of the midbrain, respectively. Nociceptive activation of these brainstem areas, together with reciprocal activation of the parabrachial nucleus, hypothalamus and the limbic system, promotes a stress response which increases alertness and generates an autonomic response.

Recently, brain imaging techniques, such as positron emission tomography (PET) and functional magnetic resonance imaging (fMRI), have been used to reveal nociceptive processing areas in higher centres (Moisset and Bouhassira, 2007). Consistent with the extensive relays from the thalamus and brainstem, most human studies show increased activity in several regions ('pain matrix'), including the somatosensory cortices I and II (SI and II), anterior cingulate gyrus (ACG) and insular cortex (IC). Others include the amygdala, premotor area (PMA), thalamus, prefrontal cortex (PFC), basal ganglia, posterior parietal cortex, brainstem and cerebellum. SI, SII and the thalamus are associated with the sensory-discriminative dimensions of pain, whereas limbic areas, including the ACG, AI and amygdala, are associated with the affective or emotional dimensions of pain. Nociceptive activation of the PFC likely relates to cognitive-interpretive aspects of the pain experience (Wiech et al., 2008).

### *1.3.3 Endogenous regulation*

Nociceptive activation of the brainstem also promotes descending inhibition of the superficial dorsal horn. Pioneering experiments by Reynolds identified a modulatory circuit, whereby electrical stimulation of the periaqueductal grey (PAG) allowed major surgeries to be performed on conscious

rats without the expression of pain behaviours (Reynolds, 1969). It is now understood that PAG induced analgesia involves synaptic recruitment of descending fibres from the rostral ventral medulla (RVM) nuclei: nucleus raphe magnus (NRM) and the gigantocellular reticular nucleus (Bardoni, 2009). The serotonergic fibres of the NRM lie in the dorsolateral funiculus of the spinal cord and, through synaptic arrangements not fully understood, serotonin release into the dorsal horn leads to the inhibition of nociceptive spinothalamic projection neurons. Besides serotonin, other neurotransmitters, including norepinephrine, GABA, glycine, somatostatin and enkephalin, contribute to the effects of RVM stimulation. The PAG-RVM circuit is one of the most characterized descending pathways, however, more recent findings suggest this circuit is also facilitatory, promoting hyperalgesia in cases of acute inflammation and after nerve injury.

### *1.4 Neuropathic Pain*

Neuropathic pain can be defined as 'pain arising as a direct consequence of a lesion or disease affecting the somatosensory system' (Treede et al., 2008). Unlike nociceptive or 'inflammatory pain' which alerts the body to actual or potential tissue damage, neuropathic pain or 'non-inflammatory pain' serves no useful purpose (Smith, 2004;Latremoliere and Woolf, 2009). Neuropathic pain can be triggered by various insults including direct nerve and spinal cord trauma; viral infections including *Herpes zoster* and HIV; or metabolic diseases including diabetes (Irving, 2005). In experimental animals, peripheral nerve damage, such as nerve sectioning (axotomy), induces pain-related behaviours that are widely

accepted as a model for human neuropathic pain. Such behaviours are associated with an enduring increase in the excitability of peripheral, primary afferent neurons and, over a period of days or weeks, leads to the generation of increased excitability and synaptic activity in second order sensory neurons within the dorsal horn of the spinal cord. This corresponds to the phenomenon of 'central sensitization' which is a major component of many persistant pain states (Latremoliere and Woolf, 2009;Woolf, 1983). Because traditional analgesics, such as morphine, have limited use in the treatment of neuropathic pain, much effort has been devoted to the understanding of how peripheral nerve injury leads to increased excitability of the spinal dorsal horn.

### *1.4.1 Pharmacological treatment of neuropathic pain*

Non-steroidal anti-inflammatory drugs (NSAIDs), acetaminophen, more powerful opioid analgesics, or local anaesthetics can adequately control acute pain (Layzell, 2008;Krenzischek et al., 2008). Chronic, neuropathic pain differs from acute pain not only in its onset and duration, but more importantly in the underlying mechanisms. Thus, neuropathic pain may not have identifiable ongoing injury or inflammation and often responds poorly to NSAIDs and opioids (Watkins et al., 2005;Arner and Meyerson, 1988;Argoff et al., 2006). Surprisingly, many of these pharmaceutical approaches have been commonly prescribed in neuropathic pain conditions. For example, in a study of 55, 686 patients, the largest percentages of patients received opioids (53.9%) followed by NSAIDS (39.7 %) for the treatment of painful peripheral neuropathies (Berger et

al., 2004). Coupled to this, the repeated use of opioids is associated with several complications, including the development of analgesic tolerance and withdrawal-induced pain enhancement (Watkins et al., 2005). Given the considerable prevalence of neuropathic pain in the general population of 1% (Tarride et al., 2006) and its strong association with nerve injury, mismanagement represents a major problem (O'Connor and Dworkin, 2009).

Although there is no single, well tolerated drug for the treatment of neuropathic pain that parallels opioids for acute pain, the current understanding of neuropathic pain reveals several potential peripheral and central targets for therapeutic intervention (Smith, 2004). First-line treatments for neuropathic pain include the use of topical agents, such as lidocaine; certain antidepressants, such as tricyclic antidepressants; and the calcium channel $\alpha 2\delta$ ligands, gabapentin and pregabalin (gabapentinoids) (Smith, 2004;O'Connor and Dworkin, 2009). One major challenge is that the side effects of individual therapies, such as the drowsiness, confusion and dizziness associated with gabapentinoids, often limit the dosages required to achieve clinical efficacy (O'Connor and Dworkin, 2009). Thus, combination therapy is frequently used where it is ideal to choose medications with different mechanisms of action, as well as, different adverse effects.

Recently, it was reported that the membrane-impermeant lidocaine derivative, QX314, can enter small DRG neurons through TRPV1 channels in a capsaicin dependent manner, producing a potent anaesthetic effect (Binshtok et al., 2007). Since, TRPV1 channels are preferentially expressed on small,

nociceptive neurons (Caterina and Julius, 2001;Caterina et al., 1997) this raises the interesting possibility of selecting combinational therapies which allow targeting of the pain pathway, thereby, maximizing therapeutic efficacy, while limiting side effects (Binshtok et al., 2009;Gerner et al., 2008). In our laboratory, we are currently testing the hypothesis that gabapentin will also enter through TRPV1 channels, thereby, increasing efficacy through improved access to the $\alpha 2\delta$ calcium channel subunit (Biggs et al., 2010).

Still yet, further opportunities include the more recently recognized alterations to NMDA receptor properties after nerve injury (Iwata et al., 2007;Geng et al., 2010) and the use of N-methyl D-aspartate receptor subtype 2B (NR2B) –selective antagonists (Wu and Zhuo, 2009). In addition, the contribution of immune and glial cells in neuropathic pain (Scholz and Woolf, 2007) and the use neuroimmunomodulatory drugs, such as thalidomide or proinflammatory cytokine receptor antagonists (Irving, 2005). Last, it is important to consider the potential benefits of non-pharmacological treatments, such as meditation, exercise therapy, transcutaneous electrical nerve stimulation (TENS) and spinal cord stimulation (Irving, 2005).

### *1.4.2 Animal models*

Better treatment of neuropathic pain will also require a clearer understanding of what leads to such persistent pain, and testing of pharmacological agents in such settings (Wang and Wang, 2003). Animal models can provide useful and essential systems to study chronic pain. Several models

have been developed in order simulate particular aspects of human neuropathic pain and typically involve physical peripheral nerve trauma or the production of a disease state. For instance, clinical limb amputation can be studied using a nerve transection (axotomy) and ligation model which is characterized by the development of nerve sprouting at the proximal nerve stump (neuroma) and the tendency for the experimental animal to attack ('autotomy') the anaesthetic limb (Wall et al., 1979;Devor and Wall, 1976). Autotomy behaviour has been proposed to be a manifestation of spontaneous pain (Wang and Wang, 2003) triggered by afferent barrages produced ectopically in the transected nerve (Wall et al., 1979). However, a complete nerve transection is not the usual antecedent for human peripheral neuropathies and neuropathic pain (Munger et al., 1992) . Thus, more recent models produce only partial nerve injury to reflect the majority of nerve traumas observed in humans.

The chronic constriction nerve injury (CCI) model of peripheral mononeuropathy was introduced by Bennett and Xie (1988) and involves 4 loose chromic gut ligatures tied around the sciatic nerve. Unlike nerve transection models, the CCI model can be used to study thermal and mechanical hyperalgesia and allodynia in addition to spontaneous pain behaviours, such as guarding of the ipsilateral paw (Bennett and Xie, 1988;Attal et al., 1990). In an effort to avoid variability in the extent of nerve injury after CCI due to inter-experimenter differences in the degree of ligature tightness, cuff neuropathy was introduced (Mosconi and Kruger, 1996). This type of injury produces similar pain-related behaviours to that observed in CCI animals, but involves placing a fixed diameter

polyethylene cuff around the sciatic nerve. To mimic the condition of spontaneous burning pain (causalgia) after partial nerve injury in humans, a partial nerve ligation (PNL) was developed and involves passing a suture through approximately half of the sciatic nerve where it is then tied tightly (Seltzer et al., 1990). After PNL, animals exhibit many of the pain-related behaviours associated with CCI, however, many of these behaviours in PNL are expressed bilaterally and have been associated with 'mirror pain' in humans. Kim and Chung (1992) also developed a model, spinal nerve ligation (SNL), to simulate causalgia and involves unilaterally tightly ligating the $5^{th}$ lumbar segment (L5) spinal nerve or both L5 and L6 spinal nerves distal to the DRG (Kim and Chung, 1992). SNL animals develop similar pain-related behaviours to PNL with the advantage of allowing researchers to study injured and uninjured spinal segments.

Since neuropathy is a common complication in diabetes patients (Dyck et al., 1993), several animal models mimicking metabolic disease have been developed, including streptozotocin (STZ)-induced diabetic neuropathy. A single injection of STZ into the rat tail vein kills insulin secreting islet cells, inducing hyperglycemia and the development of thermal and mechanical hyperalgesia, as well as, mechanical allodynia (Forman et al., 1986;Aley et al., 2000). In the case of HIV/AIDS, peripheral neuropathy and neuropathic pain are frequently observed clinically and a novel mouse model has been developed to study the effects of a HIV viral accessory protein, Viral protein R (Vpr), on the peripheral nervous system (Acharjee et al., 2010). This animal model involves the expression of the *vpr* transgene in an immunodeficient ($RAG1^{-/-}$) background and

similar to human HIV infections, mice express Vpr in the DRGs and sciatic nerve along with exhibiting mechanical allodynia.

Taken together, there are several animal models aimed at mimicking particular behaviours or nervous system insults associated with human neuropathic pain conditions. As discussed earlier, some of the major challenges related to the use of animal models include assessing affective and cognitive components of the pain experience, as well as, identifying behavioural correlates for common human neuropathic pain symptoms, such as spontaneous pain. Further, interpretations made from animal nerve injury models should be considered in the context of gender, age and species studied. Last, it appears that no animal nerve injury model is without limitations, therefore, behavioural and physiological studies can only speculate on the relevance of findings to human neuropathic pain.

### *1.4.3 Enduring increase in primary afferent activity*

Peripheral nerve injury can result in spontaneous, ectopic discharge of primary afferents as seen both experimentally and clinically (Devor, 2009). Experiments using various nerve injury animal models suggest that an enduring increase in primary afferent activity originates both from the neuroma (Govrin-Lippmann and Devor, 1978), that develops at the site of nerve injury, and from sensory cell bodies in the DRG. For instance, damage to the rat sciatic nerve, through nerve sectioning, increased spontaneous, ectopic activity in primary afferent fibres (Wall and Devor, 1983) (Figure 1-3). Spontaneous activity in

myelinated fibres ceased upon further sectioning which uncoupled the DRG from the primary afferent fibres. Similar observations were made by Kajander and colleagues (1992) where all spontaneous discharge,1-3 days after CCI, orginated in the rat DRG (Kajander et al., 1992). Thus, recordings from intact preparations support a role for the DRG in neuropathic pain and several laboratories have, since, examined the effects of nerve injury on the electrical properties of isolated DRG neurons.

Two to seven weeks post axotomy increased DRG neuron excitability through reductions in the minimum current required to discharge an AP (rheobase) and a higher frequency of evoked AP discharge in response to sustained depolarizing current (Abdulla and Smith, 2001a) (Figure 1-3). There were also increases in AP height and width. Investigation under voltage-clamp conditions also support these findings, where AP regulatory mechanisms, such as HVA $Ca^{2+}$-channel current (HVA-$I_{Ba}$) and steady state (delayed rectifier) $K^+$ current ($I_K$) are attenuated (Abdulla and Smith, 2001b). In contrast, AP generating mechanisms, such as TTX–R and/or TTX-S $Na^+$ currents ($I_{NA}$), are increased (Abdulla and Smith, 2002). Further, alterations were most prevalent in the small sized (input capacitance) DRG neurons which are, presumably, nociceptive C- and Aδ-fibres. However, with the onset of autotomy (self mutilation), which is believed to be a behavioral manifestaion of human neuropathic pain, changes became most substantial in the large (Aβ) cell bodies (Abdulla and Smith, 2001a).

Other studies also reported changes in electrical properties of DRG neurons after nerve injury that are consistent with increased primary afferent

activity. For instance, intracellular recordings from DRG bulbs with attached dorsal root revealed that sacral 1 (S1) spinal nerve transection led to a significant reduction of the rheobase in A- and C-cell types (Kim et al., 1998). The reduction of rheobase in A-cells was associated with a concomitant increase in apparent input resistance near RMP. By contrast, the rheobase reduction in C-cells was associated with a depolarizing shift of the RMP. In addition, the nerve injury produced significant action potential broadening in all cell types. After a CCI injury, isolated small, medium and large sized DRG neurons showed an increased incidence of spontaneous AP activity which was associated with a negative shift in AP threshold (Study and Kral, 1996). In small-sized DRG neurons, axotomy nerve injury also reduced AP threshold without alterations to RMP or AP shape (Zhang et al., 1997). Despite differences in the experimental approach, similarities do exist, including reduced firing threshold or rheobase in, possibly, nociceptive, as well as, non-nociceptive sensory neurons.

In contrast to the findings reported by Abdulla and Smith (2002), Waxman and colleagues (1997) reported that axotomy injury resulted in the down regulation of TTX-R sodium current in small- and large-sized rat DRG neurons, leaving TTX-S sodium currents to make a greater proportion of the total sodium current in both cell populations (Everill et al., 2001;Cummins and Waxman, 1997). Similar observations were reported by Zhang and colleagues (1997) after an axotomy injury (Zhang et al., 1997). Further, the reduction in TTX-R sodium currents was paralleled by the emergence of a rapidly repriming TTX-S sodium current in small DRG neurons after axotomy. Rapidly repriming TTX-S current

permits neuronal firing at higher than normal frequencies (Cummins and Waxman, 1997;Cummins et al., 2001) and upregulation of its corresponding transcript, $Na_V1.3$, as well as, protein product have been observed in DRG neurons of adult rats after axotomy (Waxman et al., 1994;Dib-Hajj et al., 1996;Black et al., 1999), CCI (Dib-Hajj et al., 1999) and SNL (Kim et al., 2001). In contrast, transcripts encoding TTX-R sodium currents are down regulated in small DRG neurons following axotomy (Dib-Hajj et al., 1996;Dib-Hajj et al., 1998b). These alterations may, in part, be explained by a loss of target derived neurotrophic factors after peripheral nerve injuries. For instance, partial restoration of TTX-R currents, along with upregulation of alpha-SNS transcript, was reported after the administration of NGF to the proximal nerve stump (Dib-Hajj et al., 1998a). Further, intrathecal GDNF treatment prevented sensory hypersensitivity after SNL injury and was associated with block of A-fibre ectopic discharge and normalization of $Na_V1.3$ expression in injured DRG (Boucher et al., 2000). In addition to the emergence of rapidly-repriming TTX-S sodium currents, loss of target derived GDNF is associated with a reduction in TTX-R currents in small IB4-positive DRG neurons, whereas, loss of NGF is associated with a reduction in TTX-R currents in small peptidergic cells (Fjell et al., 1999). Taken together, it appears that nerve injury is commonly associated with a reduction in TTX-R sodium currents, allowing TTX-S currents to dominate as the major generators of AP upstroke and, possibly, spontaneous ectopic AP discharge in injured sensory neurons. However, $Na_V1.8$ upregulation, along with the presence of functional TTX-R sodium channels, have been associated with

abberrant activity in uninjured C-fibres and neuropathic pain behaviours after partial nerve injury (Gold et al., 2003). Therefore, the relevance of particular sodium channel isoforms to neuropathic pain may depend on the extent of nerve injury and, possibly, the degree of associated inflammation.

In large cutaneous afferent DRG neurons, a sustained potassium current component, as well as, the transient current, $I_A$, but not $I_D$ were reduced after axotomy (Everill and Kocsis, 1999). Compared to contralateral controls, mRNA expression for genes which encode delayed rectifier ($K_V$ 1.1 and 1.2) and A-type ($K_V$ 1.4, 2.2, 4.2, and 4.3) voltage-gated potassium channels were reduced in ipsilateral lumbar 4,5 and 6 DRG one week following CCI (Kim et al., 2002). Unlike changes in $I_{K,Ca}$ after axotomy (Abdulla and Smith, 2001b), L5 SNL decreased $I_{K,Ca}$ due to a direct effect on $I_{K,Ca}$ channels (Sarantopoulos et al., 2007). Though all $I_{K,Ca}$ subtypes were decreased in small- and medium-sized DRG neurons from the injured nerve, medium-sized DRG neurons from the adjacent uninjured L4 nerve had increased iberiotoxin sensitive (large conductance) and clotrimazole sensitive (intermediate conductance) $I_{K,Ca}$. In injured human peripheral nerves, there was a decrease in human intermediate conductance calcium-activated potassium channel 1 (hIK1)-like immunoreactivity predominately in large-, but also, in medium- and small-sized DRG neurons when compared to controls (Boettger et al., 2002). Like sodium channels, these changes are attributed to a decrease in retrograde transport of neurotrophic factors in injured sensory neurons. Taken together, it appears that nerve injury promotes a reduction in sustained and/or A-type potassium currents which could account for

broadening of APs, as well as, contributing to sensory neuron hyperexcitability through a reduction in spike adaptation. Further, a reduction in $I_{K,\ Ca}$, whether directly or secondary to reductions in HVA calcium currents (see below) serves as an additional ionic mechanism for AP broadening and aberrant activity in sensory neurons after peripheral nerve injury.

Two weeks after axotomy, the density of omega-conotoxin GVIA-sensitive (N-type) calcium current decreased and was concurrent with a depolarizing shift in the voltage dependence of inactivation and faster inactivation kinetics in large-sized DRG neurons associated with cutaneous afferents (Baccei and Kocsis, 2000). T-type current percent distribution was unaffected. On the other hand, in small-sized rat DRG neurons, T-type calcium current density was increased, without changes in voltage- and time-dependent parameters following CCI (Jagodic et al., 2008). Onset of diabetic neuropathy was also associated with increased T-type, but not HVA, current density with a depolarizing shift in steady-state inactivation in IB4-positive, capsaicin responsive medium-sized rat DRG neurons (Jagodic et al., 2007). Although the changes in calcium current are variable and likely depend on the nerve injury model and DRG neuron-type studied, alterations are consistent with increased excitability of sensory neurons. For instance, the reduction in HVA or N-type calcium current could underlie decreased calcium-dependent potassium current after injury (Abdulla and Smith, 2001b) which, in turn, would be expected to decrease amplitude and shorten AHP duration, ultimately, increasing firing frequency (Titmus and Faber, 1990). In contrast, the increase in T-type current has been correlated closely to more

prominent afterdepolarizing potentials (ADP), as well as, a lowered RB for AP firing (Jagodic et al., 2007).

More recently, the role of the pacemaker current ($I_H$) in neuropathic pain has been examined since $I_H$ acts to induce a depolarization after a hyperpolarizing event and, if upregulated after nerve injury, may contribute to enhanced neuronal excitability. Chronic compression of the DRG (CCD) can be achieved by the insertion of L-shaped rods into the intervertebral foramina, producing cutaneous hyperalgesia and enhancing excitability of neuronal somata in the compressed ganglion (Yao et al., 2003). Compared with control, CCD increased $I_H$ current density and rate of activation, without changing its reversal potential, voltage dependence of activation, or rate of deactivation in medium-sized rat DRG neurons associated with cutaneous afferents (Yao et al., 2003). Further, SNL injury markedly increased pacemaker currents in large-diameter DRG cells (Chaplan et al., 2003). *Ex vivo* recording of single spontaneously active units demonstrated the presence of pacemaker-driven spontaneous action potentials in the ligated nerve as indicated by decreased firing frequency of ectopic discharges originating in Aβ- and Aδ-fibers and concurrent reversal of mechanical allodynia after pharmacological blockade with ZD7288. The increase in $I_H$ appears to contrast with the results obtained in our lab after axotomy (Abdulla and Smith, 2001a) as indicated by decreased time-dependent rectification (TDR) or voltage-sag in response to hyperpolarizing current pulses. One possibility is that HCN channel protein accumulates in axons rather than in DRG cell bodies, such as that reported after CCI (Jiang et al., 2008). In this CCI study, the function of

accumulated channels was verified by local application of ZD7288 which suppressed the ectopic discharges from injured nerve fibres and relieved mechanical allodynia, but not thermal hyperalgesia. Despite some discrepancies, increases in $I_H$ maybe of relevance in particular nerve injuries, involving alterations in larger primary afferents and the associated development of mechanical allodynia.

### *1.4.4 Central sensitization*

In 1983, Clifford Woolf's study of injury induced changes to the cutaneous receptive field properties of flexor motor neurons in rat provided the first pieces of evidence for spinal cord plasticity and central sensitization (Woolf, 1983). Essentially, repeated noxious heat stimuli presented to the paw produced a sustained increase in the excitability of the flexion reflex which was characterized by: Aβ–fibre recruitment to the, normally, nociceptor specific reflex; enlargement of the receptive field which was unresponsive to local anaesthetics applied to the site of injury; and, all of which, could be mimicked by C-fibre strength electrical stimulations of the sural nerve. Since these characteristics were difficult to explain within the context of a peripherally driven mechanism, such as in nociceptive pain, a central process was conceived. It is now appreciated that central sensitization is a form of nervous system plasticity composed of increases in membrane excitability (Dalal et al., 1999), synaptic facilitation (Woolf and Thompson, 1991;Garraway et al., 2003), loss of inhibition (Baba et al., 2003) and reversal of inhibition (disinhibition) (Coull et al., 2003) of central circuitry which

promotes spontaneous pain, allodynia and hyperalgesia after inflammation or lesions to the nervous system (Latremoliere and Woolf, 2009) (Figure 1-3). The net effect is the recruitment of previously subthreshold inputs from low-threshold receptors and high-threshold receptors from outside a given receptive field to the output of central nociceptive neurons. These inputs can be experimentally revealed in the spinal cord after the administration of synaptic blockers of inhibitory transmission, such as $GABA_A$ receptor antagonists, which result in Aβ input into the superficial dorsal horn (Baba et al., 2003) and pain-like responses elicited by the movement of hairs (Sivilotti and Woolf, 1994). This heightened pain response is protective when maintained by peripheral mechanisms responding to inflammatory cues which subside over the course of healing. A major feature of neuropathic pain, however, is that it is a manifestation of plasticity in the nervous system where changes to the nociceptive pathway, enabling central sensitization, do not return to pre-injury status (Costigan et al., 2009). Therefore, the somatosensory system is left in a persistent state where it can no longer distinguish innocuous information from nociceptive information.

In the context of neuropathic pain, the mechanisms responsible for the establishment and maintenance of central sensitization remain poorly understood. What seems clear is that multiple mechanisms are involved after nerve injury to increase excitability and reduce inhibition (Latremoliere and Woolf, 2009). In our laboratory, we have demonstrated that 13-25 days of sciatic nerve CCI produces changes in the synaptic excitation of SG neurons, where there is a decrease in excitatory synaptic drive to tonic cells and an increase in excitatory

synaptic drive to SG neurons exhibiting other discharge patterns, including delay cells (Balasubramanyan et al., 2006). It was suggested that these changes, which were concurrent with the onset of mechanical allodynia and hyperalgesia, relate to the putative roles of tonic- and delay cells as inhibitory GABAergic interneurons and excitatory output neurons of the SG, respectively. One of the early consequences of CCI is the activation of spinal microglia and the release of BDNF (Coull et al., 2005). Since nervous system injury is associated with elevated levels of BDNF (Dougherty et al., 2000) and neuropathic pain-related behaviours are attenuated by sequestering BDNF (Coull et al., 2005), BDNF has become a molecule of interest in nerve injury related central sensitization. Our lab demonstrated that spinal cord cultures exposed to 5-6 days of BDNF produced a similar 'electrophysiological signature' to that seen with CCI (Lu et al., 2007) and that activated microglia enhanced overall dorsal horn excitability, as indicated by measurements of cytosolic $Ca^{2+}$ in response to high $K^{+}$ challenge, was BDNF mediated (Lu et al., 2009). Microglia derived BDNF has also been shown to mediate nerve injury induced disinhibition through causing the collapse of the transmembrane anion gradient and compromising control over firing rate in LI neurons (Coull et al., 2005;Prescott et al., 2006). In addition to reducing inhibitory tone in the dorsal horn, BDNF release has been associated with the enhancement of N-methyl-d-aspartate (NMDA) receptor mediated depolarizations in the rat spinal cord (Kerr et al., 1999) as well as the enhancement of NMDA receptor mediated excitatory post synaptic currents (epscs) in LII dorsal horn neurons (Garraway et al., 2003). It was further demonstrated that ATP and its

release from damaged cells can activate microglia and, through $P2X_4$ purinergic receptor ($P2X_4R$) stimulation, promotes the release of BDNF (Ulmann et al., 2008).

Taken together, it is possible that peripheral nerve injury causes sufficient release of ATP to activate microglia, triggering the release of BDNF which promotes an increase in superficial dorsal horn excitability through a functional loss of inhibitory circuits and enhancement of synaptic strength at excitatory synapses. BDNF is, however, only one piece to a very complicated puzzle and several studies have described contributions of other molecules, cell types and processes to the establishment and maintenance of central sensitization after nerve injury (Costigan et al., 2009;Latremoliere and Woolf, 2009).

### *1.5 Nerve Injury*

Ectopic discharge in primary afferents is secondary to direct axonal damage and disruption of the myelin sheath that surrounds many axons. Cutting an axon, results in degeneration of the distal segment as a consequence of interruption in axonal flow and transport which deprives the distal axon and nerve ending of its normal metabolic interaction with the cell body. Wallerian degeneration leads to loss of the distal axonal segment and involves responses from glial cells, immune cells, in addition to peripheral nerves. The proximal portion of damaged primary afferents can undergo phenotypic switch in response to retrograde loss of target-derived trophic factors. However, the electrical behaviour of, both, injured and uninjured nerve fibres is altered in response to

injury (Gold et al., 2003;Ma et al., 2003). In parallel, the chemical environment is changed and several mediators are known to interact with sensory neurons. Alterations in sensory neuron phenotype and electrical activity likely contribute to central sensitization and neuropathic pain.

*1.5.1 Nerve degeneration*

Nerve degeneration is not limited to nerve transections, but exists in other models of nerve injury (Mosconi and Kruger, 1996), as well as, in disease states and infections (Jones et al., 2007;Acharjee et al., 2010). In the case of axotomy, the proximal axonal segment and attached cell body becomes isolated from the distal segment (Kelley, 1985). Cytoplasmic materials build up as the ends of both segments become sealed, forming swollen retraction bulbs. In a process known as Wallerian degeneration, the distal axon swells and becomes a series of beaded fragments. Cellular debris from the terminal and distal axon is then cleared by phagocytic cells, such as macrophages. Although variable among species, Wallerian degeneration in rodent models of peripheral nerve injury occurs within a few days following injury (Tsao et al., 1999;Luttges et al., 1976;Perrin et al., 2005). In contrast, the proximal segment is spared since it is still metabolically coupled to the surviving cell body. During degeneration, retrograde signals produce changes in the cell body and include swelling, eccentric positioning of the nucleus and the breaking apart of rough endoplasmic reticulum (chromatolysis) (Wells and Vaidya, 1989). These changes are associated with the massive production of protein required for nerve regeneration and cease once

connections are restored. If the cell body dies, the degenerative process spreads to the remaining proximal segment. Thus, nerve degeneration occurs over several days, affects the entire neuron and involves several cell types.

*1.5.2 Inflammation*

Injury to the peripheral nerve results in a local inflammatory response characterized by the activation of resident cells, such as mast cells and macrophages, supportive Schwann cells along the axon and satellite cells in the DRG (Sorkin and Schafers, 2007;Scholz and Woolf, 2007). In addition, the inflammatory response is augmented by the infiltration of circulating phagocytes (macrophages and neutrophils), T-lymphocytes and natural killer cells which contribute to the removal of cellular debris, neutralization of pathogens, regeneration of axons and formation of a neuroma (Xie et al., 2006;Scholz and Woolf, 2007). Corresponding to these events, an 'inflammatory soup' of bradykinins, substance P, hydrogen ions, NGF, prostaglandins, histamine, ATP and proinflammatory cytokines is produced (Irving, 2005).

Several lines of evidence underline the importance of the local inflammatory response in the generation of centralized pain. For instance, cardinal signs of inflammation, such as the presence of edema and build-up of intraneurial pressure, correlates more strongly with nocifensive behaviours than the extent of fibre loss after fixed-diameter polyethylene cuff nerve injury (Mosconi and Kruger, 1996). Encasing the nerve stump after sciatic nerve transection, in order to minimize contact with infiltrating immune cells and inflammatory mediators,

attenuates pain-related behaviours, such as autotomy (Okuda et al., 2006). The local response of early inflammatory cellular mediators, including the degranulation of mast cells and the accumulation of neutrophils, is important in the generation of hyperalgesia after partial nerve injuries (Zuo et al., 2003;Perkins and Tracey, 2000). Cui and colleagues (2000) demonstrated a strong correlation between degree of local macrophage/monocyte infiltration among three nerve injury models and the presence of mechanical allodynia. Lastly, peripheral nerve injuries such as CCI are associated with an inflammatory response of higher magnitiude than sciatic nerve transections (Cui et al., 2000) and invoke downregulation of GABAergic functions in the superficial dorsal horn while axotomy is ineffective (Moore et al., 2002).

Several inflammatory mediators released from cells and damaged tissue alter the electrical properties of sensory neurons. For instance, hydrogen ions and ATP act through the non-selective cation channels TRPV1, ASICs and P2X to depolarize sensory neurons towards AP threshold (Chen et al., 1995;Chen et al., 1998;Tominaga et al., 1998). *In vivo* administration of SP to glabrous skin produces hyperalgesia and allodynia (Nakamura-Craig and Gill, 1991;Carlton et al., 1996). Further, SP release depolarizes and excites small nociceptive sensory neurons (Abdulla et al., 2001;Dray and Pinnock, 1982) which express the SP receptor, neurokinin-1(NK1) (Li and Zhao, 1998). Excitation of peptidergic fibres, not only leads to neuropeptide release centrally, but antidromic propagation of APs can also result in peripheral release and further exacerbate inflammation (neurogenic inflammation) (Yonehara and Yoshimura,

2001;Richardson and Vasko, 2002). In support, NK-1 receptor antagonists applied either centrally (Cahill and Coderre, 2002;Lee and Kim, 2007) or peripherally (Jang et al., 2004), attenuate or delay the onset of pain-related behaviours in response to nerve injury.

The involvement of NGF in inflammatory pain is well documented, however, NGF expression is upregulated in several cell types, including DRG neurons (Herzberg et al., 1997), Schwann cells (Scholz and Woolf, 2007) and satellite cells (Zhou et al., 1999) after nerve injury. Consistent with a role in nerve injury and, perhaps, neuropathic pain, NGF antagonism, with anti-serum application at the site of nerve injury, attenuated or delayed the onset of hyperalgesia after CCI (Herzberg et al., 1997;Ro et al., 1999). NGF release can enhance excitability of primary afferents in several ways, including an increase in TRPV1 activity (Chuang et al., 2001), sensitivity (Shu and Mendell, 2001) and expression (Ji et al., 2002). In addition to the maintenance of TTX-R sodium currents ($Na_v1.8$) through trk receptors (Fjell et al., 1999), NGF signalling through the p75 neurotrophin receptor, can increase AP firing and is concurrent with an enhancement of TTX-R sodium current and a suppression of delayed rectifier-like potassium current (Zhang et al., 2008).

Proteases, such as trypsin, activate tethered-ligand protease-activated receptors 2 (PAR-2), a novel class of G-protein coupled receptors (GPCR), expressed on small-sized nociceptive DRG neurons (Amadesi et al., 2004) and PAR-2 activation reduces M-current which results in membrane depolarization and the generation of APs (Linley et al., 2008;Alier et al., 2008). In *in vivo*

studies, injection of PAR-2 agonists induces pain-related behaviours (Vergnolle et al., 2001), whereas, antagonists produce antinociceptive effects (Cenac et al., 2007). Similar to the activation of metabotropic P2Y purinergic receptors (Tominaga et al., 2001;Kress and Guenther, 1999) and bradykinin-2 (B2) receptors (Cesare and McNaughton, 1996), PAR-2 activation sensitizes TRP channels which is associated with hyperalgesia (Amadesi et al., 2004;Dai et al., 2007).

The association of eicosanoids and their synthesizing enzymes, cyclo-oxygenase- 1 (COX-1) and particularly the inducible COX-2, with inflammation and pain is well documented (Salmon and Higgs, 1987;Kiefer and Dannhardt, 2005). For instance, prostaglandin $E_2$ ($PGE_2$) or prostaglandin $I_2$ ($PGI_2$; prostacyclin) administration induces hyperalgesia (Ferreira et al., 1978;Higgs et al., 1978). Further, $PGI_2$ and $PGE_2$ enhance the sensitivity of primary afferents to either mechanical or chemical stimulation (Schepelmann et al., 1992;Birrell et al., 1991;Devor et al., 1992). $PGE_2$ and $PGI_2$ receptors (EP and IP, respectively) are expressed in sensory neurons (Oida et al., 1995;Sugimoto et al., 1994;Matsumura et al., 1995) and *in vitro* application of $PGE_2$ or $PGI_2$ on DRG neurons lowers firing threshold (Schaible and schmidt, 1988) and increases AP firing upon current injection, elevated potassium or bradykinin application (Nicol and Cui, 1994;Nicol et al., 1997). Consistent with hyperexcitability, $PGE_2$ and a $PGI_2$ analogue suppress a sustained-type potassium current (Nicol et al., 1997) and, similar to serotonin, prostaglandins upregulate TTX-R sodium currents (Gold et al., 1996a). In addition, $I_H$ is positively modulated by $PGE_2$ in trigeminal ganglion

neurons (Ingram and Williams, 1996). Through a receptor mediated mechanism of action, $PGE_2$ and $PGI_2$ also sensitize TRPV1 channels, producing hyperalgesia in mice (Moriyama et al., 2005). Last, it has also been suggested that hyperalgesia induced by bradykinin, norepinephrine and cytokines is secondary to the production of prostaglandins (Taiwo and Levine, 1988).

*1.5.3 Phenotypic switch*

After nerve injury, there are also several neuropeptide and neurotrophin related changes relevant to sensory neurons. Though CGRP and SP expression is largely regarded to be downregulated in injured sensory neurons (Sommer and Myers, 1995;Marchand et al., 1994), respective receptor antagonists applied either centrally (Cahill and Coderre, 2002;Lee and Kim, 2007;Bennett et al., 2000) or peripherally (Jang et al., 2004), attenuate or delay the onset of pain-related behaviours in response to nerve injury. This apparent paradox may be explained by phentoypic shifts and / or contributions from uninjured sensory neurons after nerve injury. For instance, some nerve injuries (Baranowski et al., 1993) result in a reversed pattern (phenotypic shift) where large, rather than small, sensory neurons begin to express (Noguchi et al., 1994;Noguchi et al., 1995) and become responsive to SP (Abdulla et al., 2001). Another example of phenotypic switch pertains to BDNF. Under normal circumstances, BDNF mRNA and protein is expressed in nociceptive sensory neurons (Michael et al., 1997), however, BDNF becomes upregulated in large-diameter DRG neurons and is concurrent with increased anterograde transport to the dorsal horn after sciatic axotomy (Tonra et

al., 1998). Phenotypic shift in sensory neurons is likely to alter the efficacy of their synaptic input into the spinal cord (Scholz and Woolf, 2007).

### *1.5.4 Summary*

Taken together, there is strong evidence linking the inflammatory milieu after nerve injury with changes in the electrical activity of sensory neurons and pain-related behaviours. Coupled to this, a phenotypic switch may drive changes in the dorsal horn unique to nerve injury. The net effect is that primary afferents send volleys of spontaneous, ectopic discharge to the dorsal horn which can then trigger central sensitization. Last, an association between enduring increases in primary afferent activity after peripheral nerve injury and neuropathic pain has been established, however, the role of inflammatory mediators in this process remains to be elucidated.

## ***1.6 Cytokines***

Cytokines are a diverse group of small proteins that are critical for communication between cells and, therefore, help to coordinate the inflammatory/immune response (Morales and Gereau IV, 2007). Cytokines not only influence the local environment produced after inflammation or injury, but have actions that modify systemic functions, including appetite, slow-wave sleep, body temperature and neuroendocrine function. Many of these systemic responses, such as the resetting in set-point of hypothalamic thermoregulation to induce fever, contribute to host defense during infection (Vitkovic et al.,

2000;Kluger et al., 1998). Cytokines can be broadly classified as pro- or anti-inflammatory depending on their effects on immune cells, such as lymphocytes (Schafers et al., 2007). Chemokines or chemotactic cytokines are an additional family of cytokines that are characterized by their ability to stimulate chemotaxis in non-excitable cells, including leukocytes (White et al., 2007). Though cytokines and chemokines are necessary for the course of recovery after injury, both are implicated in the production of pain-related behaviours.

### *1.6.1 Adaptation*

Cytokines and chemokines are involved in the orchestration of events following peripheral nerve injury which permit nerve regeneration. For instance, chemokine (Cysteine-X-Cysteine motif) ligand 1 (CXCL1) are thought to attract neutrophils to the site of injury in the very early events of the immune response (Scholz and Woolf, 2007), while chemokine ( C-C motif) ligands 2 and 3 (CCL2 and CCL3) are responsible for the activation of resident macrophages and the infiltration of monocytes from the blood (Perrin et al., 2005). Activated macrophages secrete several pro-inflammatory mediators, including the cytokines: interleukin-1β (IL-1β) and IL-6, interferon-γ, leukemia inhibitory factor (LIF) and tumor necrosis factor-α (TNF-α) (Tofaris et al., 2002). TNF-α mediated signalling stimulates the autocrine synthesis and release of cytokines from macrophages, as well as, reinforcing the infiltration of macrophages by inducing the release of proteases and the upregulation of adhesion molecules (Scholz and Woolf, 2007). IL-1 (subtype unspecified) induces the synthesis and

release of NGF from Schwann cells (Lindholm et al., 1987) which can act retrogradely in injured sensory neuron cell bodies to promote expression of genes necessary for axonal growth and remyelination (Esper and Loeb, 2004). Immune responses at the site of injury generally cease with the removal of myelin debris during Wallerian degeneration.

In addition to the site of nerve injury, T lymphocytes and macrophages can be attracted to the DRG through the release of chemokines, such as soluble-fractalkine and CCL2, from sensory neurons and satellite glia (McLachlan and Hu, 2007). A large proportion of the macrophages in the DRG become phagocytic and are thought to clear cellular debris associated with the death of injured sensory neurons (Hu and McLachlan, 2003). In certain nerve injuries, such as L5 SNL, the inflammatory response can trigger invasion of macrophages and lymphocytes into uninjured L4 DRG (Hu and McLachlan, 2002). Further, the release of pro-inflammatory cytokines from infiltrating macrophages promotes sympathetic nerve sprouting and alterations to sensory neurons, including the expression of neuropeptide transmitters and development of spontaneous ectopic discharge (Scholz and Woolf, 2007). The immune response in the DRG, characterized by the accumulation of macrophages immunoreactive for major histocompatibility factor II (MHC II) around injured sensory neuron cell bodies, can persist for several weeks to months after nerve injury (Hu and McLachlan, 2003). Therefore, cytokines and chemokines are involved in various stages following nerve injury and it is expected that at least some remain present until nerve regeneration is complete.

*1.6.2 Maladaptation*

There is mounting evidence that the inflammatory response, intrinsic to Wallerian degeneration, is important in the establishment of neuropathic pain. For instance, mutant C57BL/6/Ola mice have delayed Wallerian degeneration (Lunn et al., 1989). After nerve injury, these mice have reduced pain-related behaviours concurrent with a delayed immune response characterized by a decreased upregulation of TNF-α and IL-1β in macrophages and Schwann cells (Sommer and Schafers, 1998). In other studies, intraplantar administration of pro-inflammatory cytokines, such as TNF-α or IL-1β, induces mechanical and/or thermal hyperalgesia (Ferreira et al., 1988;Cunha et al., 1992;Sachs et al., 2002). In addition, direct application of IL-1β or TNF-α to the DRG or sciatic nerve results in mechanical allodynia (Zelenka et al., 2005;Homma et al., 2002;Schafers et al., 2003). Further, interruption of IL-1β and/or TNF-α biological activity attenuates pain-related behaviours after nerve injury (Sweitzer et al., 2001;Lindenlaub et al., 2000;Sommer et al., 2001;Sommer et al., 1999;Wolf et al., 2006). Blocking TNF-α production in monocytes with thalidomide, prevented hypersensitivity associated with inflammation in uninjured L4 and L5 DRG after L5 ventral root transection, indicating that the cytokine response, and not necessarily direct axonal damage, is involved in pain-related behaviours after nerve injury (Xu et al., 2006). Last, IL-6 knock-out mice have delayed mechanical allodynia after L5 SNL which was associated with reduced sympathetic sprouting to the DRG, suggesting cytokines can induce sympathetic-sensory coupling and sympathetic-dependent pain after nerve injury (Ramer et al., 1998). Collectively,

these observations suggest an important role for particular pro-inflammatory cytokines in the development neuropathic pain.

Although it would be reasonable to study the actions of any major pro-inflammatory cytokine, such as TNF-α or IL-6, the remainder of my thesis will focus on the cellular effects of IL-1β in sensory neurons. My choice is supported by several recent observations (discussed below) which implicate direct involvement of IL-1β in the enduring increase in sensory neuron excitability commonly observed after peripheral nerve injury. Since changes in injured sensory neurons may lead to central sensitization, IL-1β may be of particular importance in the establishment of neuropathic pain.

### *1.7 IL-1beta*

The IL-1 superfamily of pleiotropic cytokines is evolutionarily conserved in vertebrates and includes the cytokines: IL-1α, IL-1β and IL-18 (Allan et al., 2005). Recently, a number of other proteins show similarity to this cytokine group and there are now at least ten known members. The IL-1 family is an important part of the innate immune system, playing an important role in host defence against microorganisms that divide inside cells, such as mycobacteria or listeria (Braddock and Quinn, 2004). IL-1α and IL-1β were the first members of the IL-1 family to be identified (March et al., 1985) and have since been the most extensively characterized members of the IL-1 family. The family also contains an endogenous IL-1 receptor antagonist (IL-1Ra) that inhibits IL-1 actions mediated by type I IL-1 receptor (IL-1RI). IL-1α and IL-1β are highly potent,

eliciting biological effects in the $10^{-14}$ to $10^{-13}$ M range (Orencole and Dinarello, 1989). Although IL-1α and IL-1β are products of two different genes, they have high sequence homology and exert similar biological effects, however, IL-1β is more potent in activating humoral immune responses (Nakae et al., 2001). Furthermore, of the two agonists, IL-1β is the major secretory form and is known to have neurotoxic actions (Allan and Rothwell, 2001).

### *1.7.1 IL-1β production*

IL-1β is synthesized as a large precursor protein (pro-IL-1β) by various cells of the peripheral and central immune system, such as lymphocytes and monocytes (Allan et al., 2005). Under physiological conditions IL-1β protein is expressed at very low levels (<5 pg/mL), however, in response to infection or injury, its expression is rapidly upregulated to the ng/mL range in serum (Dinarello, 2005) and in tissue (Kawasaki et al., 2008;Xie et al., 2006). The production and secretion of mature, biologically active IL-1β protein is a two step process. At the transcriptional level, gene expression of IL-1β can be induced by various pro-inflammatory stimuli, including microbial products, other pro-inflammatory cytokines (such as TNF), cellular injury and hypoxia (Hsu and Wen, 2002;Perregaux et al., 2002). Even IL-1β, itself, is a potent stimulator of its own gene expression (Schindler et al., 1990). These inflammatory cues signal transcription through the recruitment of various factors that recognize and bind DNA regulatory regions, such as the cyclic AMP response element, the activator protein-1 (AP1) binding site, the NF-κB binding site and the lipopolysaccharide

(LPS)-response enhancer site (Takeuchi and Akira, 2010;Auron and Webb, 1994). Suppressors of IL-1 transcription include glucocorticoids and their anti-inflammatory mediator, annexin-1 (also known as lipocortin-1) (Perretti and D'Acquisto, 2009), as well as, the anti-inflammatory cytokines, such as IL-4, IL-10 and IL-13 (Dinarello, 2000).

At the post-translational level, pro-IL-1β (31 kDa) in the cytosol is biologically inactive and, therefore, the regulation of cellular release is another control point for changes in IL-1β levels (Dinarello, 2005). Cytosolic pro-IL-1β moves into specialized secretory lysosomes where it co-localizes with pro-caspase-1, an intracellular cysteine protease. The next step involves the processing of pro-caspase-1 into caspase-1 (also known as IL-1β converting enzyme (ICE)) *via* a protein complex termed the 'IL-1β inflammasome' (Martinon et al., 2007). A number of molecules, indicative of injury or infection, can activate inflammasomes, including ATP release from damaged tissue (Schroder and Tschopp, 2010). ATP binds the P2X7 ligand gated ion channel which allows an efflux of potassium and, through a series of events that remain uncertain (Schroder and Tschopp, 2010), leads to the cleavage of pro-IL-1β and subsequent cellular release of mature IL-1β (Petrilli et al., 2007).

The two-step process described above appears to be highly coordinated. For example, treatment of microglial cells or macrophages with LPS induces expression of pro-IL-1β, but not cleavage or release. In LPS-primed macrophages, however, activation of $P2X_7$ by ATP or ADP elicits both cleavage and release of IL-1β via caspase-1 (Le Feuvre et al., 2002). On the other hand,

caspase-1 activation is not the only mechanism leading to the processing of pro-IL-1β into its mature form. For instance, pro-IL-1β can also be processed through neutrophil derived serine proteases, such as proteinase-3 (Coeshott et al., 1999). Last, in local inflammatory reactions, precursor IL-1β can be released then processed into biologically active IL-1β by a variety of extracellular proteases found in the inflammatory milieu, including the matrix metalloproteases (MMP) - 2, 3 and 9 (Schonbeck et al., 1998;Kawasaki et al., 2008).

### *1.7.2 IL-1β signalling*

The members of the IL-1 family all bind membrane bound IL-1RI with similar affinities. As opposed to IL-1Ra, IL-1β binding to IL-1RI leads to the formation of a heterodimer with IL-1 receptor accessory protein (IL-1RAcP) (Greenfeder et al., 1995). IL-1RI and IL-1RAcP belong to the Toll-like receptor (TLR) superfamily which plays a key role in the immune response (Dunne and O'Neill, 2003). These related receptors all have sequence similarity in their cytosolic regions that contains amino acids related to those found in a gene (Toll) required for embryonic development of *Drosophilia* (Gay and Keith, 1991). This conserved region has been termed the Toll-IL-1 receptor (TIR) domain (Dinarelllo, 2010). The formation of a heterodimer between IL-1RI and IL-1RAcP results in the physical approximation of the TIR domains which triggers a complex series of signalling events in the target cell.

Signalling is characterized by the recruitment of several adaptor proteins and downstream kinases, including myeloid differentiation protein (MyD88), IL-

1RI receptor-associated kinase (IRAK),TNF receptor-associated factor-6 (TRAF6) and transforming growth factor β – activated kinase-1(Tak1) that results in the activation of the transcription factor, nuclear factor-κB (NF-κB), as well, as the stress-related mitogen activated protein kinases (MAPKs) (Andre et al., 2006;Ninomiya-Tsuji et al., 1999;Landstrom, 2010). This is followed by transcription of multiple inflammation-associated genes, including those that encode type II phospholipase $A_2$ ($PLA_2$(II)); cyclo-oxygenase-2 (COX-2); inducible NO synthase (iNOS); chemokines, such as fractalkine; cytokines, such as IL-6 and TNF; and adhesion molecules, such as endothelial-cell selectin (E-selectin) and intracellular adhesion molecule-1 (ICAM1) (Subramaniam et al., 2004;Dinarello, 2000). The IL-1β receptor signalling pathway is versatile and can also lead to the activation of many other cascades such as the tyrosine kinase / PKC and phosphatidyl inositol-3 kinase (PI3K) / Akt pathways which are also relevant to neuropathic pain (Diem et al., 2003;Roux et al., 2005;Obreja et al., 2002;Funakoshi et al., 2001;Zhuang et al., 2006).

In addition to the endogenous receptor antagonist IL-1Ra, IL-1 receptors can regulate the inflammatory effects of IL-1β. For instance, the type II IL-1 receptor (IL-1RII) has a short cytosolic domain and, therefore, it is believed to serve as a decoy receptor, competing with IL-1RI for binding of IL-1(Allan et al., 2005). Last, all three IL-1 receptors can be shed from cell membranes where soluble IL-1RI (sIL-1RI), sIL-1RII and sIL-1RAcP are thought to interefere with IL-1β signalling, thereby, further restricting the effects of IL-1β on target cells (Allan et al., 2005).

*1.7.3 IL-1β influence on electrical membrane properties of sensory neurons*

The pain-related behaviours produced by peripheral administration of IL-1β suggest that primary afferent fibres have become hypersensitive. Consistent with this hypothesis, *in vivo* recordings from DRG revealed that intraplantar injections of IL-1β led to increased spontaneous discharge, as well as, elevated discharge rate and lowered firing thresholds in response to polymodal receptor activation (Fukuoka et al., 1994). In another study, IL-1β application was followed by an increase in myelinated fibre spontaneous discharge rate and a decrease in mechanical threshold (Ozaktay et al., 2006). There are several ways IL-1β can modulate sensory neuron electrical behaviour, including effects secondary to the production of other inflammatory mediators. For example, Inoue and colleagues (1999) demonstrated that IL-1β mediated release of SP in DRG sensory neuron cultures required the upregulation of COX-2, suggesting that the pro-inflammatory effects of IL-1β, including hypersensitivity, require the production of prostaglandins (Inoue et al., 1999). In support, hyperalgesia after intraplantar injection of IL-1β could be attenuated by indomethacin pretreatment (Ferreira et al., 1988).

More recently, it was determined that IL-1RI mRNA is expressed in most sensory neurons (Copray et al., 2001), as well as, protein expression on the somata of small and larger sized neurons (Liu et al., 2006;Binshtok et al., 2008). This implies that IL-1β can directly affect primary afferents. Coupled to this, many of the hypersensitive responses occur within minutes after *in vivo* IL-1β application, suggesting fast (transcription-independent) receptor signalling is

involved (Fukuoka et al., 1994;Ozaktay et al., 2006;Tadano et al., 1999). In agreement, *in vitro* whole-cell recordings have revealed changes in the electrical properties of sensory neurons consistent with hyperexcitability after acute IL-1β applications. After 30 seconds of IL-1β (1 nM), Takeda and colleagues (2007) reported that small-sized trigeminal ganglion neurons became depolarized with decreased input resistance and displayed increased firing frequency in response to depolarizing current pulses (Takeda et al., 2007). These effects were IL-1RI dependent since they were attenuated in the presence IL-1Ra and were concurrent with a reduction in transient and sustained potassium current components (Takeda et al., 2008;Takeda et al., 2007). Similar increases in excitability were reported in small-sized DRG neurons after 10 minute applications of IL-1β (0.6 nM) (Binshtok et al., 2008). The authors further demonstrated that IL-1β acts in a p38 mitogen-activated protein kinase (p38 MAP kinase)-dependent manner to shift the voltage-dependency of slow-inactivation and activation of TTX-R sodium channels which augment sodium currents that determine AP threshold and upstroke. Last, a 90 second IL-1β (1 nM) incubation potentiated noxious heat-evoked currents in small-sized DRG neurons and involved the IL-1RI-tyrosine kinase-PKC pathway (Obreja et al., 2002). Taken together, sensory neurons can directly detect the acute presence of inflammatory mediators, such as IL-1β, with alterations in ionic currents that are consistent with increased cell excitability and the development of pain-related behaviours.

*1.7.4 IL-1β relevance to neuropathic pain*

IL-1β is produced and secreted under neuropathic pain states and, consequently, has been an intensly investigated pro-inflammatory cytokine (Sommer and Kress, 2004). For instance, IL-1 activity in mouse peripheral nerve, as assessed by stimulation of thymocyte proliferation, was increased within hours following nerve lesion and one week thereafter (Rotshenker et al., 1992). Centrally, immunoreactivity for IL-1β protein in LI dorsal horn was increased for several weeks and paralled the development of mechanical allodynia, following a freeze lesion of the sciatic nerve (sciatic cryoneurolysis) (DeLeo et al., 1997). IL-1β mRNA expression was upregulated in spinal cord tissue beginning one week after L5 SNL (Winkelstein et al., 2001). In another L5 SNL study, time-dependent upregulation of MMP-9 and MMP-2 characterized early- and late-phase development of neuropathic pain-related behaviours, respectively (Kawasaki et al., 2008). The investigators concluded that MMP-9 induces neuropathic pain-related behaviours through IL-1β processing and activation of microglia at early times (1-3 days), whereas, MMP-2 maintains neuropathic pain-related behaviours through IL-1β processing and astrocyte activation at later times (>7days) after nerve injury. Neuropathic pain-related behaviours, such as mechanical allodynia, could be reversed by a single dose of IL-1β receptor antagonist, IL-1Ra, 4 days after peripheral nerve injury (Gabay et al., 2010). Lastly, IL-1β is elevated in the cerebrospinal fluid (CSF) of neuropathic pain patients (Alexander et al., 2005). Taken together, the continued presence and

activity of IL-1β for several days to weeks after nerve injury may form the etiological basis for the development of neuropathic pain.

### *1.8 A Hypothesis*

'It is not hard to conceive that a substance produced by cell damage and capable of exciting sensory units of the polymodal fibers could produce a long-lasting increase in sensitivity produced by its continued presence in small quantities'.

-Bessou and Perl (1969)

Peripheral nerve injury promotes an enduring increase in the excitability of primary afferent neurons. This change, which likely contributes to the development of neuropathic pain, may be a consequence of prolonged (days to weeks) exposure of primary afferent neurons to inflammatory mediators such as cytokines. IL-1β may be critical to this process, since its receptor, IL-1RI, is present on sensory neurons (Liu et al., 2006;Copray et al., 2001) and short-term (seconds to minutes) applications are known to increase sensory neuron excitability (Binshtok et al., 2008;Takeda et al., 2007). However, the effects of long-term IL-1β exposure, as may occur after nerve injury (Kawasaki et al., 2008;Gabay et al., 2010), have yet to be examined. In order to emulate the release of IL-1β after peripheral nerve injury, I, therefore, exposed defined medium cultured rat DRG neurons to 100 pM IL-1β for 5-6 days and tested the HYPOTHESIS that such an application will promote an enduring increase in their excitability.

The following questions will be addressed:

1. Will 5-6 days of IL-1β exposure increase the excitability of DRG neurons under current-clamp conditions? More specifically, does IL-1β increase the ability of DRG neurons to fire action potentials in response to depolarizing current commands?

2. Is the effect of IL-1β differential among DRG neuron subpopulations?

3. Are the effects of IL-1β mediated by IL-1RI, thus, can changes in excitability be antagonized by the IL1-RI receptor antagonist, IL-1Ra?

4. Which ion channels are affected by IL-1β under voltage-clamp conditions?

***Table 1-1: Summary table of the classification of primary afferent fibres***

Primary afferents carry sensory information from specialized receptors or free nerve endings in the periphery into the dorsal horn of the spinal cord. Primary afferents can be classified based on properties summarized in this table. Soma diameter and neurochemistry of primary afferent cell bodies are commonly used to distinguish sensory neurons *in vitro*.

| | **Aα/β** | **Aδ** | **C** |
|---|---|---|---|
| **Neuronal Classification** | Large | Medium | Small |
| **Soma Diameter** | >40 μm | 30-40 μm | <30 μm |
| **$C_{in}$** | >90 pF | 70-90 pF | <70 pF |
| **Myelination** | Heavy | Thin | None |
| **Conduction Velocity** | 14-55 m/s | 2.2-8 m/s | <1.4 m/s |
| **Information Sent** | Light touch, hair bending | Innocuous or Nociception | Nociception |
| **Spinal Cord Innervations** | Lamina III and IV | Lamina I, II,III and V | Lamina I, II and V |
| **Neurochemical Markers** | Phosphorylated-NF200 (RT97) | Phosphorylated-NF200 (RT97) | IB4,$P2X_3$ (non-peptidergic); CGRP,SP (peptidergic) |
| **Neurotrophin Receptor** | TrkC; TrkB | TrkC (D-hairs); TrkB | GDNF receptor components (non-peptidergic); TrkA (peptidergic); TrkB |

***Table 1-2: Summary table of the classification of sensory nerve endings in the skin according to modality***

Within the skin, there are several morphologically distinct nerve endings which can be classified according to sensory modality. In general, free nerve endings (pain and temperature) are associated with Aδ– and C-primary afferent fibres, while more specialized receptors (tactile) are associated with Aα/β–primary afferent fibres.

Adapted from Perl (1992).

| Receptor Type | Fibre Group | Modality |
|---|---|---|
| Hair Follicle | Aα/β/δ | Tactile |
| Meissner Corpuscle | Aα/β | Tactile |
| Ruffini Ending | Aα/β | Tactile |
| Merkel Cell | Aα/β | Tactile |
| Pacinian Corpuscle | Aα/β/δ | Tactile |
| Free Nerve Ending | Aδ, C | Pain and temperature |

***Table 1-3: Summary table of the classification of specialized receptors in the skin according to size of receptive field and adaptation***

Within the skin, there at least four morphologically distinct, specialized receptors which can be classified according to the size of receptive field and extent of (rapid or slow) action potential adaptation upon static, mechanical skin displacement. Adapted from Brodal (2010).

| Receptive Fields | Adaptation | |
|---|---|---|
| | **Rapid** | **Slow** |
| **Small** | **Meissner Corpuscles:**<br>Glabrous skin, in dermal papillae<br>Touch: moving stimuli<br>Vibration < 100 Hz | **Merkel Cells:**<br>Close to the epithelium<br>Touch: judging form and surface of objects |
| **Large** | **Pacinian Corpuscles:**<br>Border dermis-subcutis<br>Vibration > 100 Hz | **Ruffini Endings:**<br>Dermis, parallel to the skin surface; stretch of the skin (friction) |

***Figure 1-1: Definitions for hyperalgesia and allodynia***

A: Hyperalgesia. $T_0$ refers to the normal pain threshold. After sensitization of nociceptive high-threshold (HT) fibres, there is pain amplification or *hyperalgesia* (red arrow and red area) which is characterized by the lowering in pain thresholds ($T_S$).

B: Allodynia. Only if pain is cleary induced by low-threshold (LT) fibres should the term *allodynia* be used (blue arrow). $T_{0/S}$ refers to the normal threshold for touch sensation which is identical to (or near) the stimulation threshold for allodynia. In all cases where it is not known whether low- or high-threshold sensory nerve fibres are involved, the umbrella term *hyperalgesia* should be used.

Adapted from Sandkuhler (2009).

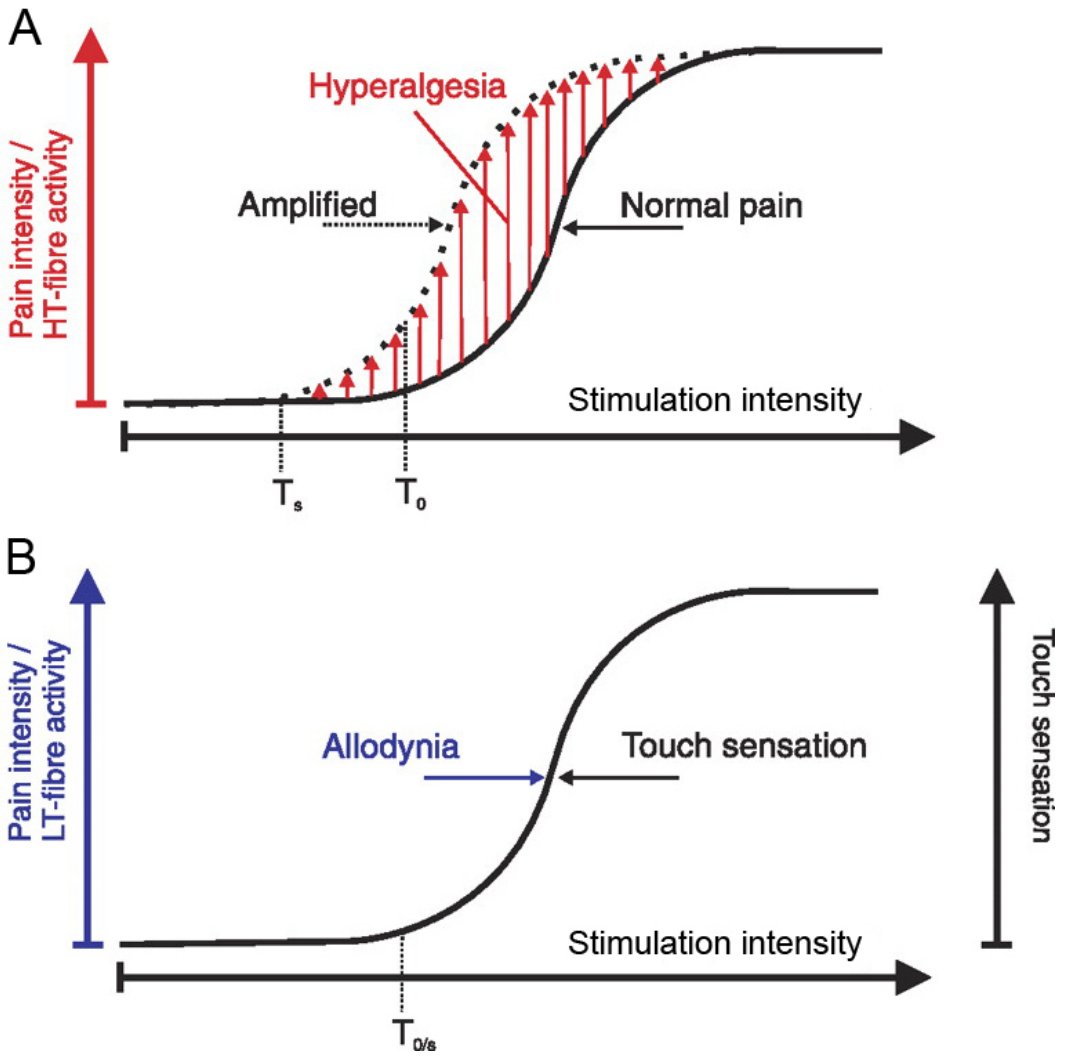
A
Pain intensity / HT-fibre activity
Hyperalgesia
Amplified
Normal pain
Stimulation intensity
$T_s$
$T_0$
B
Pain intensity / LT-fibre activity
Allodynia
Touch sensation
Touch sensation
Stimulation intensity
$T_{0/s}$

***Figure 1-2: Primary afferent terminations in the dorsal horn***

The identities of primary afferents that terminate and release neurotransmitters, such as glutamate, within the marginal layer lamina (LI), the *substantia gelatinosa* (LII), the *nucleus proprius* (LIII to LIV) and LV of the spinal cord are shown.

-Large myelinated Aβ-fibres (thick black lines) have extensive terminations in LIII and IV.

-Peptidergic C-fibres (thin black lines) terminate in LI, IIo and V.

-Non-peptidergic C-fibres (thin green lines) terminate dorsally within inner lamina II (LIIi).

-Nociceptive, high threshold mechanoreceptive Aδ-fibres (grey lines) terminate in laminae I and V.

-Innocuous Aδ-fibres (red lines), innervating D-hairs terminate in the deeper part of lamina II and lamina III.

Taken together, the superficial layers of the dorsal horn (LI and LIIo) receive heavy nociceptive input, while deeper laminae, with the exception of L5, receive non-nociceptive input.

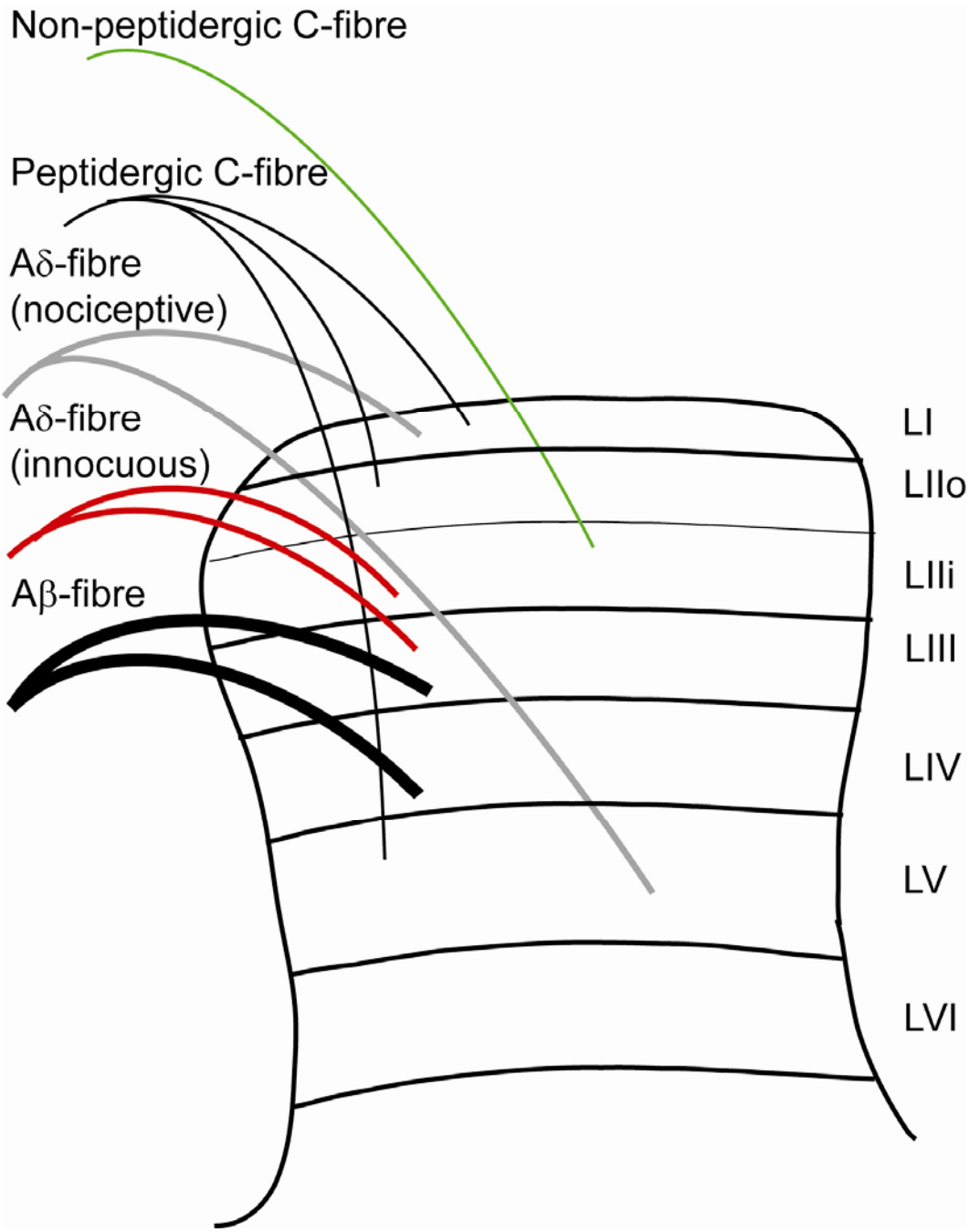
Non-peptidergic C-fibre
Peptidergic C-fibre
Aδ-fibre
(nociceptive)
Aδ-fibre
(innocuous)
Aβ-fibre
LI
LIIo
LIIi
LIII
LIV
LV
LVI

***Figure 1-3: Summary of changes in nociceptive signalling following peripheral nerve injury in animal models of neuropathic pain***

This diagram shows the primary afferent fibre with both peripheral and central terminals, the dorsal root ganglion which houses the cell bodies of primary afferents, and the dorsal horn of the spinal cord.

Following peripheral nerve injury, a progressive enhancement of neuronal excitability from peripheral to central neurons occurs in a process known as 'central sensitization'.

Adapted from Lu (2007).

*References:*

1. Abdulla and Smith (2001a).

2. Govrin-Lippmann and Devor (1978)

3. Wall and Devor (1983)

4. Dalal et al. (1999)

5. Baba et al. (2003)

6. Coull et al. (2003)

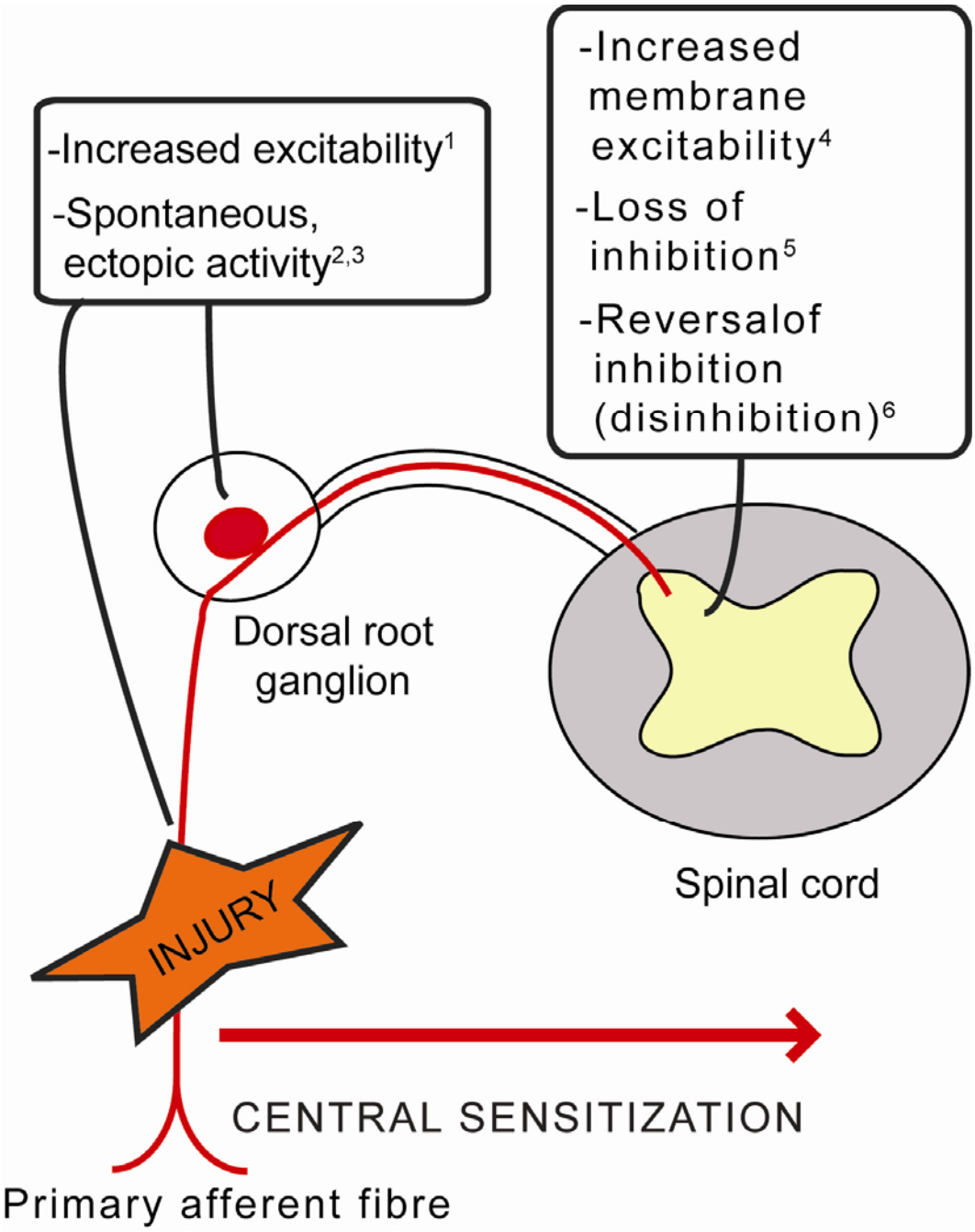
-Increased membrane excitability[4]
-Loss of inhibition[5]
-Reversalof inhibition (disinhibition)[6]
-Increased excitability[1]
-Spontaneous, ectopic activity[2,3]
Dorsal root ganglion
Spinal cord
INJURY
CENTRAL SENSITIZATION
Primary afferent fibre

### *1.9 References*


1. Abdulla FA, Smith PA (2001a) Axotomy- and autotomy-induced changes in the excitability of rat dorsal root ganglion neurons. J Neurophysiol 85: 630-643.

2. Abdulla FA, Smith PA (2002) Changes in Na(+) channel currents of rat dorsal root ganglion neurons following axotomy and axotomy-induced autotomy. J Neurophysiol 88: 2518-2529.

3. Abdulla FA, Stebbing MJ, Smith PA (2001) Effects of substance P on excitability and ionic currents of normal and axotomized rat dorsal root ganglion neurons. Eur J Neurosci 13: 545-552.

4. Abdulla FA, Smith PA (2001b) Axotomy- and Autotomy-Induced Changes in Ca2+and K+ Channel Currents of Rat Dorsal Root Ganglion Neurons. J Neurophysiol 85: 644-658.

5. Acharjee S, Noorbakhsh F, Stemkowski PL, Olechowski C, Cohen EA, Ballanyi K, Kerr B, Pardo C, Smith PA, Power C (2010) HIV-1 viral protein R causes peripheral nervous system injury associated with in vivo neuropathic pain. FASEB J.

6. Acosta CG, Lopez HS (1999) delta Opioid Receptor Modulation of Several Voltage-Dependent Ca2+ Currents in Rat Sensory Neurons. J Neurosci 19: 8337-8348.

7. Airaksinen MS, Koltzenburg M, Lewin GR, Masu Y, Helbig C, Wolf E, Brem G, Toyka KV, Thoenen H, Meyer M (1996) Specific subtypes of cutaneous mechanoreceptors require neurotrophin-3 following peripheral target innervation. Neuron 16: 287-295.

8. Airaksinen MS, Saarma M (2002) The GDNF family: Signalling, biological functions and therapeutic value. Nat Rev Neurosci 3: 383-394.

9. Akopian AN, Sivilotti L, Wood JN (1996) A tetrodotoxin-resistant voltage-gated sodium channel expressed by sensory neurons. Nature 379: 257-262.

10. Alessandri-Haber N, Joseph E, Dina OA, Liedtke W, Levine JD (2005) TRPV4 mediates pain-related behavior induced by mild hypertonic stimuli in the presence of inflammatory mediator. Pain 118: 70-79.

11. Alexander GM, van Rijn MA, van Hilten JJ, Perreault MJ, Schwartzman RJ (2005) Changes in cerebrospinal fluid levels of pro-inflammatory cytokines in CRPS. Pain 116: 213-219.

12. Aley KO, Messing RO, Mochly-Rosen D, Levine JD (2000) Chronic hypersensitivity for inflammatory nociceptor sensitization mediated by the epsilon isozyme of protein kinase C. J Neurosci 20: 4680-4685.

13. Alier KA, Endicott JA, Stemkowski PL, Cenac N, Cellars L, Chapman K, Andrade-Gordon P, Vergnolle N, Smith PA (2008) Intrathecal administration of proteinase-activated receptor-2 agonists produces hyperalgesia by exciting the cell bodies of primary sensory neurons. J Pharmacol Exp Ther 324: 224-233.

14. Allan SM, Rothwell NJ (2001) Cytokines and acute neurodegeneration. Nat Rev Neurosci 2: 734-744.

15. Allan SM, Tyrrell PJ, Rothwell NJ (2005) Interleukin-1 and neuronal injury. Nat Rev Immunol 5: 629-640.

16. Alloui A, Zimmermann K, Mamet J, Duprat F, Noel J, Chemin J, Guy N, Blondeau N, Voilley N, Rubat-Coudert C, Borsotto M, Romey G, Heurteaux C, Reeh P, Eschalier A, Lazdunski M (2006) TREK-1, a K+ channel involved in polymodal pain perception. EMBO J 25: 2368-2376.

17. Alvarez FJ, Fyffe RE (2000) Nociceptors for the 21st century. Curr Rev Pain 4: 451-458.

18. Amadesi S, Nie J, Vergnolle N, Cottrell GS, Grady EF, Trevisani M, Manni C, Geppetti P, McRoberts JA, Ennes H, Davis JB, Mayer EA, Bunnett NW (2004) Protease-activated receptor 2 sensitizes the capsaicin receptor transient receptor potential vanilloid receptor 1 to induce hyperalgesia. J Neurosci 24: 4300-4312.

19. Andre R, Moggs JG, Kimber I, Rothwell NJ, Pinteaux E (2006) Gene regulation by IL-1beta independent of IL-1R1 in the mouse brain. Glia 53: 477-483.

20. Aoki Y, Takahashi Y, Ohtori S, Moriya H, Takahashi K (2004) Distribution and immunocytochemical characterization of dorsal root ganglion neurons innervating the lumbar intervertebral disc in rats: A review. Life Sciences 74: 2627-2642.

21. Aoki YM, Ohtori SM, Takahashi KM, Ino HM, Douya HM, Ozawa TM, Saito TM, Moriya HM (2005) Expression and Co-Expression of VR1, CGRP, and IB4-Binding Glycoprotein in Dorsal Root Ganglion Neurons in Rats: Differences Between the Disc Afferents and the Cutaneous Afferents. [Miscellaneous Article]. Spine 30: 1496-1500.

22. Argoff CE, Backonja MM, Belgrade MJ, Bennett GJ, Clark MR, Cole BE, Fishbain DA, Irving GA, McCarberg BH, McLean MJ (2006) Consensus

guidelines: treatment planning and options. Diabetic peripheral neuropathic pain. Mayo Clin Proc 81: S12-S25.

23. Arner S, Meyerson BA (1988) Lack of analgesic effect of opioids on neuropathic and idiopathic forms of pain. Pain 33: 11-23.

24. Attal N, Jazat F, Kayser V, Guilbaud G (1990) Further evidence for 'pain-related' behaviours in a model of unilateral peripheral mononeuropathy. Pain 41: 235-251.

25. Auron PE, Webb AC (1994) Interleukin-1: a gene expression system regulated at multiple levels. Eur Cytokine Netw 5: 573-592.

26. Averill S, McMahon SB, Clary DO, Reichardt LF, Priestley JV (1995) Immunocytochemical localization of trkA receptors in chemically identified subgroups of adult rat sensory neurons. Eur J Neurosci 7: 1484-1494.

27. Baba H, Ji RR, Kohno T, Moore KA, Ataka T, Wakai A, Okamoto M, Woolf CJ (2003) Removal of GABAergic inhibition facilitates polysynaptic A fiber-mediated excitatory transmission to the superficial spinal dorsal horn. Mol Cell Neurosci 24: 818-830.

28. Baccei ML, Kocsis JD (2000) Voltage-Gated Calcium Currents in Axotomized Adult Rat Cutaneous Afferent Neurons. J Neurophysiol 83: 2227-2238.

29. Backonja MM, Stacey B (2004) Neuropathic pain symptoms relative to overall pain rating. J Pain 5: 491-497.

30. Bahia PK, Suzuki R, Benton DC, Jowett AJ, Chen MX, Trezise DJ, Dickenson AH, Moss GW (2005) A functional role for small-conductance calcium-activated potassium channels in sensory pathways including nociceptive processes. J Neurosci 25: 3489-3498.

31. Balasubramanyan S, Stemkowski PL, Stebbing MJ, Smith PA (2006) Sciatic chronic constriction injury produces cell-type-specific changes in the electrophysiological properties of rat substantia gelatinosa neurons. J Neurophysiol 96: 579-590.

32. Bandell M, Story GM, Hwang SW, Viswanath V, Eid SR, Petrus MJ, Earley TJ, Patapoutian A (2004) Noxious cold ion channel TRPA1 is activated by pungent compounds and bradykinin. Neuron 41: 849-857.

33. Baranowski AP, Priestley JV, McMahon S (1993) Substance P in cutaneous primary sensory neurons--a comparison of models of nerve

injury that allow varying degrees of regeneration. Neuroscience 55: 1025-1036.

34. Bardoni R (2009) Postnatal development shifts the balance of pain descending control. J Physiol 587: 2711-2712.

35. Bayliss DA, Barrett PQ (2008) Emerging roles for two-pore-domain potassium channels and their potential therapeutic impact. Trends in Pharmacological Sciences 29: 566-575.

36. Beneski DA, Catterall WA (1980) Covalent labeling of protein components of the sodium channel with a photoactivable derivative of scorpion toxin. Proceedings of the National Academy of Sciences of the United States of America 77: 639-643.

37. Bennett AD, Chastain KM, Hulsebosch CE (2000) Alleviation of mechanical and thermal allodynia by CGRP(8-37) in a rodent model of chronic central pain. Pain 86: 163-175.

38. Bennett DL, Averill S, Clary DO, Priestley JV, McMahon SB (1996) Postnatal changes in the expression of the trkA high-affinity NGF receptor in primary sensory neurons. Eur J Neurosci 8: 2204-2208.

39. Bennett DLH, Michael GJ, Ramachandran N, Munson JB, Averill S, Yan Q, McMahon SB, Priestley JV (1998) A distinct subgroup of small DRG cells express GDNF receptor components and GDNF is protective for these neurons after nerve injury. J Neurosci 18: 3059-3072.

40. Bennett GJ, Xie YK (1988) A peripheral mononeuropathy in rat that produces disorders of pain sensation like those seen in man. Pain 33: 87-107.

41. Berger A, Dukes EM, Oster G (2004) Clinical characteristics and economic costs of patients with painful neuropathic disorders. The Journal of Pain 5: 143-149.

42. Bessou P, Perl ER (1969) Response of cutaneous sensory units with unmyelinated fibers to noxious stimuli. J Neurophysiol 32: 1025-1043.

43. Biggs, J. E., Stemkowski, P. L., Ballanyi, K., and Smith, P. A. 'Spicing up' the gabapentinoids. 13th World Congress on Pain IASP abtracts . 2-9-2010.

44. Binshtok AM, Bean BP, Woolf CJ (2007) Inhibition of nociceptors by TRPV1-mediated entry of impermeant sodium channel blockers. Nature 449: 607-610.

45. Binshtok AM, Gerner P, Oh SB, Puopolo M, Suzuki S, Roberson DP, Herbert T, Wang CF, Kim D, Chung G, Mitani AA, Wang GK, Bean BP, Woolf CJ (2009) Coapplication of lidocaine and the permanently charged sodium channel blocker QX-314 produces a long-lasting nociceptive blockade in rodents. Anesthesiology 111: 127-137.

46. Binshtok AM, Wang H, Zimmermann K, Amaya F, Vardeh D, Shi L, Brenner GJ, Ji RR, Bean BP, Woolf CJ, Samad TA (2008) Nociceptors are interleukin-1beta sensors. J Neurosci 28: 14062-14073.

47. Birrell GJ, McQueen DS, Iggo A, Coleman RA, Grubb BD (1991) PGI2-induced activation and sensitization of articular mechanonociceptors. Neuroscience Letters 124: 5-8.

48. Black JA, Cummins TR, Plumpton C, Chen YH, Hormuzdiar W, Clare JJ, Waxman SG (1999) Upregulation of a Silent Sodium Channel After Peripheral, but not Central, Nerve Injury in DRG Neurons. J Neurophysiol 82: 2776-2785.

49. Boettger MK, Till S, Chen MX, Anand U, Otto WR, Plumpton C, Trezise DJ, Tate SN, Bountra C, Coward K, Birch R, Anand P (2002) Calcium-activated potassium channel SK1- and IK1-like immunoreactivity in injured human sensory neurones and its regulation by neurotrophic factors. Brain 125: 252-263.

50. Botchkarev VA VA, Kief S, Paus R, Moll I (1999) Overexpression of Brain-Derived Neurotrophic Factor Increases Merkel Cell Number in Murine Skin. 113: 691-692.

51. Boucher TJ, Okuse K, Bennett DL, Munson JB, Wood JN, McMahon SB (2000) Potent analgesic effects of GDNF in neuropathic pain states. Science 290: 124-127.

52. Boulais N, Misery L (2007) Merkel cells. Journal of the American Academy of Dermatology 57: 147-165.

53. Bradbury EJ, Burnstock G, McMahon SB (1998) The expression of P2X3 purinoreceptors in sensory neurons: effects of axotomy and glial-derived neurotrophic factor. Mol Cell Neurosci 12: 256-268.

54. Braddock M, Quinn A (2004) Targeting IL-1 in inflammatory disease: new opportunities for therapeutic intervention. Nat Rev Drug Discov 3: 330-339.

55. Brodal P (2010) Peripheral Parts of the Somatosensory System. In: The Central Nervous System Structure and Function (Brodal P, ed), pp 165-189. New York: Oxford University Press.

56. Brown AG, Fyffe RE, Noble R (1980) Projections from Pacinian corpuscles and rapidly adapting mechanoreceptors of glabrous skin to the cat's spinal cord. J Physiol 307: 385-400.

57. Brown AG, Fyffe RE, Rose PK, Snow PJ (1981) Spinal cord collaterals from axons of type II slowly adapting units in the cat. J Physiol 316: 469-480.

58. Brown AG, Rose PK, Snow PJ (1977) The morphology of hair follicle afferent fibre collaterals in the spinal cord of the cat. J Physiol 272: 779-797.

59. Brown AG, Rose PK, Snow PJ (1978) Morphology and organization of axon collaterals from afferent fibres of slowly adapting type I units in cat spinal cord. J Physiol 277: 15-27.

60. Brown HF, DiFrancesco D, Noble SJ (1979) How does adrenaline accelerate the heart? Nature 280: 235-236.

61. Burgess PR, Perl ER (1967) Myelinated afferent fibres responding specifically to noxious stimulation of the skin. The Journal of Physiology 190: 541-562.

62. Caffrey JM, Eng DL, Black JA, Waxman SG, Kocsis JD (1992) Three types of sodium channels in adult rat dorsal root ganglion neurons. Brain Research 592: 283-297.

63. Cahill CM, Coderre TJ (2002) Attenuation of hyperalgesia in a rat model of neuropathic pain after intrathecal pre- or post-treatment with a neurokinin-1 antagonist. Pain 95: 277-285.

64. Carlton SM, Zhou S, Coggeshall RE (1996) Localization and activation of substance P receptors in unmyelinated axons of rat glabrous skin. Brain Res 734: 103-108.

65. Carroll P, Lewin GR, Koltzenburg M, Toyka KV, Thoenen H (1998) A role for BDNF in mechanosensation. Nat Neurosci 1: 42-46.

66. Catacuzzeno L, Fioretti B, Pietrobon D, Franciolini F (2008) The differential expression of low-threshold K+ currents generates distinct firing patterns in different subtypes of adult mouse trigeminal ganglion neurones. J Physiol 586: 5101-5118.

67. Caterina MJ, Julius D (2001) The vanilloid receptor: a molecular gateway to the pain pathway. Annu Rev Neurosci 24: 487-517.

68. Caterina MJ, Schumacher MA, Tominaga M, Rosen TA, Levine JD, Julius D (1997) The capsaicin receptor: a heat-activated ion channel in the pain pathway. Nature 389: 816-824.

69. Catterall WA, Goldin AL, Waxman SG (2005a) International Union of Pharmacology. XLVII. Nomenclature and structure-function relationships of voltage-gated sodium channels. Pharmacol Rev 57: 397-409.

70. Catterall WA, Perez-Reyes E, Snutch TP, Striessnig J (2005b) International Union of Pharmacology. XLVIII. Nomenclature and structure-function relationships of voltage-gated calcium channels. Pharmacol Rev 57: 411-425.

71. Catterall WA (2000a) From Ionic Currents to Molecular Mechanisms: The Structure and Function of Voltage-Gated Sodium Channels. Neuron 26: 13-25.

72. Catterall WA (2000b) STRUCTURE AND REGULATION OF VOLTAGE-GATED Ca2+ CHANNELS. Annual Review of Cell and Developmental Biology 16: 521-555.

73. Cenac N, Andrews CN, Holzhausen M, Chapman K, Cottrell G, Andrade-Gordon P, Steinhoff M, Barbara G, Beck P, Bunnett NW, Sharkey KA,

Ferraz JG, Shaffer E, Vergnolle N (2007) Role for protease activity in visceral pain in irritable bowel syndrome. J Clin Invest 117: 636-647.

74. Cesare P, McNaughton P (1996) A novel heat-activated current in nociceptive neurons and its sensitization by bradykinin. Proc Natl Acad Sci U S A 93: 15435-15439.

75. Chaplan SR, Guo HQ, Lee DH, Luo L, Liu C, Kuei C, Velumian AA, Butler MP, Brown SM, Dubin AE (2003) Neuronal hyperpolarization-activated pacemaker channels drive neuropathic pain. J Neurosci 23: 1169-1178.

76. Chen CC, Akopian AN, Sivilotti L, Colquhoun D, Burnstock G, Wood JN (1995) A P2X purinoceptor expressed by a subset of sensory neurons. Nature 377: 428-431.

77. Chen CC, England S, Akopian AN, Wood JN (1998) A sensory neuron-specific, proton-gated ion channel. Proc Natl Acad Sci U S A 95: 10240-10245.

78. Christensen BN, Perl ER (1970) Spinal neurons specifically excited by noxious or thermal stimuli: marginal zone of the dorsal horn. J Neurophysiol 33: 293-307.

79. Christian EP, Togo J, Naper KE (1994) Guinea pig visceral C-fiber neurons are diverse with respect to the K+ currents involved in action-potential repolarization. J Neurophysiol 71: 561-574.

80. Chuang HH, Prescott ED, Kong H, Shields S, Jordt SE, Basbaum AI, Chao MV, Julius D (2001) Bradykinin and nerve growth factor release the capsaicin receptor from PtdIns(4,5)P2-mediated inhibition. Nature 411: 957-962.

81. Coeshott C, Ohnemus C, Pilyavskaya A, Ross S, Wieczorek M, Kroona H, Leimer AH, Cheronis J (1999) Converting enzyme-independent release of tumor necrosis factor alpha and IL-1beta from a stimulated human monocytic cell line in the presence of activated neutrophils or purified proteinase 3. Proc Natl Acad Sci U S A 96: 6261-6266.

82. Connor JA, Stevens CF (1971) Voltage clamp studies of a transient outward membrane current in gastropod neural somata. J Physiol 213: 21-30.

83. Copray JC, Mantingh I, Brouwer N, Biber K, Kust BM, Liem RS, Huitinga I, Tilders FJ, Van Dam AM, Boddeke HW (2001) Expression of interleukin-1 beta in rat dorsal root ganglia. J Neuroimmunol 118: 203-211.

84. Cosens DJ, Manning AUBR (1969) Abnormal Electroretinogram from a Drosophila Mutant. Nature 224: 285-287.

85. Costigan M, Scholz J, Woolf CJ (2009) Neuropathic pain: a maladaptive response of the nervous system to damage. Annu Rev Neurosci 32: 1-32.

86. Coull JA, Beggs S, Boudreau D, Boivin D, Tsuda M, Inoue K, Gravel C, Salter MW, De Koninck Y (2005) BDNF from microglia causes the shift in neuronal anion gradient underlying neuropathic pain. Nature 438: 1017-1021.

87. Coull JA, Boudreau D, Bachand K, Prescott SA, Nault F, Sik A, De Koninck P, De Koninck Y (2003) Trans-synaptic shift in anion gradient in spinal lamina I neurons as a mechanism of neuropathic pain. Nature 424: 938-942.

88. Cox JJ, Reimann F, Nicholas AK, Thornton G, Roberts E, Springell K, Karbani G, Jafri H, Mannan J, Raashid Y, Al Gazali L, Hamamy H, Valente EM, Gorman S, Williams R, McHale DP, Wood JN, Gribble FM, Woods CG (2006) An SCN9A channelopathy causes congenital inability to experience pain. Nature 444: 894-898.

89. Cui JG, Holmin S, Mathiesen T, Meyerson BA, Linderoth B (2000) Possible role of inflammatory mediators in tactile hypersensitivity in rat models of mononeuropathy. Pain 88: 239-248.

90. Cummins TR, Aglieco F, Renganathan M, Herzog RI, Dib-Hajj SD, Waxman SG (2001) Nav1.3 sodium channels: rapid repriming and slow closed-state inactivation display quantitative differences after expression in a mammalian cell line and in spinal sensory neurons. J Neurosci 21: 5952-5961.

91. Cummins TR, Dib-Hajj SD, Black JA, Akopian AN, Wood JN, Waxman SG (1999) A Novel Persistent Tetrodotoxin-Resistant Sodium Current In SNS-Null And Wild-Type Small Primary Sensory Neurons. J Neurosci 19: 43RC.

92. Cummins TR, Waxman SG (1997) Downregulation of Tetrodotoxin-Resistant Sodium Currents and Upregulation of a Rapidly Repriming Tetrodotoxin-Sensitive Sodium Current in Small Spinal Sensory Neurons after Nerve Injury. J Neurosci 17: 3503-3514.

93. Cunha FQ, Poole S, Lorenzetti BB, Ferreira SH (1992) The pivotal role of tumour necrosis factor alpha in the development of inflammatory hyperalgesia. Br J Pharmacol 107: 660-664.

94. Dai Y, Wang S, Tominaga M, Yamamoto S, Fukuoka T, Higashi T, Kobayashi K, Obata K, Yamanaka H, Noguchi K (2007) Sensitization of TRPA1 by PAR2 contributes to the sensation of inflammatory pain. J Clin Invest 117: 1979-1987.

95. Dalal A, Tata M, Allegre G, Gekiere F, Bons N, Albe-Fessard D (1999) Spontaneous activity of rat dorsal horn cells in spinal segments of sciatic projection following transection of sciatic nerve or of corresponding dorsal roots. Neuroscience 94: 217-228.

96. DeLeo JA, Colburn RW, Rickman AJ (1997) Cytokine and growth factor immunohistochemical spinal profiles in two animal models of mononeuropathy. Brain Res 759: 50-57.

97. Denda M, Nakatani M, Ikeyama K, Tsutsumi M, Denda S (2007) Epidermal keratinocytes as the forefront of the sensory system. Exp Dermatol 16: 157-161.

98. Devor M (2009) Ectopic discharge in Abeta afferents as a source of neuropathic pain. Exp Brain Res 196: 115-128.

99. Devor M, Wall PD (1976) Type of sensory nerve fibre sprouting to form a neuroma. Nature 262: 705-708.

100. Devor M, White DM, Goetzl EJ, Levine JD (1992) Eicosanoids, but not tachykinins, excite C-fiber endings in rat sciatic nerve-end neuromas. Neuroreport 3: 21-24.

101. Dhaka A, Viswanath V, Patapoutian A (2006) TRP ION CHANNELS AND TEMPERATURE SENSATION. Annual Review of Neuroscience 29: 135-161.

102. Dib-Hajj S, Black JΓ, Felts P, Waxman SΓ (1996) Down-regulation of transcripts for Na channel +¦-SNS in spinal sensory neuronsΓÇëfollowingΓÇëaxotomy. Proceedings of the National Academy of Sciences of the United States of America 93: 14950-14954.

103. Dib-Hajj SD, Black JA, Cummins TR, Kenney AM, Kocsis JD, Waxman SG (1998a) Rescue of alpha -SNS Sodium Channel Expression in Small Dorsal Root Ganglion Neurons After Axotomy by Nerve Growth Factor In Vivo. J Neurophysiol 79: 2668-2676.

104. Dib-Hajj SD, Tyrrell L, Black JA, Waxman SG (1998b) NaN, a novel voltage-gated Na channel, is expressed preferentially in peripheral sensory neurons and down-regulated after axotomy. Proceedings of the National Academy of Sciences of the United States of America 95: 8963-8968.

105. Dib-Hajj SD, Fjell J, Cummins TR, Zheng Z, Fried K, LaMotte R, Black JA, Waxman SG (1999) Plasticity of sodium channel expression in DRG neurons in the chronic constriction injury model of neuropathic pain. Pain 83: 591-600.

106. Diem R, Hobom M, Grotsch P, Kramer B, Bahr M (2003) Interleukin-1 beta protects neurons via the interleukin-1 (IL-1) receptor-mediated Akt pathway and by IL-1 receptor-independent decrease of transmembrane currents in vivo. Mol Cell Neurosci 22: 487-500.

107. DiFrancesco D, Ojeda C (1980) Properties of the current if in the sino-atrial node of the rabbit compared with those of the current iK, in Purkinje fibres. J Physiol 308: 353-367.

108. Dinarello CA (2000) Proinflammatory cytokines. Chest 118: 503-508.

109. Dinarello CA (2005) Interleukin-1beta. Crit Care Med 33: S460-S462.

110. Djouhri L, Bleazard L, Lawson SN (1998) Association of somatic action potential shape with sensory receptive properties in guinea-pig dorsal root ganglion neurones. J Physiol 513 ( Pt 3): 857-872.

111. Doubell TP, Mannion RJ, Woolf CJ (1999) The dorsal horn: state-dependent sensory processing, plasticity and the generation of pain. In:

Textbook of Pain (Wall PD, Melzack R, eds), pp 165-181. London: Harcourt Publishers Limited.

112. Dougherty KD, Dreyfus CF, Black IB (2000) Brain-derived neurotrophic factor in astrocytes, oligodendrocytes, and microglia/macrophages after spinal cord injury. Neurobiol Dis 7: 574-585.

113. Dray A, Pinnock RD (1982) Effects of substance P on adult rat sensory ganglion neurones in vitro. Neurosci Lett 33: 61-66.

114. Duce IR, Keen P (1977) An ultrastructural classification of the neuronal cell bodies of the rat dorsal root ganglion using zinc iodide-osmium impregnation. Cell Tissue Res 185: 263-277.

115. Dunne A, O'Neill LA (2003) The interleukin-1 receptor/Toll-like receptor superfamily: signal transduction during inflammation and host defense. Sci STKE 2003: re3.

116. Dyck PJ, Kratz KM, Karnes JL, Litchy WJ, Klein R, Pach JM, Wilson DM, O'Brien PC, Melton III LJ (1993) The prevalence by staged severity of various types of diabetic neuropathy, retinopathy, and nephropathy in a population-based cohort: The Rochester Diabetic Neuropathy Study. Neurology 43: 817-824.

117. Esper RM, Loeb JA (2004) Rapid axoglial signaling mediated by neuregulin and neurotrophic factors. J Neurosci 24: 6218-6227.

118. Everill B, Cummins TR, Waxman SG, Kocsis JD (2001) Sodium currents of large (A[beta]-type) adult cutaneous afferent dorsal root ganglion neurons display rapid recovery from inactivation before and after axotomy. Neuroscience 106: 161-169.

119. Everill B, Kocsis JD (1999) Reduction in Potassium Currents in Identified Cutaneous Afferent Dorsal Root Ganglion Neurons After Axotomy. J Neurophysiol 82: 700-708.

120. Everill B, Rizzo MA, Kocsis JD (1998) Morphologically Identified Cutaneous Afferent DRG Neurons Express Three Different Potassium Currents in Varying Proportions. J Neurophysiol 79: 1814-1824.

121. Fang X, McMullan S, Lawson SN, Djouhri L (2005) Electrophysiological differences between nociceptive and non-nociceptive dorsal root ganglion neurones in the rat in vivo. The Journal of Physiology 565: 927-943.

122. Fang X, Djouhri L, McMullan S, Berry C, Waxman SG, Okuse K, Lawson SN (2006) Intense Isolectin-B4 Binding in Rat Dorsal Root Ganglion Neurons Distinguishes C-Fiber Nociceptors with Broad Action Potentials and High Nav1.9 Expression. J Neurosci 26: 7281-7292.

123. Ferreira SH, Lorenzetti BB, Bristow AF, Poole S (1988) Interleukin-1 beta as a potent hyperalgesic agent antagonized by a tripeptide analogue. Nature 334: 698-700.

124. Ferreira SH, Nakamura M, de Abreu Castro MS (1978) The hyperalgesic effects of prostacyclin and prostaglandin E2. Prostaglandins 16: 31-37.

125. Ferri GL, Sabani A, Abelli L, Polak JM, Dahl D, Portier MM (1990) Neuronal intermediate filaments in rat dorsal root ganglia: differential distribution of peripherin and neurofilament protein immunoreactivity and effect of capsaicin. Brain Res 515: 331-335.

126. Fjell J, Cummins TR, Dib-Hajj SD, Fried K, Black JA, Waxman SG (1999) Differential role of GDNF and NGF in the maintenance of two TTX-resistant sodium channels in adult DRG neurons. Brain Res Mol Brain Res 67: 267-282.

127. Forman LJ, Estilow S, Lewis M, Vasilenko P (1986) Streptozocin diabetes alters immunoreactive +¦-endorphin levels and pain perception after 8 wk in female rats. Diabetes 35: 1309-1313.

128. Fuchs A, Rigaud M, Sarantopoulos CD, Filip P, Hogan QH (2007) Contribution of calcium channel subtypes to the intracellular calcium

signal in sensory neurons: the effect of injury. Anesthesiology 107: 117-127.

129. Fukuoka H, Kawatani M, Hisamitsu T, Takeshige C (1994) Cutaneous hyperalgesia induced by peripheral injection of interleukin-1 beta in the rat. Brain Res 657: 133-140.

130. Funakoshi M, Sonoda Y, Tago K, Tominaga S, Kasahara T (2001) Differential involvement of p38 mitogen-activated protein kinase and phosphatidyl inositol 3-kinase in the IL-1-mediated NF-kappa B and AP-1 activation. Int Immunopharmacol 1: 595-604.

131. Gabay E, Wolf G, Shavit Y, Yirmiya R, Tal M (2010) Chronic blockade of interleukin-1 (IL-1) prevents and attenuates neuropathic pain behavior and spontaneous ectopic neuronal activity following nerve injury. Eur J Pain.

132. Garraway SM, Petruska JC, Mendell LM (2003) BDNF sensitizes the response of lamina II neurons to high threshold primary afferent inputs. Eur J Neurosci 18: 2467-2476.

133. Gasser HS (1937) The Control of Excitation in the Nervous System. Bull N Y Acad Med 13: 324-348.

134. Gay NJ, Keith FJ (1991) Drosophila Toll and IL-1 receptor. Nature 351: 355-356.

135. Geng SJ, Liao FF, Dang WH, Ding X, Liu XD, Cai J, Han JS, Wan Y, Xing GG (2010) Contribution of the spinal cord BDNF to the development of neuropathic pain by activation of the NR2B-containing NMDA receptors in rats with spinal nerve ligation. Experimental Neurology 222: 256-266.

136. Gerke MB, Plenderleith MB (2001) Binding sites for the plant lectin Bandeiraea simplicifolia I-isolectin B(4) are expressed by nociceptive primary sensory neurones. Brain Res 911: 101-104.

137. Gerner P, Binshtok AM, Wang CF, Hevelone ND, Bean BP, Woolf CJ, Wang GK (2008) Capsaicin combined with local anesthetics preferentially prolongs sensory/nociceptive block in rat sciatic nerve. Anesthesiology 109: 872-878.

138. Ghatta S, Nimmagadda D, Xu X, O'Rourke ST (2006) Large-conductance, calcium-activated potassium channels: structural and functional implications. Pharmacol Ther 110: 103-116.

139. Gilron I, Johnson AP (2010) Economics of chronic pain: How can science guide health policy? Can J Anaesth 57: 530-538.

140. Gold MS, Reichling DB, Shuster MJ, Levine JD (1996a) Hyperalgesic agents increase a tetrodotoxin-resistant Na+ current in nociceptors. Proc Natl Acad Sci U S A 93: 1108-1112.

141. Gold MS, Shuster MJ, Levine JD (1996b) Characterization of six voltage-gated K+ currents in adult rat sensory neurons. J Neurophysiol 75: 2629-2646.

142. Gold MS, Shuster MJ, Levine JD (1996c) Role of a Ca(2+)-dependent slow afterhyperpolarization in prostaglandin E2-induced sensitization of cultured rat sensory neurons. Neurosci Lett 205: 161-164.

143. Gold MS, Weinreich D, Kim CS, Wang R, Treanor J, Porreca F, Lai J (2003) Redistribution of Na(V)1.8 in uninjured axons enables neuropathic pain. J Neurosci 23: 158-166.

144. Goldin AL, Barchi RL, Caldwell JH, Hofmann F, Howe JR, Hunter JC, Kallen RG, Mandel G, Meisler MH, Netter YB, Noda M, Tamkun MM, Waxman SG, Wood JN, Catterall WA (2000) Nomenclature of Voltage-Gated Sodium Channels. Neuron 28: 365-368.

145. Goldstein ME, House SB, Gainer H (1991) NF-L and peripherin immunoreactivities define distinct classes of rat sensory ganglion cells. J Neurosci Res 30: 92-104.

146. González-Martínez T, Fariñas I, Valle MEd, Feito J, Germanà G, Cobo J, Vega JA (2005) BDNF, but not NT-4, is necessary for normal development of Meissner corpuscles. Neuroscience Letters 377: 12-15.

147. González-Martínez T, Germanà, P., Monjil DF, Silos-Santiago I, de Carlos F, Germanà G, Cobo J, Vega JA (2004) Absence of Meissner corpuscles in the digital pads of mice lacking functional TrkB. Brain Research 1002: 120-128.

148. Gover TD, Moreira TH, Weinreich D (2009) Role of Calcium in Regulating Primary Sensory Neuronal Excitability. pp 563-587.

149. Govrin-Lippmann R, Devor M (1978) Ongoing activity in severed nerves: source and variation with time. Brain Research 159: 406-410.

150. Greenfeder SA, Varnell T, Powers G, Lombard-Gillooly K, Shuster D, McIntyre KW, Ryan DE, Levin W, Madison V, Ju G (1995) Insertion of a structural domain of interleukin (IL)-1 beta confers agonist activity to the IL-1 receptor antagonist. Implications for IL-1 bioactivity. J Biol Chem 270: 22460-22466.

151. Grudt TJ, Perl ER (2002) Correlations between neuronal morphology and electrophysiological features in the rodent superficial dorsal horn. J Physiol 540: 189-207.

152. Guo A, Vulchanova L, Wang J, Li X, Elde R (1999) Immunocytochemical localization of the vanilloid receptor 1 (VR1): relationship to neuropeptides, the P2X3 purinoceptor and IB4 binding sites. Eur J Neurosci 11: 946-958.

153. Gutman GA, Chandy KG, Grissmer S, Lazdunski M, McKinnon D, Pardo LA, Robertson GA, Rudy B, Sanguinetti MC, Stuhmer W, Wang X (2005) International Union of Pharmacology. LIII. Nomenclature and molecular relationships of voltage-gated potassium channels. Pharmacol Rev 57: 473-508.

154. Handwerker HO, Kilo S, Reeh PW (1991) Unresponsive afferent nerve fibres in the sural nerve of the rat. J Physiol 435: 229-242.

155. Harper AA, Lawson SN (1985a) Conduction velocity is related to morphological cell type in rat dorsal root ganglion neurones. J Physiol 359: 31-46.

156. Harper AA, Lawson SN (1985b) Electrical properties of rat dorsal root ganglion neurones with different peripheral nerve conduction velocities. J Physiol 359: 47-63.

157. Herzberg U, Eliav E, Dorsey JM, Gracely RH, Kopin IJ (1997) NGF involvement in pain induced by chronic constriction injury of the rat sciatic nerve. Neuroreport 8: 1613-1618.

158. Hibino H, Inanobe A, Furutani K, Murakami S, Findlay I, Kurachi Y (2010) Inwardly Rectifying Potassium Channels: Their Structure, Function, and Physiological Roles. Physiol Rev 90: 291-366.

159. Higgs EA, Moncada S, Vane JR (1978) Inflammatory effects of prostacyclin (PGI2) and 6-oxo-PGF1[alpha] in the rat paw. Prostaglandins 16: 153-162.

160. Hodgkin AL, Huxley AF (1952) A quantitative description of membrane current and its application to conduction and excitation in nerve. The Journal of Physiology 117: 500-544.

161. Hofmann F, Biel M, Flockerzi V (1994) Molecular basis for Ca2+ channel diversity. Annu Rev Neurosci 17: 399-418.

162. Hokfelt T, Elde R, Johansson O, Luft R, Nilsson G, Arimura A (1976) Immunohistochemical evidence for separate populations of somatostatin-containing and substance P-containing primary afferent neurons in the rat. Neuroscience 1: 131-136.

163. Hokfelt T, Kellerth JO, Nilsson G, Pernow B (1975) Substance P: localization in the central nervous system and in some primary sensory neurons. Science 190: 889-890.

164. Homma Y, Brull SJ, Zhang JM (2002) A comparison of chronic pain behavior following local application of tumor necrosis factor alpha to the normal and mechanically compressed lumbar ganglia in the rat. Pain 95: 239-246.

165. Honore P, Rogers SD, Schwei MJ, Salak-Johnson JL, Luger NM, Sabino MC, Clohisy DR, Mantyh PW (2000) Murine models of inflammatory, neuropathic and cancer pain each generates a unique set of neurochemical changes in the spinal cord and sensory neurons. Neuroscience 98: 585-598.

166. Hsu HY, Wen MH (2002) Lipopolysaccharide-mediated reactive oxygen species and signal transduction in the regulation of interleukin-1 gene expression. J Biol Chem 277: 22131-22139.

167. Hu P, McLachlan EM (2002) Macrophage and lymphocyte invasion of dorsal root ganglia after peripheral nerve lesions in the rat. Neuroscience 112: 23-38.

168. Hu P, McLachlan EM (2003) Selective reactions of cutaneous and muscle afferent neurons to peripheral nerve transection in rats. J Neurosci 23: 10559-10567.

169. Hummel M, Lu P, Cummons TA, Whiteside GT (2008) The persistence of a long-term negative affective state following the induction of either acute or chronic pain. Pain 140: 436-445.

170. Ingram SL, Williams JT (1996) Modulation of the hyperpolarization-activated current (Ih) by cyclic nucleotides in guinea-pig primary afferent neurons. J Physiol 492 ( Pt 1): 97-106.

171. Inoue A, Ikoma K, Morioka N, Kumagai K, Hashimoto T, Hide I, Nakata Y (1999) Interleukin-1beta induces substance P release from primary afferent neurons through the cyclooxygenase-2 system. J Neurochem 73: 2206-2213.

172. Irving GA (2005) Contemporary assessment and management of neuropathic pain. Neurology 64: S21-S27.

173. Iwata H, Takasusuki T, Yamaguchi S, Hori Y (2007) NMDA receptor 2B subunit-mediated synaptic transmission in the superficial dorsal horn of peripheral nerve-injured neuropathic mice. Brain Research 1135: 92-101.

174. Jagodic MM, Pathirathna S, Joksovic PM, Lee W, Nelson MT, Naik AK, Su P, Jevtovic-Todorovic V, Todorovic SM (2008) Upregulation of the T-Type Calcium Current in Small Rat Sensory Neurons After Chronic Constrictive Injury of the Sciatic Nerve. J Neurophysiol 99: 3151-3156.

175. Jagodic MM, Pathirathna S, Nelson MT, Mancuso S, Joksovic PM, Rosenberg ER, Bayliss DA, Jevtovic-Todorovic V, Todorovic SM (2007) Cell-Specific Alterations of T-Type Calcium Current in Painful Diabetic Neuropathy Enhance Excitability of Sensory Neurons. J Neurosci 27: 3305-3316.

176. Jang JH, Nam TS, Paik KS, Leem JW (2004) Involvement of peripherally released substance P and calcitonin gene-related peptide in mediating mechanical hyperalgesia in a traumatic neuropathy model of the rat. Neurosci Lett 360: 129-132.

177. Ji RR, Samad TA, Jin SX, Schmoll R, Woolf CJ (2002) p38 MAPK activation by NGF in primary sensory neurons after inflammation increases TRPV1 levels and maintains heat hyperalgesia. Neuron 36: 57-68.

178. Jiang YQ, Xing GG, Wang SL, Tu HY, Chi YN, Li J, Liu FY, Han JS, Wan Y (2008) Axonal accumulation of hyperpolarization-activated cyclic

nucleotide-gated cation channels contributes to mechanical allodynia after peripheral nerve injury in rat. Pain 137: 495-506.

179. Johnson KO (2001) The roles and functions of cutaneous mechanoreceptors. Current Opinion in Neurobiology 11: 455-461.

180. Jones GJ, Barsby NL, Cohen EA, Holden J, Harris K, Dickie P, Jhamandas J, Power C (2007) HIV-1 Vpr Causes Neuronal Apoptosis and In Vivo Neurodegeneration. J Neurosci 27: 3703-3711.

181. Kajander KC, Wakisaka S, Bennett GJ (1992) Spontaneous discharge originates in the dorsal root ganglion at the onset of a painful peripheral neuropathy in the rat. Neurosci Lett 138: 225-228.

182. Kameyama M (1983) Ionic currents in cultured dorsal root ganglion cells from adult guinea pigs. J Membr Biol 72: 195-203.

183. Kasai H, Kameyama M, Yamaguchi K, Fukuda J (1986) Single transient K channels in mammalian sensory neurons. Biophys J 49: 1243-1247.

184. Kaupp UB, Seifert R (2001) Molecular diversity of pacemaker ion channels. Annu Rev Physiol 63: 235-257.

185. Kawasaki Y, Xu ZZ, Wang X, Park JY, Zhuang ZY, Tan PH, Gao YJ, Roy K, Corfas G, Lo EH, Ji RR (2008) Distinct roles of matrix metalloproteases in the early- and late-phase development of neuropathic pain. Nat Med 14: 331-336.

186. Kelley J (1985) Reactions of neurons to injury. In: Principles of Neural Science (Kandel ER, Schwartz JH, eds), pp 187-195. New York: Elsevier Science Publishings Co., Inc.

187. Kerr BJ, Bradbury EJ, Bennett DL, Trivedi PM, Dassan P, French J, Shelton DB, McMahon SB, Thompson SW (1999) Brain-derived neurotrophic factor modulates nociceptive sensory inputs and NMDA-evoked responses in the rat spinal cord. J Neurosci 19: 5138-5148.

188. Kiefer W, Dannhardt G (2005) COX-2 inhibition and pain management: a review summary. Expert Rev Clin Immunol 1: 431-442.

189. Kim CH, Oh Y, Chung JM, Chung K (2001) The changes in expression of three subtypes of TTX sensitive sodium channels in sensory neurons after spinal nerve ligation. Brain Res Mol Brain Res 95: 153-161.

190. Kim DS, Choi JO, Rim HD, Cho HJ (2002) Downregulation of voltage-gated potassium channel [alpha] gene expression in dorsal root ganglia

following chronic constriction injury of the rat sciatic nerve. Molecular Brain Research 105: 146-152.

191. Kim SH, Chung JM (1992) An experimental model for peripheral neuropathy produced by segmental spinal nerve ligation in the rat. Pain 50: 355-363.

192. Kim YI, Na HS, Kim SH, Han HC, Yoon YW, Sung B, Nam HJ, Shin SL, Hong SK (1998) Cell type-specific changes of the membrane properties of peripherally-axotomized dorsal root ganglion neurons in a rat model of neuropathic pain. Neuroscience 86: 301-309.

193. Kluger MJ, Kozak W, Leon LR, Soszynski D, Conn CA (1998) Fever and antipyresis. Prog Brain Res 115: 465-475.

194. Knyihar-Csillik E, Csillik B (1981) FRAP: histochemistry of the primary nociceptive neuron. Prog Histochem Cytochem 14: 1-137.

195. Koerber HR, Druzinsky RE, Mendell LM (1988) Properties of somata of spinal dorsal root ganglion cells differ according to peripheral receptor innervated. J Neurophysiol 60: 1584-1596.

196. Koerber HR, Mendell LM (1992) Functional Heterogeneity of Dorsal Root Ganglion Cells. In: Sensory Neurons Diversity, Development, and Plasticity (Scott SA, ed), pp 77-96. New York: Oxford University Press.

197. Kostyuk PG, Veselovsky NS, Fedulova SA, Tsyndrenko AY (1981a) Ionic currents in the somatic membrane of rat dorsal root ganglion neurons-III. Potassium currents. Neuroscience 6: 2439-2444.

198. Kostyuk PG, Veselovsky NS, Tsyndrenko AY (1981b) Ionic currents in the somatic membrane of rat dorsal root ganglion neurons-I. Sodium currents. Neuroscience 6: 2423-2430.

199. Kouranova EV, Strassle BW, Ring RH, Bowlby MR, Vasilyev DV (2008) Hyperpolarization-activated cyclic nucleotide-gated channel mRNA and protein expression in large versus small diameter dorsal root ganglion neurons: correlation with hyperpolarization-activated current gating. Neuroscience 153: 1008-1019.

200. Krenzischek DA, Dunwoody CJ, Polomano RC, Rathmell JP (2008) Pharmacotherapy for Acute Pain: Implications for Practice. Journal of PeriAnesthesia Nursing 23: S28-S42.

201. Kress M, Guenther S (1999) Role of [Ca2+]i in the ATP-induced heat sensitization process of rat nociceptive neurons. J Neurophysiol 81: 2612-2619.

202. Kruger L, Perl ER, Sedivec MJ (1981) Fine structure of myelinated mechanical nociceptor endings in cat hairy skin. J Comp Neurol 198: 137-154.

203. Kwan KY, Allchorne AJ, Vollrath MA, Christensen AP, Zhang DS, Woolf CJ, Corey DP (2006) TRPA1 contributes to cold, mechanical, and chemical nociception but is not essential for hair-cell transduction. Neuron 50: 277-289.

204. Landstrom M (2010) The TAK1-TRAF6 signalling pathway. The International Journal of Biochemistry & Cell Biology 42: 585-589.

205. Latremoliere A, Woolf CJ (2009) Central sensitization: a generator of pain hypersensitivity by central neural plasticity. J Pain 10: 895-926.

206. Lawson SN, Caddy KW, Biscoe TJ (1974) Development of rat dorsal root ganglion neurones. Studies of cell birthdays and changes in mean cell diameter. Cell Tissue Res 153: 399-413.

207. Lawson SN, Harper AA, Harper EI, Garson JA, Anderton BH (1984) A monoclonal antibody against neurofilament protein specifically labels a subpopulation of rat sensory neurones. J Comp Neurol 228: 263-272.

208. Lawson SN, Harper EI, Harper AA, Garson JA, Coakham HB, Randle BJ (1985) Monoclonal antibody 2C5: a marker for a subpopulation of small neurones in rat dorsal root ganglia. Neuroscience 16: 365-374.

209. Layzell M (2008) Current interventions and approaches to postoperative pain management. Br J Nurs 17: 414-419.

210. Le Feuvre R, Brough D, Rothwell N (2002) Extracellular ATP and P2X7 receptors in neurodegeneration. Eur J Pharmacol 447: 261-269.

211. Lee MC, Mouraux A, Iannetti GD (2009) Characterizing the cortical activity through which pain emerges from nociception. J Neurosci 29: 7909-7916.

212. Lee SE, Kim JH (2007) Involvement of substance P and calcitonin gene-related peptide in development and maintenance of neuropathic pain from spinal nerve injury model of rat. Neuroscience Research 58: 245-249.

213. Lee Y, Kawai Y, Shiosaka S, Takami K, Kiyama H, Hillyard CJ, Girgis S, MacIntyre I, Emson PC, Tohyama M (1985a) Coexistence of calcitonin

gene-related peptide and substance P-like peptide in single cells of the trigeminal ganglion of the rat: immunohistochemical analysis. Brain Research 330: 194-196.

214. Lee Y, Takami K, Kawai Y, Girgis S, Hillyard CJ, MacIntyre I, Emson PC, Tohyama M (1985b) Distribution of calcitonin gene-related peptide in the rat peripheral nervous system with reference to its coexistence with substance P. Neuroscience 15: 1227-1237.

215. Lesage F, Lazdunski M (2000) Molecular and functional properties of two-pore-domain potassium channels. Am J Physiol Renal Physiol 279: F793-F801.

216. Li HS, Zhao ZQ (1998) Small sensory neurons in the rat dorsal root ganglia express functional NK-1 tachykinin receptor. Eur J Neurosci 10: 1292-1299.

217. Li W, Gao SB, Lv CX, Wu Y, Guo ZH, Ding JP, Xu T (2007) Characterization of voltage-and Ca2+-activated K+ channels in rat dorsal root ganglion neurons. J Cell Physiol 212: 348-357.

218. Light AR, Perl ER (1979) Spinal termination of functionally identified primary afferent neurons with slowly conducting myelinated fibers. J Comp Neurol 186: 133-150.

219. Light AR, Perl ER (2003) Unmyelinated afferent fibers are not only for pain anymore. J Comp Neurol 461: 137-139.

220. Light AR, Trevino DL, Perl ER (1979) Morphological features of functionally defined neurons in the marginal zone and substantia gelatinosa of the spinal dorsal horn. J Comp Neurol 186: 151-171.

221. Lindenlaub T, Teuteberg P, Hartung T, Sommer C (2000) Effects of neutralizing antibodies to TNF-alpha on pain-related behavior and nerve regeneration in mice with chronic constriction injury. Brain Res 866: 15-22.

222. Lindholm D, Heumann R, Meyer M, Thoenen H (1987) Interleukin-1 regulates synthesis of nerve growth factor in non-neuronal cells of rat sciatic nerve. Nature 330: 658-659.

223. Lindsay RM (1992) The Role of Neurotrophic Factors in Functional Maintenance of Mature Sensory Neurons. In: Sensory Neurons Diversity, Development, and Plasticity (Scott SA, ed), pp 404-420. New York.

224. Linley JE, Rose K, Patil M, Robertson B, Akopian AN, Gamper N (2008) Inhibition of M current in sensory neurons by exogenous proteases: a signaling pathway mediating inflammatory nociception. J Neurosci 28: 11240-11249.

225. Liu L, Yang TM, Liedtke W, Simon SA (2006) Chronic IL-1beta signaling potentiates voltage-dependent sodium currents in trigeminal nociceptive neurons. J Neurophysiol 95: 1478-1490.

226. Lu SG, Zhang X, Gold MS (2006) Intracellular calcium regulation among subpopulations of rat dorsal root ganglion neurons. The Journal of Physiology 577: 169-190.

227. Lu, V. B. BDNF in neuropathic pain. 1-357. 13-9-2007. University of Alberta.

228. Lu VB, Ballanyi K, Colmers WF, Smith PA (2007) Neuron type-specific effects of brain-derived neurotrophic factor in rat superficial dorsal horn and their relevance to 'central sensitization'. J Physiol 584: 543-563.

229. Lu VB, Biggs JE, Stebbing MJ, Balasubramanyan S, Todd KG, Lai AY, Colmers WF, Dawbarn D, Ballanyi K, Smith PA (2009) Brain-derived neurotrophic factor drives the changes in excitatory synaptic transmission in the rat superficial dorsal horn that follow sciatic nerve injury. J Physiol 587: 1013-1032.

230. Lu Y, Perl ER (2003) A specific inhibitory pathway between substantia gelatinosa neurons receiving direct C-fiber input. J Neurosci 23: 8752-8758.

231. Lu Y, Perl ER (2005) Modular organization of excitatory circuits between neurons of the spinal superficial dorsal horn (laminae I and II). J Neurosci 25: 3900-3907.

232. Lumpkin EA, Bautista DM (2005) Feeling the pressure in mammalian somatosensation. Curr Opin Neurobiol 15: 382-388.

233. Lumpkin EA, Caterina MJ (2007) Mechanisms of sensory transduction in the skin. Nature 445: 858-865.

234. Lunn ER, Perry VH, Brown MC, Rosen H, Gordon S (1989) Absence of Wallerian Degeneration does not Hinder Regeneration in Peripheral Nerve. Eur J Neurosci 1: 27-33.

235. Luo W, Wickramasinghe SR, Savitt JM, Griffin JW, Dawson TM, Ginty DD (2007) A Hierarchical NGF Signaling Cascade Controls Ret-Dependent and Ret-Independent Events during Development of Nonpeptidergic DRG Neurons. Neuron 54: 739-754.

236. Luttges MW, Kelly PT, Gerren RA (1976) Degenerative changes in mouse sciatic nerves: electrophoretic and electrophysiologic characterizations. Exp Neurol 50: 706-733.

237. Ma C, Shu Y, Zheng Z, Chen Y, Yao H, Greenquist KW, White FA, LaMotte RH (2003) Similar electrophysiological changes in axotomized and neighboring intact dorsal root ganglion neurons. J Neurophysiol 89: 1588-1602.

238. Mackie M, Hughes DI, Maxwell DJ, Tillakaratne NJ, Todd AJ (2003) Distribution and colocalisation of glutamate decarboxylase isoforms in the rat spinal cord. Neuroscience 119: 461-472.

239. Maingret F, Lauritzen I, Patel AJ, Heurteaux C, Reyes R, Lesage F, Lazdunski M, Honore E (2000) TREK-1 is a heat-activated background K(+) channel. EMBO J 19: 2483-2491.

240. March CJ, Mosley B, Larsen A, Cerretti DP, Braedt G, Price V, Gillis S, Henney CS, Kronheim SR, Grabstein K, . (1985) Cloning, sequence and expression of two distinct human interleukin-1 complementary DNAs. Nature 315: 641-647.

241. Marchand JE, Wurm WH, Kato T, Kream RM (1994) Altered tachykinin expression by dorsal root ganglion neurons in a rat model of neuropathic pain. Pain 58: 219-231.

242. Martin JH (1985a) Receptor physiology and submodality coding in the somatic sensory system. In: Principles of Neurral Science (Kandel ER, Schwartz JH, eds), pp 287-300. New York: Elsevier.

243. Martin JH (1985b) Receptor physiology and submodality coding in the somatic sensory system. In: Principles of Neurral Science (Kandel ER, Schwartz JH, eds), pp 287-300. New York: Elsevier.

244. Martinon F, Gaide O, Petrilli V, Mayor A, Tschopp J (2007) NALP inflammasomes: a central role in innate immunity. Semin Immunopathol 29: 213-229.

245. Matsuda Y, Yoshida S, Yonezawa T (1978) Tetrodotoxin sensitivity and Ca component of action potentials of mouse dorsal root ganglion cells cultured in vitro. Brain Res 154: 69-82.

246. Matsumura K, Watanabe Y, Onoe H, Watanabe Y (1995) Prostacyclin receptor in the brain and central terminals of the primary sensory neurons: An autoradiographic study using a stable prostacyclin analogue [3H]iloprost. Neuroscience 65: 493-503.

247. Maxwell DJ, Belle MD, Cheunsuang O, Stewart A, Morris R (2007) Morphology of inhibitory and excitatory interneurons in superficial laminae of the rat dorsal horn. The Journal of Physiology 584: 521-533.

248. Mayer ML, Westbrook GL (1983) A voltage-clamp analysis of inward (anomalous) rectification in mouse spinal sensory ganglion neurones. J Physiol 340: 19-45.

249. Maylie J, Bond CT, Herson PS, Lee WS, Adelman JP (2004) Small conductance Ca2+-activated K+ channels and calmodulin. The Journal of Physiology 554: 255-261.

250. McCaffery M, Pasero C (1999) Pain : clinical manual. St. Louis: Mosby.

251. McFarlane S, Cooper E (1991) Kinetics and voltage dependence of A-type currents on neonatal rat sensory neurons. J Neurophysiol 66: 1380-1391.

252. McLachlan EM, Hu P (2007) Inflammation of Dorsal Root Ganglia: Satellite Cell Activation and Immune Cell Recruitment after Nerve Injury. In: Immune and Glial Regulation of Pain (DeLeo JA, Sorkin LS, Watkins LR, eds), pp 167-185. Seattle: IASP Press.

253. McMahon SB, Armanini MP, Ling LH, Phillips HS (1994) Expression and coexpression of Trk receptors in subpopulations of adult primary sensory neurons projecting to identified peripheral targets. Neuron 12: 1161-1171.

254. Merskey H, Bogduk N (1994) Part III: Pain Terms, A Current List with Definitions and Notes on Usage. In: Classification of Chronic Pain Descriptions of Chronic Pain Syndromes and Definitions of Pain Terms, (Merskey H, Bogduk N, eds), pp 209-214. Seattle: IASP Press.

255. Michael GJ, Averill S, Nitkunan A, Rattray M, Bennett DL, Yan Q, Priestley JV (1997) Nerve growth factor treatment increases brain-derived neurotrophic factor selectively in TrkA-expressing dorsal root ganglion cells and in their central terminations within the spinal cord. J Neurosci 17: 8476-8490.

256. Michaelis M, Habler HJ, Jaenig W (1996) Silent afferents: a separate class of primary afferents? Clin Exp Pharmacol Physiol 23: 99-105.

257. Mogil JS, Crager SE (2004) What should we be measuring in behavioral studies of chronic pain in animals? Pain 112: 12-15.

258. Mogil JS (2009) Animal models of pain: progress and challenges. Nat Rev Neurosci 10: 283-294.

259. Moisset X, Bouhassira D (2007) Brain imaging of neuropathic pain. NeuroImage 37: S80-S88.

260. Molliver DC, Wright DE, Leitner ML, Parsadanian AS, Doster K, Wen D, Yan Q, Snider WD (1997) IB4-binding DRG neurons switch from NGF to GDNF dependence in early postnatal life. Neuron 19: 849-861.

261. Momin A, Cadiou H, Mason A, McNaughton PA (2008) Role of the hyperpolarization-activated current Ih in somatosensory neurons. J Physiol 586: 5911-5929.

262. Mongan LC, Hill MJ, Chen MX, Tate SN, Collins SD, Buckby L, Grubb BD (2005) The distribution of small and intermediate conductance calcium-activated potassium channels in the rat sensory nervous system. Neuroscience 131: 161-175.

263. Montell C (2005) TRP channels in Drosophila photoreceptor cells. J Physiol 567: 45-51.

264. Moore KA, Kohno T, Karchewski LA, Scholz J, Baba H, Woolf CJ (2002) Partial peripheral nerve injury promotes a selective loss of GABAergic inhibition in the superficial dorsal horn of the spinal cord. J Neurosci 22: 6724-6731.

265. Morales MEP, Gereau IV RW (2007) Cytokine Regulation of Ion Channels in the Pain Pathway. In: Immune and Glial Regulation of Pain

(DeLeo JA, Sorkin LS, Watkins LR, eds), pp 189-207. Seattle: IASP Press.

266. Morita K, Katayama Y (1989) Calcium-dependent slow outward current in visceral primary afferent neurones of the rabbit. Pflugers Arch 414: 171-177.

267. Moriyama T, Higashi T, Togashi K, Iida T, Segi E, Sugimoto Y, Tominaga T, Narumiya S, Tominaga M (2005) Sensitization of TRPV1 by EP1 and IP reveals peripheral nociceptive mechanism of prostaglandins. Molecular Pain 1: 3.

268. Morris CE, Juranka PF (2007) Nav channel mechanosensitivity: activation and inactivation accelerate reversibly with stretch. Biophys J 93: 822-833.

269. Mosconi T, Kruger L (1996) Fixed-diameter polyethylene cuffs applied to the rat sciatic nerve induce a painful neuropathy: ultrastructural morphometric analysis of axonal alterations. Pain 64: 37-57.

270. Munger BL, Bennett GJ, Kajander KC (1992) An experimental painful peripheral neuropathy due to nerve constriction. I. Axonal pathology in the sciatic nerve. Exp Neurol 118: 204-214.

271. Munger BL, Ide C (1988) The structure and function of cutaneous sensory receptors. Arch Histol Cytol 51: 1-34.

272. Nakae S, Asano M, Horai R, Iwakura Y (2001) Interleukin-1 beta, but not interleukin-1 alpha, is required for T-cell-dependent antibody production. Immunology 104: 402-409.

273. Nakamura-Craig M, Gill BK (1991) Effect of neurokinin A, substance P and calcitonin gene related peptide in peripheral hyperalgesia in the rat paw. Neurosci Lett 124: 49-51.

274. Nicholls JG, Baylor DA (1968) Specific modalities and receptive fields of sensory neurons in CNS of the leech. J Neurophysiol 31: 740-756.

275. Nicol GD, Cui M (1994) Enhancement by prostaglandin E2 of bradykinin activation of embryonic rat sensory neurones. J Physiol 480 ( Pt 3): 485-492.

276. Nicol GD, Vasko MR, Evans AR (1997) Prostaglandins suppress an outward potassium current in embryonic rat sensory neurons. J Neurophysiol 77: 167-176.

277. Ninomiya-Tsuji J, Kishimoto K, Hiyama A, Inoue J, Cao Z, Matsumoto K (1999) The kinase TAK1 can activate the NIK-I kappaB as well as the MAP kinase cascade in the IL-1 signalling pathway. Nature 398: 252-256.

278. Noguchi K, Dubner R, De Leon M, Senba E, Ruda MA (1994) Axotomy induces preprotachykinin gene expression in a subpopulation of dorsal root ganglion neurons. J Neurosci Res 37: 596-603.

279. Noguchi K, Kawai Y, Fukuoka T, Senba E, Miki K (1995) Substance P induced by peripheral nerve injury in primary afferent sensory neurons and its effect on dorsal column nucleus neurons. J Neurosci 15: 7633-7643.

280. Nowycky MC (1992) Voltage-Gated Ion Channels in Dorsal Root Ganglion Neurons. In: Sensory Neurons Diversity, Development, and Plasticity (Scott SA, ed), pp 97-115. New York: Oxford University Press.

281. O'Connor AB, Dworkin RH (2009) Treatment of Neuropathic Pain: An Overview of Recent Guidelines. The American Journal of Medicine 122: S22-S32.

282. Obreja O, Rathee PK, Lips KS, Distler C, Kress M (2002) IL-1 beta potentiates heat-activated currents in rat sensory neurons: involvement of IL-1RI, tyrosine kinase, and protein kinase C. FASEB J 16: 1497-1503.

283. Ocaña M, Cendán CM, Cobos EJ, Entrena JM, Baeyens JM (2004) Potassium channels and pain: present realities and future opportunities. European Journal of Pharmacology 500: 203-219.

284. Oida H, Namba T, Sugimoto Y, Ushikubi F, Ohishi H, Ichikawa A, Narumiya S (1995) In situ hybridization studies of prostacyclin receptor mRNA expression in various mouse organs. British Journal of Pharmacology 116: 2828-2837.

285. Olausson H, Lamarre Y, Backlund H, Morin C, Wallin BG, Starck G, Ekholm S, Strigo I, Worsley K, Vallbo AB, Bushnell MC (2002) Unmyelinated tactile afferents signal touch and project to insular cortex. Nat Neurosci 5: 900-904.

286. Orencole SF, Dinarello CA (1989) Characterization of a subclone (D10S) of the D10.G4.1 helper T-cell line which proliferates to attomolar concentrations of interleukin-1 in the absence of mitogens. Cytokine 1: 14-22.

287. Orio P, Madrid R, de la PE, Parra A, Meseguer V, Bayliss DA, Belmonte C, Viana F (2009) Characteristics and physiological role of hyperpolarization activated currents in mouse cold thermoreceptors. J Physiol 587: 1961-1976.

288. Ozaktay AC, Kallakuri S, Takebayashi T, Cavanaugh JM, Asik I, DeLeo JA, Weinstein JN (2006) Effects of interleukin-1 beta, interleukin-6, and tumor necrosis factor on sensitivity of dorsal root ganglion and peripheral receptive fields in rats. Eur Spine J 15: 1529-1537.

289. Pape HC (1996) Queer current and pacemaker: the hyperpolarization-activated cation current in neurons. Annu Rev Physiol 58: 299-327.

290. Patel AJ, Honore E, Maingret F, Lesage F, Fink M, Duprat F, Lazdunski M (1998) A mammalian two pore domain mechano-gated S-like K+ channel. EMBO J 17: 4283-4290.

291. Pearce RJ, Duchen MR (1994) Differential expression of membrane currents in dissociated mouse primary sensory neurons. Neuroscience 63: 1041-1056.

292. Peier AM, Moqrich A, Hergarden AC, Reeve AJ, Andersson DA, Story GM, Earley TJ, Dragoni I, McIntyre P, Bevan S, Patapoutian A (2002) A TRP channel that senses cold stimuli and menthol. Cell 108: 705-715.

293. Penner R, Petersen M, Pierau FK, Dreyer F (1986) Dendrotoxin: a selective blocker of a non-inactivating potassium current in guinea-pig dorsal root ganglion neurones. Pflugers Arch 407: 365-369.

294. Perkins NM, Tracey DJ (2000) Hyperalgesia due to nerve injury: role of neutrophils. Neuroscience 101: 745-757.

295. Perl ER (1992) Function of Dorsal Root Ganglion Neurons: An Overview. In: Sensory Neurons Diversity, Development, and Plasticity (Sheryl A.Scott, ed), pp 3-23. New York: Oxford University Press.

296. Perregaux DG, Bhavsar K, Contillo L, Shi J, Gabel CA (2002) Antimicrobial peptides initiate IL-1 beta posttranslational processing: a novel role beyond innate immunity. J Immunol 168: 3024-3032.

297. Perretti M, D'Acquisto F (2009) Annexin A1 and glucocorticoids as effectors of the resolution of inflammation. Nat Rev Immunol 9: 62-70.

298. Perrin FE, Lacroix S, Aviles-Trigueros M, David S (2005) Involvement of monocyte chemoattractant protein-1, macrophage inflammatory protein-1alpha and interleukin-1beta in Wallerian degeneration. Brain 128: 854-866.

299. Perry MJ, Lawson SN (1998) Differences in expression of oligosaccharides, neuropeptides, carbonic anhydrase and neurofilament in rat primary afferent neurons retrogradely labelled via skin, muscle or visceral nerves. Neuroscience 85: 293-310.

300. Petrilli V, Papin S, Dostert C, Mayor A, Martinon F, Tschopp J (2007) Activation of the NALP3 inflammasome is triggered by low intracellular potassium concentration. Cell Death Differ 14: 1583-1589.

301. Pischalnikova A, Sokolova O (2009) The Domain and Conformational Organization in Potassium Voltage-Gated Ion Channels. Journal of Neuroimmune Pharmacology 4: 71-82.

302. Polgar E, Fowler JH, McGill MM, Todd AJ (1999) The types of neuron which contain protein kinase C gamma in rat spinal cord. Brain Res 833: 71-80.

303. Prescott SA, De Koninck Y (2002) Four cell types with distinctive membrane properties and morphologies in lamina I of the spinal dorsal horn of the adult rat. J Physiol 539: 817-836.

304. Prescott SA, Sejnowski TJ, De Koninck Y (2006) Reduction of anion reversal potential subverts the inhibitory control of firing rate in spinal lamina I neurons: towards a biophysical basis for neuropathic pain. Mol Pain 2: 32.

305. Price DD (2000) Psychological and Neural Mechanisms of the Affective Dimension of Pain. Science 288: 1769-1772.

306. Rainville P, Carrier B, Hofbauer RK, Bushnell MC, Duncan GH (1999) Dissociation of sensory and affective dimensions of pain using hypnotic modulation. Pain 82: 159-171.

307. Rainville P, Duncan GH, Price DD, Carrier B, Bushnell MC (1997) Pain affect encoded in human anterior cingulate but not somatosensory cortex. Science 277: 968-971.

308. Ramer MS, Murphy PG, Richardson PM, Bisby MA (1998) Spinal nerve lesion-induced mechanoallodynia and adrenergic sprouting in sensory ganglia are attenuated in interleukin-6 knockout mice. Pain 78: 115-121.

309. Ramsey IS, Delling M, Clapham DE (2006) An introduction to TRP channels. Annu Rev Physiol 68: 619-647.

310. REXED B (1952) The cytoarchitectonic organization of the spinal cord in the cat. J Comp Neurol 96: 414-495.

311. REXED B (1954) A cytoarchitectonic atlas of the spinal cord in the cat. J Comp Neurol 100: 297-379.

312. Reynolds DV (1969) Surgery in the rat during electrical analgesia induced by focal brain stimulation. Science 164: 444-445.

313. Ribeiro-da-Silva A, Cuello AC (1995) Organization of peptidergic neurons in the dorsal horn of the spinal cord: anatomical and functional correlates. Prog Brain Res 104: 41-59.

314. Richardson JD, Vasko MR (2002) Cellular mechanisms of neurogenic inflammation. J Pharmacol Exp Ther 302: 839-845.

315. Rizzo MA, Kocsis JD, Waxman SG (1994) Slow sodium conductances of dorsal root ganglion neurons: intraneuronal homogeneity and interneuronal heterogeneity. J Neurophysiol 72: 2796-2815.

316. Ro LS, Chen ST, Tang LM, Jacobs JM (1999) Effect of NGF and anti-NGF on neuropathic pain in rats following chronic constriction injury of the sciatic nerve. Pain 79: 265-274.

317. Robinson DR, Gebhart GF (2008) Inside Information: The Unique Features of Visceral Sensation. Molecular Interventions 8: 242-253.

318. Rose RD, Koerber HR, Sedivec MJ, Mendell LM (1986) Somal action potential duration differs in identified primary afferents. Neurosci Lett 63: 259-264.

319. Rotshenker S, Aamar S, Barak V (1992) Interleukin-1 activity in lesioned peripheral nerve. J Neuroimmunol 39: 75-80.

320. Roux J, Kawakatsu H, Gartland B, Pespeni M, Sheppard D, Matthay MA, Canessa CM, Pittet JF (2005) Interleukin-1beta decreases expression of the epithelial sodium channel alpha-subunit in alveolar epithelial cells via a p38 MAPK-dependent signaling pathway. J Biol Chem 280: 18579-18589.

321. Rush AM, Cummins TR, Waxman SG (2007) Multiple sodium channels and their roles in electrogenesis within dorsal root ganglion neurons. J Physiol 579: 1-14.

322. Sachs D, Cunha FQ, Poole S, Ferreira SH (2002) Tumour necrosis factor-[alpha], interleukin-1[beta] and interleukin-8 induce persistent mechanical nociceptor hypersensitivity. Pain 96: 89-97.

323. Salmon JA, Higgs GA (1987) Prostaglandins and leukotrienes as inflammatory mediators. Br Med Bull 43: 285-296.

324. Sandkuhler J (2009) Models and mechanisms of hyperalgesia and allodynia. Physiol Rev 89: 707-758.

325. Sangameswaran L, Delgado SG, Fish LM, Koch BD, Jakeman LB, Stewart GR, Sze P, Hunter JC, Eglen RM, Herman RC (1996) Structure and Function of a Novel Voltage-gated, Tetrodotoxin-resistant Sodium

Channel Specific to Sensory Neurons. Journal of Biological Chemistry 271: 5953-5956.

326. Santoro B, Liu DT, Yao H, Bartsch D, Kandel ER, Siegelbaum SA, Tibbs GR (1998) Identification of a gene encoding a hyperpolarization-activated pacemaker channel of brain. Cell 93: 717-729.

327. Sarantopoulos CD, McCallum JB, Rigaud M, Fuchs A, Kwok WM, Hogan QH (2007) Opposing effects of spinal nerve ligation on calcium-activated potassium currents in axotomized and adjacent mammalian primary afferent neurons. Brain Res 1132: 84-99.

328. Schafers M, Lee DH, Brors D, Yaksh TL, Sorkin LS (2003) Increased sensitivity of injured and adjacent uninjured rat primary sensory neurons to exogenous tumor necrosis factor-alpha after spinal nerve ligation. J Neurosci 23: 3028-3038.

329. Schafers M, Sommer C, Sorkin LS (2007) Proinflammatory Cytokines and Neuropathic Pain: Retrograde Signaling and Dorsal Root Ganglion Changes after Peripheral Nerve Injury. In: Immune and Glial Regulation of Pain (DeLeo JA, Sorkin LS, Watkins LR, eds), pp 85-105. Seattle: IASP Press.

330. Schaible HG, schmidt RF (1988) Excitation and sensitization of fine articular afferents from cat's knee joint by prostaglandin E2. J Physiol 403: 91-104.

331. Schepelmann K, linger K, Schaible HG, schmidt RF (1992) Inflammatory mediators and nociception in the joint: Excitation and sensitization of slowly conducting afferent fibers of cat's knee by prostaglandin I2. Neuroscience 50: 237-247.

332. Schepers RJ, Ringkamp M (2009) Thermoreceptors and thermosensitive afferents. Neuroscience & Biobehavioral Reviews 33: 205-212.

333. Schindler R, Ghezzi P, Dinarello CA (1990) IL-1 induces IL-1. IV. IFN-gamma suppresses IL-1 but not lipopolysaccharide-induced transcription of IL-1. J Immunol 144: 2216-2222.

334. Scholz A, Gruss M, Vogel W (1998) Properties and functions of calcium-activated K+ channels in small neurones of rat dorsal root ganglion studied in a thin slice preparation. J Physiol 513 ( Pt 1): 55-69.

335. Scholz J, Woolf CJ (2007) The neuropathic pain triad: neurons, immune cells and glia. Nat Neurosci 10: 1361-1368.

336. Schonbeck U, Mach F, Libby P (1998) Generation of biologically active IL-1 beta by matrix metalloproteinases: a novel caspase-1-independent pathway of IL-1 beta processing. J Immunol 161: 3340-3346.

337. Schroder K, Tschopp J (2010) The Inflammasomes. Cell 140: 821-832.

338. Schroeder JE, Fischbach PS, McCleskey EW (1990) T-type calcium channels: heterogeneous expression in rat sensory neurons and selective modulation by phorbol esters. J Neurosci 10: 947-951.

339. Scott SA (1992) Sensory Neurons Diversity, Development, and Plasticity. New York: Oxford University Press.

340. Scroggs RS, Fox AP (1992) Calcium current variation between acutely isolated adult rat dorsal root ganglion neurons of different size. J Physiol 445: 639-658.

341. Scroggs RS, Todorovic SM, Anderson EG, Fox AP (1994) Variation in IH, IIR, and ILEAK between acutely isolated adult rat dorsal root ganglion neurons of different size. J Neurophysiol 71: 271-279.

342. Seltzer Z, Dubner R, Shir Y (1990) A novel behavioral model of neuropathic pain disorders produced in rats by partial sciatic nerve injury. Pain 43: 205-218.

343. Shu X, Mendell LM (2001) Acute sensitization by NGF of the response of small-diameter sensory neurons to capsaicin. J Neurophysiol 86: 2931-2938.

344. Silverman JD, Kruger L (1990) Selective neuronal glycoconjugate expression in sensory and autonomic ganglia: relation of lectin reactivity to peptide and enzyme markers. Journal of Neurocytology 19: 789-801.

345. Sivilotti L, Woolf CJ (1994) The contribution of GABAA and glycine receptors to central sensitization: disinhibition and touch-evoked allodynia in the spinal cord. J Neurophysiol 72: 169-179.

346. Smith PA (2004) Neuropathic pain: drug targets for current and future interventions. Drug News Perspect 17: 5-17.

347. Sommer C, Kress M (2004) Recent findings on how proinflammatory cytokines cause pain: peripheral mechanisms in inflammatory and neuropathic hyperalgesia. Neurosci Lett 361: 184-187.

348. Sommer C, Lindenlaub T, Teuteberg P, Schafers M, Hartung T, Toyka KV (2001) Anti-TNF-neutralizing antibodies reduce pain-related behavior in two different mouse models of painful mononeuropathy. Brain Res 913: 86-89.

349. Sommer C, Myers RR (1995) Neurotransmitters in the spinal cord dorsal horn in a model of painful neuropathy and in nerve crush. Acta Neuropathol 90: 478-485.

350. Sommer C, Petrausch S, Lindenlaub T, Toyka KV (1999) Neutralizing antibodies to interleukin 1-receptor reduce pain associated behavior in mice with experimental neuropathy. Neurosci Lett 270: 25-28.

351. Sommer C, Schafers M (1998) Painful mononeuropathy in C57BL/Wld mice with delayed wallerian degeneration: differential effects of cytokine production and nerve regeneration on thermal and mechanical hypersensitivity. Brain Res 784: 154-162.

352. Sommer EW, Kazimierczak J, Droz B (1985) Neuronal subpopulations in the dorsal root ganglion of the mouse as characterized by combination of ultrastructural and cytochemical features. Brain Res 346: 310-326.

353. Sorkin LS, Schafers M (2007) Immune Cells in Peripheral Nerve. In: Immune and Glia Regulation of Pain (DeLeo JA, Sorkin LS, Watkins LR, eds), pp 3-19. Seattle: IASP Press.

354. Stansfeld C, Feltz A (1988) Dendrotoxin-sensitive K+ channels in dorsal root ganglion cells. Neurosci Lett 93: 49-55.

355. Stansfeld CE, Marsh SJ, Halliwell JV, Brown DA (1986) 4-Aminopyridine and dendrotoxin induce repetitive firing in rat visceral sensory neurones by blocking a slowly inactivating outward current. Neurosci Lett 64: 299-304.

356. Stephens HE, Belliveau AC, Gupta JS, Mirkovic S, Kablar B (2005) The role of neurotrophins in the maintenance of the spinal cord motor neurons and the dorsal root ganglia proprioceptive sensory neurons. Int J Dev Neurosci 23: 613-620.

357. Stewart WF, Ricci JA, Chee E, Morganstein D, Lipton R (2003) Lost Productive Time and Cost Due to Common Pain Conditions in the US Workforce. JAMA 290: 2443-2454.

358. Stucky CL, DeChiara T, Lindsay RM, Yancopoulos GD, Koltzenburg M (1998) Neurotrophin 4áIs Required for the Survival of a Subclass of Hair Follicle Receptors. J Neurosci 18: 7040-7046.

359. Study RE, Kral MG (1996) Spontaneous action potential activity in isolated dorsal root ganglion neurons from rats with a painful neuropathy. Pain 65: 235-242.

360. Subramaniam S, Stansberg C, Cunningham C (2004) The interleukin 1 receptor family. Dev Comp Immunol 28: 415-428.

361. Sugimoto Y, Shigemoto R, Namba T, Negishi M, Mizuno N, Narumiya S, Ichikawa A (1994) Distribution of the messenger rna for the prostaglandin e receptor subtype ep3 in the mouse nervous system. Neuroscience 62: 919-928.

362. Sugiura Y, Terui N, Hosoya Y (1989) Difference in distribution of central terminals between visceral and somatic unmyelinated (C) primary afferent fibers. J Neurophysiol 62: 834-840.

363. Suzuki M, Mizuno A, Kodaira K, Imai M (2003a) Impaired pressure sensation in mice lacking TRPV4. J Biol Chem 278: 22664-22668.

364. Suzuki M, Watanabe Y, Oyama Y, Mizuno A, Kusano E, Hirao A, Ookawara S (2003b) Localization of mechanosensitive channel TRPV4 in mouse skin. Neuroscience Letters 353: 189-192.

365. Sweitzer S, Martin D, DeLeo JA (2001) Intrathecal interleukin-1 receptor antagonist in combination with soluble tumor necrosis factor receptor exhibits an anti-allodynic action in a rat model of neuropathic pain. Neuroscience 103: 529-539.

366. Tadano T, Namioka M, Nakagawasai O, Tan-No K, Matsushima K, Endo Y, Kisara K (1999) Induction of nociceptive responses by intrathecal injection of interleukin-1 in mice. Life Sci 65: 255-261.

367. Taiwo YO, Levine JD (1988) Characterization of the arachidonic acid metabolites mediating bradykinin and noradrenaline hyperalgesia. Brain Research 458: 402-406.

368. Takeda M, Kitagawa J, Takahashi M, Matsumoto S (2008) Activation of interleukin-1beta receptor suppresses the voltage-gated potassium currents in the small-diameter trigeminal ganglion neurons following peripheral inflammation. Pain 139: 594-602.

369. Takeda M, Tanimoto T, Kadoi J, Nasu M, Takahashi M, Kitagawa J, Matsumoto S (2007) Enhanced excitability of nociceptive trigeminal ganglion neurons by satellite glial cytokine following peripheral inflammation. Pain 129: 155-166.

370. Takeuchi O, Akira S (2010) Pattern Recognition Receptors and Inflammation. Cell 140: 805-820.

371. Tarride J, Collet J, Choiniere M, Rousseau C, Gordon A (2006) The economic burden of neuropathic pain in Canada. Journal of Medical Economics 9: 55-68.

372. Terlau H, Heinemann SH, St³hmer W, Pusch M, Conti F, Imoto K, Numa S (1991) Mapping the site of block by tetrodotoxin and saxitoxin of sodium channel II. FEBS Letters 293: 93-96.

373. Titmus MJ, Faber DS (1990) Axotomy-induced alterations in the electrophysiological characteristics of neurons. Progress in Neurobiology 35: 1-51.

374. Todd AJ (2002) Anatomy of primary afferents and projection neurones in the rat spinal dorsal horn with particular emphasis on substance P and the neurokinin 1 receptor. Exp Physiol 87: 245-249.

375. Todd AJ, Hughes DI, Polgar E, Nagy GG, Mackie M, Ottersen OP, Maxwell DJ (2003) The expression of vesicular glutamate transporters VGLUT1 and VGLUT2 in neurochemically defined axonal populations in the rat spinal cord with emphasis on the dorsal horn. Eur J Neurosci 17: 13-27.

376. Todd AJ, McKenzie J (1989) GABA-immunoreactive neurons in the dorsal horn of the rat spinal cord. Neuroscience 31: 799-806.

377. Todorovic SM, Jevtovic-Todorovic V (2006) The role of T-type calcium channels in peripheral and central pain processing. CNS Neurol Disord Drug Targets 5: 639-653.

378. Tofaris GK, Patterson PH, Jessen KR, Mirsky R (2002) Denervated Schwann cells attract macrophages by secretion of leukemia inhibitory

factor (LIF) and monocyte chemoattractant protein-1 in a process regulated by interleukin-6 and LIF. J Neurosci 22: 6696-6703.

379. Tominaga M, Caterina MJ, Malmberg AB, Rosen TA, Gilbert H, Skinner K, Raumann BE, Basbaum AI, Julius D (1998) The cloned capsaicin receptor integrates multiple pain-producing stimuli. Neuron 21: 531-543.

380. Tominaga M, Wada M, Masu M (2001) Potentiation of capsaicin receptor activity by metabotropic ATP receptors as a possible mechanism for ATP-evoked pain and hyperalgesia. Proc Natl Acad Sci U S A 98: 6951-6956.

381. Tonra JR, Curtis R, Wong V, Cliffer KD, Park JS, Timmes A, Nguyen T, Lindsay RM, Acheson A, DiStefano PS (1998) Axotomy upregulates the anterograde transport and expression of brain-derived neurotrophic factor by sensory neurons. J Neurosci 18: 4374-4383.

382. Traub RJ, Mendell LM (1988) The spinal projection of individual identified A-delta- and C-fibers. J Neurophysiol 59: 41-55.

383. Traub RJ, Solodkin A, Ruda MA (1989) Calcitonin gene-related peptide immunoreactivity in the cat lumbosacral spinal cord and the effects of multiple dorsal rhizotomies. J Comp Neurol 287: 225-237.

384. Treede RD, Jensen TS, Campbell JN, Cruccu G, Dostrovsky JO, Griffin JW, Hansson P, Hughes R, Nurmikko T, Serra J (2008) Neuropathic pain: redefinition and a grading system for clinical and research purposes. Neurology 70: 1630-1635.

385. Trevino DL, Carstens E (1975) Confirmation of the location of spinothalamic neurons in the cat and monkey by the retrograde transport of horseradish peroxidase. Brain Res 98: 177-182.

386. Tsao JW, George EB, Griffin JW (1999) Temperature Modulation Reveals Three Distinct Stages of Wallerian Degeneration. J Neurosci 19: 4718-4726.

387. Tu H, Deng L, Sun Q, Yao L, Han JS, Wan Y (2004) Hyperpolarization-activated, cyclic nucleotide-gated cation channels: roles in the differential electrophysiological properties of rat primary afferent neurons. J Neurosci Res 76: 713-722.

388. Ulens C, Tytgat J (2001) Functional heteromerization of HCN1 and HCN2 pacemaker channels. J Biol Chem 276: 6069-6072.

389. Ulmann L, Hatcher JP, Hughes JP, Chaumont S, Green PJ, Conquet F, Buell GN, Reeve AJ, Chessell IP, Rassendren F (2008) Up-regulation of

P2X4 receptors in spinal microglia after peripheral nerve injury mediates BDNF release and neuropathic pain. J Neurosci 28: 11263-11268.

390. Valdés-Sánchez T, Kirstein M, Pérez-Villalba A, Antonio Vega J, Isabel Fariñas (2010) Dev Biol 339: 465-476.

391. Vergnolle N, Bunnett NW, Sharkey KA, Brussee V, Compton SJ, Grady EF, Cirino G, Gerard N, Basbaum AI, Andrade-Gordon P, Hollenberg MD, Wallace JL (2001) Proteinase-activated receptor-2 and hyperalgesia: A novel pain pathway. Nat Med 7: 821-826.

392. Viana F, Belmonte C (2008) Funny currents are becoming serious players in nociceptor's sensitization. J Physiol 586: 5841-5842.

393. Villiere V, McLachlan EM (1996) Electrophysiological properties of neurons in intact rat dorsal root ganglia classified by conduction velocity and action potential duration. J Neurophysiol 76: 1924-1941.

394. Vitkovic L, Bockaert J, Jacque C (2000) "Inflammatory" cytokines: neuromodulators in normal brain? J Neurochem 74: 457-471.

395. Voets T, Droogmans G, Wissenbach U, Janssens A, Flockerzi V, Nilius B (2004) The principle of temperature-dependent gating in cold- and heat-sensitive TRP channels. Nature 430: 748-754.

396. Vogalis F, Harvey JR, Furness JB (2003a) PKA-mediated inhibition of a novel K+ channel underlies the slow after-hyperpolarization in enteric AH neurons. J Physiol 548: 801-814.

397. Vogalis F, Storm JF, Lancaster B (2003b) SK channels and the varieties of slow after-hyperpolarizations in neurons. Eur J Neurosci 18: 3155-3166.

398. Vydyanathan A, Wu ZZ, Chen SR, Pan HL (2005) A-type voltage-gated K+ currents influence firing properties of isolectin B4-positive but not isolectin B4-negative primary sensory neurons. J Neurophysiol 93: 3401-3409.

399. Wall PD (1999) Introduction to the fourth edition. In: Textbook of Pain (Wall PD, melzack R, eds), pp 1-8. London: Harcourt Publishers Limited.

400. Wall PD, Devor M (1983) Sensory afferent impulses originate from dorsal root ganglia as well as from the periphery in normal and nerve injured rats. Pain 17: 321-339.

401. Wall PD, Devor M, Inbal R, Scadding JW, Schonfeld D, Seltzer Z, Tomkiewicz MM (1979) Autotomy following peripheral nerve lesions: experimental anesthesia dolorosa. Pain 7: 103-113.

402. Wang H, Woolf CJ (2005) Pain TRPs. Neuron 46: 9-12.

403. Wang LX, Wang ZJ (2003) Animal and cellular models of chronic pain. Advanced Drug Delivery Reviews 55: 949-965.

404. Watkins LR, Hutchinson MR, Johnston IN, Maier SF (2005) Glia: novel counter-regulators of opioid analgesia. Trends Neurosci 28: 661-669.

405. Waxman SG, Kocsis JD, Black JA (1994) Type III sodium channel mRNA is expressed in embryonic but not adult spinal sensory neurons, and is reexpressed following axotomy. J Neurophysiol 72: 466-470.

406. Wells MR, Vaidya U (1989) Morphological alterations in dorsal root ganglion neurons after peripheral axon injury: association with changes in metabolism. Exp Neurol 104: 32-38.

407. White FA, Monahan PE, LaMotte RH (2007) Chemokines and Their Receptors in the Nervous System: A Link to Neuropathic Pain. In: Immune and Glial Regulation of Pain (DeLeo JA, Sorkin LS, Watkins LR, eds), pp 123-142. Seattle: IASP Press.

408. Wiech K, Ploner M, Tracey I (2008) Neurocognitive aspects of pain perception. Trends in Cognitive Sciences 12: 306-313.

409. Winkelstein BA, Rutkowski MD, Sweitzer SM, Pahl JL, DeLeo JA (2001) Nerve injury proximal or distal to the DRG induces similar spinal glial

activation and selective cytokine expression but differential behavioral responses to pharmacologic treatment. J Comp Neurol 439: 127-139.

410. Wolf G, Gabay E, Tal M, Yirmiya R, Shavit Y (2006) Genetic impairment of interleukin-1 signaling attenuates neuropathic pain, autotomy, and spontaneous ectopic neuronal activity, following nerve injury in mice. Pain 120: 315-324.

411. Woolf CJ (1983) Evidence for a central component of post-injury pain hypersensitivity. Nature 306: 686-688.

412. Woolf CJ (1987) Central terminations of cutaneous mechanoreceptive afferents in the rat lumbar spinal cord. J Comp Neurol 261: 105-119.

413. Woolf CJ, Thompson SW (1991) The induction and maintenance of central sensitization is dependent on N-methyl-D-aspartic acid receptor activation; implications for the treatment of post-injury pain hypersensitivity states. Pain 44: 293-299.

414. Wright DE, Snider WD (1995) Neurotrophin receptor mRNA expression defines distinct populations of neurons in rat dorsal root ganglia. J Comp Neurol 351: 329-338.

415. Wu LJ, Zhuo M (2009) Targeting the NMDA Receptor Subunit NR2B for the Treatment of Neuropathic Pain. Neurotherapeutics 6: 693-702.

416. Xie WR, Deng H, Li H, Bowen TL, Strong JA, Zhang JM (2006) Robust increase of cutaneous sensitivity, cytokine production and sympathetic sprouting in rats with localized inflammatory irritation of the spinal ganglia. Neuroscience 142: 809-822.

417. Xu JT, Xin WJ, Zang Y, Wu CY, Liu XG (2006) The role of tumor necrosis factor-alpha in the neuropathic pain induced by Lumbar 5 ventral root transection in rat. Pain 123: 306-321.

418. Yao H, Donnelly DF, Ma C, LaMotte RH (2003) Upregulation of the hyperpolarization-activated cation current after chronic compression of the dorsal root ganglion. J Neurosci 23: 2069-2074.

419. Yasaka T, Kato G, Furue H, Rashid MH, Sonohata M, Tamae A, Murata Y, Masuko S, Yoshimura M (2007) Cell-type-specific excitatory and inhibitory circuits involving primary afferents in the substantia gelatinosa of the rat spinal dorsal horn in vitro. The Journal of Physiology 581: 603-618.

420. Yonehara N, Yoshimura M (2001) Influence of painful chronic neuropathy on neurogenic inflammation. Pain 92: 259-265.

421. Yoshida S, Matsuda Y, Samejima A (1978) Tetrodotoxin-resistant sodium and calcium components of action potentials in dorsal root ganglion cells of the adult mouse. J Neurophysiol 41: 1096-1106.

422. Yoshida S, Matsumoto S (2005) Effects of +¦-Dendrotoxin on K+ Currents and Action Potentials in Tetrodotoxin-Resistant Adult Rat Trigeminal Ganglion Neurons. J Pharmacol Exp Ther 314: 437-445.

423. Yusaf SP, Goodman J, Pinnock RD, Dixon AK, Lee K (2001) Expression of voltage-gated calcium channel subunits in rat dorsal root ganglion neurons. Neuroscience Letters 311: 137-141.

424. Zamponi GW, Lewis RJ, Todorovic SM, Arneric SP, Snutch TP (2009) Role of voltage-gated calcium channels in ascending pain pathways. Brain Research Reviews 60: 84-89.

425. Zelenka M, Schafers M, Sommer C (2005) Intraneural injection of interleukin-1beta and tumor necrosis factor-alpha into rat sciatic nerve at physiological doses induces signs of neuropathic pain. Pain 116: 257-263.

426. Zhang JM, Donnelly DF, Song XJ, Lamotte RH (1997) Axotomy Increases the Excitability of Dorsal Root Ganglion Cells With Unmyelinated Axons. J Neurophysiol 78: 2790-2794.

427. Zhang XF, Gopalakrishnan M, Shieh CC (2003) Modulation of action potential firing by iberiotoxin and NS1619 in rat dorsal root ganglion neurons. Neuroscience 122: 1003-1011.

428. Zhang XL, Mok LP, Katz EJ, Gold MS (2010) BKCa currents are enriched in a subpopulation of adult rat cutaneous nociceptive dorsal root ganglion neurons. Eur J Neurosci 31: 450-462.

429. Zhang YH, Chi XX, Nicol GD (2008) Brain-derived neurotrophic factor enhances the excitability of rat sensory neurons through activation of the p75 neurotrophin receptor and the sphingomyelin pathway. J Physiol 586: 3113-3127.

430. Zhou XF, Deng YS, Chie E, Xue Q, Zhong JH, McLachlan EM, Rush RA, Xian CJ (1999) Satellite-cell-derived nerve growth factor and neurotrophin-3 are involved in noradrenergic sprouting in the dorsal root ganglia following peripheral nerve injury in the rat. Eur J Neurosci 11: 1711-1722.

431. Zhuang ZY, Wen YR, Zhang DR, Borsello T, Bonny C, Strichartz GR, Decosterd I, Ji RR (2006) A peptide c-Jun N-terminal kinase (JNK) inhibitor blocks mechanical allodynia after spinal nerve ligation: respective roles of JNK activation in primary sensory neurons and spinal

astrocytes for neuropathic pain development and maintenance. J Neurosci 26: 3551-3560.

432. Zuo Y, Perkins NM, Tracey DJ, Geczy CL (2003) Inflammation and hyperalgesia induced by nerve injury in the rat: a key role of mast cells. Pain 105: 467-479.

# CHAPTER 2

Methods

### *2.1 Primary Cell Cultures*

Establishment of (dorsal root ganglion) DRG cell cultures was a modification of procedures previously decribed by Lindsay (1988) and Acheson et al. (1995). Male Sprague Dawley rats (18–20 days old) were anaesthetized with 1g/mL ethyl carbamate (Sigma, St. Louis, MO, USA). DRGs (14-21/animal) were aseptically dissected from thoracic and lumbar spinal segments and collected in Dulbecco's Modified Eagle Medium supplemented with 10% heat inactivated horse serum (both from Gibco, Grand Island, NY, USA) (DMEMHS). Ganglia were enzymatically treated for 1.5 hrs with 0.125% type IV collagenase (Worthington, Lakewood, NJ, USA), washed twice in $Ca^{2+}$/$Ba^{2+}$-free Phosphate Buffer Solution (PBS), treated with 0.25% trypsin (from bovine pancreas, Sigma) in PBS for 30 min, washed 3 times in DMEMHS and finally taken up in 2 ml of DMEMHS containing 80 ug/mL type IV DNAse (Sigma) and 100 ug/mL soybean trypsin inhibitor (Worthington). A single cell suspension was then readily obtained by trituration of the enzymatically softened ganglia by 6-8 passages through the tip of a 1mL Eppendorf pipette. Neurons were plated the following day after neuronal cell enrichment (purification).

#### *2.1.1 Neuronal cell enrichment*

Neuronal cell enrichment (Figure 2-1) was aimed at minimizing the effects of IL-1β secondary to the involvement of mitotic (non-neuronal) cells (Lindsay, 1988). Non-neuronal cells were largely eliminated at outset by the use of differential adhesion and treatment with anti-mitotic agents, followed by

differential sedimentation procedures. More specifically, dissociated ganglia were plated (in DMEMHS supplemented with the anti-mitotic combination: Cytosine 3-D-Arabino-Furanoside (Ara-C), uridine and 5-fluoro-2'-deoxyuridine (all from Sigma and all at 10 μM)) in two 50 mm culture dishes (preplates) (Corning, NY, USA) previously coated with 3 ug/mL polyornithine (Sigma). After 15-20 hr, the non-neuronal cells become firmly attached to the dish, while most of the neurons (large, phase-bright cells; also see Figure 2-2) are only weakly adherent to the dish or to flattened non-neuronal cells. Then, by carefully removing the culture medium, most dead cells and axonal / myelin debris were discarded prior to selectively dislodging the attached neurons with a gentle stream of serum free defined medium (1:3 F12:DMEM supplemented with 1/100 N-2 supplement and 1/100 Penicillin/Streptomycin/Amphotericin B (all from Gibco)) delivered from a 1 mL Eppendorf pipette. The neurons from the two preplates were collected in a total of 12 mL of defined medium in a conical tube. Further neuronal enrichment was achieved by centrifugation of the cell suspension at 500 rpm for 5 min, whereupon viable neurons are lightly pelleted, leaving myelin debris, dead cells, and small non-neuronal cells in suspension. The supernatant was discarded and the cells were then re-suspended in 1 mL of defined medium. At 100 μL volumes, the cells were plated into 35 mm tissue culture dishes (Nunc, Roskilde, Denmark) pre-coated with 3 ug/mL polyornithine (Sigma) and 2 ug/mL laminin (Sigma). All dishes were then filled with a neurotrophin- and serum-free defined medium at ~ 2 mL/ dish. Cells were maintained at $36.5^0$C, 95% air : 5% $CO_2$. Defined medium was exchanged every 72 hrs.

*2.1.2 Treatment of DRG neurons*

Since DRG neuron phenotypic shift is likely to occur in long-term cell cultures (Aguayo et al., 1991), a preliminary attempt to curtail this effect involved the maintenance of cell cultures in DMEMHS with 50 ng/mL exogenously added nerve growth factor (NGF). Under investigation using enzyme-linked immunosorbent assay (ELISA), however, ambient concentrations of IL-1β in control DRG cell cultures were unstable and approached test concentrations of IL-1β (100 pM). In contrast, control cell cultures maintained in defined medium, without NGF, produced IL-1β concentrations which were consistently near or below the detection limit for ELISA (≤ 5pM, see below; Figure 2-3) and, therefore, became the accepted approach.

To this end, after 3 days in culture with defined medium, dishes were divided into 2 treatment groups (Figure 2-4): 100 pM IL-1β (Peprotech, Rocky Hill, NJ, USA; prepared in 0.1% Bovine Serum Albumin (BSA) (Sigma)) and control (0.1% BSA). For antagonist experiments (IL-1Ra; R & D systems, Minneapolis, MN, USA), the two treatment groups were: IL-1β + 100 ng/mL IL-1Ra (prepared in 0.1% BSA) and control + IL-1Ra (which will be referred to as internal control). Treatments were applied for the following 5-6 days, with defined medium exchanges every 72 hrs.

***2.2 Enzyme-Linked Immunosorbent Assay (ELISA)***

Sandwich ELISAs were used to measure ambient IL-1β levels *as per* standard protocols used by Dr. Aaron Lai and Dr. Kathryn Todd (Centre for

Neuroscience, University of Alberta, Edmonton, AB, Canada). The capture antibody (R&D, #AF-501-NA), diluted 200 ng/mL in TBS-T (Tris-buffered saline with 0.1% Tween), was coated on 96-well plates overnight. The coated plates were blocked with 1% albumin (in TBS-T; Sigma) for two hours. The samples (obtained from DRG culture medium exchanges) were then added to the wells and incubated for four hours. The plates were then incubated with the detection antibody (R&D, #MAB5011), diluted 500 ng/mL in TBS-T, for four hours, followed by incubation with biotinylated 1:1000 anti-mouse IgG (Serotec, Raleigh, NC, USA) for 30 minutes, then with 1:1000 horseradish peroxidase-conjugated strepavidin (Dako, Burlington, ON, Canada), both diluted in TBS-T, for 30 minutes. Colour development was produced by the addition of the chromagen tetramethylbenzidine (Biosource, Camarillo, CA, USA), and the reaction was stopped with equal volume of 3M sulfuric acid. All steps above were carried out at room temperature, and three TBS-T washes were applied in between each step. The developed plates were read on a spectrophotometer at 450 nm. Signal intensities from a sample were compared to signal intensities from the respective calibrated standard curve to permit protein quantification. Each sample was run in duplicate, and IL-1β concentrations will be reported as averages.

### *2.3 Subclassification of DRG Neurons*

Based on previously established criteria, DRG neurons were classified according to soma diameter as 'small' (< 30 μm), 'medium' (30-40 μm), or 'large' (>40 μm) as measured with a calibrated micrometer that fits on the eye

piece of a Nikon TE300 inverted fluorescence microscope (Nikon, Toronto, ON, Canada) (Lu et al., 2006;Caffrey et al., 1992;Scroggs and Fox, 1992). Thus, DRG neurons with large-sized cell bodies are likely to be non-nociceptive afferents (Aα/β –fibres), while small-sized cell bodies are likely to be nociceptive afferents (C-fibres) (Caffrey et al., 1992;Lu et al., 2006;Lawson, 2002;Harper and Lawson, 1985). Medium-sized cell bodies likely represent a mixed population of nociceptive and non-nociceptive afferents (Aδ-fibres).

Since small diameter IB4-positive and –negative sensory neurons are believed to be functionally distinct with regard to pain physiology (Fang et al., 2006;Fjell et al., 1999;Stucky and Lewin, 1999;Snider and McMahon, 1998), the plant (*Griffonia simplicifolia*) lectin, isolectin B4 (IB4), was added in selected DRG cell cultures on day 1 (preplates for 30 minutes before removal) at 30 μg/mL (Fjell et al., 1999) (Figure 2-4). Under fluorescence microscopy, binding to IB4 Alexa Fluor® 488 conjugate (Invitrogen, Eugene, OR, USA ) identified small neurons as IB4-positive or –negative (Silverman and Kruger, 1990). To limit misclassification of small IB4-negative or, possibly, peptidergic (CGRP-positive) visceral DRG neurons as small IB4-positive (Robinson et al., 2004), only the most intensely stained small DRG neurons were considered IB4-positive.

### *2.4 Electrophysiology*

Whole-cell recordings (at room temperature, 22°C) were made using an AXOCLAMP 2A amplifier (Axon Instruments, Foster City, CA, USA) in either bridge-balance current-clamp mode or discontinuous single-electrode voltage-

clamp mode as described previously (Abdulla and Smith, 2001b;Abdulla and Smith, 2001a;Abdulla and Smith, 2002). With regard to voltage-clamp studies, low resistance patch electrodes (2-5 MΩ) permitted the use of high switching frequencies >30 kHz with high clamp gains (8-30 mV/nA). The effectiveness of the voltage-clamp was confirmed by examining recordings of the command voltage and recording from neurons where the voltage trace was slow to rise or distorted were discarded. The total volume of fluid in the recording dishes was ~1 mL. The Petri dishes were superfused at a flow rate of 2 mL/min. Input capacitance ($C_{in}$) was calculated from the membrane time constant and input resistance or by the integration of the capacitative transient generated by a 10 mV voltage step (Abdulla and Smith, 1997).

### *2.4.1 Action potential (AP) recordings*

For action potential (AP) recordings, external solution contained (in mM) 127 NaCl, 2.5 KCl, 1.2 $NaH_2PO_4$, 26 $NaHCO_3$, 2.5 $CaCl_2$, 1.3 $MgSO_4$ and 25 D-glucose saturated with 95% $O_2$ – 5% $CO_2$. Internal (pipette) solution contained (in mM) 130 KGluconate, 4 Mg-ATP, 0.3 Na-GTP, 10 EGTA, 2 $CaCl_2$ and 10 HEPES (adjusted to pH 7.2 with KOH; osmolarity 310-320 mOsm). Current-clamp recordings were made at RMP and APs were generated using 5 ms depolarizing current pulses. Rheobase was defined as the minimum amount of depolarizing current that discharged an AP in 50% of trials. Spike width (AP

duration) was measured at 50% maximum amplitude. Afterhyperpolarization (AHP) duration was measured at 50 and at 25% repolarization. To quantify changes in excitability in response to a series of 450 ms current ramps and 800 ms current steps, the latency of each AP (cumulative latency), AP firing frequency and AP number were measured. In order to assess the response of DRG neurons to membrane hyperpolarization, voltage sag was measured in response to an 800 ms step at -0.1 nA.

### *2.4.2 Sodium current ($I_{Na}$) recordings*

To limit contributions from voltage-gated $Ca^{2+}$ and $K^+$ currents, $I_{Na}$ was recorded in an external solution containing the following (in mM): 75 mM TEA-Cl, 50 NaCl (to improve voltage-clamp control), 5 KCl, 4 $MgCl_2$, 10 HEPES and 60 D-glucose (adjusted to pH 7.4 with NaOH; osmolarity 330 mOsm). Internal solution contained the following (in mM): 140 CsCl, 10 NaCl, 2 MgATP, 0.3 $Na_2GTP$, 2 EGTA, 10 HEPES and 2 $MgCl_2$ (adjusted to pH 7.2 with NaOH; osmolarity 300-310 mOsm). Tetrodotoxin (TTX) (Alomone Labs, Jerusalem, Israel) (300 nM) was applied by superfusion. Total $I_{Na}$ was recorded in response to 40 ms depolarizing voltage commands from a holding potential ($V_h$ = -90 mV) and leak subtracted by means of a p/4 protocol. Thus, a series of one-fourth amplitude, reversed polarity voltage commands were applied, and the recorded currents multiplied by four and added to the recordings of $I_{Na}$. Current decay (fast inactivation) was fitted with a single exponent function: $f(t)=\sum_{i=1}^{n} Ai\, e^{-t/\tau i}$ + C.

For voltage dependence of activation, normalized ($I/I_{-20}$ ) *I-V* curves were fit with a single Boltzmann function: y = A2 + (A1-A2)/(1 + exp((x-x0)/dx)). $I_{Na}$ steady-state fast inactivation protocol involved 300 ms incremental depolarizing prepulses preceded 10 ms test pulses to -10 mV to determine the fraction of current available ($I/I_{-110}$). $I_{Na}$ steady-state slow inactivation protocol involved 5 s prepulses, followed by 20 ms recovery pulses to -120 mV (to allow recovery from fast inactivation), preceded 10 ms test pulses to -10 mV to determine the fraction of current available ($I/I_{-120}$). To obtain the TTX-S and TTX-R components of the current, currents persisting in the presence of 300 nM TTX were subtracted from the corresponding values of total $I_{Na}$.

### *2.4.3 Hyperpolarization-activated cation current ($I_H$) recordings*

$I_H$ was recorded in an external solution containing the following (in mM): 150 NaCl, 5 KCl, 2.5 $CaCl_2$, 1 $MgCl_2$, 10 HEPES and 10 D-glucose (adjusted to pH 7.4 with NaOH; osmolarity 330-340 mOsm). Internal solution contained (in mM) 130 KGluconate, 2 Mg-ATP, 0.3 Na-GTP, 11 EGTA, 10 HEPES and 1 $CaCl_2$ (adjusted to pH 7.2 with KOH; osmolarity 310-320 mOsm). $I_H$ was elicited by a series of hyperpolarizing voltage commands (from -60 mV to -130 mV) that were also incremental in duration (from 4.25 s to 2.5 s) from a $V_h$ of -50 mV. When possible, the presence of $I_H$ was confirmed with block by ZD7288 (100 μM; Tocris, Ellisville, MO, USA). The time course for the activation of $I_H$

was fit with the sum of a two exponential function: $f(t)=\sum_{i=1}^{n} Ai\ e^{-t/\tau i}$ + C. For the voltage dependence of activation, the conductance ratio, $G/G_{-130}$, was calculated from tail current ($I_{H,Tail}$) amplitudes measured 100 – 200 ms after repolarization and curves were fit with a single Boltzmann function: y = A2 + (A1-A2)/(1 + exp((x-x0)/dx)).

### *2.4.4 Calcium current ($I_{Ba}$) recordings*

$Ca^{2+}$ channel currents ($I_{Ca}$) were measured using $Ba^{2+}$ as a charge carrier ($I_{Ba}$). For these experiments, external "$Ba^{2+}$" solution contained (in mM) 160 TEA-Cl, 10 HEPES, 2 $BaCl_2$, 10 D-glucose and 300 nM TTX (adjusted to pH 7.4 with TEA-OH; osmolarity 330-340 mOsm). Internal solution contained (in mM) 120 CsCl, 5 Mg-ATP, 0.4 $Na_2$-GTP, 10 EGTA and 20 HEPES (adjusted to pH 7.2 with CsOH; osmolarity 300-310 mOsm). $I_{Ba}$ currents were evoked using a series of 150 ms depolarizing voltage commands from $V_h$ = -100 mV or $V_h$ = -60 mV and leak subtracted by means of a p/6 protocol. For the voltage dependency of $I_{Ba}$ inactivation, the fraction of current available at $V_{cmd}$ = -10 mV was determined in response to a series of 3.5 s incremental prepulses from $V_h$ = -100 mV. Normalized ($I/I_{-110}$) inactivation curves were fit with a single Boltzmann function: y = A2 + (A1-A2)/(1 + exp((x-x0)/dx)).

*2.4.5 Potassium current ($I_K$) recordings*

For recording $K^+$ currents, external solution contained (in mM) 145 *N*-methyl-D-glucamine (NMG)Cl, 10 KCl, 2.5 $CaCl_2$, 10 HEPES, 1.0 $MgCl_2$ and 10 D-glucose (adjusted to pH 7.4 with HCl; 320 mosm). Internal solution contained (in mM) 100 K gluconate, 40 NMG-Cl, 2 Mg-ATP, 0.3 $Na_2GTP$, 11 EGTA, 10 HEPES and 0.1 $CaCl_2$ (adjusted to pH 7.2 with HCl; 300 mosm). In view of the complexity and variability of potassium currents in DRG neurons (Akins and McCleskey, 1993;Gold et al., 1996), a relatively simplified approach has been used for their isolation in my study. $I_K$ currents were recorded at voltages between -60 mV and +60 mV (from a holding potential ($V_h$) of -80 mV) after a 500 ms conditioning prepulse ($V_p$) to -120 mV or -30 mV and leak subtracted by means of a p/6 protocol. Digital subtraction (Vp = -120 mV – Vp = -30 mV) revealed the presence of an inactivating current component and is likely attributed to the presence of A-type potassium currents and/or the presence of $I_{K,Ca}$ which may decline as a consequence to the inactivation of calcium conductances (Abdulla and Smith, 2001b). In the presence of 5 mM $Mn^{2+}$ (to block $I_{Ca}$), a steady-state non-inactivating component could be measured at the end of the stimulation pulse when preceded by $V_p$ = -30 mV and is likely to be delayed-rectifier potassium current (referred to as non-inactivating $I_K$). To isolate A-type currents, the subtraction process was repeated in the presence of 5 mM $Mn^{2+}$. Since A-type currents in DRG neurons may reflect the existence of $I_{Af}$, $I_{As}$ (or $I_D$) and $I_{Aht}$ (Gold et al., 1996;Everill et al., 1998), in this study they are collectively referred to as inactivating $Mn^{2+}$-resistant ($Mn^{2+}$ -R) $I_K$. Last, digital subtraction of

outward current (recorded at $V_p$ = -120 mV) remaining in the presence of 5mM $Mn^{2+}$ from total outward current yielded $I_{K,Ca}$ (referred to as inactivating $Mn^{2+}$ -sensitive ($Mn^{2+}$ -S) $I_K$).

### *2.5 Analysis and Statistics*

All electrophysiological data were acquired and analyzed using pCLAMP 10 software (Axon Instruments). Figures were produced with Origin 8.0 (OriginLab, Northampton, MA, USA) or Adobe Illustrator 10 (Adobe Software, San Jose, CA, USA). Where applicable, data were presented as mean ± standard error of mean (s.e.m.). Statistical comparisons were made with unpaired t-test, Mann-Whitney U test, Fisher's exact-test or one-way analysis of variance (ANOVA) with post-hoc Tukey's multiple comparisons test. *P values* from these statistical tests were generated using GraphPad Prism 5.00 (GraphPad Software, San Diego, CA, USA). Statistical significance was taken as $p<0.05$.

***Figure 2-1: Neuronal cell enrichment strategy***

Neuronal cell enrichment was aimed at minimizing the effects of IL-1β secondary to the involvement of mitotic (non-neuronal) cells. *As per* Lindsay (1988), non-neuronal cells were largely eliminated at outset by the use of differential adhesion (1) and treatment with anti-mitotic agents (2), followed by differential sedimentation procedures (3).

1) Differential adhesion in preplates. Dissociated ganglia were plated in 50 mm culture dishes (preplates) coated with 3 ug/mL polyornithine (O). After 15-20 hr, the non-neuronal cells become firmly attached to the dish, while most of the neurons (large, phase-bright cells; also see Figure 2-2) are only weakly adherent to the dish or to flattened non-neuronal cells.

2) Treatment with anti-mitotic agents. Preplates were filled with DMEMHS supplemented with the anti-mitotic combination: Cytosine 3-D-Arabino-Furanoside (Ara-C), uridine and 5-fluoro-2'-deoxyuridine (all at 10 μM).

3) Differential sedimentation. The neurons from the two preplates were collected in a total of 12 mL of defined medium in a conical tube and centrifugation of the cell suspension at 500 rpm for 5 min lightly pelleted viable neurons, leaving myelin debris, dead cells, and small non-neuronal cells in suspension. The supernatant was discarded and the cells were then re-suspended in 1 mL of defined medium. At 100 μL volumes, the cells were plated into 35 mm tissue culture dishes pre-coated with 3 ug/mL polyornithine and 2 ug/mL laminin (L).

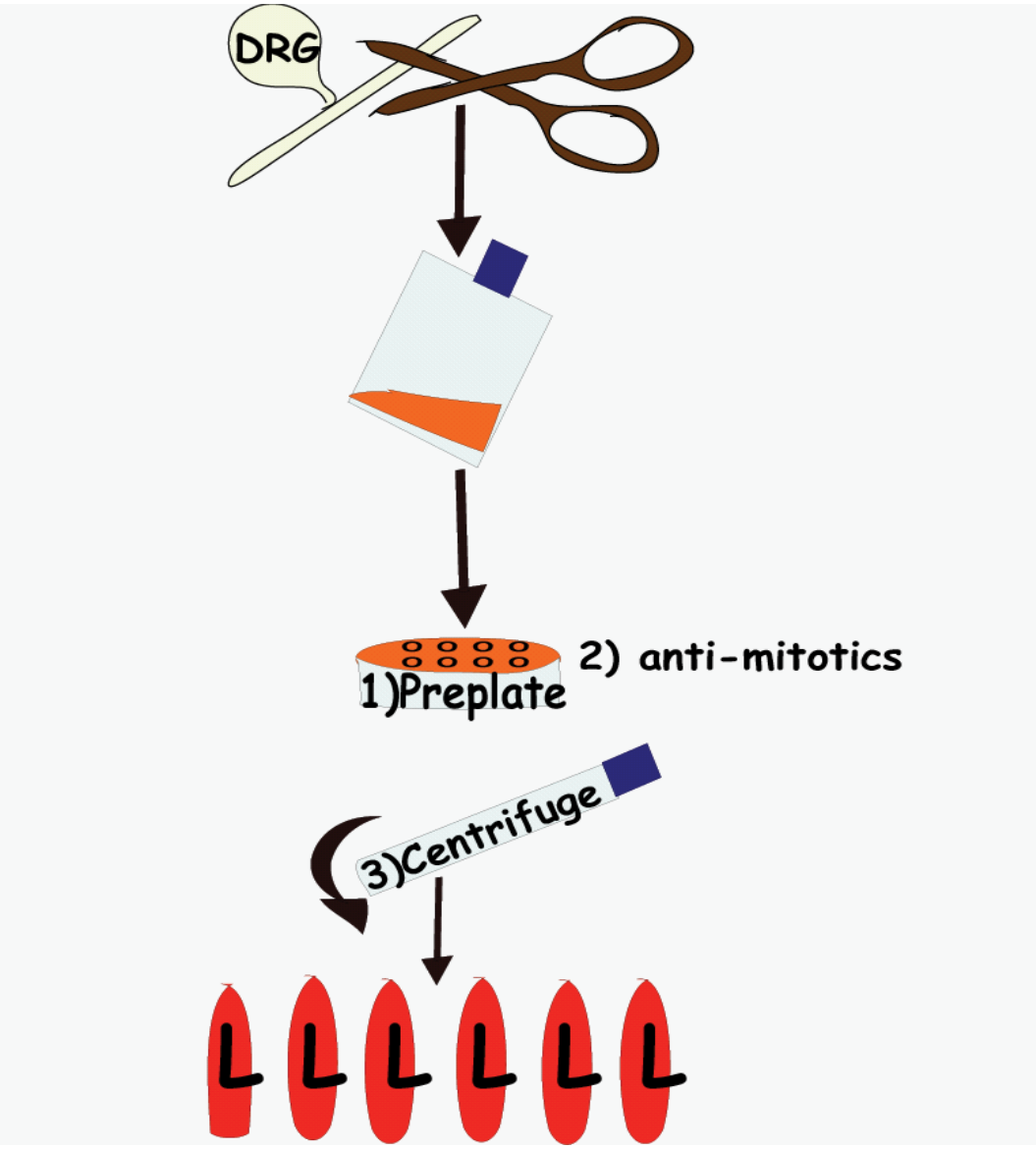
DRG
1)Preplate
2) anti-mitotics
3)Centrifuge

***Figure 2-2: Phase-contrast images of dissociated DRG cultures and the effect of neuronal cell enrichment***

A) Preplates (0 days in culture). In preplates, the small dark non-neuronal cells (likely to be fibroblasts and Schwann cells) become firmly attached to the dish, while most of the neurons (large, phase-bright cells; yellow arrows) are only weakly adherent to the dish or to flattened non-neuronal cells.

B) Neuronal cell enrichment (9 days in culture). Neuronal cell enrichment yielded low density cell cultures where individual neurons (yellow arrow) appeared to be isolated from other DRG cells.

C) Without enrichment (9 days in culture). In the absence of neuronal cell enrichment, non-neuronal cells continued to proliferate and formed a confluent monolayer within 1 week. Under these conditions, individual neurons (yellow arrow) could not be isolated for other DRG cells.

Scale bar, 50 μm.

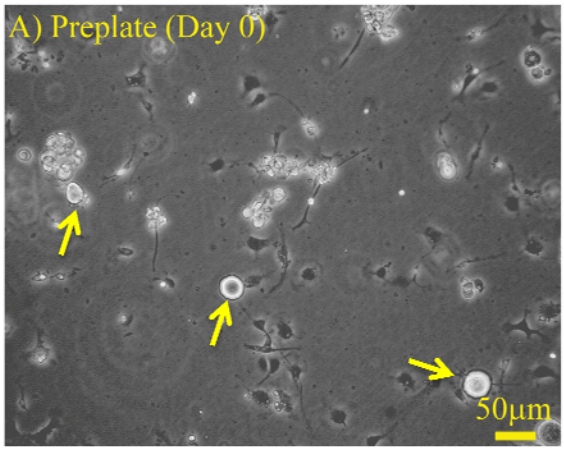
A) Preplate (Day 0)
50µm

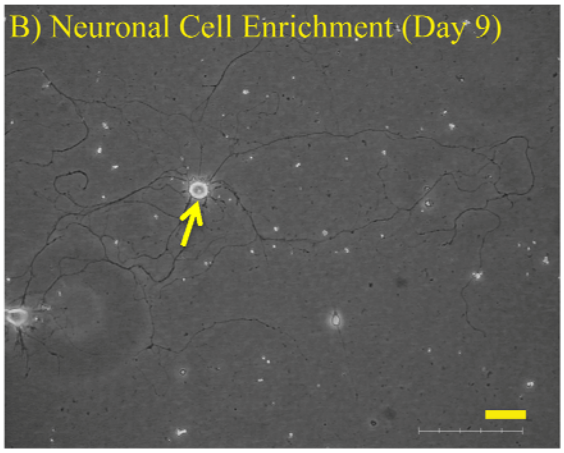
B) Neuronal Cell Enrichment (Day 9)

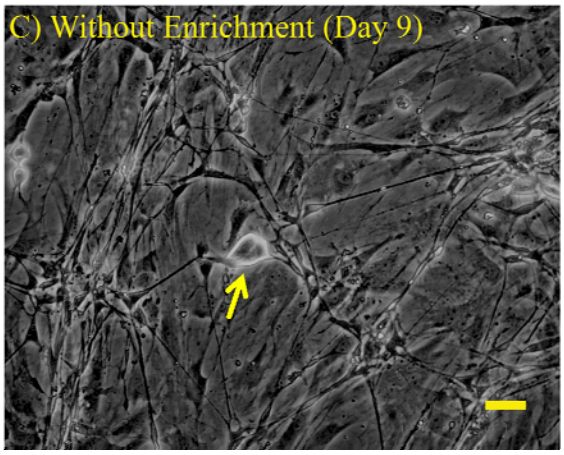
C) Without Enrichment (Day 9)

***Figure 2-3: ELISA measurements of ambient IL-1β levels in culture***

Under investigation using enzyme-linked immunosorbent assay (ELISA), ambient concentrations of IL-1β in control DRG cell cultures maintained in neurotrophin- and serum free- (defined) medium, produced IL-1β concentrations which were consistently near or below the detection limit for ELISA (≤ 5pM).

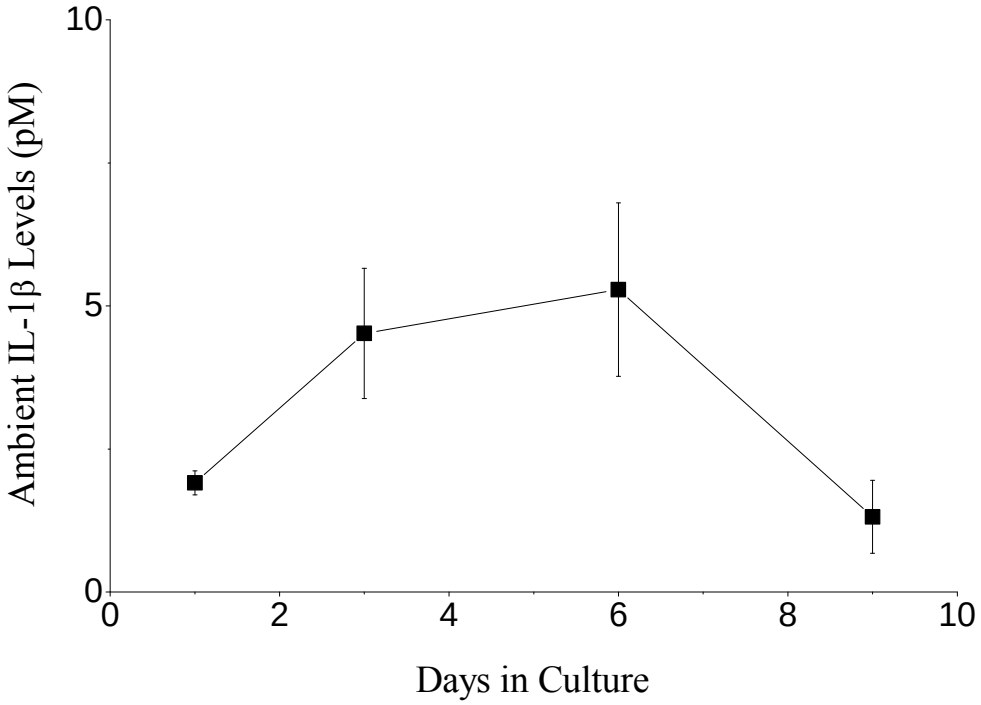
Ambient IL-1β Levels (pM)
10
5
0
0
2
4
6
8
10
Days in Culture

***Figure 2-4: DRG cell culture treatment protocols***

After 15-20 hrs in preplates with DMEMHS, the plant (*Griffonia simplicifolia*) lectin, isolectin $B_4$ ($IB_4$), was added in selected DRG cell cultures for 30 minutes before removal at 30 μg/mL (Fjell et al., 1999).

After 3 days in cell culture with defined medium, dishes were divided into 2 treatment groups: 100 pM IL-1β (prepared in 0.1% BSA) and control (0.1% BSA). For antagonist experiments, the two treatment groups were: 100 pM IL-1β + 100 ng/mL IL-1Ra (prepared in 0.1% BSA) and control + IL-1Ra (which will be referred to as internal control). Treatments were applied for the following 5-6 days, with defined medium exchanges every 72 hrs.

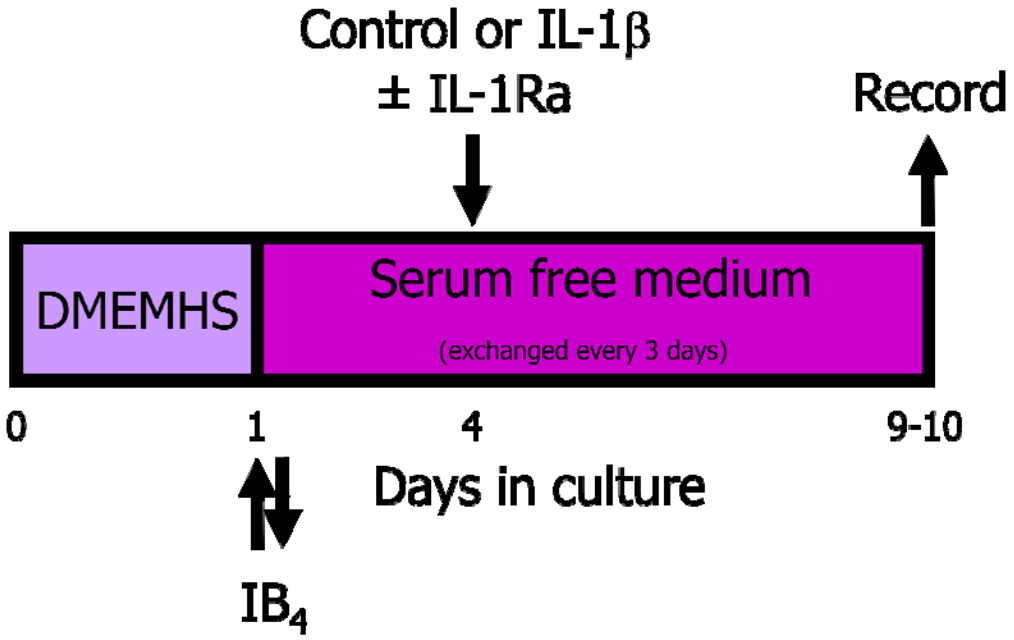
Control or IL-1β
± IL-1Ra
Record
DMEMHS
Serum free medium
(exchanged every 3 days)
0
1
4
9-10
Days in culture
IB4

### *2.6 References*


1. Abdulla FA, Smith PA (1997) Ectopic alpha2-adrenoceptors couple to N-type Ca2+ channels in axotomized rat sensory neurons. J Neurosci 17: 1633-1641.

2. Abdulla FA, Smith PA (2001a) Axotomy- and autotomy-induced changes in the excitability of rat dorsal root ganglion neurons. J Neurophysiol 85: 630-643.

3. Abdulla FA, Smith PA (2002) Changes in Na(+) channel currents of rat dorsal root ganglion neurons following axotomy and axotomy-induced autotomy. J Neurophysiol 88: 2518-2529.

4. Abdulla FA, Smith PA (2001b) Axotomy- and Autotomy-Induced Changes in Ca2+and K+ Channel Currents of Rat Dorsal Root Ganglion Neurons. J Neurophysiol 85: 644-658.

5. Acheson A, Conover JC, Fandl JP, DeChiara TM, Russell M, Thadani A, Squinto SP, Yancopoulos GD, Lindsay RM (1995) A BDNF autocrine loop in adult sensory neurons prevents cell death. Nature 374: 450-453.

6. Aguayo LG, Weight FF, White G (1991) TTX-sensitive action potentials and excitability of adult rat sensory neurons cultured in serum- and exogenous nerve growth factor-free medium. Neurosci Lett 121: 88-92.

7. Akins PT, McCleskey EW (1993) Characterization of potassium currents in adult rat sensory neurons and modulation by opioids and cyclic AMP. Neuroscience 56: 759-769.

8. Caffrey JM, Eng DL, Black JA, Waxman SG, Kocsis JD (1992) Three types of sodium channels in adult rat dorsal root ganglion neurons. Brain Research 592: 283-297.

9. Everill B, Rizzo MA, Kocsis JD (1998) Morphologically Identified Cutaneous Afferent DRG Neurons Express Three Different Potassium Currents in Varying Proportions. J Neurophysiol 79: 1814-1824.

10. Fang X, Djouhri L, McMullan S, Berry C, Waxman SG, Okuse K, Lawson SN (2006) Intense Isolectin-B4 Binding in Rat Dorsal Root Ganglion Neurons Distinguishes C-Fiber Nociceptors with Broad Action Potentials and High Nav1.9 Expression. J Neurosci 26: 7281-7292.

11. Fjell J, Cummins TR, Dib-Hajj SD, Fried K, Black JA, Waxman SG (1999) Differential role of GDNF and NGF in the maintenance of two

TTX-resistant sodium channels in adult DRG neurons. Brain Res Mol Brain Res 67: 267-282.

12. Gold MS, Shuster MJ, Levine JD (1996) Characterization of six voltage-gated K+ currents in adult rat sensory neurons. J Neurophysiol 75: 2629-2646.

13. Harper AA, Lawson SN (1985) Conduction velocity is related to morphological cell type in rat dorsal root ganglion neurones. J Physiol 359: 31-46.

14. Lawson SN (2002) Phenotype and function of somatic primary afferent nociceptive neurones with C-, Adelta- or Aalpha/beta-fibres. Exp Physiol 87: 239-244.

15. Lindsay RM (1988) Nerve growth factors (NGF, BDNF) enhance axonal regeneration but are not required for survival of adult sensory neurons. J Neurosci 8: 2394-2405.

16. Lu SG, Zhang X, Gold MS (2006) Intracellular calcium regulation among subpopulations of rat dorsal root ganglion neurons. The Journal of Physiology 577: 169-190.

17. Robinson DR, McNaughton PA, Evans ML, Hicks GA (2004) Characterization of the primary spinal afferent innervation of the mouse colon using retrograde labelling. Neurogastroenterology & Motility 16: 113-124.

18. Scroggs RS, Fox AP (1992) Calcium current variation between acutely isolated adult rat dorsal root ganglion neurons of different size. J Physiol 445: 639-658.

19. Silverman JD, Kruger L (1990) Selective neuronal glycoconjugate expression in sensory and autonomic ganglia: relation of lectin reactivity to peptide and enzyme markers. Journal of Neurocytology 19: 789-801.

20. Snider WD, McMahon SB (1998) Tackling Pain at the Source: New Ideas about Nociceptors. Neuron 20: 629-632.

21. Stucky CL, Lewin GR (1999) Isolectin B(4)-positive and -negative nociceptors are functionally distinct. J Neurosci 19: 6497-6505.

# CHAPTER 3

The Effects of Long-term IL-1β Exposure on DRG Neuron Excitability

### *3.1 Results*

*3.1.1 Electrical properties of control DRG neurons in long-term cell culture*

All neurons were recorded at RMP. Neurons with RMP less than -40 mV had a tendency not to fire APs and were omitted from further study. Figure 3-1A illustrates representative recordings of APs elicited in 12 large, 36 medium, 20 small IB4-positive and 23 small IB4-negative control neurons by a 5 ms pulse of depolarizing current set at rheobase. Evident from the traces and summarized in Table 3-1, small IB4-negative neurons had the broadest spike width (measured at half maximal AP height) along with a prominent shoulder on the AP falling phase. The maximal rate of repolarization in the falling phase of small IB4-negative neuron APs was also slower and significant (ANOVA-Tukey test, $p<0.05$) when compared to the fastest rates exhibited in large neurons (Table 3-1). Small IB4-positive neurons had a larger AHP amplitude than small-sized IB4-negative neurons (ANOVA-Tukey test, $p<0.05$). In contrast, AHP duration at 25% and 50% repolarization was unaltered among the four DRG neuron types. However, some neurons had a more gradual repolarization and did not achieve 50% or, in some cases, 25% recovery within the sweep duration (83 ms) remaining after the square current pulse. For instance, 2 (10% of total) small IB4-positive and 4 (17.4% of total) small IB4-negative neurons failed to repolarize to 50%, while 1 (8.3% of total) large neuron failed to repolarize to 25%. In medium neurons, rheobase was significantly greater when compared to small IB4-positive and –negative neurons (ANOVA-Tukey test, $p<0.05$ and $p<0.001$, respectively), whereas, RMP was significantly greater than that recorded in large and small IB4-

negative neurons (ANOVA-Tukey test, $p<0.01$ and $p<0.05$, respectively). Of the total 91 control neurons recorded, after-depolarization (ADP) and spontaneous discharge were never observed.

Passive properties were measured from membrane responses to hyperpolarizing current pulses 800 ms in duration at RMP. Large neurons exhibited the smallest input resistances and were significantly smaller than in both small IB4-positive and –negative neurons (ANOVA-Tukey test, $p<0.001$; Table 3-1). In addition, large, medium and small IB4-positive neurons had significantly smaller input resistances than small IB4-negative neurons (ANOVA-Tukey test, $p<0.001$, $p<0.001$ and $p<0.05$, respectively). Medium neurons had the largest input capacitances and these were significantly larger than in both large and small IB4-negative neurons (ANOVA-Tukey test, $p<0.05$ and $p<0.001$, respectively). Last, membrane time constants were shortest in large-sized neurons with significance when compared to both medium and small IB4-positive neurons (ANOVA-Tukey test, $p<0.05$).

### *3.1.2 Effect of acute IL-β exposure on DRG neuron excitability in long-term cell culture*

Since acutely isolated sensory neurons are known to express functional IL-1RI receptors (Binshtok et al., 2008;Copray et al., 2001), the response of neurons to IL-1β after four days in culture was examined. As depicted with a representative experiment in Figure 3-2, acute (60 s) application of 100 pM IL-1β produced a rapid increase in DRG neuron excitability. A medium neuron unable

to fire in response to a 2 nA depolarizing current ramp (Figure 3-2A), suddenly began to fire after focal perfusion with IL-1β for 1 minute (Figure 3-2B).

### *3.1.3 Effects of long-term IL-β exposure on DRG neuron AP parameters and passive membrane properties*

#### *3.1.3.1 Effects of IL-1β exposure on medium neurons*

After 5-6 days exposure, the effects of 100 pM IL-1β were most prominent in medium DRG neurons (Table 3-2). IL-1β application significantly reduced rheobase (Figure 3-3A) and increased the maximal rates of both depolarization and repolarization (Figure 3-3B) in response to depolarizing current pulses 5 ms in duration (unpaired t-test, $p<0.05$, $p<0.001$ and $p<0.01$, respectively). As depicted in Figure 3-1, IL-1β significantly increased AP height, reduced AHP amplitude and shortened AHP duration at 50% repolarization (unpaired t-test, $p<0.01$; also see Table 3-2 and Figure 3-3C). However, 5 (13.2% of total) medium neurons failed to reach 50% repolarization after IL-1β exposure, whereas, all control neurons achieved 50% repolarization (Fisher's exact-test, $p>0.05$; Table 3-2). Last, IL-1β significantly reduced average input capacitance along with a faster membrane time constant (unpaired t-test, $p<0.01$ and $p<0.05$, respectively), but without alteration to input resistance.

#### *3.1.3.2 Effects of IL-1β exposure on small IB4-positive neurons*

These included a significant increase in spike width (Figure 3-1B inset) along with a concurrent decrease in the rate of repolarization (unpaired t-test, $p<0.01$ and $p<0.05$, respectively; Table 3-2 and Figure 3-3B). In addition, both

control and IL-1β treated cultures had small IB4-positive neurons (10% and 9.5% of total, respectively; Fisher's exact-test, $p>0.05$) in which the AHP did not reach 50% repolarization (Table 3-2).

*3.1.3.3 Effects of IL-1β exposure on large neurons*

There was no significant difference in the proportion of large neurons to recover from membrane hyperpolarization at 25% repolarization (8.3% of total control neurons vs. 10% of total IL-1β neurons; Fisher's exact-test, $p>0.05$; Table 3-2). In the absence of further changes to control neurons, 7 (70% of total) IL-1β treated large neurons significantly failed to reach 50% repolarization (Fisher's exact-test, $p<0.01$; Table 3-2). Additionally, large neurons had a significant increase in rheobase and a significantly longer duration to 25% repolarization after IL-1β exposure (unpaired t-test, $p<0.05$ and $p<0.01$, respectively; Figure 3-3A and 3C, respectively).

*3.1.3.4 Effects of IL-1β exposure on small IB4-negative neurons*

IL-1β application had no significant effects on AP characteristics or passive properties of small IB4-negative neurons, however, ADP was evident in 1 (4.2% of total) neuron (Fisher's exact-test, $p>0.05$).

Last, none of the total 93 DRG neurons recorded in IL-1β treated cultures displayed spontaneous firing.

*3.1.4 Effects of long-term IL-β exposure on DRG neuron excitability in response to current steps*

The influence of 100 pM IL-1β exposure on DRG neuron excitability was assessed from membrane responses to 800 ms depolarizing current steps evoked from RMP. Comparisons in discharge pattern and AP number were made at the minimum depolarizing current step to elicit firing in the greatest proportion of neurons. Thus, 800 pA current commands discharged all large and medium-sized neurons, whereas, 500 pA steps discharged all small IB4-positive neurons and 95.3% (41/43) of the total small IB4-negative DRG cells. As depicted in Figure 3-4, four different discharge patterns were observed. Some neurons discharged a single spike before accommodating and, under control conditions, this occurred in 66.7% of large neurons, 25% of medium neurons, 10% of small IB4-positive neurons and 34.8% of small IB4-negative neurons (Figure 3-5A). Other DRG neurons were slightly more excitable and discharged more than one AP before eventually accommodating (phasic discharge). In control cell cultures, phasic discharge was seen in 0% of large neurons, 41.7% of medium neurons, 50% of small IB4-positive neurons and 26.1% of small IB4-negative neurons. The third group of neurons displayed tonic discharge and fired APs throughout the application of depolarizing current. Under control conditions, tonic discharge was observed in 33.3% of large neurons, 33.3% of medium neurons, 40% of small IB4-positive neurons and 39.1% of small IB4-negative neurons. The fourth pattern, where discharge occurs intermittently throughout the current command (irregular discharge), was only observed in 1 (2.6% of total) IL-1β treated

medium neuron. As summarized in Figure 3-5A, the proportion of discharge patterns was not significantly altered in the presence of 5-6 days of IL-1β (Fisher's exact-test, $p>0.05$). In contrast, the average AP number in tonic discharging neurons was significantly increased in medium neurons exposed to IL-1β and a similar trend was apparent in small IB4-positive neurons (unpaired t-test, $p<0.05$ and $0.05<p\leq0.1$, respectively; Figure 3-5B). Since large neurons typically displayed single spike discharge behaviour, they were omitted from further current step analysis.

Multiple firing neurons have short interspike intervals or high frequency discharge (instantaneous frequency) between the initial two spikes (Figure 3-4C). As firing continues, however, the rate of discharge slows towards a steady-state frequency as indicated by wider interspike intervals between the final two spikes. Thus, the effect of IL-1β on repetitive discharge was analyzed more extensively through the plotting of frequency – current (*f-I*) curves (Figure 3-6). DRG neurons that discharged a single AP have an infinite initial and steady-state interspike interval, whereas, neurons that exhibited 2 APs have an initial discharge frequency and an infinite steady-state interspike interval (Abdulla and Smith, 2001). Infinite interspike intervals were excluded from discharge frequency analysis. Results for the instantaneous firing frequency are indicated in Figure 3-6A, while those for steady-state frequency are in Figure 3-6B. Qualitatively, the slopes of *f-I* curves were steeper (higher in gain) in IL-1β exposed medium neurons when compared to control conditions. Further, IL-1β exposure resulted in significantly higher instantaneous discharge frequencies for both medium and

small IB4-positive neurons (unpaired t-test, $p<0.05$; Figure 3-6A, Figures 3-7A and 3-7B). In response to the largest current injection (800 pA), steady-state frequency was also significantly increased in IL-1β treated medium neurons and a similar trend was observed in small IB4-positive neurons (unpaired t-test, $p<0.05$ and $0.05<p\leq0.1$, respectively; Figure 3-6B). No differences were observed in the repetitive firing behaviour of small IB4-negative neurons (Figures 3-5 and 3-6).

### *3.1.5 Effects of long-term IL-β exposure on DRG neuron excitability in response to current ramps*

The influence of 100 pM IL-1β exposure on DRG neuron repetitive discharge was also examined from membrane responses to 450 ms depolarizing current ramps (Figure 3-8A). All excitability analysis was conducted on ramps to 2 nA since this ramp resulted in the greatest number of DRG neurons to fire APs. In control cell cultures, discharge in response to 2 nA current ramps was seen in 41.7% of large neurons, 80.6% of medium neurons, 90% of small IB4-positive neurons and 81.8% of small IB4-negative neurons (Figure 3-8B). As summarized in Figure 3-8B, these proportions, in both medium and small neurons, were not significantly altered by 5-6 days exposure to IL-1β (Fisher's exact-test, $p>0.05$). In contrast, IL-1β exposure significantly increased the percentage of large neurons (90% vs. 41.7%) which discharged on current ramps (Fisher's exact-test, $p<0.05$; Figure 3-8B). Individual DRG neurons that did not fire were excluded from subsequent repetitive discharge analysis.

Further alterations in membrane excitability were determined through measurements of latencies to the formation of respective APs (cumulative latency; Figure 3-8A) and the total number of APs generated during current application (Figures 3-9A and 3-9B). As illustrated in Figure 3-9A, IL-1β treated small IB4-positive neurons had subtle, yet significant decreases in cumulative AP latencies where differences became progressively larger with each successive AP ($p<0.05$ for the fourth AP and $p<0.01$ for the eighth AP; also see Figure 3-10A). In contrast, large neurons had significant increases in the latencies for successive AP discharge (unpaired t-test, $p<0.05$). Although cumulative latency was unaffected in medium neurons, significantly more APs developed in response to the ramp commands in IL-1β treated cultures (unpaired t-test, $p<0.05$; Figure 3-9B and Figure 3-10B). In large neurons, IL-1β application resulted in significantly increased AP cumulative latencies and decreased average number of APs generated during current application (unpaired t-test, $p<0.05$; Figures 3-9A and 3-9B, respectively). Similar to the findings in the step protocol, no differences were observed in the repetitive firing behaviour of small IB4-negative neurons in response to ramp current commands (Figure 3-9).

### *3.1.6 Effects of long-term IL-β exposure on DRG neuron voltage sag*

Many DRG neurons exhibit a time-dependent change in voltage or 'sag' in response to hyperpolarizing current (Czeh et al., 1977;Abdulla and Smith, 2001;Villiere and McLachlan, 1996). As depicted in Figure 3-11A, voltage sag is characterized by an initial transient peak voltage response ($V_{Peak}$) which settles to

a less negative steady-state ($V_{SS}$) level within a few hundred milliseconds. Voltage sag was quantified as the percent difference between $V_{Peak}$ and $V_{SS}$ (% voltage sag) and analysis revealed that voltage sag was most prominent in control large neurons with significant differences when compared to control medium and small IB4-positive neurons (one-way ANOVA-Tukey test, $p<0.01$for both; Figure 3-11B). With the exception of medium neurons, long-term IL-1β exposure yielded a trend towards a decrease in voltage sag (Figure 3-11B).

### *3.1.7 Effects of long-term IL-β exposure on small IB4-positive and medium DRG neuron electrical behaviour in the presence of IL-1Ra*

Since IL-1β treated small IB4-positive and medium neurons displayed many features consistent with hyperexcitability, including enhanced firing frequencies and increased AP number, they became the primary focus for further investigation. To explore the possibility that alterations to DRG neuron electrical behaviour are IL-1β receptor-mediated, primary DRG cultures were co-treated for 5-6 days with IL-1β and the IL-1RI antagonist, IL-1Ra.

Internal controls for antagonist experiments (BSA + IL-1Ra) were performed in order to correct for possible changes that 100 ng/mL IL-1Ra may introduce to DRG cultures. Direct statistical comparisons were avoided between cultures with and without IL-1Ra, because the final concentration of the stabilizing agent, BSA, was double (0.001% vs. 0.002%) in antagonist experiments. Qualitatively, however, medium control neurons appeared to be similar in many of the different AP parameters measured with the exception that

AHP duration to 50% repolarization is shortened, whereas, input resistances, input capacitances and membrane time constants were all decreased (Table 3-3). After IL-1Ra exposure, small IB4-positive neuron AP height appeared larger, while AP width became broader. AHP amplitude was also decreased and AHP duration at 25% repolarization appeared longer. Last, small IB4-positive DRG neuron average input resistance and membrane time constant were visibly increased, while input capacitance was unchanged in cell cultures exposed to antagonist. No additional differences were apparent in measured parameters of repetitive discharge for both DRG neuron subtypes.

Comparisons between IL-1β and internal controls, with regard to AP characteristics and passive membrane properties, are summarized in Table 3-4. In medium neurons, 100 ng/ml IL-1Ra was unable to attenuate differences in rheobase and AP height (unpaired t-test, $p<0.05$ and $p<0.01$, respectively; also see Figures 3-13A and 3-12). In contrast, IL-1Ra co-application antagonized IL-1β effects on medium neuron maximal rate of repolarization in the descending phase of the AP and AHP duration at 50% repolarization (Table 3-4 and Figures 3-13A and 3-13B). Additionally, IL-1Ra application reduced statistical differences produced by IL-1β on AHP amplitude and maximal rate of depolarization (unpaired t-test, $0.05<p\leq0.1$ *vs.* $p<0.01$ and $p<0.05$ *vs.* $p<0.001$, respectively; Table 3-4 vs. Table 3-2, also see Figures 3-12 and 3-13B). IL-1Ra also attenuated differences in the mean input capacitance and membrane time constant. In the presence of IL-1Ra, IL-1β exposure produced novel and significant increases in the AP width (Figure 3-12B inset) and input resistances of

medium neurons (unpaired t-test, $p<0.05$ and $p<0.001$, respectively; Table 3-4). Similar to IL-1β alone, antagonist experiments yielded no significant differences in the proportion of medium or small IB4-positive neurons achieving 25% and 50% repolarization (Fisher's exact-test, $p>0.05$). Last, the effects of IL-1β exposure on small IB4-positive neuron spike width (Figure 3-12) and rate of repolarization (Figure 3-13B) were reduced in the presence of IL-1Ra (unpaired t-test, $p>0.05$ and $0.05<p\leq0.1$, respectively; Table 3-4).

IL-1β receptor-mediated effects on small IB4-positive and medium neuron repetitive discharge were also investigated. In the presence of IL-1Ra, 800 pA current step commands discharged 97.8% (45/46) of the total medium neurons, while 500 pA steps discharged all small IB4-positive neurons. Tonic, phasic and single-spike discharge patterns were again consistently observed and, in internal control medium neurons, these patterns appeared in 19%, 38.1%, and 42.9% of cells, respectively (Figure 3-14A). In small IB4-positive neurons, these same patterns were seen in 18.2%, 54.5% and 27.3% cells. Similar to IL-1β alone, irregular discharge behaviour emerged after IL-1β exposure in 2 (18% of total) medium neurons (Figure 3-14A). Despite the appearance of a fourth AP firing pattern, IL-1β exposure did not significantly alter the proportions of the four discharge patterns in either DRG neuron (Fisher's exact-test, $p>0.05$; Figure 3-14A). IL-1Ra co-treatment attenuated the increase in AP number observed in tonic discharging medium neurons and small IB4-positive neurons exposed to IL-1β (Mann-Whitney U test, $p>0.05$; Figure 3-14B). As indicated in Figures 3-15A and 3-15B, increases in small IB4-positive and medium neuron repetitive firing

frequencies were also abolished in the presence of antagonist. With regard to 2 nA current ramps, AP discharge was seen in 63.6% of internal control medium neurons and 100% of internal control small IB4-positive neurons and these proportions were not significantly altered in the presence of IL-1β (Fisher's exact-test, $p>0.05$; Figure 3-16). Similar to current step findings, IL-1Ra attenuated the effects of IL-1β on small IB4-positive neuron cumulative latency and medium neuron total AP number (Figure 3-17A and 3-17B, respectively).

## *3.2 Discussion*

### *3.2.1 Identification DRG neuron subpopulations*

An obvious limitation to *in vitro* studies of the DRG is that it is impossible to know the precise sensory modality transduced by an individual sensory neuron in the absence of the associated sensory terminal and receptive field. To avoid this uncertainty, DRG neurons were subclassified according to cell body size (diameter; Figure 2-2) to which a rough correlation with conduction velocity and other electrical properties has been previously established (Harper and Lawson, 1985;Lawson, 2002). Thus, DRG neurons with large-diameter cell bodies are proposed to be non-nociceptive afferents, while small-diameter cell bodies are proposed to be nociceptive afferents (Caffrey et al., 1992;Lu et al., 2006). In addition, medium-diameter cell bodies likely represent a mixed population of nociceptive and non-nociceptive afferents. Last, the ability to bind the isolectin, IB4, was used to further distinguish subpopulations of small, nociceptive neurons which are believed to be functionally distinct with regard to pain physiology

(Fang et al., 2006;Fjell et al., 1999;Stucky and Lewin, 1999b;Snider and McMahon, 1998).

A drawback to the use of the above criteria for sensory neuron classification is that it is strictly relevant to cutaneous afferents and not to sensory neurons with other targets of innervations (Robinson and Gebhart, 2008). This is of potential concern in my investigation, since the DRG were harvested from multiple spinal segments and likely included cutaneous, visceral and muscle afferents. Therefore, it is possible that there are misclassified DRG neurons in my study. For instance, visceral DRG neurons that give rise to Aδ- and C-fibres have, on average, larger cell body diameters than those considered to be non-visceral nociceptors (Perry and Lawson, 1998;Gold and Traub, 2004;Sugiura et al., 2005). In addition, there is considerable variability among the proportion of identified cutaneous, muscle and visceral afferents that bind IB4 (Robinson and Gebhart, 2008). Coupled to this, it has been reported that nearly all (> 90%) IB4-positive colonic DRG neurons are immunoreactive for CGRP, whereas, only 20% of the total DRG population show co-localization (Robinson et al., 2004). This finding suggests that IB4 binding is not a reliable marker of non-peptidergic DRG neuron subpopulations when considering visceral afferents. Taken together, it is likely that a higher proportion of larger-sized DRG neurons in my study (than in cutaneous DRG neuron studies) would correspond to 'Aδ and C-fibres'. Similarly, there would be a higher proportion of small IB4-positive neurons that are peptidergic.

While DRG neuron misclassification would limit specific interpretations made on a given subpopulation (in addition to the phenotypic shift discussed below), it is important to emphasize that the same methods for DRG neuron isolation were followed regardless of treatment condition (Chapter 2). Therefore, it is expected that such a complication would not introduce an additional source of variability between control and IL-1β treated cell cultures. To this end, the results obtained here could be verified in future studies, involving retrogradely labeled cutaneous DRG neurons.

### *3.2.2 Passive membrane properties of control DRG neurons in long-term cell cultures*

Measurement of 'passive' membrane properties in my study was complicated by at least two factors: 1) the presence of neurites on DRG neurons in long-term cell culture (see Figure 2-2B) introduced unaccounted cell membrane surface area; and 2) the activation of $I_H$ (see Figures 5-8A and 5-8B; also see Figure 3-11B) contaminated measurements of passive membrane properties derived from hyperpolarizing current commands. Therefore, values obtained for input capacitance ($C = \tau/R$) were not in agreement with cell body size (Table 3-1). For instance, large neuron input capacitance was smaller than expected and may be attributed to the significantly faster membrane time constant observed in the large-sized population. In addition, the unexpected difference in input capacitance between small IB4-positive and -negative neurons may be related to significant

differences in input resistance. As a result, input capacitance was avoided as an additional criterion of DRG cell body size.

*3.2.3 AP parameters of control DRG neurons in long-term cell cultures*

Although correlations between DRG neuron morphology and electrophysiology have been firmly established in acutely isolated DRG neuron preparations, very few studies have investigated these correlations in long-term (9-10 days) cell cultures. Somal AP width or duration correlates well with afferent type (Lawson, 2002) and has been one of the most consistently reported electrophysiological characteristics that distinguish subpopulations of sensory neurons (Fang et al., 2005;Abdulla and Smith, 2001;Villiere and McLachlan, 1996;Petruska et al., 2000). In contrast with the literature, AP width, as measured at half maximal AP height, was uniform among small IB4-positive, medium and large -sized DRG neurons (Table 3-1). Small IB4-negative DRG neurons, on the other hand, had the broadest APs (3.29 ± 0.43 ms) with prominent shoulders on the AP falling phase, suggesting these neurons, coupled to their slower rates of AP depolarization and repolarization, are likely to be nociceptive C-fibre conducting afferents (Waddell and Lawson, 1990). Interestingly, both small IB4 -negative and –positive neuron AP widths were considerably narrower than the nociceptor AP widths (typically ≥ 5 ms) found in other *in vitro* DRG studies (Abdulla and Smith, 2001;Stucky and Lewin, 1999a;Snape et al., 2009;Binshtok et al., 2008). Given the association between AP width and the expression of TTX-R sodium channels, one possible explanation for this discrepancy might be that

heterogeneous sodium channel isoform expression was not maintained in long-term cell cultures devoid of neurotrophin supplementation, such as NGF and /or GDNF (Fjell et al., 1999) (also see Chapters 2, 4 and 5). Further, Since TTX-R channel isoforms are known to be expressed at lower levels in large, non-nociceptive DRG neurons (Caffrey et al., 1992;Rizzo et al., 1994;Lai et al., 2004), losses would be expected to have less impact on AP shape. Consistent with this, narrow AP widths were preserved in large DRG neurons (Figure 3-1A and Table 3-1).

Other parameters, in relation to DRG cell body diameter and afferent type, appear to be less consistent in the literature and are reflected in my findings. For instance, afterhyperpolarization (AHP) durations were similar among all DRG neuron subtypes in long-term cell culture (Table 3-1) and is in agreement with a poor correlation to conduction velocity (Lawson, 2002;Ritter and Mendell, 1992) and, perhaps, soma diameter. However, intact and acutely dissociated DRG studies have reported that AHP duration decreases with increases in conduction velocity and soma size as measured by membrane capacitance (Abdulla and Smith, 2001;Villiere and McLachlan, 1996). This discrepancy may be reconciled by the observation that long AHP durations and large AHP amplitudes correspond to high threshold mechanoreceptors (HTMRs) and not necessarily conduction velocity (Ritter and Mendell, 1992;Lawson, 2002;Waddell and Lawson, 1990). This would also explain the significantly larger AHP amplitude in small IB4-positive DRG neurons from my study, as well as, the cases where AHP duration exceeded the sweep duration of the current pulse protocol in large and small DRG

neurons (Table 3-1). Waddell and colleagues (1990) also found that multiple firing in response to sustained current injection was strongly correlated with AHP duration and, therefore, the uniform AHP durations observed in my investigation may explain the rather uniform proportion of neurons that fired tonically (Figure 3-5A). In another example, RMP was uniform among large and small DRG neurons and this finding is consistent with reports from other studies (Abdulla and Smith, 2001;Petruska et al., 2000;Stucky and Lewin, 1999c). Medium neurons, however, were considerably more hyperpolarized (Table 3-1) and, therefore, relates well with findings from Gold and colleagues (1996) that larger-sized DRG neurons have a more hyperpolarized RMP. In addition to RMP, Abdulla and Smith (2001) reported that rheobase was uniform across acutely isolated DRG neuron subpopulations. This was also found in my study with the exception of a significantly increased rheobase in medium neurons which was likely related to the hyperpolarized RMP.

In agreement with the literature (Villiere and McLachlan, 1996;Abdulla and Smith, 2001;Czeh et al., 1977;Gurtu and Smith, 1988), the magnitude of voltage sag (% voltage sag) was greatest in large DRG neurons (Figure 3-11B). The large voltage sag found in small IB4-negative neurons may be related to reports that a subpopulation of small-diameter cold-sensitive thermoreceptive sensory neurons express large amounts of $I_H$ which is kinetically similar to $I_H$ found in large neurons (Reid et al., 2002;Viana et al., 2002;Momin et al., 2008;Orio et al., 2009).

In summary, it appears that many of the incongruent findings, with regard to DRG neuron AP parameters, reflect limitations inherent with the study of DRG neurons *in vitro* (Fang et al., 2005) rather than solely artifacts of long-term cell culture. As opposed to *in vivo* or *in situ* studies, it is not possible to know*, in vitro*, whether the receptive terminal is high or low threshold. This is further complicated by the finding that A- and C-fibres can both have populations of low and high threshold receptors where some AP parameters correlate better to one classification versus the other (Lawson, 2002;Ritter and Mendell, 1992;Djouhri et al., 1998). It does appear, however, that phenotypic shift did occur in response to long-term cell culturing conditions and is evidenced by a deviation from expected AP width in small IB4-positive DRG neurons.

### *3.2.4 Effects of long-term IL-β exposure on DRG neuron AP parameters and passive membrane properties*

Investigations into the long-term effects of inflammatory mediators on isolated sensory neurons are virtually non-existent and, therefore, it is difficult to make straightforward comparisons with my findings. Furthermore, the effects of IL-1β (Binshtok et al., 2008;Takeda et al., 2007;Liu et al., 2006) and other cytokine (Jin and Gereau, 2006) applications often focus on the relevance to inflammatory pain and, consequently, studies are restricted to small, putatively, nociceptive sensory neurons. After nerve injury, however, there is a trend towards increased excitability, reduced rheobase and increased spike width in subpopulations of DRG neurons that likely include small, nociceptive, as well as,

large, non-nociceptive sensory neurons (Abdulla and Smith, 2001). Since the underlying aim in my thesis was to test the relevance of IL-1β to the development of neuropathic pain, I have decided to compare my findings, primarily, to the pattern of changes observed after peripheral nerve injury.

A reduction in rheobase or AP threshold is one of the most consistent changes reported in DRG neurons after nerve injury, as well as, in response to acute IL-1β applications (Abdulla and Smith, 2001;Binshtok et al., 2008;Kim et al., 1998;Study and Kral, 1996;Zhang et al., 1997;Fukuoka et al., 1994). Interestingly, medium neurons were the only subpopulation to respond significantly ($p<0.05$) in this manner after long-term IL-1β exposure (Table 3-2). Also similar to axotomy nerve injury and acute IL-1β studies, changes in medium neuron rheobase were not associated with increases in input resistance and/or membrane depolarization (Binshtok et al., 2008;Abdulla and Smith, 2001;Zhang et al., 1997). In contrast, more depolarizing current was required to elicit discharge in large neurons in the presence of IL-1β, suggesting that this effect would not likely contribute to large sensory neuron hyperexcitability and the onset of allodynia observed after nerve injury (Devor, 2009). Surprisingly, small IB4-negative DRG neurons were not affected and this was a consistent feature of this cell-type throughout the course of investigation.

Although changes to sensory neuron AHP amplitude and duration are more variable after nerve injury (Stebbing et al., 1999;Abdulla and Smith, 2001;Gallego et al., 1987;Gurtu and Smith, 1988), intracellular recordings from DRG with attached dorsal root and peripheral nerve have revealed that short AHP

durations enable neurons to fire multiple APs and follow higher frequencies of stimulation (Waddell and Lawson, 1990;Villiere and McLachlan, 1996). Consistent with changes that support increases in excitability, IL-1β exposure resulted in a significant ($p<0.01$) decrease in medium neuron AHP duration at 50% repolarization (Table 3-2). Similar to the consequences of axotomy nerve injury on A-fibres (Gurtu and Smith, 1988;Stebbing et al., 1999), medium neuron AHP amplitude was significantly ($p<0.01$) decreased in the absence of changes to RMP. Again and conducive to hypoexcitability, large neurons exposed to IL-1β had a significantly ($p<0.01$) longer AHP duration to 25% recovery, while a significant ($p<0.01$) proportion of large neurons failed to recover to 50% repolarization (Table 3-2).

After long-term IL-1β exposure, small IB4-positive DRG neurons displayed significantly ($p<0.01$; Table 3-2 and Figure 3-1B, inset) broader APs which is consistent with findings after nerve injury (Stebbing et al., 1999;Abdulla and Smith, 2001;Kim et al., 1998). Interestingly, medium neurons, which responded in several ways consistent with nerve injury, did not display increases in AP width (Table 3-2). However, in agreement with axotomy nerve injury (Abdulla and Smith, 2001), medium neuron AP height became significantly ($p<0.01$) increased after long-term IL-1β exposure (Table 3-2 and Figure 3-1). Furthermore, the significant changes in the rates of depolarization and/or repolarization after long-term IL-1β exposure are likely to be associated with alterations to AP shape and underlying active membrane properties in medium and small IB4-positive neurons (Waddell and Lawson, 1990). Last, the

significantly faster membrane time constant and concurrent decrease in input capacitance ($p<0.05$ and $p<0.01$, respectively) in medium neurons exposed to IL-1β approached time constants observed in the large neurons and, as discussed above, may be associated with a change in active properties inherent of larger-sized sensory neurons (Table 3-2 and Chapter 5).

### *3.2.5 Effects of long-term IL-β exposure on DRG neuron excitability*

Depolarizing current steps and ramps can be used in the examination of DRG neuron repetitive discharge. Similar to the enhanced repetitive discharge reported after nerve injury and acute IL-1β application (Abdulla and Smith, 2001;Binshtok et al., 2008;Takeda et al., 2007), both medium and small IB4-positive DRG neurons had increases in excitability after long-term IL-1β exposure. For instance, hyperexcitability in response to current ramps was characterized by significant reductions in small IB4-positive neuron cumulative AP latencies (Figure 3-9A), as well as, a significant ($p<0.05$) increase in medium neuron total AP number (Figure 3-9B). Analysis of DRG neurons displaying tonic firing patterns revealed that medium neurons exposed to IL-1β had a significant ($p<0.05$) increase in AP number (Figure 3-5B). Last, long-term IL-1β exposure led to significant increases in step firing frequencies in both medium and small IB4-positive neurons (Figures 3-6A and 3-6B).

The characterization of hyperexcitability in IL-1β exposed medium and small IB4-positive neurons, thus, appeared distinct in many aspects, including

increases in AP number versus reductions in AP cumulative latencies, respectively. Despite these differences, which are likely to be consequences of inherently different contributing ionic mechanisms (Chapters 4 and 5), neither DRG neuron subpopulation responded in a similar manner to large neurons. As alluded to from increased rheobase and prolonged AHP durations, large neurons exposed to IL-1β displayed many features consistent with hypoexcitability which are opposite to findings from nerve injury studies. With the exception of a significant ($p<0.05$) increase in the ability to respond to depolarizing current ramps (Figure 3-8B), deficits in large neuron repetitive discharge included significant increases in AP cumulative latencies concurrent with a significant ($p<0.05$) decrease in total AP number. In contrast to all other DRG neuron subtypes and suggestive of an inability to respond to IL-1β in long-term culture conditions, small IB4-negative neurons displayed no measureable changes in excitability.

### *3.2.6 Effects of long-term IL-β exposure on DRG neuron spontaneous activity*

The above sections dealt with effects of IL-1β on DRG neuron excitability driven by various types of depolarizing current stimuli. In addition to this, spontaneous activity can originate in injured DRG *in vivo* (Wall and Devor, 1983) or *ex vivo* (Study and Kral, 1996) and in response to acute applications of IL-1β *in vitro* (Binshtok et al., 2008), therefore, the possibility exists that IL-1β is responsible for the generation of spontaneous activity after nerve injury. However, the absence of spontaneous activity in the whole DRG neuron

population, from both control and IL-1β exposed cell cultures, seems inconsistent with this possibility. One explanation could be that the functional expression of a particular ion channel or cell signalling molecule, crucial to spontaneous activity, is down-regulated in long-term DRG cell cultures (Chapter 4). Alternatively, the concentration of IL-1β used by Binshtok and colleagues (2008) was six-fold greater than the concentration added to my DRG cell cultures and, therefore, spontaneous activity may be a concentration dependent effect of IL-1β. Last, Abdulla and Smith (2001) reported a lack of spontaneous activity in injured DRG neurons *in vitro* and attributed their discrepancy to a lack of features inherent of dissociated neurons which exist *in vivo*. This could include trophic support from intact DRG and/or from target tissues. Furthermore, injured DRG neurons *in vivo* may be subject to chemical cross-excitation (Amir and Devor, 1996) and ongoing effects of secreted mediators such as, noradrenaline (McLachlan et al., 1993).

### *3.2.7 Effects of long-term IL-β exposure on DRG neuron electrical behaviour in the presence of IL-1Ra*

Since the effects of long-term IL-1β exposure on medium and small IB4-positive DRG neurons were consistent with hyperexcitability after nerve injury, subsequent investigations were limited to these two neuron subtypes. Importantly, it was observed that the addition of IL-1Ra (100 ng/mL) in long-term cell cultures, under internal control (BSA + IL-1Ra) conditions, was associated with qualitative changes in the electrical behaviour of DRG neurons relative to controls

in the absence of cytokines (Table 3-3). Possible explanations for these artifacts include:

1. Although ambient levels for IL-1β were near the detection threshold for ELISA (≤ 5 pM; Figure 2-3), biological effects of IL-1β have been reported in the sub-picomolar range (Ferreira et al., 1988;Fukuoka et al., 1994;Orencole and Dinarello, 1989). Therefore, it is possible that the addition of IL-1Ra nullified a basal effect of IL-1β on cultured DRG neurons.

2. It is also possible that IL-1Ra has previously undocumented biological activity. However, *in vitro* and *in vivo* studies have reported that IL-1ra at concentrations 100,000 and a million -fold greater than IL-1β, respectively, have no agonist activity (Granowitz et al., 1992;Hannum et al., 1990).

3. Finally, these observations may also be related to the slightly higher final concentration of the cytokine stabilizing agent, BSA, required in antagonist experiments. Regardless of the root cause, the receptor mediated effects of IL-1β were only determined relative to internal controls in the presence of IL-1Ra.

IL-1Ra co-application antagonized or mitigated several aspects of the increase in excitability promoted by long-term IL-1β exposure. This included the shortening of AHP duration in medium neurons (Table 3-4 and Figure 3-11C), the broadening of APs in small IB4-positive neurons (Table 3-4 and Figure 3-10B, inset) and the enhancement of repetitive discharge in both DRG cell-types (Figures 3-12 to 3-14). Although these effects on DRG cell electrical behaviour are concluded to be receptor-mediated, two anomalies need to be addressed. First, IL-1Ra was unable to attenuate differences in medium neuron rheobase and AP

height ($p<0.05$ and $p<0.01$, respectively; Table 3-4, also see Figures 3-13A and 3-12). These findings may be attributed to the possibility that IL-1β has biological activity independent of IL-1RI signalling which has been reported *in vivo*, as well as, in cell culture (Humphreys and Grencis, 2009;Herseth et al., 2009;Diem et al., 2003;Andre et al., 2006). On the other hand, the reduction in rheobase may be secondary to the unexpected significant increase in medium neuron input resistance (see below). Second, IL-1β and IL-1Ra co-treatment produced novel and significant increases in medium neuron AP width (Figure 3-12B inset) and input resistance ($p<0.05$ and $p<0.001$, respectively; Table 3-4). Since IL-1Ra is a competitive antagonist (Hannum et al., 1990), it is unlikely that IL-1Ra would act synergistically with IL-1β. In addition, nanomolar range IL-1Ra is sufficient to attenuate the *in vitro* effects of short-term (≤ 24 hrs) IL-1β applications at concentrations in excess of 100 pM (Liu et al., 2006;Takeda et al., 2008;Takeda et al., 2007). However, the possibility remains that 100 ng/mL (~6 nM) IL-1Ra was unable to completely attenuate the effects of 100 pM IL-1β in long-term cell culturing conditions. Coupled to this, the expression of IL-1RI is dynamically regulated (Takii et al., 1992;Takii et al., 1994) such that more receptors may appear overtime in the DRG cell cultures and, owing to the potency of IL-1β, only a few receptors need be present on the cell surface to elicit a biological response (Dinarello, 1998). Therefore, the novel effects of IL-1β in the presence of IL-1Ra could be related to receptor availability and an apparent dose-dependent effect where lower concentrations of IL-1β have been previously suggested to have

contrasting effects to higher concentrations (Oka et al., 1993;Oka et al., 1994;Andrew and Mary, 2000).

*3.2.8 Conclusion*

The effects of long-term IL-1β exposure were sensory neuron specific. Similar to nerve injury and acute IL-1β application, long-term IL-1β exposure produced several changes in medium and small IB4-positive neurons which were consistent with hyperexcitability. In contrast, large neurons responded in an opposite manner, whereas, small IB4-negative neurons were devoid of any measurable response. Since *in vivo* and *in vitro* nerve injury studies report hyperexcitability in small, nociceptive and large, non-nociceptive sensory neurons subpopulations, the hypoexcitability of large neurons in IL-1β exposed cultures suggests that IL-1β has a restricted role in injured sensory neuron electrical activity. This is further supported by the lack of response from small IB4-negative neurons, as well as, the absence of spontaneous activity in IL-1β exposed DRG cell cultures. Therefore, other molecules or processes may be required, in addition to the release of IL-1β, for these further changes observed after peripheral nerve injury.

My findings on long-term IL-1β exposure and DRG neuron excitability are intriguing in the following ways:

1. Hyperexcitability in medium DRG neurons exposed to IL-1β likely includes mixed populations of neurons corresponding to nociceptive and non-nociceptive

primary afferent fibres and, therefore, has relevance to hyperalgesia and allodynia, respectively.

2. The responsiveness of small IB4-positive DRG neurons, but not IB4-negative, to prolonged IL-1β exposure is consistent with the suggestion that small, nociceptive IB4-negative afferents are involved in inflammatory pain, while small, IB4-positive afferents are involved neuropathic pain (Snider and McMahon, 1998).

3. The inability of IL-1Ra to attenuate reductions in rheobase suggests that IL-1β can contribute to hyperexcitability independent of IL-1RI signalling and this should be taken into account when targeting IL-1β, or more specifically IL-1RI, in the management of neuropathic pain.

4. Last, the expression of IL-1RI (Liu et al., 2006;Copray et al., 2001) by most sensory neurons and the hyperexcitability observed in sensory neurons with acute IL-1β applications (Binshtok et al., 2008;Takeda et al., 2007), as well as, after 5-6 days of IL-1β exposure suggests that sensory neurons are detectors of sustained IL-1β release. However, the effects of long-term IL-1β exposure may be less directly mediated, involving the, yet to be determined, production of $PGE_2$ (Maier et al., 1990) and/or NGF (Safieh-Garabedian et al., 1995). Taken together, these findings may have identified critical features to the enduring increase in excitability of injured primary afferents that is thought to be involved in the establishment of central sensitization and, possibly, neuropathic pain.

In Chapters 4 and 5, I examine possible ionic mechanisms responsible for hyperexcitability in small IB4-positive and medium DRG neurons exposed to

long-term IL-1β. Since phenotypic shift was observed in long-term DRG cell cultures, this may impact the contribution of specific ion channels to hyperexcitability. For example, TTX-R sodium currents drive AP upstroke, contribute to the broad AP widths and repetitive discharge in small-sized DRG neurons (Caffrey et al., 1992;Rizzo et al., 1994;Lai et al., 2004;Fjell et al., 1999;Renganathan et al., 2001) and alterations to channel function and/or expression are commonly observed after nerve injury (Gold et al., 2003;Abdulla and Smith, 2002;Dib-Hajj et al., 1998;Zhang et al., 1997) or in the presence of inflammatory mediators, including IL-1β (Binshtok et al., 2008;Liu et al., 2006). The potential loss of functional TTX-R sodium channel isoforms, as discussed above, would obviously impact the baseline electrical activity of small-sized DRG neurons, as well as, their response to IL-1β. In addition, T-type calcium currents underlie after-depolarization potential (ADP) in sensory neurons (Abdulla and Smith, 2001;White et al., 1989) and the absence of ADP suggests a loss in the functional expression of T-type calcium channels in long-term DRG cell cultures. Because T-type calcium currents are involved in burst firing (White et al., 1989;Zamponi et al., 2009;Jevtovic-Todorovic and Todorovic, 2006) and can be upregulated after nerve injury (Jagodic et al., 2007;Jagodic et al., 2008), their potential absence may further restrict interpretations made regarding the role of IL-1β in injured sensory neuron hyperexcitability.

Despite the potential limitations imposed upon DRG neurons in long-term cell culture, medium and small IB4-positive sensory neuron subpopulations displayed distinct alterations in electrical activity in response to long-term IL-

1β exposure, suggesting phenotypic differences still existed. Furthermore, it is expected that differences in phenotype extend to the ionic mechanisms which drive increases in excitability.

***Figure 3-1: Representative AP traces in DRG neurons and the effects of IL-1β on AP shape***

A: Representative recordings of APs elicited in 23 small IB4-negative, 20 small IB4-positive, 36 medium and 12 large control neurons by a 5 ms pulse of depolarizing current set at rheobase (black traces). Small IB4-negative neurons had the longest duration APs (broadest spike width) along with a prominent shoulder on the AP falling phase.

B: Effects of long-term IL-1β exposure on AP shapes (red traces) in DRG neurons. In medium neurons, IL-1β increased AP height, reduced AHP amplitude and shortened AHP duration (inset). In small IB4-positive neurons, IL-1β increased AP width (inset). No changes were observed in the overall AP shapes for large and small IB4-negative neurons.

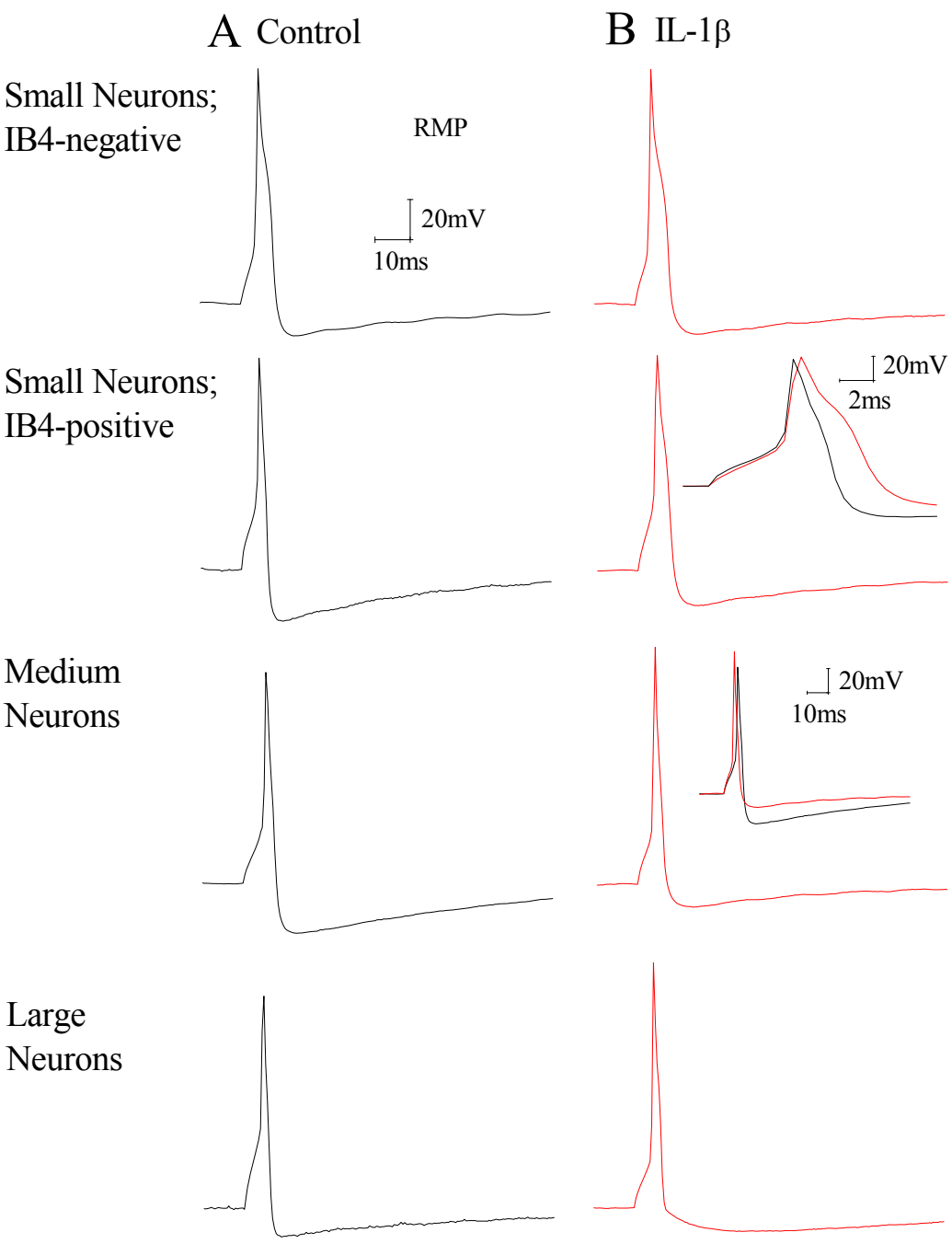
A Control
B IL-1β
Small Neurons;
IB4-negative
RMP
20mV
10ms
Small Neurons;
IB4-positive
20mV
2ms
Medium
Neurons
20mV
10ms
Large
Neurons

***Table 3-1: Summary of AP parameters and passive membrane properties of control DRG neurons***

Statistical significance determined with one-way ANOVA and post-hoc Tukey's multiple comparisons test. * = $p<0.05$, † = $p<0.01$, § = $p<0.001$.

a = significant difference vs. large neuron

b = significant difference vs. medium neuron

c = significant difference vs. small IB4-positive neuron

d = significant difference vs. small IB4-negative neuron

| *Parameter* | *Large Neuron*<br><br>*Control*<br><br>*Value ± s.e.m. (n)* | *Medium Neuron*<br><br>*Control*<br><br>*Value ± s.e.m. (n)* | *Small $IB_4$ +ve Neuron*<br><br>*Control*<br><br>*Value ± s.e.m. (n)* | *Small $IB_4$ -ve Neuron*<br><br>*Control*<br><br>*Value ± s.e.m. (n)* |
|---|---|---|---|---|
| *RMP (mV)* | -54.3 ± 1.9 (12) | -61.4 ± 0.8 (36)$^{a\dagger d*}$ | -58.5 ± 1.4 (20) | -57.0 ± 1.4 (23) |
| *Spike Height (mV)* | 101.3 ± 6.5 (12) | 97.3 ± 2.5 (36) | 103.8 ± 3.4 (20) | 104.6 ± 4.0 (23) |
| *Spike Width (ms)* | 2.00 ± 0.39 (12) | 2.05 ± 0.15 (36) | 1.86 ± 0.12 (20) | 3.29 ± 0.43 (23)$^{a*, b\dagger, c\dagger}$ |
| *Maximal Rate of Depolarization (mV/ms)* | 124.5 ± 17.2 (12) | 95.5 ± 5.8 (36) | 110.0 ± 7.4 (20) | 107.9 ± 9.7 (23) |
| *Maximal Rate of Repolarization (mV/ms)* | -68.2 ± 8.8 (12) | -52.1 ± 2.5 (36) | -57.9 ± 3.3 (20) | -49.0 ± 4.5 (23)$^{a*}$ |
| *AHP Amplitude (mV)* | -16.9 ± 1.8 (12) | -17.7 ± 0.8 (36) | -20.1 ± 0.9 (20)$^{d*}$ | -15.4 ± 1.4 (23) |
| *AHP Duration at 25% Repolarization (ms)* | 11.45 ± 1.90 (11) | 15.88 ± 0.92 (36) | 17.75 ± 2.00 (20) | 13.89 ± 1.5 (23) |
| *AHP Duration at 50% Repolarization (ms)* | 25.42 ± 4.62 (11) | 34.99 ± 2.15 (36) | 35.2 6± 3.65 (18) | 30.06 ± 3.01 (19) |
| *Rheobase (nA)* | 0.39 ± 0.05 (12) | 0.49 ± 0.03 (36)$^{c*, d\S}$ | 0.37 ± 0.03 (20) | 0.27 ± 0.02 (23) |
| *Input Resistance (MΩ)* | 192 ± 30 (12) | 330 ± 23 (36) | 453± 35 (20)$^{a\S}$ | 603 ± 50 (23)$^{a\S, b\S, c*}$ |
| *Input Capacitance (pF)* | 107 ± 11.8 (12) | 180.8 ± 17.8 (36)$^{a*,d\S}$ | 127.4 ± 10.5 (20) | 72.2 ± 7.6 (23) |
| *Membrane Time Constant (ms)* | 21.46 ± 5.17 (12)$^{b*, c*}$ | 62.2 ± 8.33 (36) | 59.24 ± 6.48 (20) | 43.06 ± 6.07 (23) |

***Figure 3-2: Effect of acute IL-β exposure on DRG neuron excitability in long-term cell culture***

Qualitatively, 100 pM IL-1β produced a rapid increase in DRG neuron excitability. A medium-sized neuron unable to elicit AP discharge in response to a 2 nA depolarizing current ramp (A; black trace), began to fire after focal perfusion with IL-1β for 1 minute (B; red trace).

A Control

B IL-1β; 1min.

Medium Neuron

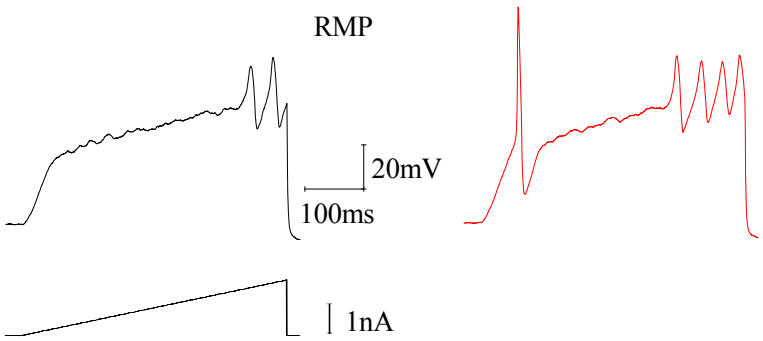

***Figure 3-3: Effects of IL-1β on DRG neuron rheobase, AP rates and AHP duration***

A: Effects of IL-1β exposure on rheobase. IL-1β treatment significantly reduced rheobase in medium neurons (0.49 ± 0.03 nA, n = 36 vs. 0.41 ± 0.02, n = 38; $p<0.05$) and increased rheobase in large neurons (0.39 ± 0.05 nA, n= 12 vs. 0.54 ± 0.04, n = 10; $p<0.05$).

B: Effects of IL-1β exposure on maximal rates of depolarization and repolarization. In small IB4-positive neurons, IL-1β treatment significantly decreased maximal rate of repolarization (-57.9 ± 3.3 mV/ms, n = 20 vs. -46.6 ± 2.9, n = 21; $p<0.05$). In medium neurons, IL-1β treatment significantly increased the maximal rates of both depolarization (95.5 ± 5.8 mV/ms, n = 36 vs. 124.6 ± 6.1, n = 38; $p<0.001$) and repolarization (-52.1 ± 2.5 mV/ms, n = 36 vs. -66.8 ± 4.1, n = 38; $p<0.01$).

C: Effects of IL-1β exposure on AHP duration at 25% and 50% repolarization. In medium neurons, IL-1β treatment significantly shortened AHP duration at 50% repolarization (34.99 ± 2.15 ms, n = 36 vs. 26.68 ± 1.93 n = 33; $p<0.01$). In large neurons, IL-1β treatment significantly increased AHP duration at 25% repolarization (11.45 ± 1.90 ms, n = 11 vs. 35.26 ± 6.71, n = 9; $p<0.01$).

Error bars indicate means ± s.e.m. Significant difference vs. control * = $p<0.05$, † = $p<0.01$and § = $p<0.001$ with unpaired t-test. For clarity, error bars are omitted in 3D bar graphs.

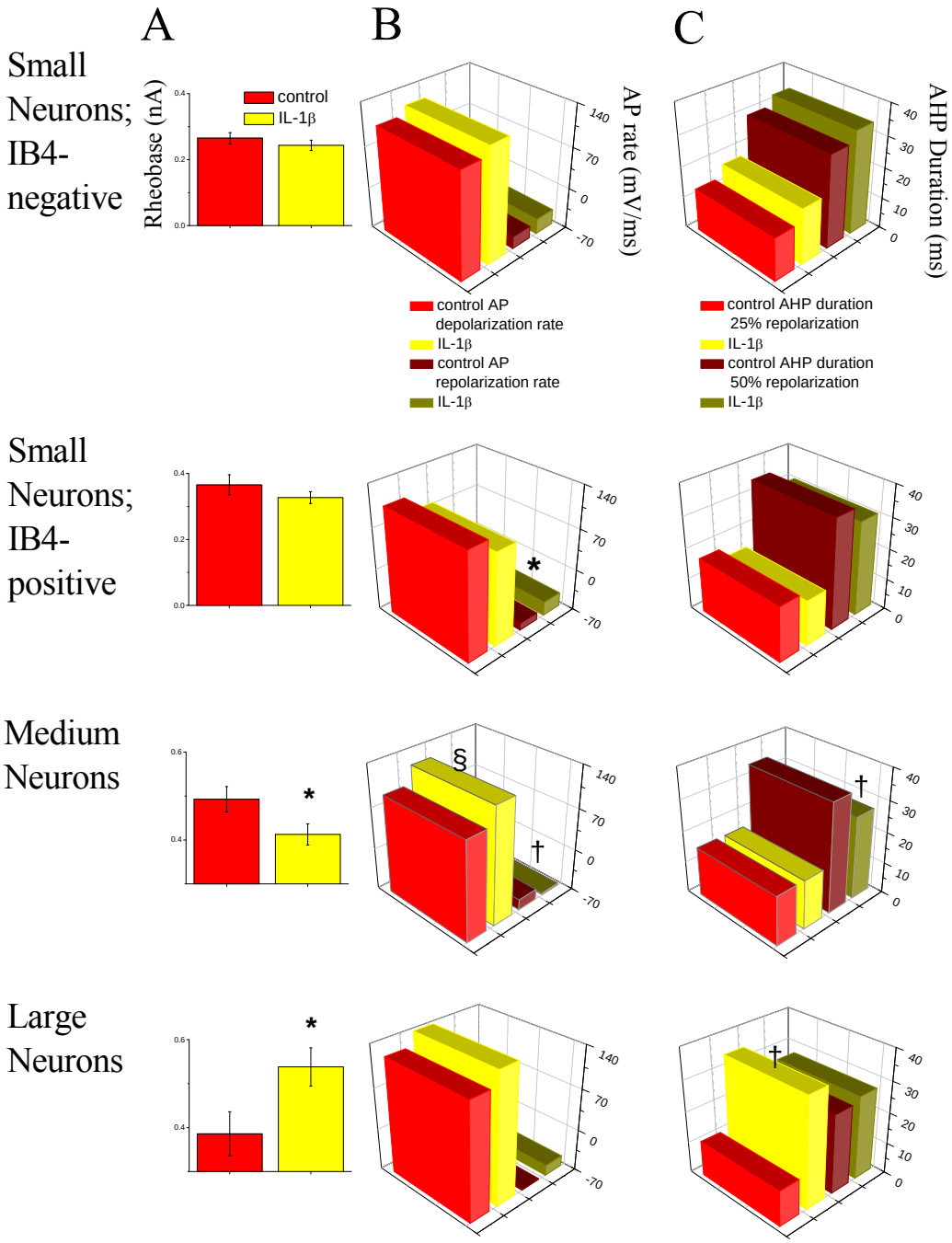
A
B
C
Small Neurons; IB4-negative
Small Neurons; IB4-positive
Medium Neurons
Large Neurons
Rheobase (nA)
control
IL-1β
AP rate (mV/ms)
AHP Duration (ms)
control AP depolarization rate
IL-1β
control AP repolarization rate
IL-1β
control AHP duration 25% repolarization
IL-1β
control AHP duration 50% repolarization
IL-1β
*
§
†

***Table 3-2: Summary of AP parameters and passive membrane properties in control versus IL-1β treated DRG neurons***

Statistical significance determined with unpaired t-test or Fisher's exact-test. Significant difference vs. control * = $p<0.05$, † = $p<0.01$and § = $p<0.001$ with unpaired t-test; # = $p<0.01$ with Fisher's exact-test.

| *Parameter* | *Large Neuron*<br><br>*Control*<br><br>*Value ± s.e.m. (n)* | *Large Neuron*<br><br>*IL-1β*<br><br>*Value ± s.e.m. (n)* | *Medium Neuron*<br><br>*Control*<br><br>*Value ± s.e.m. (n)* | *Medium Neuron*<br><br>*IL-β*<br><br>*Value ± s.e.m. (n)* | *Small $IB_4$ +ve Neuron*<br><br>*Control*<br><br>*Value ± s.e.m. (n)* | *Small $IB_4$ +ve Neuron*<br><br>*IL-1β*<br><br>*Value ± s.e.m. (n)* | *Small $IB_4$ -ve Neuron*<br><br>*Control*<br><br>*Value ± s.e.m. (n)* | *Small $IB_4$ -ve Neuron*<br><br>*IL-1β*<br><br>*Value ± s.e.m. (n)* |
|---|---|---|---|---|---|---|---|---|
| *RMP (mV)* | -54.3 ± 1.9 (12) | -57.9 ± 1.0 (10) | -61.4 ± 0.8 (36) | -59.5 ± 1.0 (38) | -58.5 ± 1.4 (20) | -57.0 ± 1.9 (21) | -57.0 ± 1.4 (23) | -57.3 ± 1.5 (24) |
| *Spike Height (mV)* | 101.3 ± 6.5 (12) | 115.3 ± 4.0 (10) | 97.3 ± 2.5 (36) | 106.6 ± 2.3 (38)$^{\dagger}$ | 103.8 ± 3.4 (20) | 95.6 ± 4.9 (21) | 104.6 ± 4.0 (23) | 107.6 ± 3.2 (24) |
| *Spike Width (ms)* | 2.00 ± 0.39 (12) | 2.59± 0.42 (10) | 2.05 ± 0.15 (36) | 2.24 ± 0.29 (38) | 1.86 ± 0.12 (20) | 2.52 ± 0.16 (21)$^{\dagger}$ | 3.29 ± 0.43 (23) | 3.39 ± 0.29 (24) |
| *Maximal Rate of Depolarization (mV/ms)* | 124.5 ± 17.2 (12) | 146.9 ± 11.4 (10) | 95.5 ± 5.8 (36) | 124.6 ± 6.1 (38)$^{\S}$ | 110.0 ± 7.4 (20) | 84.9 ± 10.0 (21) | 107.9 ± 9.7 (23) | 122.2 ± 7.3 (24) |
| *Maximal Rate of Repolarization (mV/ms)* | -68.2 ± 8.8 (12) | -52.1 ± 5.1 (10) | -52.1 ± 2.5 (36) | -66.8 ± 4.1 (38)$^{\dagger}$ | -57.9 ± 3.3 (20) | -46.6 ± 2.9 (21)$^{*}$ | -49.0 ± 4.5 (23) | -43.9 ± 2.3 (24) |
| *AHP Amplitude (mV)* | -16.9 ± 1.8 (12) | -13.1 ± 0.8 (10) | -17.7 ± 0.8 (36) | -14.2 ± 1.0 (38)$^{\dagger}$ | -20.1 ± 0.9 (20) | -18.3 ± 1.0 (21) | -15.4 ± 1.4 (23) | -13.9 ± 1.8 (24) |
| *AHP Duration at 25% Repolarization (ms)* | 11.45 ± 1.90 (11) | 35.26 ± 6.71 (9)$^{\dagger}$ | 15.88 ± 0.92 (36) | 15.72 ± 1.89 (38) | 17.75 ± 2.00 (20) | 14.50 ± 1.70 (21) | 13.89 ± 1.5 (23) | 17.92 ± 1.95 (20) |
| *AHP Duration at 50% Repolarization (ms)* | 25.42 ± 4.62 (11) | 26.93 ± 9.49 (3)$^{\#}$ | 34.99 ± 2.15 (36) | 26.68 ± 1.93(33)$^{\dagger}$ | 35.2 6± 3.65 (18) | 30.26 ± 3.39 (19) | 30.06 ± 3.01 (19) | 33.31 ± 3.78 (16) |
| *Rheobase (nA)* | 0.39 ± 0.05 (12) | 0.54 ± 0.04$^{*}$ (10) | 0.49 ± 0.03 (36) | 0.41 ± 0.02 (38)$^{*}$ | 0.37 ± 0.03 (20) | 0.33 ± 0.02 (21) | 0.27 ± 0.02 (23) | 0.24 ± 0.02 (24) |
| *Input Resistance (MΩ)* | 192 ± 30 (12) | 190 ± 37 (10) | 330 ± 23 (36) | 297± 23 (38) | 453± 35 (20) | 490 ± 55 (21) | 603 ± 50 (23) | 679 ± 46 (22) |
| *Input Capacitance (pF)* | 107 ± 11.8 (12) | 119.8 ± 13.1 (10) | 180.8 ± 17.8 (36) | 121.3 ± 11.1 (38)$^{\dagger}$ | 127.4 ± 10.5 (20) | 109.7 ± 13.6 (21) | 72.2 ± 7.6 (23) | 64.7 ± 5.8 (22) |
| *Membrane Time Constant (ms)* | 21.46 ± 5.17 (12) | 21.03 ± 3.63 (10) | 62.2 ± 8.33 (36) | 38.5 ± 5.25 (38)$^{*}$ | 59.24 ± 6.48 (20) | 54.44 ± 8.79 (21) | 43.06 ± 6.07 (23) | 42.6 ± 4.33 (24) |

***Figure 3-4: DRG neuron firing patterns in response to 800 ms step current commands***

DRG neuron excitability was assessed from membrane responses to 800 ms depolarizing current steps. As depicted in the representative traces, four different discharge patterns were observed.

A: Single-spike neurons fired a single spike before accommodating.

B: Phasic discharge neurons were slightly more excitable and fired more than one AP before eventually accommodating.

C: Tonic discharge neuron fired APs throughout the application of depolarizing current. Arrows: multiple firing neurons can be further characterized by narrow interspike intervals (instantaneous frequency) between the initial two spikes and wider interspike intervals (steady-state frequency) between the final two spikes.

D: Irregular discharge neurons fired intermittently throughout the current command.

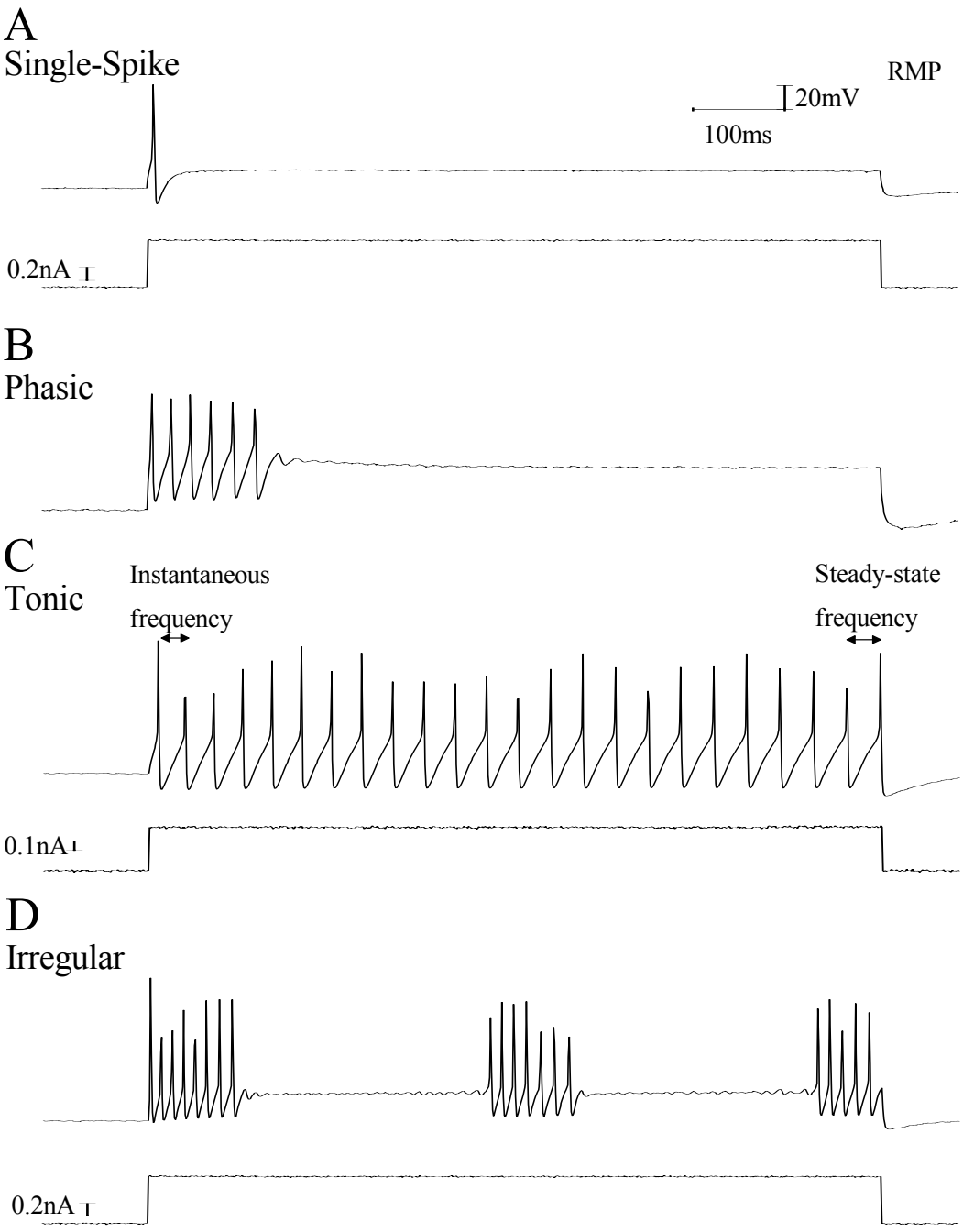
A
Single-Spike
RMP
20mV
100ms
0.2nA
B
Phasic
C
Tonic
Instantaneous
frequency
Steady-state
frequency
0.1nA
D
Irregular
0.2nA

***Figure 3-5: DRG neuron distribution of firing patterns and total AP number***

Comparisons in discharge pattern and concurrent AP number were made using 800 pA steps for all large and medium neurons and 500 pA steps for all small neurons.

A: Proportion of discharge patterns among DRG neuron subpopulations. Under control conditions, single-spike discharge occurred in 66.7% (8/12) of large neurons, 25% (9/36) of medium neurons, 10% (2/20) of small IB4-positive neurons and 34.8% (8/23) of small IB4-negative neurons. Phasic discharge was seen in 0% (0/12) of large neurons, 41.7% (15/36) of medium neurons, 50% (10/20) of small IB4-positive neurons and 26.1% (6/23) of small IB4-negative neurons. Tonic discharge was observed in 33.3% (4/12) of large neurons, 33.3% (12/36) of medium neurons, 40% (8/20) of small IB4-positive neurons and 39.1% (9/23) of small IB4-negative neurons. Irregular discharge, was never observed under control conditions. The proportion of discharge patterns was not significantly altered in the presence of 5-6 days of IL-1β (Fisher's exact-test, $p>0.05$).

B: Total AP number in DRG neurons with phasic and tonic –discharge patterns. Total AP number in tonic discharging neurons was significantly increased in medium neurons exposed to IL-1β (33.0 ± 3.2, n = 12 vs. 44.4 ± 4.4, n = 13; $p<0.05$) and a similar trend was apparent in small IB4-positive neurons (25.4 ± 2.2, n = 8 vs. 32.0 ± 2.6, n = 6; $p=0.07$). Error bars indicate means ± s.e.m. Significant difference vs. control * = $p<0.05$ with unpaired t-test.

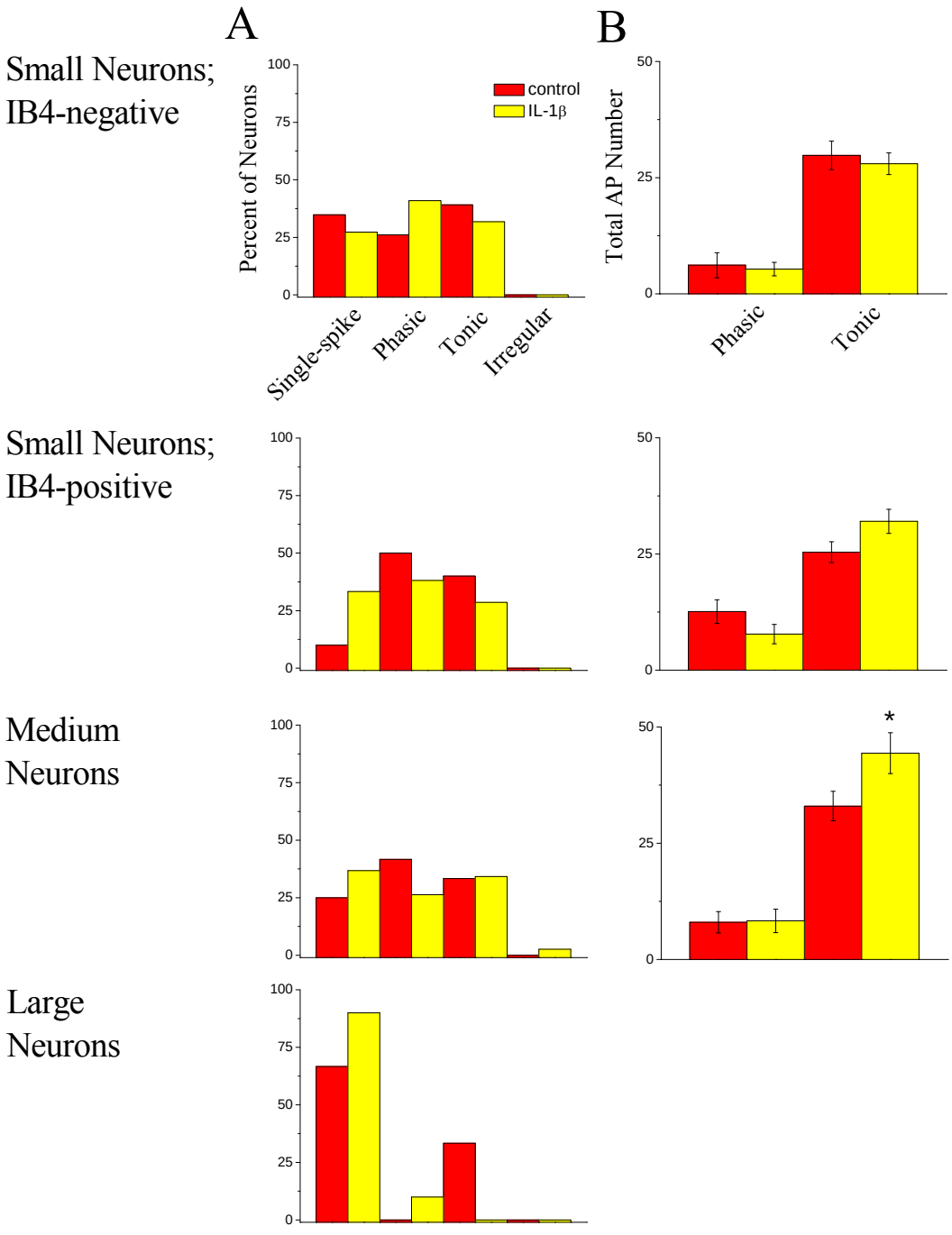
A
B
Small Neurons;
IB4-negative
Small Neurons;
IB4-positive
Medium
Neurons
Large
Neurons
Percent of Neurons
Total AP Number
control
IL-1β
Single-spike
Phasic
Tonic
Irregular
Phasic
Tonic
*

***Figure 3-6: IL-1β effects on DRG neuron repetitive firing frequencies***

Frequency – current (*f-I*) curves illustrate the effect of IL-1β exposure on DRG neuron repetitive discharge in response to 800 ms depolarizing current steps.

A: Instantaneous firing frequency *f-I* curves as measured from the first interspike interval (see Figure 3-4C). In a manner dependent on the magnitude of current injection, IL-1β exposure resulted in significantly higher instantaneous discharge frequencies for both small IB4-positive neurons (at 0.2 nA: 26.4 ± 0.9 Hz, n = 16 vs. 29.9 ± 1.3, n = 15; $p<0.05$) and medium (at 0.5 nA: 38.8 ± 2.7 Hz, n = 28 vs. 50.4 ± 4.6, n = 23; $p<0.05$; at 0.8 nA: 47.4 ± 3.5 Hz, n = 27 vs. 62.6 ± 6.8 Hz, n = 24; $p<0.05$).

B: Steady-state frequency *f-I* curves as measure from the steady-state interspike interval (see Figure 3-4C). In response to the largest current injection (800 pA), IL-1β exposure resulted in a significantly higher steady-state discharge frequency (37.8 ± 2.1 Hz, n = 24 vs. 46.5 ± 3.9, n = 22; $p<0.05$). A similar trend was observed in small IB4-positive neurons at a current injection of 0.5 nA (35.0 ± 1.2 Hz, n = 18 vs. 38.6 ± 1.6, n = 13; $p = 0.08$).

Error bars indicate means ± s.e.m. Significant difference vs. control * = $p<0.05$ with unpaired t-test.

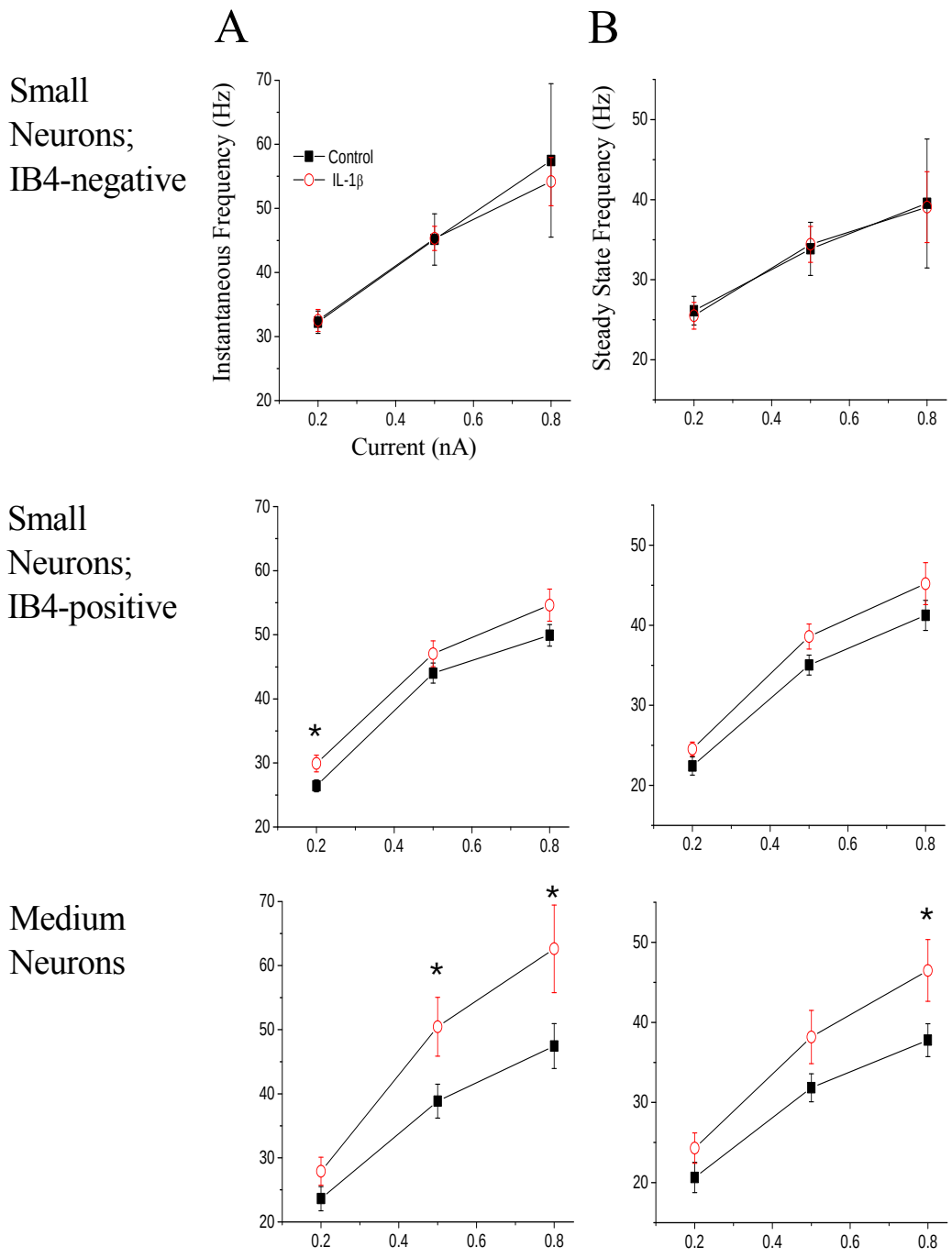
A
B
Small Neurons; IB4-negative
Small Neurons; IB4-positive
Medium Neurons
Instantaneous Frequency (Hz)
Steady State Frequency (Hz)
Current (nA)
Control
IL-1β
*

***Figure 3-7: Illustration of the effects of IL-1β exposure on DRG neuron repetitive discharge in response to depolarizing current steps***

Representative traces of DRG neuron repetitive discharge in response to 800 ms depolarizing current steps at 0.2 nA (A: small IB4-positive neurons) and at 0.8 nA (B: medium neurons).

A: Illustration of the effect of IL-1β treatment on instantaneous firing frequency in small IB4-positive neurons. Barbells: indicate interspike interval for control neuron (black trace). Interspike interval became narrower (higher discharge frequency) in IL-1β treated neuron (red trace).

B: Illustration of the effect of IL-1β treatment on instantaneous and steady-state firing frequencies in medium neurons. Barbells: indicate interspike intervals for control neuron (black trace). Interspike intervals became narrower (higher discharge frequency) in IL-1β treated neuron (red trace).

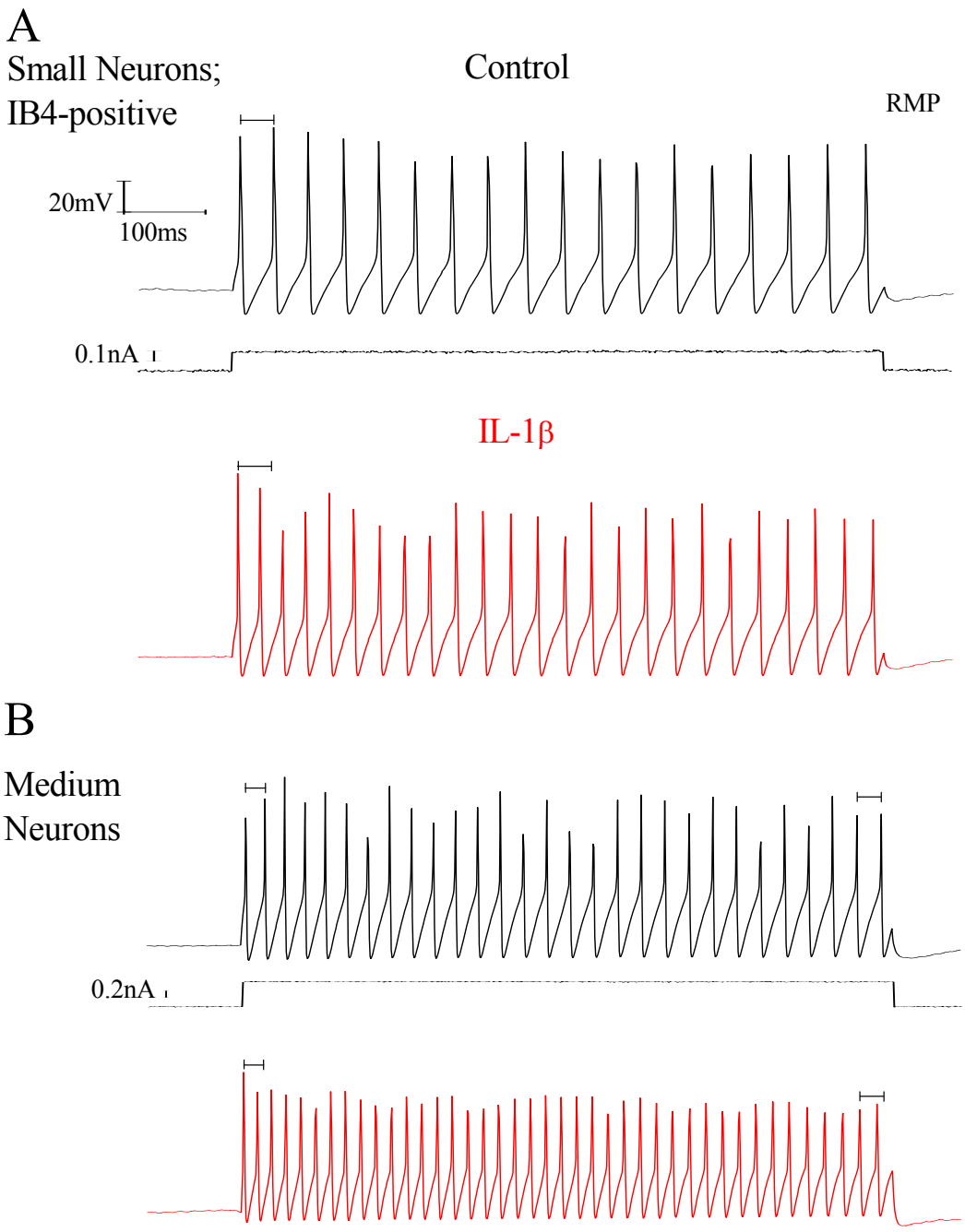
A
Small Neurons;
IB4-positive
Control
RMP
20mV
100ms
0.1nA
IL-1β
B
Medium
Neurons
0.2nA

***Figure 3-8: DRG neuron discharge in responses to current ramps and the effect of IL-1β exposure on firing capability***

A: DRG neuron excitability was also examined from membrane responses to 450 ms depolarizing current ramps. Arrows: illustrations of cumulative latency measurements for successive AP discharge.

B: All excitability analysis was conducted on ramps to 2 nA since this ramp resulted in the greatest number of DRG neurons to fire APs. In control cell cultures, AP discharge was seen in 41.7% (5/12) of large neurons, 80.6% (29/36) of medium neurons, 90% (18/20) of small IB4-positive neurons and 81.8% (18/22) of small IB4-negative neurons. IL-1β exposure significantly increased the percentage, from 41.7% (5/12) to 90% (9/10), of large neurons which discharged on current ramps ($p<0.05$). In both medium and small neurons, proportions of neurons that fired were not significantly altered in the presence of 5-6 days of IL-1β ($p>0.05$).

Significant difference vs. control * = $p<0.05$ with Fisher's exact-test.

A

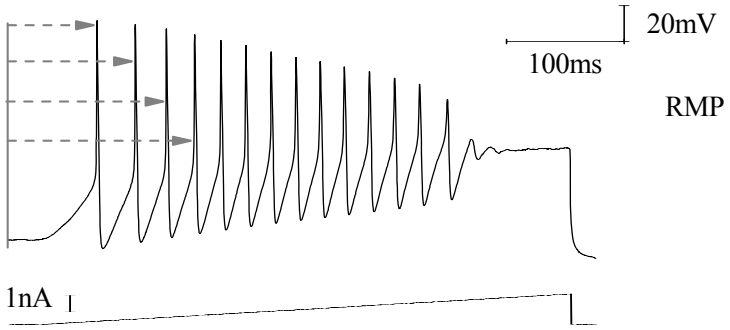
20mV
100ms
RMP
1nA

B

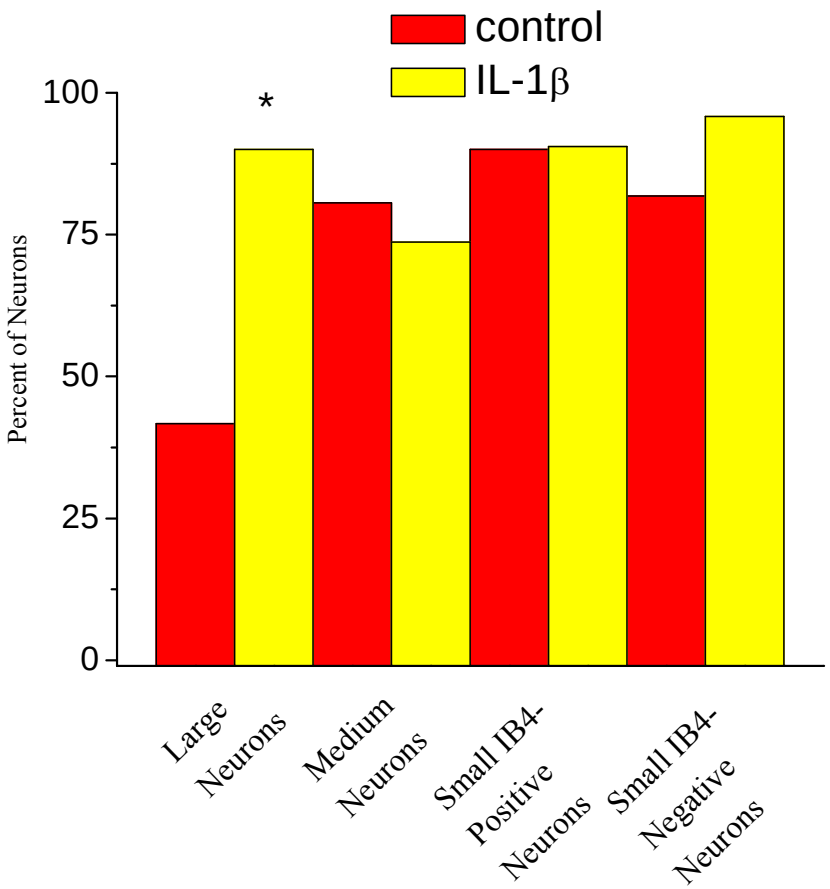
control
IL-1β
100
75
50
25
0
Percent of Neurons
*
Large Neurons
Medium Neurons
Small IB4-Positive Neurons
Small IB4-Negative Neurons

***Figure 3-9: Effects of IL-1β exposure on DRG neuron cumulative AP latency and total AP number in response to current ramps***

A: Effects of IL-1β exposure on DRG neuron cumulative AP latencies. IL-1β treated small IB4-positive neurons had significant decreases in cumulative AP latencies where differences became progressively larger with each successive AP ($p<0.05$ for the fourth AP and $p<0.01$ for the eighth AP). Large neurons exposed to IL-1β had significant increases in cumulative AP latencies ($p<0.05$).

B: Effects of IL-1β exposure on DRG neuron total AP number. In medium neurons, significantly more APs developed in response to the ramp commands in IL-1β treated cultures (10.2 ± 1.4 APs, n = 29 vs. 15.3 ± 1.9, n = 28; $p<0.05$). In large neurons, IL-1β exposure significantly decreased average number of APs generated during current application (18.2 ± 4.4 APs, n = 5 vs. 5.4 ± 1.1, n = 9; $p<0.05$).

Error bars indicate means ± s.e.m. Significant difference vs. control * = $p<0.05$ and † = $p<0.01$ with unpaired t-test. Data for the control group from 18 small IB4-negative, 18 small IB4-positive, 29 medium and 5 large neurons. Data for the IL-1β treated group from 23 small IB4-negative, 19 small IB4-positive, 28 medium and 9 large neurons.

Small Neurons; IB4-negative

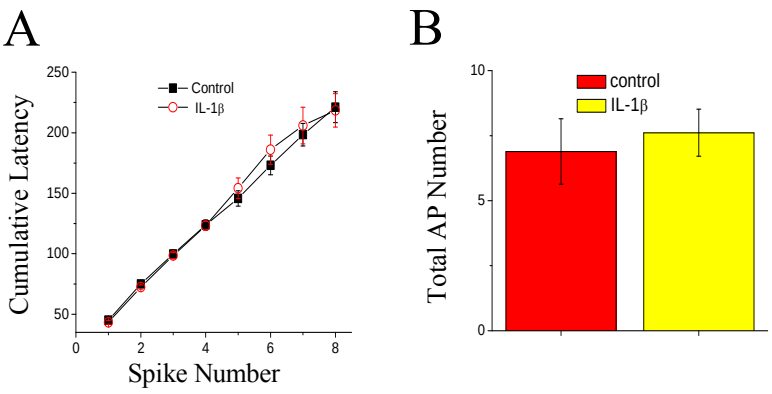


Small Neurons; IB4-positive

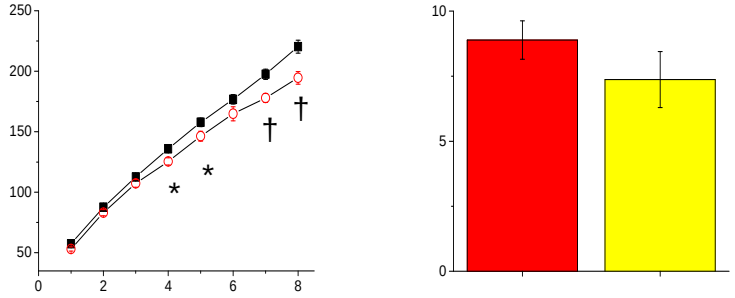


Medium Neurons

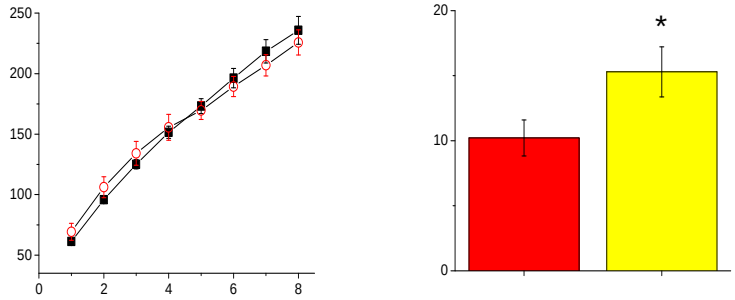


Large Neurons

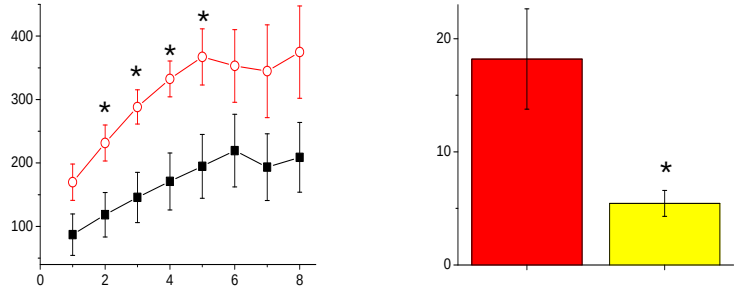

***Figure 3-10: Illustration of the effects of IL-1β exposure on DRG neuron repetitive discharge in response to depolarizing current ramps***

Representative traces of DRG neuron repetitive discharge in response to 2 nA depolarizing current ramps.

A: Illustration of the effect of IL-1β treatment on cumulative AP latency in small IB4-positive neurons. Arrows: cumulative AP latencies for control neuron (black trace). Cumulative latencies became progressively shorter with each successive AP in IL-1β treated neuron (red trace).

B: Illustration of the effect of IL-1β treatment on total AP number in medium neurons. Control neuron (black trace) generated less APs than IL-1β treated neuron (red trace).

A

Small Neurons; IB4-positive

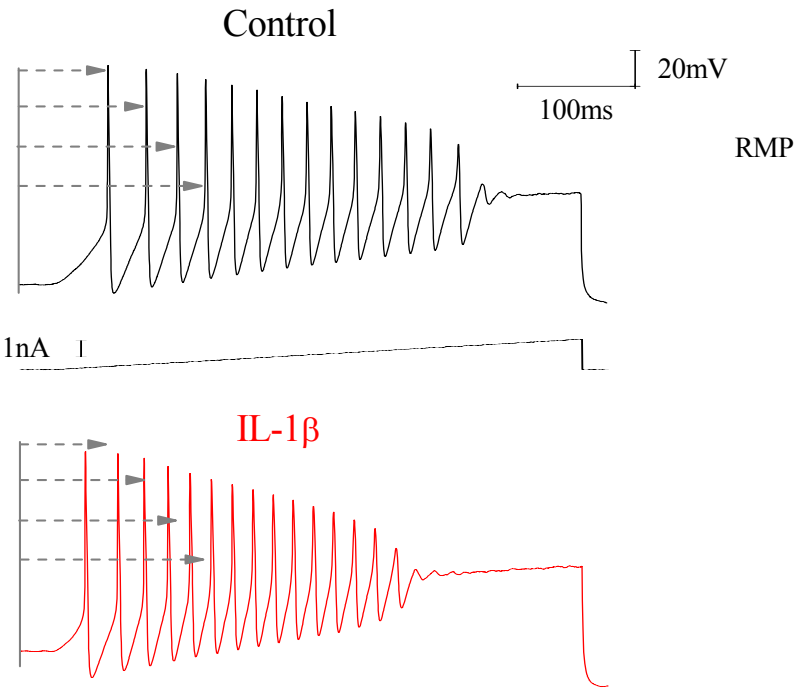


B

Medium Neurons

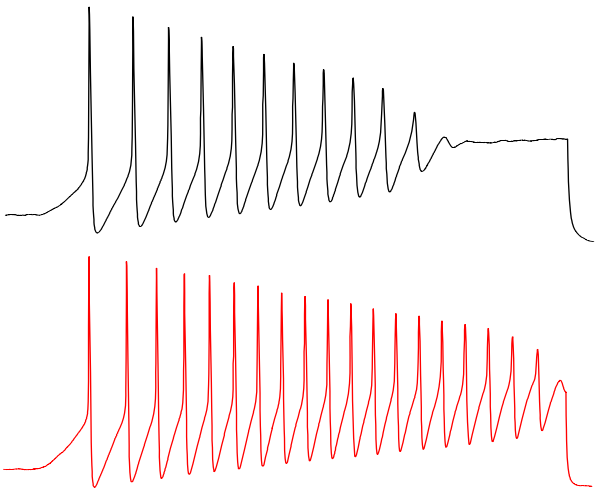

***Figure 3-11: DRG neuron responses to hyperpolarizing current steps (voltage sag) in long-term cell culture and the effect of IL-1β***

A: Quantification of voltage sag in DRG neurons. Voltage sag is characterized by an initial transient peak voltage response ($V_{Peak}$) which settles to a less negative steady-state ($V_{SS}$) level within a few hundred milliseconds. Voltage sag was quantified as the percent difference between $V_{Peak}$ and $V_{SS}$ (% voltage sag) in response to a 800 ms step at -0.1 nA.

B: Effects of IL-1β on the magnitude of voltage sag among DRG neuron subpopulations. Voltage sag was greatest in control large neurons with significant differences when compared to control medium and small IB4-positive neurons (38.6 ± 3.4%, n = 12 vs. 22.7 ± 3.0, n = 36; $p<0.01$ and 18.8 ± 2.5, n = 20; $p<0.01$; respectively). With the exception of medium neurons, long-term IL-1β exposure yielded a trend towards a decrease in voltage sag.

Error bars indicate means ± s.e.m. Significant difference vs. large neurons † = $p<0.01$ with one-way ANOVA-Tukey test.

A

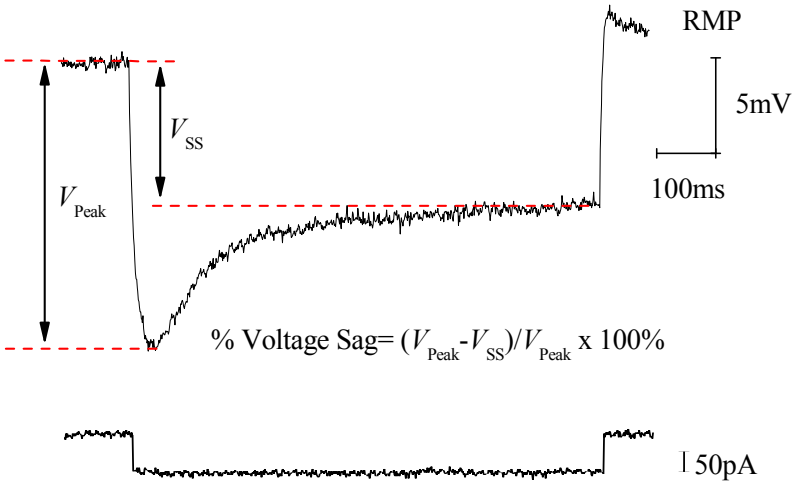
RMP
5mV
100ms
$V_{SS}$
$V_{Peak}$
% Voltage Sag= ($V_{Peak}$-$V_{SS}$)/$V_{Peak}$ x 100%
50pA

B

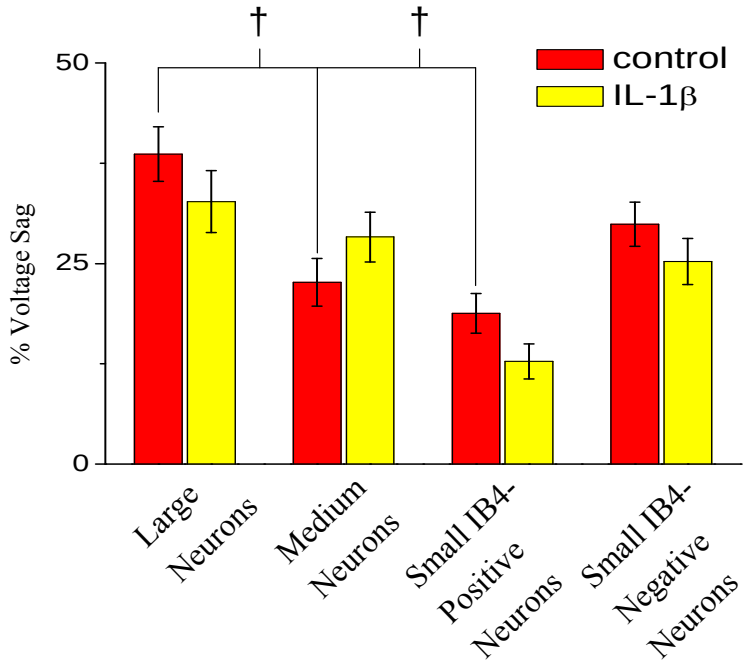
†
†
control
IL-1β
% Voltage Sag
50
25
0
Large Neurons
Medium Neurons
Small IB4-Positive Neurons
Small IB4-Negative Neurons

***Table 3-3: Comparisons of control DRG neuron AP parameters and passive membrane properties with and without IL-1Ra co-treatment***

Direct statistical comparisons were avoided between cultures with and without IL-1Ra, because the final concentration of the stabilizing agent, BSA, was double (0.001% vs. 0.002%) in antagonist experiments.

Medium Neurons: After IL-1Ra exposure, medium neurons appeared to be similar in many of the different AP parameters measured with the exception that AHP duration to 50% repolarization is shortened, whereas, input resistances, input capacitances and membrane time constants were all decreased.

Small IB4-positive neurons: After IL-1Ra exposure, small IB4-positive neuron AP height appeared larger, while AP width became broader. AHP amplitude was also decreased and AHP duration at 25% repolarization appeared longer. Small IB4-positive DRG neuron average input resistance and membrane time constant were visibly increased, while input capacitance was unchanged in cell cultures exposed to antagonist.

| *Parameter* | *Medium Neuron*<br><br>*Control*<br><br>*Value ± s.e.m. (n)* | *Medium Neuron*<br><br>*Control + IL-1Ra*<br><br>*Value ± s.e.m. (n)* | *Small $IB_4$ +ve Neuron*<br><br>*Control*<br><br>*Value ± s.e.m. (n)* | *Small $IB_4$ +ve Neuron*<br><br>*Control + IL-1Ra*<br><br>*Value ± s.e.m. (n)* |
|---|---|---|---|---|
| *RMP (mV)* | -61.4 ± 0.8 (36) | -60.5 ± 0.9 (22) | -58.5 ± 1.4 (20) | -60.2± 1.4 (22) |
| *Spike Height (mV)* | 97.3 ± 2.5 (36) | 100.2 ± 3.6 (22) | 103.8 ± 3.4 (20) | 113.9 ± 3.0 (22) |
| *Spike Width (ms)* | 2.05 ± 0.15 (36) | 1.85 ± 0.13 (22) | 1.86 ± 0.12 (20) | 2.51 ± 0.21 (22) |
| *Maximal Rate of Depolarization (mV/ms)* | 95.5 ± 5.8 (36) | 109.3 ± 9.1 (22) | 110.0 ± 7.4 (20) | 101.5 ± 5.7(22) |
| *Maximal Rate of Repolarization (mV/ms)* | -52.1 ± 2.5 (36) | -58.0 ± 3.9 (22) | -57.9 ± 3.3 (20) | -54.0 ± 3.6 (22) |
| *AHP Amplitude (mV)* | -17.7 ± 0.8 (36) | -15.5 ± 1.1 (22) | -20.1 ± 0.9 (20) | -16.7 ± 1.0 (22) |
| *AHP Duration at 25% Repolarization (ms)* | 15.88 ± 0.92 (36) | 14.53 ± 1.31 (22) | 17.75 ± 2.00 (20) | 25.28 ± 3.11 (22) |
| *AHP Duration at 50% Repolarization (ms)* | 34.99 ± 2.15 (36) | 26.44 ± 3.08 (21) | 35.2 6± 3.65 (18) | 39.45 ± 4.49 (15) |
| *Rheobase (nA)* | 0.49 ± 0.03 (36) | 0.51 ± 0.04 (22) | 0.37 ± 0.03 (20) | 0.36 ± 0.02 (22) |
| *Input Resistance (MΩ)* | 330 ± 23 (36) | 225 ± 18 (22) | 453± 35 (20) | 591± 31 (22) |
| *Input Capacitance (pF)* | 180.8 ± 17.8 (36) | 149.4 ± 17.7 (22) | 127.4 ± 10.5 (20) | 129 ± 13.6 (22) |
| *Membrane Time Constant (ms)* | 62.2 ± 8.33 (36) | 34.27 ± 5.16 (22) | 59.24 ± 6.48 (20) | 72.85 ± 6.93 (22) |

***Table 3-4: Summary of the effects of IL-1β exposure on DRG neuron AP parameters and passive membrane properties with IL-1Ra co-treatment***

Statistical significance determined with unpaired t-test. Significant difference vs. control * = $p<0.05$, † = $p<0.01$and § = $p<0.001$ with unpaired t-test.

| *Parameter* | *Medium Neuron*<br><br>*Control*<br><br>*Value ± s.e.m. (n)* | *Medium Neuron*<br><br>*IL-β*<br><br>*Value ± s.e.m. (n)* | *Small $IB_4$ +ve Neuron*<br><br>*Control*<br><br>*Value ± s.e.m. (n)* | *Small $IB_4$ +ve Neuron*<br><br>*IL-1β*<br><br>*Value ± s.e.m. (n)* |
|---|---|---|---|---|
| *RMP (mV)* | -60.5 ± 0.9 (22) | -61.8 ± 1.1 (25) | -60.2± 1.4 (22) | -62.5 ± 1.3 (21) |
| *Spike Height (mV)* | 100.2 ± 3.6 (22) | 114.6 ± 2.9 (25)$^{\dagger}$ | 113.9 ± 3.0 (22) | 107.4 ± 2.9 (21) |
| *Spike Width (ms)* | 1.85 ± 0.13 (22) | 2.58 ± 0.26 (25)$^{*}$ | 2.51 ± 0.21 (22) | 3.67 ± 0.87 (21) |
| *Maximal Rate of Depolarization (mV/ms)* | 109.3 ± 9.1 (22) | 138.1 ± 7.6 (25)$^{*}$ | 101.5 ± 5.7(22) | 106.5 ± 9.2 (21) |
| *Maximal Rate of Repolarization (mV/ms)* | -58.0 ± 3.9 (22) | -54.3 ± 4.0 (25) | -54.0 ± 3.6 (22) | -44.5 ± 3.8 (21) |
| *AHP Amplitude (mV)* | -15.5 ± 1.1 (22) | -12.6 ± 1.2 (25) | -16.7 ± 1.0 (22) | -15.8 ± 1.0 (21) |
| *AHP Duration at 25% Repolarization (ms)* | 14.53 ± 1.31 (22) | 16.67 ± 1.76 (21) | 25.28 ± 3.11 (22) | 21.55 ± 2.26 (21) |
| *AHP Duration at 50% Repolarization (ms)* | 26.44 ± 3.08 (21) | 33.53 ± 3.42 (20) | 39.45 ± 4.49 (15) | 39.50 ± 4.57 (15) |
| *Rheobase (nA)* | 0.51 ± 0.04 (22) | 0.40 ± 0.04 (25)$^{*}$ | 0.36 ± 0.02 (22) | 0.37 ± 0.03 (21) |
| *Input Resistance (MΩ)* | 225 ± 18 (22) | 393± 36 (25)$^{\S}$ | 591± 31 (22) | 551 ± 41 (21) |
| *Input Capacitance (pF)* | 149.4 ± 17.7 (22) | 125.1 ± 12.8 (25) | 129 ± 13.6 (22) | 129.9 ± 16.3 (21) |
| *Membrane Time Constant (ms)* | 34.27 ± 5.16 (22) | 50.4 ± 7.32 (25) | 72.85 ± 6.93 (22) | 64.8 ± 5.99 (21) |

***Figure 3-12: Representative DRG neuron APs in IL-1Ra co-treated cultures and the effects of IL-1β***

A: Representative recordings of APs elicited in control small IB4-positive and medium neurons by a 5 ms pulse of depolarizing current set at rheobase (black traces).

B: Effects of long-term IL-1β exposure on AP shapes (blue traces) in DRG neurons with IL-1Ra co-treatment. In small IB4-positive neurons, broadening of APs in response to IL-1β exposure was still evident, but not statistically different, in the presence of IL-1Ra (inset). In medium neurons, IL-1Ra was unable to attenuate differences in AP height (dashed line). In contrast, IL-1Ra co-application antagonized IL-1β effects on medium neuron AHP amplitude (solid line). In the presence of IL-1Ra, IL-1β exposure also produced novel increases in medium neuron AP width (inset).

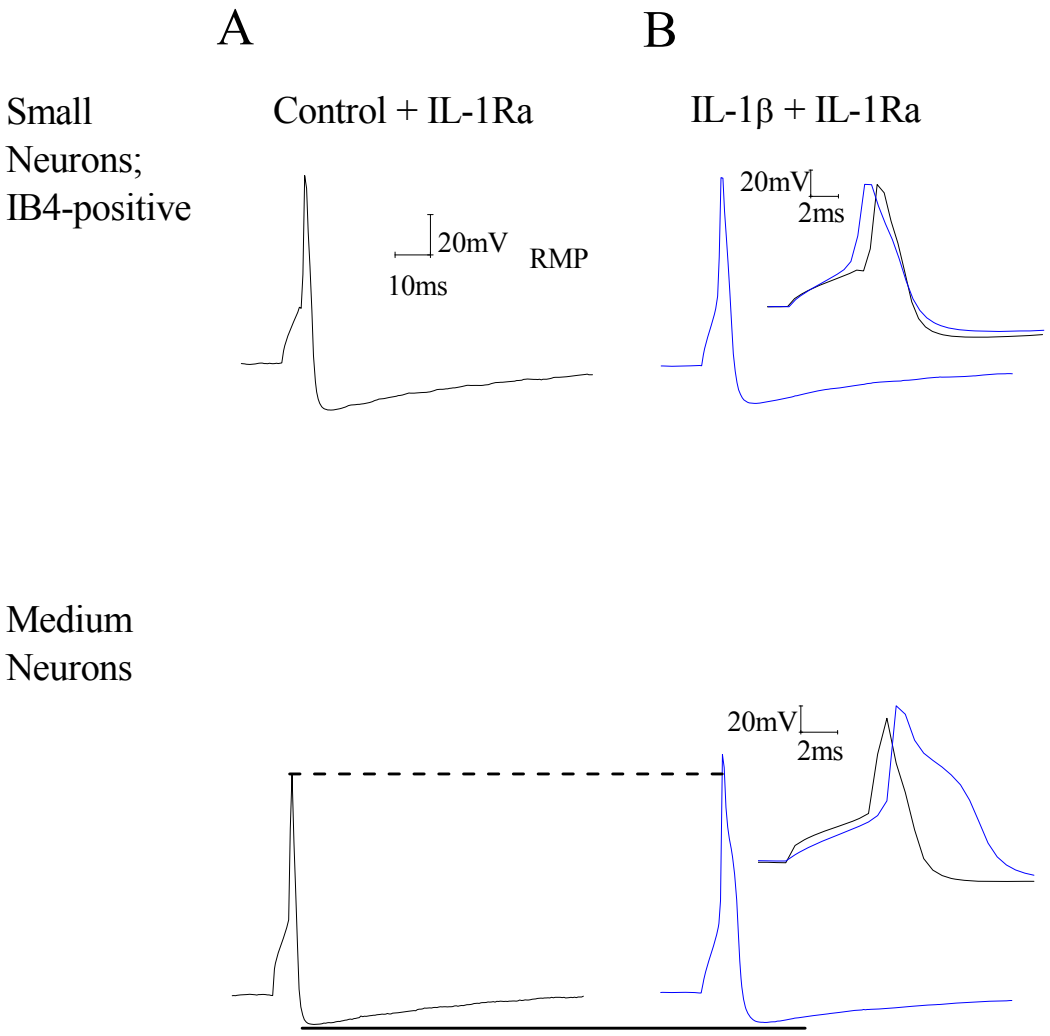
A
B
Small Neurons; IB4-positive
Control + IL-1Ra
IL-1β + IL-1Ra
20mV
10ms
RMP
20mV
2ms
Medium Neurons
20mV
2ms

***Figure 3-13: IL-1β effects on DRG neuron rheobase, AP rates and AHP duration in IL-1Ra co-treated cultures***

A: Effects of IL-1b exposure on DRG neuron rheobase in IL-1Ra co-treated cultures. In medium neurons, IL-1Ra was unable to attenuate reductions in rheobase in response to IL-1β exposure (0.51 ± 0.04 nA, n = 22 vs. 0.40 ± 0.04, n = 25; $p<0.05$).

B: Effects of IL-1β exposure on DRG neuron maximal rates of depolarization and repolarization in IL-1Ra co-treated cultures. In small IB4-positive neurons, the reduction in the maximal rate of repolarization in response to IL-1β exposure was still evident in the presence of IL-1Ra (-54.0 ± 3.6 mV/ms, n = 22 vs. -44.5 ± 3.8, n = 21; $p=0.07$). In medium neurons, IL-1Ra was unable to completely attenuate increases in the maximal rate of depolarization in response to IL-1β exposure (109.3 ± 9.1 mV/ms, n = 22 vs. 138.1 ± 7.6, n = 25; $p<0.05$). In contrast, IL-1Ra co-application antagonized the effect of IL-1β on medium neuron maximal rate of repolarization.

C: Effects of IL-1β exposure on DRG neuron AHP durations at 25% and 50% repolarization in IL-1Ra co-treated cultures. IL-1Ra co-application antagonized IL-1β effects on medium neuron AHP duration at 50% repolarization.

Error bars indicate means ± s.e.m. Significant difference vs. control * = $p<0.05$ with unpaired t-test. For clarity, error bars are omitted in 3D bar graphs.

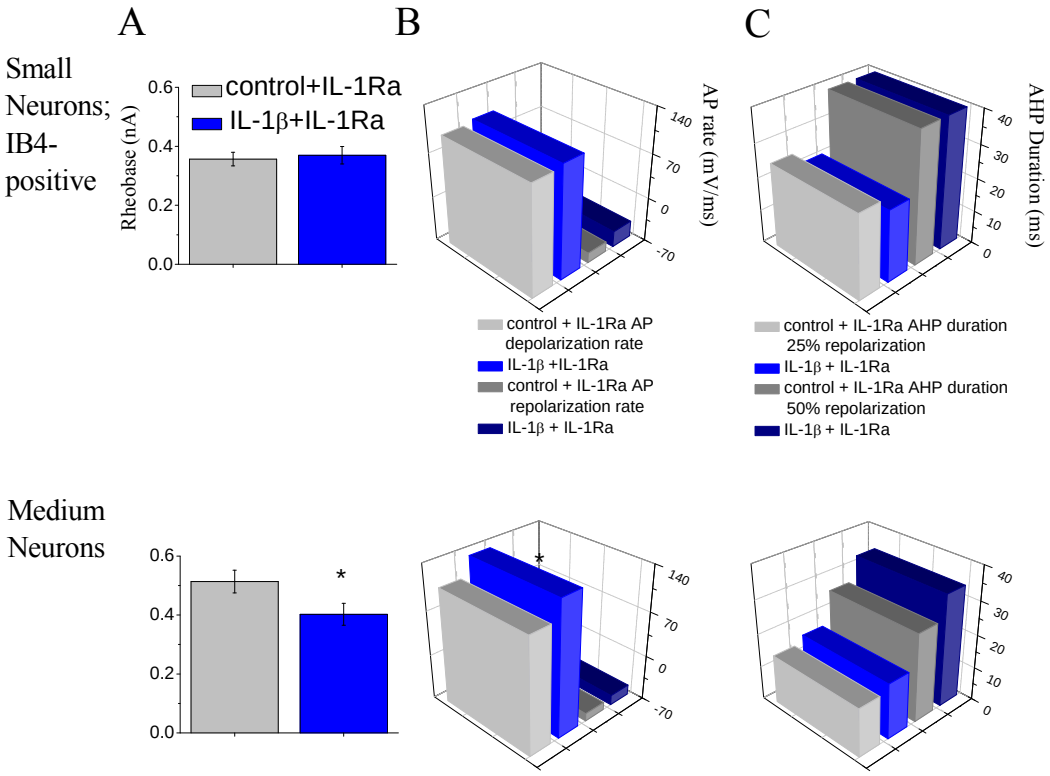
A
B
C
Small Neurons; IB4-positive
Rheobase (nA)
0.6
0.4
0.2
0.0
control+IL-1Ra
IL-1β+IL-1Ra
AP rate (mV/ms)
140
70
0
-70
control + IL-1Ra AP depolarization rate
IL-1β +IL-1Ra
control + IL-1Ra AP repolarization rate
IL-1β + IL-1Ra
AHP Duration (ms)
40
30
20
10
0
control + IL-1Ra AHP duration 25% repolarization
IL-1β + IL-1Ra
control + IL-1Ra AHP duration 50% repolarization
IL-1β + IL-1Ra
Medium Neurons
*
*

***Figure 3-14: Effects IL-1β exposure on DRG neuron distribution of firing patterns and total AP number in response to step commands in IL-1Ra co-treated cell cultures***

Comparisons in discharge pattern and concurrent AP number were made using 800 pA steps for medium neurons and 500 pA steps for small IB4-positive neurons.

A: Effects of IL-1β exposure DRG neuron firing patterns in IL-1Ra co-treated cell cultures. Single-spike, phasic and tonic discharge patterns were consistently observed and, in internal control small IB4-positive neurons, these patterns appeared in 27.3% (6/22), 54.5% (12/22), and 18.2% (4/22) of neurons, respectively. In medium neurons, these same patterns were seen in 42.9% (9/21), 38.1% (8/21) and 19% (4/21) of neurons. Similar to IL-1β in the absence of IL-1Ra, irregular discharge behaviour emerged after IL-1β exposure in 2 (18% of total) medium neurons. IL-1β exposure did not significantly alter the proportions of the four discharge patterns in either DRG neuron subpopulation (Fisher's exact-test, $p>0.05$).

B: Effect of IL-1β exposure on DRG neuron total AP number in IL-1Ra co-treated cell cultures. IL-1Ra co-treatment attenuated the increases in total AP number observed in tonic discharging small IB4-positive neurons and medium neurons exposed to IL-1β (Mann-Whitney U test, $p>0.05$). Error bars indicate means ± s.e.m.

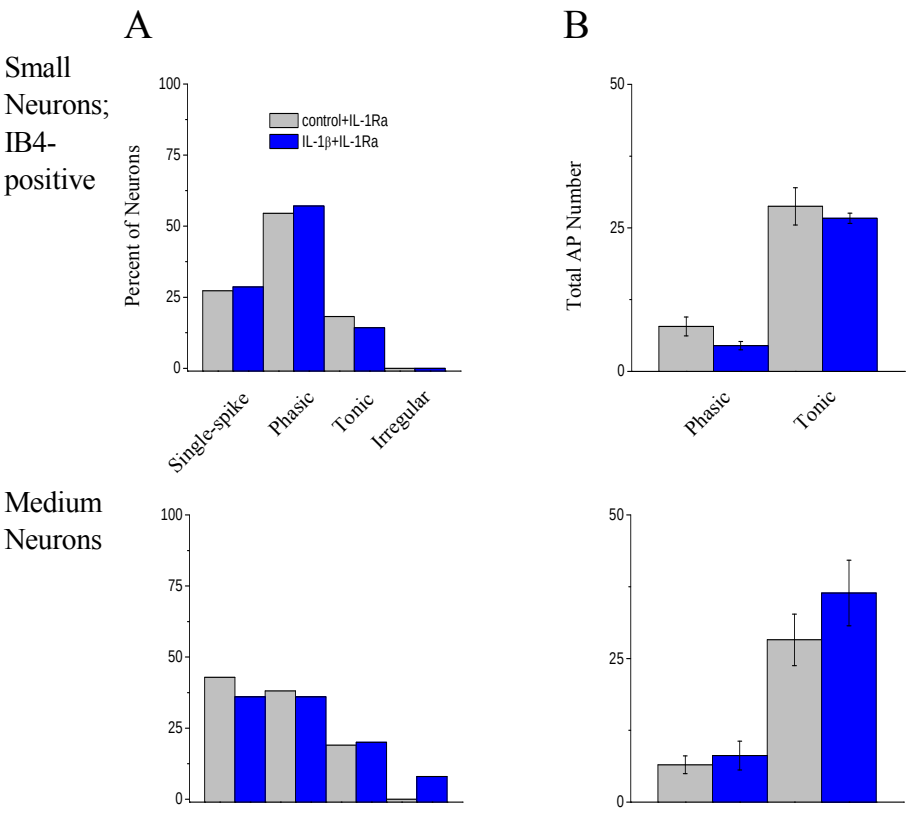
A
B
Small Neurons; IB4-positive
Medium Neurons
Percent of Neurons
control+IL-1Ra
IL-1β+IL-1Ra
Single-spike
Phasic
Tonic
Irregular
Total AP Number
Phasic
Tonic

***Figure 3-15: Effects of IL-1β exposure on DRG neuron repetitive firing frequencies in IL-1Ra co-treated cell cultures***

Frequency – current (*f-I*) curves illustrate the effect of IL-1β exposure on DRG neuron repetitive discharge in response to 800 ms depolarizing current steps in IL-1Ra co-treated cell cultures.

A: Instantaneous firing frequency *f-I* curves as measured from the first interspike interval. IL-1Ra attenuated higher instantaneous discharge frequencies for both small IB4-positive and medium neurons in response to IL-1β exposure (unpaired t-test, $p>0.05$).

B: Steady-state frequency *f-I* curves as measure from the steady-state interspike interval. IL-1Ra attenuated higher steady-state discharge frequencies for both small IB4-positive and medium neurons in response to IL-1β exposure (unpaired t-test, $p>0.05$).

Traces: small IB4-positive (top) and medium (bottom) neuron representative traces of internal control (black) versus IL-1β treated (blue) repetitive firing in response to depolarizing current steps in IL-1Ra co-treated cell cultures.

Error bars indicate means ± s.e.m.

A

B

Small Neurons; IB4-positive

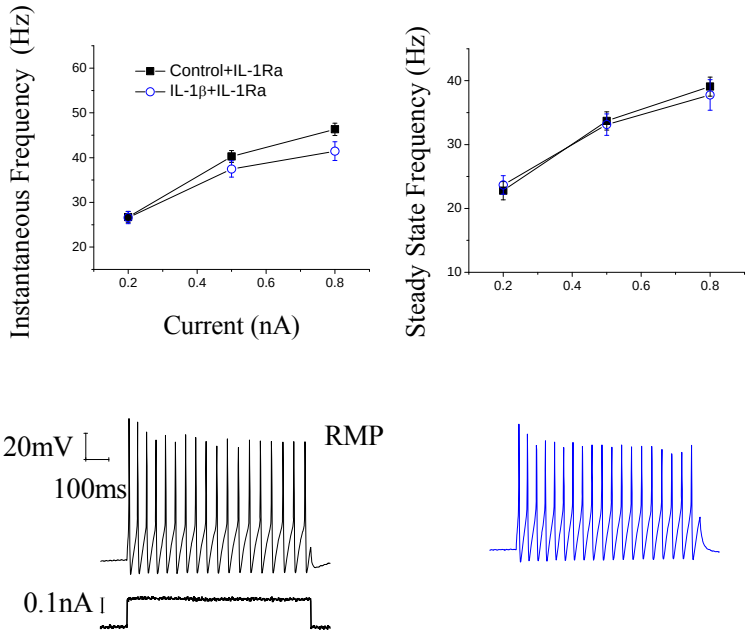


Medium Neurons

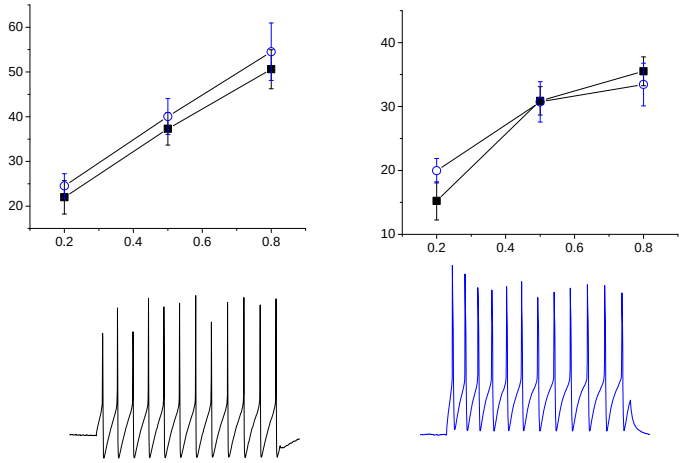

***Figure 3-16: Effect of IL-1β exposure on DRG neuron firing capability in response to current ramps in IL-1Ra co-treated cell cultures***

AP discharge was seen in 100% (22/22) of internal control small IB4-positive and 63.6% (14/22) of medium neurons and these proportions were not significantly altered in the presence of IL-1β with IL-1Ra co-treatment (Fisher's exact-test, $p>0.05$).

Small neurons; IB4-positive

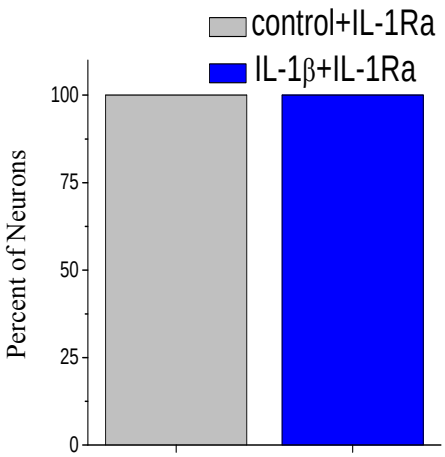


Medium Neurons

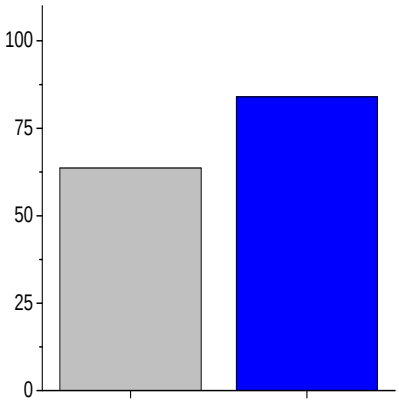

***Figure 3-17: Effects of IL-1β on DRG neuron cumulative AP latency and total AP number in response to current ramps in IL-1Ra co-treated cultures***

A: IL-1Ra attenuated decreases in small IB4-positive neuron cumulative AP latencies in response to IL-1β exposure (unpaired t-test, $p>0.05$).

B: IL-1Ra attenuated increases in medium neuron total AP number in response to IL-1β exposure (unpaired t-test, $p>0.05$).

Traces: small IB4-positive (top) and medium (bottom) neuron representative traces of internal control (black) versus IL-1β treated (blue) repetitive firing in response to depolarizing current ramps in IL-1Ra co-treated cell cultures.

Error bars indicate means ± s.e.m. Data for the control group from 22 small IB4-positive and 14 medium neurons. Data for the IL-1β treated group from 21 small IB4-positive and 21 medium neurons.

A

B

Small Neurons; IB4-positive

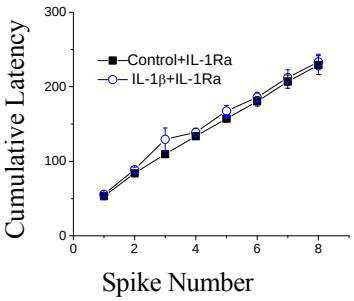


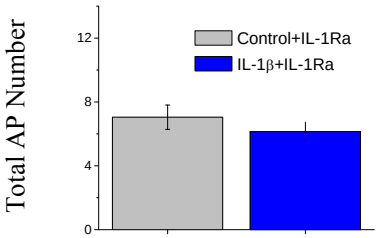


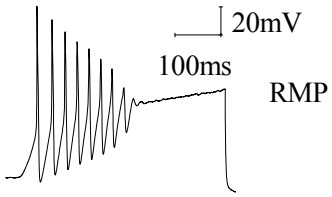


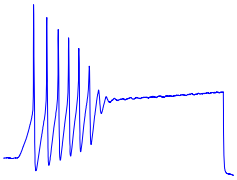

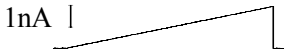


Medium Neurons

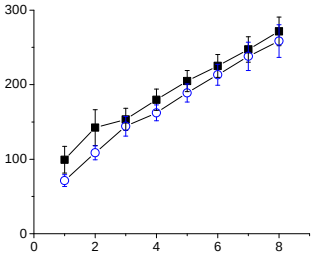


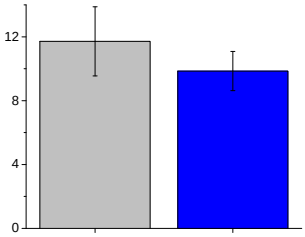


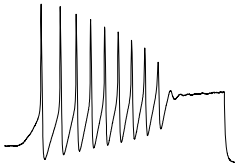

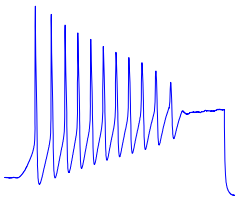

***Table 3-5: Summary of significant findings***

Table summarizes significant findings in Chapter 3. In general, long-term IL-1β exposure increased excitability in medium and small IB4-positive DRG neurons. In contrast, large neurons had reduced excitability, while small IB4-negative neurons were unresponsive. IL-1Ra attenuated some, but not all, changes in medium and small IB4-positive neurons exposed to IL-1β.

| Parameter | Effect of IL-1β | Antagonised by IL-1Ra? |
|---|---|---|
| **Large Neuron** AP shape | No change | |
| **Medium Neuron** AP shape | Taller | No |
| **Small IB4-positive Neuron** AP shape | Broader | Yes |
| **Small IB4-negative Neuron** AP shape | No change | |
| **Large Neuron** AHP shape | Longer | |
| **Medium Neuron** AHP shape | Shallower and shorter | Yes |
| **Small IB4-positive Neuron** AHP shape | No change | |
| **Small IB4-negative Neuron** AHP shape | No change | |
| **Large Neuron** RB | Increased | |
| **Medium Neuron** RB | Decreased | No |
| **Small IB4-positive Neuron** RB | No change | |
| **Small IB4-negative Neuron** RB | No change | |
| **Large Neuron** repetitive firing | Decreased | |
| **Medium Neuron** repetitive firing | Increased | Yes |
| **Small IB4-positive Neuron** repetitive firing | Increased | Yes |
| **Small IB4-negative Neuron** repetitive firing | No change | |

### *3.3 References*


1. Abdulla FA, Smith PA (2001) Axotomy- and autotomy-induced changes in the excitability of rat dorsal root ganglion neurons. J Neurophysiol 85: 630-643.

2. Abdulla FA, Smith PA (2002) Changes in Na(+) channel currents of rat dorsal root ganglion neurons following axotomy and axotomy-induced autotomy. J Neurophysiol 88: 2518-2529.

3. Aguayo LG, Weight FF, White G (1991) TTX-sensitive action potentials and excitability of adult rat sensory neurons cultured in serum- and exogenous nerve growth factor-free medium. Neurosci Lett 121: 88-92.

4. Amir R, Devor M (1996) Chemically mediated cross-excitation in rat dorsal root ganglia. J Neurosci 16: 4733-4741.

5. Andre R, Moggs JG, Kimber I, Rothwell NJ, Pinteaux E (2006) Gene regulation by IL-1beta independent of IL-1R1 in the mouse brain. Glia 53: 477-483.

6. Andrew, J. Souter and Mary, G. Garry. Spinal interleukin-1+¦ reduces inflammatory pain. Pain 86[1], 63-68. 1-5-2000.

7. Binshtok AM, Wang H, Zimmermann K, Amaya F, Vardeh D, Shi L, Brenner GJ, Ji RR, Bean BP, Woolf CJ, Samad TA (2008) Nociceptors are interleukin-1beta sensors. J Neurosci 28: 14062-14073.

8. Caffrey JM, Eng DL, Black JA, Waxman SG, Kocsis JD (1992) Three types of sodium channels in adult rat dorsal root ganglion neurons. Brain Research 592: 283-297.

9. Copray JC, Mantingh I, Brouwer N, Biber K, Kust BM, Liem RS, Huitinga I, Tilders FJ, Van Dam AM, Boddeke HW (2001) Expression of interleukin-1 beta in rat dorsal root ganglia. J Neuroimmunol 118: 203-211.

10. Czeh G, Kudo N, Kuno M (1977) Membrane properties and conduction velocity in sensory neurones following central or peripheral axotomy. J Physiol 270: 165-180.

11. Devor M (2009) Ectopic discharge in Abeta afferents as a source of neuropathic pain. Exp Brain Res 196: 115-128.

12. Dib-Hajj SD, Tyrrell L, Black JA, Waxman SG (1998) NaN, a novel voltage-gated Na channel, is expressed preferentially in peripheral sensory neurons and down-regulated after axotomy. Proceedings of the National Academy of Sciences of the United States of America 95: 8963-8968.

13. Diem R, Hobom M, Grotsch P, Kramer B, Bahr M (2003) Interleukin-1 beta protects neurons via the interleukin-1 (IL-1) receptor-mediated Akt pathway and by IL-1 receptor-independent decrease of transmembrane currents in vivo. Mol Cell Neurosci 22: 487-500.

14. Dinarello CA (1998) Interleukin-1, Interleukin-1 Receptors and Interleukin-1 Receptor Antagonist. International Reviews of Immunology 16: 457-499.

15. Djouhri L, Bleazard L, Lawson SN (1998) Association of somatic action potential shape with sensory receptive properties in guinea-pig dorsal root ganglion neurones. J Physiol 513 ( Pt 3): 857-872.

16. Fang X, McMullan S, Lawson SN, Djouhri L (2005) Electrophysiological differences between nociceptive and non-nociceptive dorsal root ganglion neurones in the rat in vivo. The Journal of Physiology 565: 927-943.

17. Fang X, Djouhri L, McMullan S, Berry C, Waxman SG, Okuse K, Lawson SN (2006) Intense Isolectin-B4 Binding in Rat Dorsal Root Ganglion Neurons Distinguishes C-Fiber Nociceptors with Broad Action Potentials and High Nav1.9 Expression. J Neurosci 26: 7281-7292.

18. Ferreira SH, Lorenzetti BB, Bristow AF, Poole S (1988) Interleukin-1 beta as a potent hyperalgesic agent antagonized by a tripeptide analogue. Nature 334: 698-700.

19. Fjell J, Cummins TR, Dib-Hajj SD, Fried K, Black JA, Waxman SG (1999) Differential role of GDNF and NGF in the maintenance of two TTX-resistant sodium channels in adult DRG neurons. Brain Res Mol Brain Res 67: 267-282.

20. Fukuoka H, Kawatani M, Hisamitsu T, Takeshige C (1994) Cutaneous hyperalgesia induced by peripheral injection of interleukin-1 beta in the rat. Brain Res 657: 133-140.

21. Gallego R, Ivorra I, Morales A (1987) Effects of central or peripheral axotomy on membrane properties of sensory neurones in the petrosal ganglion of the cat. J Physiol 391: 39-56.

22. Gold MS, Weinreich D, Kim CS, Wang R, Treanor J, Porreca F, Lai J (2003) Redistribution of Na(V)1.8 in uninjured axons enables neuropathic pain. J Neurosci 23: 158-166.

23. Gold MS, Traub RJ (2004) Cutaneous and Colonic Rat DRG Neurons Differ With Respect to Both Baseline and PGE2-Induced Changes in

Passive and Active Electrophysiological Properties. J Neurophysiol 91: 2524-2531.

24. Granowitz EV, Porat R, Mier JW, Pribble JP, Stiles DM, Bloedow DC, Catalano MA, Wolff SM, Dinarello CA (1992) Pharmacokinetics, safety and immunomodulatory effects of human recombinant interleukin-1 receptor antagonist in healthy humans. Cytokine 4: 353-360.

25. Gurtu S, Smith PA (1988) Electrophysiological characteristics of hamster dorsal root ganglion cells and their response to axotomy. J Neurophysiol 59: 408-423.

26. Hannum CH, Wilcox CJ, Arend WP, Joslin FG, Dripps DJ, Heimdal PL, Armes LG, Sommer A, Eisenberg SP, Thompson RC (1990) Interleukin-1 receptor antagonist activity of a human interleukin-1 inhibitor. Nature 343: 336-340.

27. Harper AA, Lawson SN (1985) Conduction velocity is related to morphological cell type in rat dorsal root ganglion neurones. J Physiol 359: 31-46.

28. Herseth JI, Refsnes M, Lag M, Schwarze PE (2009) Role of IL-1 beta and COX2 in silica-induced IL-6 release and loss of pneumocytes in co-cultures. Toxicol In Vitro 23: 1342-1353.

29. Humphreys NE, Grencis RK (2009) IL-1-dependent, IL-1R1-independent resistance to gastrointestinal nematodes. Eur J Immunol 39: 1036-1045.

30. Jagodic MM, Pathirathna S, Joksovic PM, Lee W, Nelson MT, Naik AK, Su P, Jevtovic-Todorovic V, Todorovic SM (2008) Upregulation of the T-Type Calcium Current in Small Rat Sensory Neurons After Chronic Constrictive Injury of the Sciatic Nerve. J Neurophysiol 99: 3151-3156.

31. Jagodic MM, Pathirathna S, Nelson MT, Mancuso S, Joksovic PM, Rosenberg ER, Bayliss DA, Jevtovic-Todorovic V, Todorovic SM (2007) Cell-Specific Alterations of T-Type Calcium Current in Painful Diabetic Neuropathy Enhance Excitability of Sensory Neurons. J Neurosci 27: 3305-3316.

32. Jevtovic-Todorovic V, Todorovic SM (2006) The role of peripheral T-type calcium channels in pain transmission. Cell Calcium 40: 197-203.

33. Jin X, Gereau RW (2006) Acute p38-mediated modulation of tetrodotoxin-resistant sodium channels in mouse sensory neurons by tumor necrosis factor-alpha. J Neurosci 26: 246-255.

34. Kim YI, Na HS, Kim SH, Han HC, Yoon YW, Sung B, Nam HJ, Shin SL, Hong SK (1998) Cell type-specific changes of the membrane properties of

peripherally-axotomized dorsal root ganglion neurons in a rat model of neuropathic pain. Neuroscience 86: 301-309.

35. Lai J, Porreca F, Hunter JC, Gold MS (2004) Voltage-gated sodium channels and hyperalgesia. Annu Rev Pharmacol Toxicol 44: 371-397.

36. Lawson SN (2002) Phenotype and function of somatic primary afferent nociceptive neurones with C-, Adelta- or Aalpha/beta-fibres. Exp Physiol 87: 239-244.

37. Lindsay RM (1988) Nerve growth factors (NGF, BDNF) enhance axonal regeneration but are not required for survival of adult sensory neurons. J Neurosci 8: 2394-2405.

38. Liu L, Yang TM, Liedtke W, Simon SA (2006) Chronic IL-1beta signaling potentiates voltage-dependent sodium currents in trigeminal nociceptive neurons. J Neurophysiol 95: 1478-1490.

39. Lu SG, Zhang X, Gold MS (2006) Intracellular calcium regulation among subpopulations of rat dorsal root ganglion neurons. The Journal of Physiology 577: 169-190.

40. Maier JA, Hla T, Maciag T (1990) Cyclooxygenase is an immediate-early gene induced by interleukin-1 in human endothelial cells. J Biol Chem 265: 10805-10808.

41. McLachlan EM, Janig W, Devor M, Michaelis M (1993) Peripheral nerve injury triggers noradrenergic sprouting within dorsal root ganglia. Nature 363: 543-546.

42. Oka T, Aou S, Hori T (1993) Intracerebroventricular injection of interleukin-1 beta induces hyperalgesia in rats. Brain Res 624: 61-68.

43. Oka T, Aou S, Hori T (1994) Intracerebroventricular injection of interleukin-1 beta enhances nociceptive neuronal responses of the trigeminal nucleus caudalis in rats. Brain Res 656: 236-244.

44. Orencole SF, Dinarello CA (1989) Characterization of a subclone (D10S) of the D10.G4.1 helper T-cell line which proliferates to attomolar concentrations of interleukin-1 in the absence of mitogens. Cytokine 1: 14-22.

45. Perry MJ, Lawson SN (1998) Differences in expression of oligosaccharides, neuropeptides, carbonic anhydrase and neurofilament in rat primary afferent neurons retrogradely labelled via skin, muscle or visceral nerves. Neuroscience 85: 293-310.

46. Petruska JC, Napaporn J, Johnson RD, Gu JG, Cooper BY (2000) Subclassified Acutely Dissociated Cells of Rat DRG: Histochemistry and Patterns of Capsaicin-, Proton-, and ATP-Activated Currents. J Neurophysiol 84: 2365-2379.

47. Renganathan M, Cummins TR, Waxman SG (2001) Contribution of Na(v)1.8 sodium channels to action potential electrogenesis in DRG neurons. J Neurophysiol 86: 629-640.

48. Ritter AM, Mendell LM (1992) Somal membrane properties of physiologically identified sensory neurons in the rat: effects of nerve growth factor. J Neurophysiol 68: 2033-2041.

49. Rizzo MA, Kocsis JD, Waxman SG (1994) Slow sodium conductances of dorsal root ganglion neurons: intraneuronal homogeneity and interneuronal heterogeneity. J Neurophysiol 72: 2796-2815.

50. Robinson DR, McNaughton PA, Evans ML, Hicks GA (2004) Characterization of the primary spinal afferent innervation of the mouse colon using retrograde labelling. Neurogastroenterology & Motility 16: 113-124.

51. Robinson DR, Gebhart GF (2008) Inside Information: The Unique Features of Visceral Sensation. Molecular Interventions 8: 242-253.

52. Safieh-Garabedian B, Poole S, Allchorne A, Winter J, Woolf CJ (1995) Contribution of interleukin-1 beta to the inflammation-induced increase in nerve growth factor levels and inflammatory hyperalgesia. Br J Pharmacol 115: 1265-1275.

53. Snape A, Pittaway JF, Baker MD (2009) Excitability parameters and sensitivity to anemone toxin ATX-II in rat small diameter primary sensory neurones discriminated by Griffonia simplicifolia Isolectin-IB4. The Journal of Physiology.

54. Snider WD, McMahon SB (1998) Tackling Pain at the Source: New Ideas about Nociceptors. Neuron 20: 629-632.

55. Stebbing MJ, Eschenfelder S, Habler HJ, Acosta MC, Janig W, McLachlan EM (1999) Changes in the action potential in sensory neurones after peripheral axotomy in vivo. Neuroreport 10: 201-206.

56. Stucky CL, Lewin GR (1999b) Isolectin B(4)-positive and -negative nociceptors are functionally distinct. J Neurosci 19: 6497-6505.

57. Stucky CL, Lewin GR (1999a) Isolectin B(4)-positive and -negative nociceptors are functionally distinct. J Neurosci 19: 6497-6505.

58. Stucky CL, Lewin GR (1999c) Isolectin B4-Positive and -Negative Nociceptors Are Functionally Distinct. J Neurosci 19: 6497-6505.

59. Study RE, Kral MG (1996) Spontaneous action potential activity in isolated dorsal root ganglion neurons from rats with a painful neuropathy. Pain 65: 235-242.

60. Sugiura T, Dang K, Lamb K, Bielefeldt K, Gebhart GF (2005) Acid-Sensing Properties in Rat Gastric Sensory Neurons from Normal and Ulcerated Stomach. J Neurosci 25: 2617-2627.

61. Takeda M, Kitagawa J, Takahashi M, Matsumoto S (2008) Activation of interleukin-1beta receptor suppresses the voltage-gated potassium currents in the small-diameter trigeminal ganglion neurons following peripheral inflammation. Pain 139: 594-602.

62. Takeda M, Tanimoto T, Kadoi J, Nasu M, Takahashi M, Kitagawa J, Matsumoto S (2007) Enhanced excitability of nociceptive trigeminal ganglion neurons by satellite glial cytokine following peripheral inflammation. Pain 129: 155-166.

63. Takii T, Akahoshi T, Kato K, Hayashi H, Marunouchi T, Onozaki K (1992) Interleukin-1 up-regulates transcription of its own receptor in a

human fibroblast cell line TIG-1: role of endogenous PGE2 and cAMP. Eur J Immunol 22: 1221-1227.

64. Takii T, Hayashi H, Marunouchi T, Onozaki K (1994) Interleukin-1 down-regulates type I interleukin 1 receptor mRNA expression in a human fibroblast cell line TIG-1 in the absence of prostaglandin E2 synthesis. Lymphokine Cytokine Res 13: 213-219.

65. Villiere V, McLachlan EM (1996) Electrophysiological properties of neurons in intact rat dorsal root ganglia classified by conduction velocity and action potential duration. J Neurophysiol 76: 1924-1941.

66. Waddell PJ, Lawson SN (1990) Electrophysiological properties of subpopulations of rat dorsal root ganglion neurons in vitro. Neuroscience 36: 811-822.

67. Wall PD, Devor M (1983) Sensory afferent impulses originate from dorsal root ganglia as well as from the periphery in normal and nerve injured rats. Pain 17: 321-339.

68. White G, Lovinger DM, Weight FF (1989) Transient low-threshold Ca2+ current triggers burst firing through an afterdepolarizing potential in an adult mammalian neuron. Proc Natl Acad Sci U S A 86: 6802-6806.

69. Zamponi GW, Lewis RJ, Todorovic SM, Arneric SP, Snutch TP (2009) Role of voltage-gated calcium channels in ascending pain pathways. Brain Research Reviews 60: 84-89.

70. Zhang JM, Donnelly DF, Song XJ, Lamotte RH (1997) Axotomy Increases the Excitability of Dorsal Root Ganglion Cells With Unmyelinated Axons. J Neurophysiol 78: 2790-2794.

# CHAPTER 4

Long-term IL-1β Exposure:

Effects On Ionic Currents In Small-sized IB4-positive DRG Neurons

## *4.1 Results*

Because long-term IL-1β exposure increased the excitability of small IB4-positive DRG neurons, I analyzed the changes in various ionic conductances that might explain these changes.

### *4.1.1 Sodium current*

As described in Methods (Chapter 2), total $I_{Na}$ was recorded from DRG cells using a series of 40 ms depolarizing voltage commands from $V_h$ = -90 mV (Figure 4-1 Ai). To improve voltage-clamp control, $Na^+$ concentration in external solution was reduced to 50 mM. Using a $Cs^+$ based electrode solution to block $K^+$ currents, neurons were then treated with 300 nM TTX to isolate TTX-sensitive (TTX-S) $I_{Na}$ from TTX-resistant (TTX-R) $I_{Na}$ (Figure 4Aii) and, interestingly, digital subtraction (Figure 4Ai-ii) revealed that all measurable current was TTX-S $I_{Na}$. Therefore, all $I_{Na}$ data discussed here is TTX-S $I_{Na}$ recorded from small IB4-positive neurons in long-term cell cultures. The *I-V* plot in Figure 4-1B indicates that peak $I_{Na}$ occurred at -20 mV in both control and IL-1β exposed neurons. Similar peak current densities were also recorded from small IB4-positive control neurons (-166 ± 27 pA/pF; n=12) and neurons after 5-6 days exposure to 100 pM IL-1β (-130 ± 14 pA/pF; n=12; unpaired t-test, $p>0.05$). In addition, curves for the voltage dependence of activation are almost entirely superimposed (Figure 4-1C, also see Table 4-1).

Comparable to activation, there were no shifts in the curves for steady-state fast inactivation (measured in response to 300 ms incremental prepulses;

Figure 4-2A) after IL-1β exposure (Figure 4-2B and Table 4-1). Since shifts in the voltage dependence of steady-state slow inactivation have been previously reported for $I_{Na}$ in the context of pain hypersensitivity (Cummins et al., 2004;Binshtok et al., 2008), five second prepulses, followed by 20 ms recovery pulses to -120 mV (to allow recovery from fast inactivation), preceded 10 ms test pulses to -10 mV to determine the fraction of current available (Figure 4-2C). As indicated from overlapping steady-state slow inactivation curves, long-term IL-1β exposure was, again, without effect (Figure 4-2D and Table 4-1).

Last, since current-clamp studies revealed a significant increase in small IB4-positive neurons AP width after IL-1β treatment (Figure 4-3A) and this change might be associated with slowed inactivation (Snape et al., 2009), fast inactivation time constants for TTX-S $I_{Na}$ were determined. Single exponent fits of $I_{Na}$ decay, revealed that IL-1β exposure significantly increased fast inactivation time constants between -40 mV and -10 mV (Figures 4-3B and 4-3C).

### *4.1.2 Potassium current*

Voltage-clamp protocols and solutions were designed to examine both $K_V$ currents and $K_{Ca}$, since reductions in these currents are commonly implicated in sensory neuron hyperexcitability and broadening of APs (Abdulla and Smith, 2001b;Vydyanathan et al., 2005;Catacuzzeno et al., 2008;Kim et al., 2002;Sarantopoulos et al., 2007;Scholz et al., 1998;Takeda et al., 2008). As described in Methods (Chapter 2), outward currents were studied in a solution designed to isolate $K^+$ currents in the absence of $Na^+$ currents (NMG-Cl rather

than $Na^+$), while preserving $Ca^{2+}$ currents. DRG neuron potassium currents ($I_K$) were initially divided biophysically into non-inactivating and inactivating components using two different prepulse voltages ($V_p$) with identical voltage command protocols ($V_{cmd}$). Figures 4-4Ai and Aii show a family of outward currents recorded at voltages between -60 mV and +60 mV (from a holding potential ($V_h$) of -80 mV) after a 500 ms conditioning prepulse to $V_p$ = -120 mV or -30 mV in the standard NMG-Cl perfusion solution. Digital subtraction (Figure 4-4Ai – Aii) revealed the presence of an inactivating current component and is likely attributed to the presence of A-type potassium currents and/or the presence of $I_{K,Ca}$ which may decline as a consequence to the inactivation of calcium conductances (Abdulla and Smith, 2001b). In the presence of 5 mM $Mn^{2+}$, a steady-state non-inactivating component could be measured at the end of the stimulation pulse when preceded by $V_p$ = -30 mV (Figure 4-4B) and is likely to be delayed-rectifier potassium current (referred to as non-inactivating $I_K$). To isolate A-type currents, the subtraction process (Figure 4-5Ai – Aii) was repeated in the presence of 5 mM $Mn^{2+}$. Since A-type currents in DRG neurons may reflect the existence of $I_{Af}$, $I_{As}$ (or $I_D$) and $I_{Aht}$ (Gold et al., 1996b;Everill et al., 1998), in this study they are collectively referred to as inactivating $Mn^{2+}$-resistant ($Mn^{2+}$ -R) $I_K$. Last, digital subtraction of outward current (recorded at $V_p$ = -120 mV) remaining in the presence of 5mM $Mn^{2+}$ from total outward current yielded $I_{K,Ca}$ (referred to as inactivating $Mn^{2+}$ -sensitive ($Mn^{2+}$ -S) $I_K$; Figure 4-6Ai - Aii).

In view of the complexity and variability of potassium currents in DRG neurons (Akins and McCleskey, 1993;Gold et al., 1996b), a relatively simplified

approach has been used here for the investigation of the effects of long-term IL-1β exposure on $I_K$. To this end, all (24/24) small IB4-positive neurons, from control and IL-1β treated cell cultures, had non-inactivating $I_K$. In addition, control and IL-1β exposed neurons had similar *I-V* plots (Figure 4-4C) with no significant difference in peak non-inactivating $I_K$ density ($V_{cmd}$ = +60 mV: +121 ± 17 pA/pF (n=12) vs. +101 ± 21 pA/pF (n=12), respectively). 75% (9/12) control and 66.7% (8/12) IL-1β small IB4-positive neurons had measurable inactivating $Mn^{2+}$ -R $I_K$ (Fisher's exact-test, $p>0.05$) and, similar to non-inactivating $I_K$, there was no significant difference in peak current density (Figure 4-5B; +14 ± 7 pA/pF (n=9) vs. +12 ± 7 pA/pF (n=8), respectively). In contrast, all (21/21) small IB4-positive neurons recorded had inactivating $Mn^{2+}$ -S $I_K$ and IL-1β exposure significantly reduced peak current density from +73 ± 7 pA/pF; n=11 to +42 ± 7 pA/pF; n=10 (unpaired t-test, $p<0.05$; Figure 4-6B, also see Figure 4-6C).

### *4.1.3 Calcium current*

In these studies, $Ba^{2+}$ was substituted for $Ca^{2+}$ as the charge carrier (Chapter 2) and currents ($I_{Ba}$) were evoked in small-sized IB4-positive DRG neurons using a series of 150 ms depolarizing voltage commands from $V_h$ = -100 mV (Figure 4-7A) or -60 mV (Figure 4-7C). As depicted in Figure 4-7B, *I-V* plots ($V_h$ = -100 mV) for control and IL-1β treated neurons were nearly superimposed. More specifically, high voltage-activated $I_{Ba}$ (HVA-$I_{Ba}$) peak densities (recorded at $V_{cmd}$ = -10 mV) in control cultures (-114 ± 14 pA/pF; n=13) were not significantly different from that in the presence of IL-1β (-119 ± 18 pA/pF; n=14).

The presence of low voltage-activated $I_{Ba}$ (LVA-$I_{Ba}$) can be determined with small depolarizing commands to -50 mV which generate a shoulder on *I-V* plots at voltages between -60 mV and -30 mV (Abdulla and Smith, 2001b;Scroggs and Fox, 1992). Since shoulders on *I-V* plots ($V_h$ = -100 mV) were absent in both control and IL-1β treated small IB4-positive neurons and no significant differences in $I_{Ba}$ density were found at $V_{cmd}$ = -50 mV, LVA-$I_{Ba}$ was not further studied. By default, most of the $I_{Ba}$ described in small IB4-positive neurons in long-term cell culture is expected to be HVA-$I_{Ba}$.

Since peripheral nerve injury has been reported to increase inactivation of $Ba^{2+}$ conductances (Baccei and Kocsis, 2000;Abdulla and Smith, 2001b), the effect of changing $V_h$ on HVA-$I_{Ba}$ was initially examined. As shown in Figure 4-7D, there were no clear differences in *I-V* plots. Small IB4-positive neuron peak HVA- $I_{Ba}$ density ($V_{cmd}$ = -10 mV) remaining at $V_h$ = -60 mV, was similar in control (-14 ± 3 pA/pF; n=11) and IL-1β (-19 ± 3 pA/pF; n=14) cell cultures. However, relative to control neurons, IL-1β exposure appeared to decrease the sensitivity of HVA-$I_{Ba}$ to holding potential (Figure 4-7B vs. 4-7D). Therefore, sensitivity to a shift in holding potential was calculated as the percent decrease in peak HVA-$I_{Ba}$ density upon depolarization (from $V_h$ = -100 mV to -60 mV; Figure 4-7E). Similar to *I-V* plots, the percent decrease in peak HVA-$I_{Ba}$ density was not significantly different between control neurons (89.1 ± 2.3%, n=11) and neurons exposed to IL-1β (82.3 ± 3.6%, n=14).

To examine more directly the possibility that long-term IL-1β affects the voltage dependency of HVA-$I_{Ba}$ inactivation, the fraction of current available at

$V_{cmd}$ = -10 mV was determined in response to a series of 3.5 s incremental prepulses (Figure 4-8A). In 33.3% (4/12) of control and 40% (4/10) of IL-1β treated small IB4-positive neurons (Fisher's exact-test, $p>0.05$), however, normalized curves for the voltage dependence of inactivation could not be described by a single Boltzmann function fit (Chapter 2) and were, therefore, excluded from HVA-$I_{Ba}$ voltage dependence of inactivation analysis. These rejected neurons likely have HVA-$I_{Ba}$ that is composed of at least two biophysically distinct VGCC subtypes, such as N and L-type channels (Fox et al., 1987), which would need to be isolated with more extensive pharmacological protocols that are beyond the scope of this study. In the remaining small IB4-positive neurons, single Boltzmann function fitting of normalized curves for the voltage dependence of inactivation revealed that values for the $V_{1/2}$ of inactivation were not significantly different after long-term IL-1β exposure (control: -57.1 ± 10.5 mV, n=8 vs. IL-1β: -54.0 ± 11.1, n=6; Figure 4-8B and Table 4-1).

## *4.2 Discussion*

### *4.2.1 Sodium currents ($I_{Na}$) in small IB4-positive DRG neurons*

#### *4.2.1.1 Absence of TTX-R $I_{Na}$ in small IB4-positive DRG neurons*

Small-sized IB4-positive DRG neurons in long-term culture had TTX-S $I_{Na}$ with no measureable TTX-R $I_{Na}$. This complete absence suggests that long-term cell cultures did not support the functional expression of TTX-R sodium channels. As mentioned in Chapters 3, this deficiency likely relates to the maintenance of DRG cell cultures in the absence of serum and exogenously added

neurotrophins, such as NGF and GDNF (Dib-Hajj et al., 1998;Fjell et al., 1999;Ford et al., 2008;Aguayo et al., 1991;Aguayo et al., 1991;Aguayo and White, 1992). Since the TTX-R sodium channels $Na_V1.8$ and 1.9 are strongly expressed in small nociceptive sensory neurons (Fang et al., 2006;Djouhri et al., 2003;Fang et al., 2002), loss of TTX-R $I_{Na}$ in small IB4-positive neurons would result in a phenotypic shift, such as the narrowing of AP width described in Chapter 3. Coupled to alterations in electrical behaviour, TTX-R $I_{Na}$ and the corresponding channel isoforms are known to be altered after nerve injury and in the presence of IL-1β, as well as, other inflammatory mediators (Rush et al., 2007;Lai et al., 2004;Waxman et al., 2000;Cummins et al., 2007;Binshtok et al., 2008). Thus, interpretations made in my investigation on the long-term effects of IL-1β exposure in small IB4-positive neurons are limited by the absence of TTX-R $I_{Na}$.

This limitation was anticipated and an effort to attenuate phenotypic shift involved a preliminary attempt to maintain cultures in horse serum supplemented DMEM with exogenously added NGF. Under investigation using ELISA, however, ambient concentrations of IL-1β in control DRG cell cultures were unstable and approached test concentrations of IL-1β (100 pM). In contrast, control DRG cell cultures maintained in defined medium (Chapter 2), without NGF, produced IL-1β concentrations which were consistently near or below the detection limit for ELISA (≤ 5pM) and, therefore, became the accepted approach. To this end, long-term IL-1β exposure resulted in changes to DRG neuron excitability (Chapter 3) and, since the effects of nerve injury and the development

of pain-related behaviours are not restricted to alterations in the function and/or expression of TTX-R sodium channels (Momin et al., 2008;Todorovic and Jevtovic-Todorovic, 2006;Wang and Woolf, 2005;Black et al., 2004), the investigation moved forward.

*4.2.1.2 Characterization of TTX-S $I_{Na}$ in small IB4-positive DRG neurons in long-term cell culture*

TTX-S $I_{Na}$ in control small IB4-positive neurons had the typical characteristics found in other DRG neuron studies. For instance, rapid activation within a couple of hundred of microseconds, thresholds of activation ~ -50 mV and maximal amplitudes ~ -20 mV(Caffrey et al., 1992;Abdulla and Smith, 2002;Lai et al., 2004;Aguayo et al., 1991;Kostyuk et al., 1981;Ogata and Tatebayashi, 1993). As opposed to the slower inactivation kinetics (~ 10 ms at -40 mV) of TTX-R $I_{Na}$ in acutely isolated DRG neurons, TTX-S $I_{Na}$ in long-term cultured small IB4-positive neurons displayed inactivation kinetics (~ 1 ms at -40 mV) that are consistent with the well established rapid inactivation of TTX-S $I_{Na}$ (Ogata and Tatebayashi, 1993;Caffrey et al., 1992;Kostyuk et al., 1981). Voltage midpoints (~ -65 mV) for TTX-S $I_{Na}$ fast inactivation are in agreement with findings form Ogata and Tatebayashi (1993), however, there appears to be substantial variability in the literature where others have found more negative voltage midpoints (~ -85 mV) for fast inactivation (Kostyuk et al., 1981;Caffrey et al., 1992). Inconsistencies are most likely attributed to the use of fluoride in electrode solutions (Kostyuk et al., 1981) which is known to affect TTX-S $I_{Na}$ fast inactivation (Ogata and Tatebayashi, 1993) and was, therefore, avoided in my

study. Last, the voltage midpoint (~ -60 mV) for slow inactivation was depolarized relative to fast inactivation and is typical for TTX-S $I_{Na}$ in sensory neurons, but opposite to the case for TTX-R $I_{Na}$ (Fazan, Jr. et al., 2001;Rush et al., 2007).

*4.2.1.3 Effect of long-term IL-1β exposure on TTX-S $I_{Na}$ in small IB4-positive neurons*

The major finding in this part of the investigation is that the rates of TTX-S $I_{Na}$ inactivation became significantly slower after long-term exposure to IL-1β (Figure 4-3B). This is in agreement with findings from Abdulla and Smith (2002) where axotomy nerve injury resulted in slower inactivation rates for sodium currents, including TTX-S $I_{Na}$, in DRG neurons. However, the authors also reported that the change in TTX-s $I_{Na}$ was concurrent with an increase in current density and, therefore, deviates from my findings where there was no significant change. On the other hand, sciatic nerve ligation and section resulted in no change to TTX-S $I_{Na}$ density (Cummins and Waxman, 1997), instead, the conductance exhibited more rapid repriming and has been attributed to the upregulation of the sodium channel isoform $Na_V1.3$ in the injured DRG (Waxman et al., 1994). Despite the variability in the literature regarding sodium currents after nerve injury which likely relates to the type of injury and, possibly, the degree of inflammation associated with the injury, the consensus appears to be that TTX-S $I_{Na}$ is upregulated in injured DRG neurons (Gold et al., 2003;Abdulla and Smith, 2002;Cummins and Waxman, 1997;Dib-Hajj et al., 1999;Rizzo et al., 1995).

Although an increase in the presence of a rapidly repriming TTX-S $I_{Na}$ after long-term IL-1β exposure was not observed in my study, the rates of inactivation reported by Cummins and Waxman (1997) were unchanged, suggesting that alternative or additional changes to TTX-S $I_{Na}$ occurred in my study. For instance, nerve injury is also known to alter the expression of auxiliary β subunits, including the upregulation of the β3 subunit in small DRG neurons (Takahashi et al., 2003;Shah et al., 2000) which can slow $Na_V1.3$ channel gating kinetics, as well as, other channel isoforms in heterologous expression systems (Morgan et al., 2000;Qu et al., 2001;Cummins et al., 2001;Cusdin et al., 2010). In support, the β1 subunit is highly homologous to β3 (Morgan et al., 2000) and NGF was reported to increase the β1 subunit expression in cultured embryonic DRG neurons (Zur et al., 1995). Whether IL-1β directly or through the generation of other inflammatory mediators, such as NGF, could increase β3 subunit expression in cultured adult DRG neurons remains to be elucidated.

Alternatively, sodium channel upregulation may not involve changes in the expression of subunits or accessory proteins, but, rather, a direct modulation of channel function. For instance, many inflammatory mediators, including $PGE_2$, modulate TTX-R $I_{Na}$ through the activation of PKC and/or PKA which influence voltage midpoints and rates of activation, as well as, inactivation (Lai et al., 2004;England et al., 1996;Gold et al., 1996a;Gold et al., 1998). Although the influence of these inflammatory mediators on TTX-S $I_{Na}$ are largely unreported, IL-1β has been demonstrated to, acutely, potentiate TTX-S $I_{Na}$ in nociceptive neurons (Binshtok et al., 2008) and possibly involves a G-protein/PKC signalling

pathway (Liu et al., 2006). The characterization of TTX-S $I_{Na}$ upregulation in response to IL-1β, however, has not been thoroughly examined and, therefore, it remains possible that IL-1β, either directly or, possibly, through the production $PGE_2$ (Maier et al., 1990), results in a decrease in the rate of TTX-S $I_{Na}$ inactivation as observed in my study.

Since sodium channels are highly sensitive to the cellular background they are expressed in, many other possibilities remain (Rush et al., 2007). Interestingly, TTX-R $I_{Na}$ did not re-emerge in response to long-term IL-1β exposure, despite the possibility that IL-1β increases the synthesis and/or release of neurotrophins known to upregulate $Na_V1.8$ and $Na_V1.9$ expression in nociceptive DRG neurons (Fjell et al., 1999), including NGF and GDNF (Safieh-Garabedian et al., 1995;Saavedra et al., 2007;Appel et al., 1997;Tanabe et al., 2009).

*4.2.1.4 Functional implications of TTX-S $I_{Na}$ regulation in small IB4-positive DRG neurons in response to long-term IL-1β exposure*

An increase in fast inactivation time constants for TTX-S $I_{Na}$ in response to IL-1β exposure may contribute to increased AP width in small IB4-positive neurons and decreased maximal rate of repolarization observed under current-clamp (Chapter 3). Although determination of AP width in small sensory neurons is likely to depend on sodium, calcium and, possibly, potassium currents (Djouhri et al., 1998;Yoshida et al., 1978;Yoshida and Matsumoto, 2005;Oyelese et al., 1997), findings from several studies support a dominant role for $I_{Na}$. For instance, Abdulla and Smith (2001b) reported that calcium influx was attenuated after axotomy nerve injury and, therefore, concurrent AP broadening likely reflected

slowed inactivation of TTX-R $I_{Na}$ (Abdulla and Smith, 2001a;Abdulla and Smith, 2002). Further, it was determined, through computer modelling, that only a slight slowing of $I_{Na}$ is required to affect AP width (Abdulla and Smith, 2002) and, therefore, may have relevance in my study.

Decreases in the rates of TTX-S $I_{Na}$ inactivation may also have relevance to repetitive discharge and sensory neuron hyperexcitability. In support, gain of function mutations in the TTX-S sodium channel, $Na_V1.1$, slow $I_{Na}$ inactivation and, thereby, prolong membrane depolarization which is thought to enhance membrane excitability and contribute to inherited human epilepsy (Lossin et al., 2002). In another example, the sea anemone toxin, ATX-II, is known to bind TTX-S sodium channels, $Na_V1.1$ and $Na_V1.2$, resulting in defective fast inactivation which is implicated in the generation of spontaneous or ectopic discharge that likely underlies part of the painful response to the toxin (Snape et al., 2009;Rogers et al., 1996). An important distinction, however, between my study and the cited literature (Snape et al., 2009;Lossin et al., 2002;Abdulla and Smith, 2002) is that slowed $I_{Na}$ inactivation, in response to long-term IL-1β exposure, did not produce persistent sodium currents (Figure 4-3C). Future studies should, therefore, involve the modelling of slowed sodium current inactivation in the absence of persistent current and assess its contribution to the current-clamp findings in Chapter 3.

*4.2.2 Potassium currents ($I_K$) in small IB4-positive DRG neurons*

*4.2.2.1 Isolation of potassium currents in small IB4-positive neurons*

In view of the complexity and variability of potassium currents in DRG neurons (Akins and McCleskey, 1993;Gold et al., 1996b), a relatively simplified approach was used to examine both $K_V$ and $K_{Ca}$ currents in my study. There are, however, some potential limitations with this methodology. For instance, in the presence of $Mn^{2+}$, inactivating A-type currents were not always clearly isolated from non-inactivating $I_K$ (delayed rectifier) currents, using 500 ms prepulses. As depicted in Figure 4-4B, some slowly inactivating current still remained after a -30 mV prepulse. This likely reflected the presence of the slowly and incompletely inactivating, dendrotoxin-sensitive current ($I_D$) (Stansfeld et al., 1986;Everill et al., 1998) or, possibly, the high threshold ($I_{Aht}$) and/or slow ($I_{As}$) A-type potassium currents identified in small DRG neurons by Gold and colleagues (1996). In an effort to curtail this uncertainty, non-inactivating $I_K$ was measured at the end of a 300 ms voltage command where there is nearly complete inactivation ( at + 30 mV) of fast-inactivating A-type currents, however, components of slow A-type currents may still be present (Gold et al., 1996b;McFarlane and Cooper, 1991). Incomplete separation would be expected to result in an overestimation of non-inactivating $I_K$ density and an underestimation of inactivating $Mn^{2+}$ -R $I_K$ density. Coupled to this, the potential presence of multiple inactivating potassium currents, such as $I_{Aht}$ and $I_{As}$, would require further pharmacological and/or biophysical protocols for their separation

(Everill and Kocsis, 1999;Gold et al., 1996b) and, therefore, limits the interpretations made here on $K_V$ currents.

Another potential problem is that the use of 5 mM $Mn^{2+}$, to block calcium-dependent components of potassium conductances, could interfere with the activation and/or inactivation of A-type currents in cultured rat DRG neurons (Mayer and Sugiyama, 1988). Alterations in A-type currents would not only affect measurements of inactivating $Mn^{2+}$ -R $I_K$, but could complicate the assumption that the amplitude of inactivating $Mn^{2+}$ -S $I_K$ ($I_{K,Ca}$) may be deduced from the difference between total outward current and $Mn^{2+}$ -resistant current. This problem, however, is not limited to the use of $Mn^{2+}$ but extends to the use of other divalent cations, such as $Cd^{2+}$ (Mayer and Sugiyama, 1988;Abdulla and Smith, 2001b). In a similar manner to $K_V$ currents, more pharmacological protocols would need to be used, such as the application of apamin and/or iberiotoxin, to isolate $K_{Ca}$ currents better, as well as, separate them into their components (Sarantopoulos et al., 2007;Zhang et al., 2010).

Taken together, the numerous potassium conductances in sensory neurons, where some have over-lapping properties, are difficult to study by any one means and ideally require a combination of pharmacological, biophysical and/or molecular approaches. Despite the potential limitations in the methodology used in my study, experiments were designed to survey families of potassium currents and assess their possible contributions to sensory neuron hyperexcitability in response to long-term IL-1β exposure. Changes in any one of, or combination of,

the three potassium currents studied in response to IL-1β exposure would, therefore, justify a more specialized approach in future studies.

*4.2.2.2 Characterization of potassium current in small IB4-positive neurons in long-term cell culture*

Based on relative densities to the other two potassium currents studied, inactivating $Mn^{2+}$ -R $I_K$ (A-type current) represented the smallest current density in control small IB4-positive neurons (Figure 4-5B vs. Figures 4-4C and 4-6B). This appears to be in contrast to findings reported by Vydyanathan and colleagues (2005) where A-type (4-AP -sensitive) current in acutely isolated small IB4-positive DRG neurons represented a greater proportion to total $K_V$ current density than delayed rectifier current (TEA –sensitive). Since 5 mM 4-AP, the concentration used by the authors to isolate A-type, does not block other $K_V$ currents in sensory neurons (Gold et al., 1996b), the difference may be attributed to a loss of A-type current in long-term cell culture or, as discussed above, related to the isolation of inactivating $Mn^{2+}$ -R $I_K$.

If differences are related to insufficient biophysical isolation, it would be expected that non-inactivating $I_K$ (the remaining $I_K$) would be out of proportion as well. This does not appear to be the case, since non-inactivating $I_K$ density in long-term cell culture is comparable to delayed rectifier $I_K$ density in acutely isolated small IB4-positive neurons (both ~ 100 pA/pF at $V_{cmd}$ = +60 mV) (Vydyanathan et al., 2005). The discrepancy also appears unrelated to alterations in gating properties in response to divalent cations, since A-type currents from acutely isolated DRG neurons were recorded in the presence of 1mM $Cd^{2+}$

(Vydyanathan et al., 2005) and, therefore, also has the potential to affect current gating (McFarlane and Cooper, 1991). Since small IB4-positive DRG neurons are highly responsive to GDNF (Bennett et al., 1998;Fjell et al., 1999;Molliver et al., 1997), the exclusion of such neurotrophins in DRG cell cultures may have downregulated A-type currents in a similar manner to TTX-R $I_{Na}$. However, this also seems unlikely, since GDNF is known to suppress A-type currents (Yang et al., 2001;Takeda et al., 2010). A final possibility is that the inclusion of visceral neurons in my study resulted in the misclassification of some peptidergic DRG neurons as small IB4-positive neurons (Chapter 3). This potential source for discrepancy between studies, however, would be expected to be limited by the selection of only the most intensely stained IB4 neurons (Chapter 2) which are thought to specify non-peptidergic (CGRP-negative) DRG neurons (Robinson et al., 2004). In addition, Vydyanathan and colleagues' (2005) investigation likely included visceral afferents, since DRG neurons were also harvested from thoracic and lumbar spinal segments. Taken together, there appears to be no straightforward explanation for the apparent reduction in small IB4-positive neuron inactivating $Mn^{2+}$ -R $I_K$ and might simply relate to recovery of DRG neurons in culture after isolation.

Consistent with sensitivity to calcium influx through voltage-gated calcium channels (VGCCs), inactivating $Mn^{2+}$ -S $I_K$ *I-V* density plots had rising- and declining- phases which are associated with the onset and offset of $Ca^{2+}$ entry, respectively (Thompson, 1977;Meech and Standen, 1975). Furthermore, this response corresponds to peaks in the densities for $I_{Ba}$ (compare Figure 4-6B with

Figure 4-7B) and is absent in *I-V* density plots where calcium entry was blocked by $Mn^{2+}$ (Figure 4-4C and Figure 4-5B). The resulting 'n'- shaped *I-V* density plot, therefore, likely indicates the presence of $K_{Ca}$ currents in small IB4-positive neurons in long-term cell culture. Inactivating $Mn^{2+}$ -S $I_K$, may include $BK_{Ca}$ and/or $SK_{Ca}$ currents, since both have been previously described in acutely isolated small sensory neurons (Gold et al., 1996c;Zhang et al., 2010;Scholz et al., 1998;Abdulla and Smith, 2001b;Bahia et al., 2005). Recently, $BK_{Ca}$ current was found to be preferentially expressed in small diameter IB4-positive DRG neurons and, therefore, likely contributes substantially to the biophysical properties of this nociceptive subpopulation (Zhang et al., 2010). Compared to $BK_{Ca}$ current isolated with the selective blocker, paxilline, in acutely isolated neurons (Zhang et al., 2010), inactivating $Mn^{2+}$ -S $I_K$ density in long-term cultured small IB4-positive neurons was one quarter the magnitude ($V_{cmd}$ = +60 mV). Similar to that discussed for A-type currents, this apparent reduction in calcium dependent $I_K$ in long-term culture might relate to differences in the methodology used to isolate $K_{Ca}$ currents, a loss of $K_{Ca}$ current components, or may be related to changes in $Ca^{2+}$ influx in long-term cell culture.

In support of differences in pharmacological protocols, the authors reported that pretreatment with $Cd^{2+}$ occluded the ability of iberiotoxin to attenuate outward potassium currents in all neurons examined, yet, paxilline is known to inhibit iberiotoxin-resistant $BK_{Ca}$ channels (Hu et al., 2001;Meera et al., 2000). This raises the possibility that paxilline may be blocking $BK_{Ca}$ current components which are less sensitive to divalent cation block of VGCCs and,

therefore, might account for a larger density of $K_{Ca}$ current in Zhang and colleagues' (2010) study. Alternatively, exclusion of exogenous neurotrophins may have downregulated $K_{Ca}$ currents and is supported by evidence that GDNF is known to upregulate $K_{Ca}$ channel expression in neurons (Martin-Caraballo and Dryer, 2002). Last, a decrease in $K_{Ca}$ current could be attributed to a reduction in VGCC density in long-term cell culture, however, $I_{Ba}$ density ($V_h$ = -100 mV; Figure 4-7B; discussed below) appears to be greater than that reported in acutely isolated small diameter IB4-positive DRG neurons (Wu et al., 2004)

*4.2.2.3 Effect of long-term IL-1β exposure on potassium currents in small IB4-positive neurons*

The principal finding in this part of the investigation is that inactivating $Mn^{2+}$ -S $I_K$ density in small IB4-positive neurons was significantly reduced in response to long-term IL-1β exposure. This finding is in agreement with changes in small sensory neurons observed after nerve injury (Abdulla and Smith, 2001b;Sarantopoulos et al., 2007), however, reductions in $K_V$ currents in injured DRG neurons have also been reported (Abdulla and Smith, 2001b;Kim et al., 2002;Everill and Kocsis, 1999) and, therefore, suggests that IL-1β has a limited role in modulating potassium currents in small diameter DRG neurons after nerve injury. This is surprising in view that acute IL-1β application on acutely isolated, small diameter trigeminal ganglion neurons suppressed $K_V$ currents, including A-type current (Takeda et al., 2008). The absence of exogenously added neurotrophins was not likely to preclude effects of IL-1β, since neurotrophins, such as GDNF, are reported to downregulate A-type current in neurons (Yang et

al., 2001;Takeda et al., 2010). As mentioned above, this does not exclude possibility that reductions in A-type current in small IB4-positive neurons, by some other means related to duration in cell culture, precluded the potential effect of IL-1β. On the other hand, the lack of an effect on inactivating $Mn^{2+}$ -R $I_K$ suggests that IL-1β exerted changes in $K_{Ca}$ currents in a manner unrelated to the IL-1β mediated production and/or release of neurotrophins (Tanabe et al., 2009). This is consistent with the finding that GDNF is known to increase, rather than decrease, $K_{Ca}$ channel expression in neurons (Martin-Caraballo and Dryer, 2002).

Unlike findings from nerve injury studies (Abdulla and Smith, 2001), reduction in inactivating $Mn^{2+}$ -S $I_K$ density in small IB4-positive neurons is not likely a consequence to a reduction in VGCC current, since there was no decrease in $I_{Ba}$ density in response to long-term IL-1β exposure (Figures 4-7B and 4-7D; discussed below). However, this does not exclude the possibility that there was a decrease in resting and/or evoked intracellular $Ca^{2+}$ ($[Ca^{2+}]_i$) in response to IL-1β exposure, similar to that reported after nerve injury (Fuchs et al., 2005;Fuchs et al., 2007a), which could result in a suppression of $K_{Ca}$ currents (Scholz et al., 1998;Gold et al., 1996c). Interestingly, chronic inflammation has been reported to increase, rather than decrease, resting $[Ca^{2+}]_i$ and evoked $Ca^{2+}$ transients in IB4-positive DRG neurons (Lu and Gold, 2008). Whether long-term IL-1β exposure produces changes in $[Ca^{2+}]_i$ handling reflective of nerve injury or chronic inflammation is uncertain and should be determined in future studies.

Alternatively, it is known that $K_{Ca}$ currents can be downregulated by prostaglandins and the adenosine 3',5' –cyclic monophosphate (cAMP) second

messenger cascade (Gold et al., 1996c;Shipston et al., 1999;Widmer et al., 2003), therefore, IL-1β could have suppressed inactivating $Mn^{2+}$ -S $I_K$ in small IB4-positive neurons secondary to the production of $PGE_2$ (Maier et al., 1990). Since IL-1β signalling is known to involve p38 MAPK (Funakoshi et al., 2001;Roux et al., 2005;Tanabe et al., 2009;Binshtok et al., 2008), long-term IL-1β exposure may have directly reduced trafficking of $K_{Ca}$ subunits to the membrane, as has been described in chick ciliary ganglion neurons (Chae and Dryer, 2005). Last, it was recently determined that rat DRG contain all 4 regulatory β–subunits for $BK_{Ca}$ channels (Zhang et al., 2010), therefore, IL-1β could have influenced $K_{Ca}$ function through interactions with β-subunits in a similar manner proposed for sodium channels (discussed above).

*4.2.2.4 Functional implications of $I_{K,Ca}$ suppression in small IB4-positive neurons in response to long-term IL-1β exposure*

An increase in AP width and a decrease in the maximal rate of repolarization in small IB4-positive neurons in response to long-term IL-1β exposure (Chapter 3) is consistent with suppression of $BK_{Ca}$ currents and similar alterations, related to AP repolarization, have been previously reported when $BK_{Ca}$ channels are blocked with iberiotoxin or charybdotoxin (Scholz et al., 1998;Li et al., 2007). Although inactivating $Mn^{2+}$ -S $I_K$ components were not separated in my study, current-clamp findings suggest suppression of inactivating $Mn^{2+}$ -S $I_K$ in response to long-term IL-1β exposure involved a reduction in $BK_{Ca}$ current density. $BK_{Ca}$ channels are also known to underlie fast afterhyperpolarization ($AHP_{fast}$) (Scholz et al., 1998) which can last for up to

several hundred milliseconds in DRG neurons (Gold et al., 1996c). Surprisingly, small IB4-positive neuron AHP amplitude and duration were not decreased which would be expected if $BK_{Ca}$ currents were suppressed. This paradox may be attributed to compensatory mechanisms, such as an alteration in $[Ca^{2+}]_i$ handling (Lu and Gold, 2008). On the other hand, current-clamp findings may be more related to alterations in sodium currents with little or no reduction in BKCa currents. Future studies, involving computer modelling, could test the possibility that interactions between $BK_{Ca}$ channels (density) and $Ca^{2+}$ (evoked transients) differentially affect repolarization and $AHP_{fast}$ in small IB4-positive DRG neurons.

Experiments involving the use of iberiotoxin or apamin to block either $BK_{Ca}$ or $SK_{Ca}$ channels, respectively, demonstrate inhibition of AHP which shortens the refractory period and enhances repetitive discharge (Gold et al., 1996c;Scholz et al., 1998;Li et al., 2007). Therefore, it is possible that suppression of inactivating $Mn^{2+}$ -S $I_K$ resulted in enhancement of repetitive discharge in small IB4-positive neurons exposed to IL-1β. As discussed above, however, this is not likely to involve reductions in $AHP_{fast}$ and $BK_{Ca}$ currents. Since AHP duration was only assessed for ~80 ms following AP generation (Chapter 3), it is likely that changes in slower AHP components, which involve more elaborate protocols, were not detected in my study. For instance, slow AHP ($AHP_{slow}$) in small DRG neurons typically develops in response to a burst of APs with a latency of several hundred milliseconds (following decay of $AHP_{fast}$) and can last for several seconds (Gold et al., 1996c). Further, inhibition of $AHP_{slow}$ with apamin, suggests

involvement of $SK_{Ca}$ channels and, therefore, $SK_{Ca}$ current could also represent a component of inactivating $Mn^{2+}$ -S $I_K$ which was suppressed in response to long-term IL-1β exposure. Since the functional roles of SK, as well as IK, channels in DRG neurons remain uncertain (Gold et al., 1996c;Abdulla and Smith, 2001b;Bahia et al., 2005), future studies should incorporate appropriate pharmacological protocols in order to assess changes in specific $K_{Ca}$ currents in response to long-term IL-1β exposure.

### *4.2.3 Calcium currents ($I_{Ba}$) in small IB4-positive DRG neurons*

#### *4.2.3.1 Characterization of $I_{Ba}$ in small IB4-positive DRG neurons in long-term cell culture*

Low voltage-activated (LVA) calcium currents are characterized by their 'low' threshold for activation which results in the formation of a shoulder in *I-V* plots at voltages between -60 to -30 mV (Fox et al., 1987;Scroggs and Fox, 1992;Abdulla and Smith, 2001b). The absence of prominent shoulders on *I-V* plots ($V_h$ = -100 mV), suggests that LVA calcium channels were not a substantial contributor to total calcium current in small IB4-positive neurons in long-term cell culture. Further, since IL-1β exposure had no clear effect on $I_{Ba}$ density in response to weak depolarizations ($V_{cmd}$ = -50 mV), LVA calcium currents were not likely to contribute to small IB4-positive neuron hyperexcitability in response to long-term IL-1β exposure.

The majority of inward current recorded is expected to be high voltage-activated $I_{Ba}$ (HVA-$I_{Ba}$) which is in agreement with several other studies in

acutely isolated small sensory neurons (Abdulla and Smith, 2001b;Pearce and Duchen, 1994;Lu et al., 2006;Scroggs and Fox, 1992). More recent investigations by Todorovic's group, however, have determined the enriched presence of T-type current in subpopulations of small to medium diameter DRG neurons that are IB4-positive (Nelson et al., 2005;Jagodic et al., 2007). There are at least a couple of reasons for conflicting findings. First, Todorovic's group used high concentrations of $Ba^{2+}$ (10 mM vs. 2-3 mM) in their external solution with a fluoride-based internal solution to facilitate 'rundown' of HVA currents which would enhance the remaining LVA-$I_{Ba}$. This isolation procedure might suggest other studies simply missed LVA currents in small sensory neurons, however, all found large LVA currents in medium-sized, rather than small, DRG neurons (Abdulla and Smith, 2001b;Pearce and Duchen, 1994;Lu et al., 2006;Scroggs and Fox, 1992). Second, this would then submit that at least some of the medium-sized neurons were IB4-positive, however, Lu and colleagues (2006) reported larger LVA current densities in medium diameter or IB4-negative than in IB4-positive DRG neurons. Since it appears either could be the case, a final possibility is that functional LVA calcium channels, if present after acute isolation, were not supported in defined medium cultures in the absence of exogenously applied neurotrophins. In support, Aguayo and colleagues (1991) also reported the absence of LVA calcium currents under similar cell culturing conditions and, therefore, might be further evidence of a phenotypic shift in small IB4-positive neurons in long-term cell culture.

Last, although DRG neurons are known to express a full complement of voltage-gated calcium channel subtypes (Wu et al., 2004;Fox et al., 1987;Scroggs and Fox, 1992;Rusin and Moises, 1995), their pharmacological separation and biophysical characterization is beyond the scope of my study. Instead, a preliminary comparison on HVA-$I_{Ba}$ from control small IB4-positive neurons in long-term cell culture is made with that from acutely isolated small DRG neurons. Consistent with the literature, HVA-$I_{Ba}$ activated at ~ -50 mV ($V_h$ = -100 mV) with peak current at ~ -10 mV (Abdulla and Smith, 2001b;Scroggs and Fox, 1992;Hogan et al., 2000;Wu et al., 2004). Interestingly, given that neurotrophins are known to upregulate HVA calcium channels (Lei et al., 1997;Woodall et al., 2008), HVA-$I_{Ba}$ peak density in my cell cultures was more comparable to acutely maintained cell cultures with NGF (Hogan et al., 2000) rather than without (Wu et al., 2004). Although there were slight differences in recording conditions which may account for some of the variation (i.e. 2 or 3 mM $Ba^{2+}$ and $V_h$ = -80 to -100 mV), other possibilities remain. For instance, it has previously been reported that BDNF supports sensory neurons in culture through autocrine release (Acheson et al., 1995) and, perhaps, such release of neurotrophins (GDNF; Chapter 1) would be sufficient to maintain the functional expression of HVA calcium channels in small IB4-positive. However, this would not explain the functional losses of TTX-R sodium channels and LVA calcium channels. Another possibility could be the use of laminin-coated culture dishes (Chapter 2) where laminin is known to bind extracellular loops of calcium channel pore forming $\alpha_1$-subunits, thereby, promoting the clustering of calcium channels along the neuronal cell membrane

(Nishimune et al., 2004). Further, since this interaction appears to be voltage-gated calcium channel subtype specific (N-type and P/Q-type), it may also explain why LVA-$I_{Ba}$ was not recorded.

*4.2.3.2 Effect of long-term IL-1β exposure on HVA-$I_{Ba}$ in small IB4-positive neurons*

The major finding in this part of the investigation is that there was no significant change in peak HVA-$I_{Ba}$ density or shift in voltage dependence of HVA-$I_{Ba}$ inactivation in small IB4-positive neurons exposed to IL-1β. This observation appears to deviate from findings in nerve injury experiments where HVA calcium currents are decreased after axotomy nerve injury which may, in part, be attributed to increased inactivation (Abdulla and Smith, 2001b;Baccei and Kocsis, 2000). Further, suppression of voltage-gated calcium currents is not limited to axotomy nerve injury as a reduction in peak $I_{Ca}$ density also occurred after CCI nerve injury (Hogan et al., 2000). Therefore, it is likely that IL-1β has a limited role in alterations to HVA calcium currents observed after nerve injury.

HVA calcium currents are also responsive to various cytokines and neurotrophins. For instance, N-type calcium current, as well as, corresponding $Ca_V2.2$ expression were downregulated in postganglionic sympathetic neurons after a 24 hr exposure to the proinflammatory cytokine, tumor necrosis factor-α (TNF-α) (Motagally et al., 2009). Since this suppression occurred through signalling pathways commonly shared by IL-1β, including the activation of nuclear factor κB (NFκB) (Ninomiya-Tsuji et al., 1999), it would be expected that IL-1β has the same effect. In support, cortical neuron N-type calcium current and

channel protein were suppressed after a 24 hour exposure to IL-1β (Zhou et al., 2006). Conversely, neurotrophins that are potentially produced and released in response to IL-1β, such as NGF and GDNF (Safieh-Garabedian et al., 1995;Tanabe et al., 2009;Appel et al., 1997;Saavedra et al., 2007), are known to upregulate HVA calcium channels and/or increase HVA-$I_{Ba}$ densities in DRG and sympathetic ganglion cell cultures (Lei et al., 1997;Woodall et al., 2008). Taken together, a change in HVA-$I_{Ba}$, either up or down, would have been expected from these studies. In view of the several other changes discussed above for $I_{Na}$ and $I_K$, as well as, $I_{Ca}$ in medium neurons (Chapter 5), there is no straightforward explanation.

Finally, since HVA calcium current in DRG neurons can be composed of several biophysically and pharmacologically distinct conductances, including N and/or L-type currents (Wu et al., 2004;Fox et al., 1987;Scroggs and Fox, 1992;Rusin and Moises, 1995), I cannot dismiss the possibility that there were changes in their relative contributions to total HVA-$I_{Ba}$ density in response to long-term IL-1β exposure. In support, reductions in the relative contribution of N-type and R-type channel subtypes to calcium influx in injured small DRG neurons were reported after SNL injury (Fuchs et al., 2007b). Since changes in the contributions of calcium channel subtypes could reflect changes at central terminals which control neurotransmitter release and the transmission of nociceptive information (Rycroft et al., 2007;Passmore, 2005), future studies should test this possibility in small IB4-positive neurons exposed to IL-1β.

*4.2.3.3 Functional implications for a lack in change to $I_{Ba}$ in small IB4-positive DRG neurons in response to long-term IL-1β exposure*

No change in $I_{Ba}$, suggests VGCCs were unaffected in small IB4-positive neurons exposed to IL-1β. Therefore, broadening of APs and hyperexcitability are likely to be the consequence of changes observed for TTX-S $I_{Na}$ and $Mn^{2+}$ -S $I_K$. This also implies that alterations in small IB4-positive neurons were not secondary to changes in VGCCs, including the suppression of $K_{Ca}$ currents, as well as, calcium-dependent processes not examined in my study. Last, I cannot rule out the possibility that small IB4-positive neuron phenotypic shift in long-term cell culture precluded potential effects of IL-1β, such as the possible loss of functional LVA calcium channels and their contribution to sensory neuron excitability.

*4.2.4 Conclusion on the effects of IL-1β exposure on ionic currents in small IB4-positive DRG neurons*

The effects of short-term (minutes to hours) IL-1β application on sodium, calcium and potassium conductances have been previously described in various *in vitro* preparations, including small, nociceptive sensory neurons of the DRG and trigeminal ganglia. My study expands on these findings by examining the effects of long-term IL-1β exposure on sensory neuron excitability and its relation to changes in sensory neurons observed after nerve injury. In Chapter 3, I not only confirmed that IL-1β enhances DRG neuron excitability after short-term applications, but further demonstrated hyperexcitability in medium and small IB4-

positive sensory neuron subpopulations after 5 to 6 days exposure. I interpret these findings to be the *in vitro* equivalent to the enduring increase in primary afferent excitability reported after nerve injury and, therefore, would expand the recognized role of IL-1β in acute inflammatory pain to neuropathic pain. To further establish this possibility, I hypothesized that long-term IL-1β exposure would alter ionic currents in a manner consistent with sensory neuron hyperexcitability.

In this chapter, the two major findings were the decrease in the rate of TTX-S $I_{Na}$ inactivation and the suppression of $K_{Ca}$ current densities in small IB4-positive DRG neurons exposed to IL-1β (Table 4-2). These changes are in agreement with findings after nerve injury (Sarantopoulos et al., 2007;Abdulla and Smith, 2001b;Abdulla and Smith, 2002), however, the effects of IL-1β appeared relatively restricted when compared to broad spectrum of changes observed in injured small sensory neurons. There are at least a couple possibilities for differences:

1. Phenotypic shift, as a consequence of serum and exogenous neurotrophin – free cell culturing conditions, likely precluded potential effects of IL-1β on additional ionic conductances. This included the loss of TTX-R $I_{Na}$ and the minimal support of A-type potassium currents which are both known to be enriched in acutely isolated small IB4-positive sensory neurons (Fang et al., 2006;Vydyanathan et al., 2005;Fjell et al., 1999) and modulated by short-term IL-1β applications (Takeda et al., 2008;Binshtok et al., 2008).

2. It is also possible that biophysical and pharmacological protocols used in my study were not sufficient to monitor all changes produced by IL-1β. For example, I did not assess rapid repriming of TTX-S $I_{Na}$ or the relative contributions of VGCC subtypes to total HVA-$I_{Ba}$ current. Taken together, my study may underestimate the importance of IL-1β to the generation of sensory neuron hyperexcitability after nerve injury.

Despite several limitations, the changes described here for small IB4-positive neurons, relate well to my current-clamp findings (Table 3-5) and to pain mechanisms. For instance, the decrease in the rate of TTX-S $I_{Na}$ inactivation would be expected to the broaden APs which would in turn sustain membrane depolarization and enhance small IB4-positive sensory neuron excitability. Coupled to this, the suppression of $K_{Ca}$ current density may be associated with the attenuation of the AHP which would increase repetitive AP discharge. Although the physiological relevance of these alterations in the cell bodies of small IB4-positive is uncertain, it is possible that IL-1β would produce similar changes at central nerve terminals, leading to increased $Ca^{2+}$ entry and, therefore, increased neurotransmitter release for this functionally distinct class of nociceptors. Finally, it would be interesting to model the observed changes and examine their applicability to the generation of small IB4-positive sensory neuron hyperexcitability in response to long-term IL-1β exposure.

***Figure 4-1: $I_{Na}$ in long-term cell culture and the effect of IL-1β on TTX-sensitive $I_{Na}$ activation in small IB4-positive DRG neurons***

A: All small IB4-positive neuron $I_{Na}$ in long-term cell culture was TTX-S $I_{Na}$. Total $I_{Na}$ (black traces) was recorded from DRG neurons using a series of 40 ms depolarizing voltage commands from $V_h$ = -90 mV (Ai). Neurons were then treated with 300 nM TTX (grey traces) to isolate TTX-S $I_{Na}$ from TTX-R $I_{Na}$ (Aii) and digital subtraction (Ai-ii) revealed that all measurable current was TTX-S $I_{Na}$.

B: Effect of IL-1β exposure on TTX-S $I_{Na}$ density. *I-V* plot indicates that peak TTX-S $I_{Na}$ density occurred at -20 mV in both control and IL-1β exposed small IB4-positive neurons. IL-1β had no significant effect on peak TTX-S $I_{Na}$ density (-166 ± 27 pA/pF, n=12 vs. -130 ± 14 pA/pF, n=12; *p>0.05*).

C: Effect of IL-1β exposure on TTX-S $I_{Na}$ on voltage dependence of activation. Normalized ($I/I_{-20}$ ) *I-V* curves were fit with a single Boltzmann function (Chapter 2). IL-1β had no significant effect on values for the voltage midpoint ($V_{1/2}$) (-35.6 ± 1.8 mV, n=12 vs. -35.6 ± 1.8, n=12; *p>0.05*) or slope factor (3.0 ± 0.5 mV, n=12 vs. 4.2 ± 0.9, n=12; *p>0.05*).

Error bars indicate means ± SE. Significant difference vs. control * = *p<0.05*, † = *p<0.01*and § = *p<0.001* with unpaired t-test. Traces in A were not subtracted for leak current.

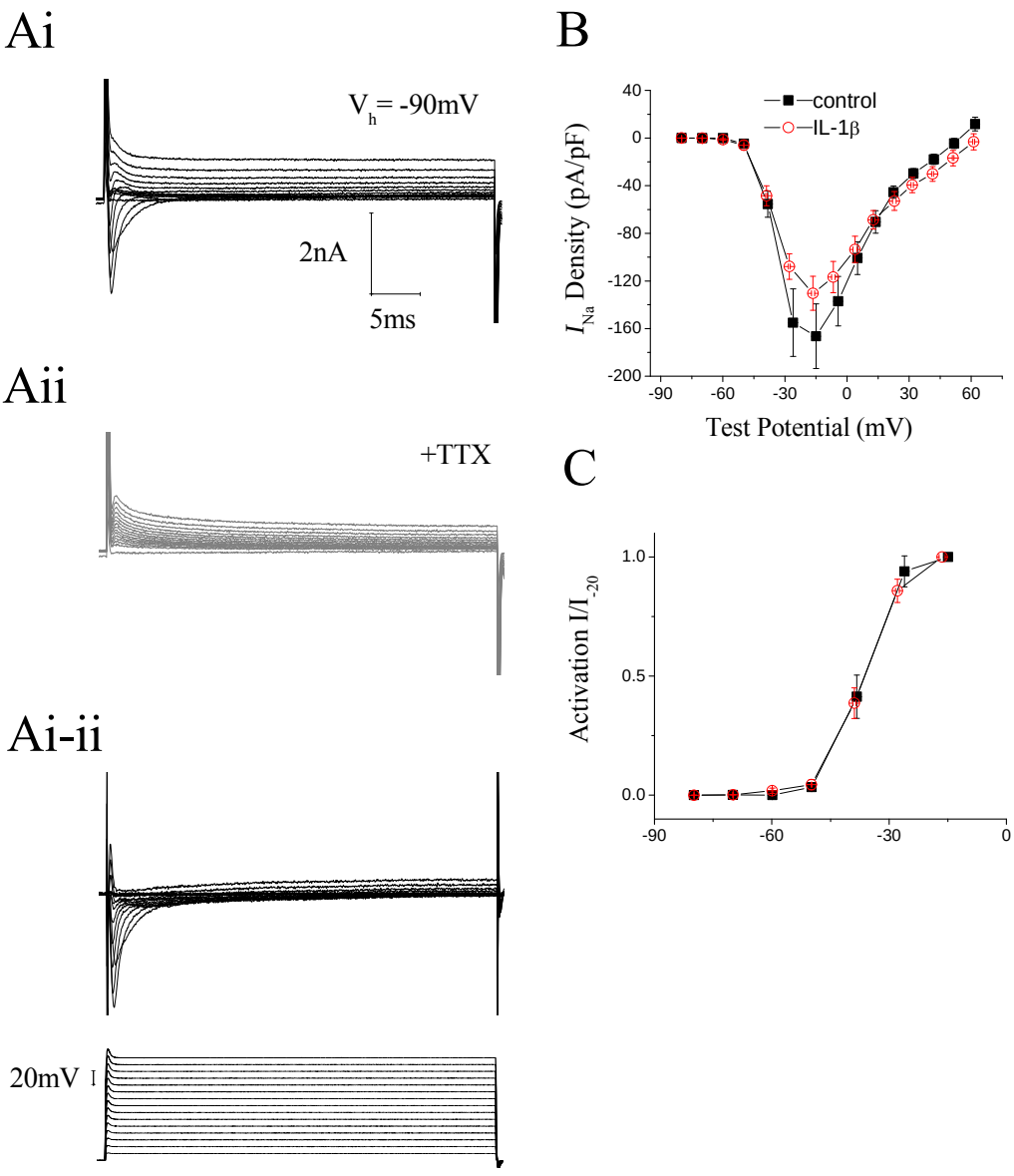
Ai
$V_h$= -90mV
2nA
5ms
Aii
+TTX
Ai-ii
20mV
B
control
IL-1β
$I_{Na}$ Density (pA/pF)
40
0
-40
-80
-120
-160
-200
-90
-60
-30
0
30
60
Test Potential (mV)
C
Activation $I/I_{-20}$
1.0
0.5
0.0
-90
-60
-30
0

***Figure 4-2: Effect of long-term IL-1β exposure on TTX-sensitive $I_{Na}$ steady-state inactivation in small IB4-positive DRG neurons***

A: TTX-S $I_{Na}$ steady-state fast inactivation protocol. From a $V_h$ = -90 mV, 300 ms incremental depolarizing prepulses preceded 10 ms test pulses to -10 mV to determine the fraction of current available.

B: Effect of IL-1β exposure on TTX-S $I_{Na}$ steady-state fast inactivation. Normalized ($I/I_{-110}$) steady-state fast inactivation curves were fit with a single Boltzmann function (Chapter 2). IL-1β had no significant effect on values for $V_{1/2}$ (-66.5 ± 1.1 mV, n=12 vs. -68.1 ± 2.3, n=12; *p>0.05*) or slope factor (6.9 ± 0.5 mV, n=12 vs. 9.1 ± 1.4, n=12; *p>0.05*).

C: TTX-S $I_{Na}$ steady-state slow inactivation protocol. From $V_h$ = -90 mV, 5 s prepulses, followed by 20 ms recovery pulses to -120 mV (to allow recovery from fast inactivation), preceded 10 ms test pulses to -10 mV to determine the fraction of current available ($I/I_{-120}$).

D: Effect of IL-1β exposure on TTX-S $I_{Na}$ steady-state slow inactivation. Normalized steady-state slow inactivation curves were fit with a single Boltzmann function (Chapter 2). IL-1β had no significant effect on values for $V_{1/2}$ (-64.2 ± 3.2 mV, n=11 vs. -57.7 ± 3.6, n=11; *p>0.05*) or slope factor (16.7 ± 2.0 mV, n=11 vs. 15.9 ± 1.6, n=11; *p>0.05*). Error bars indicate means ± SE. Significant difference vs. control * = *p<0.05*, † = *p<0.01*and § = *p<0.001* with unpaired t-test. Traces in A and C were not subtracted for leak current.

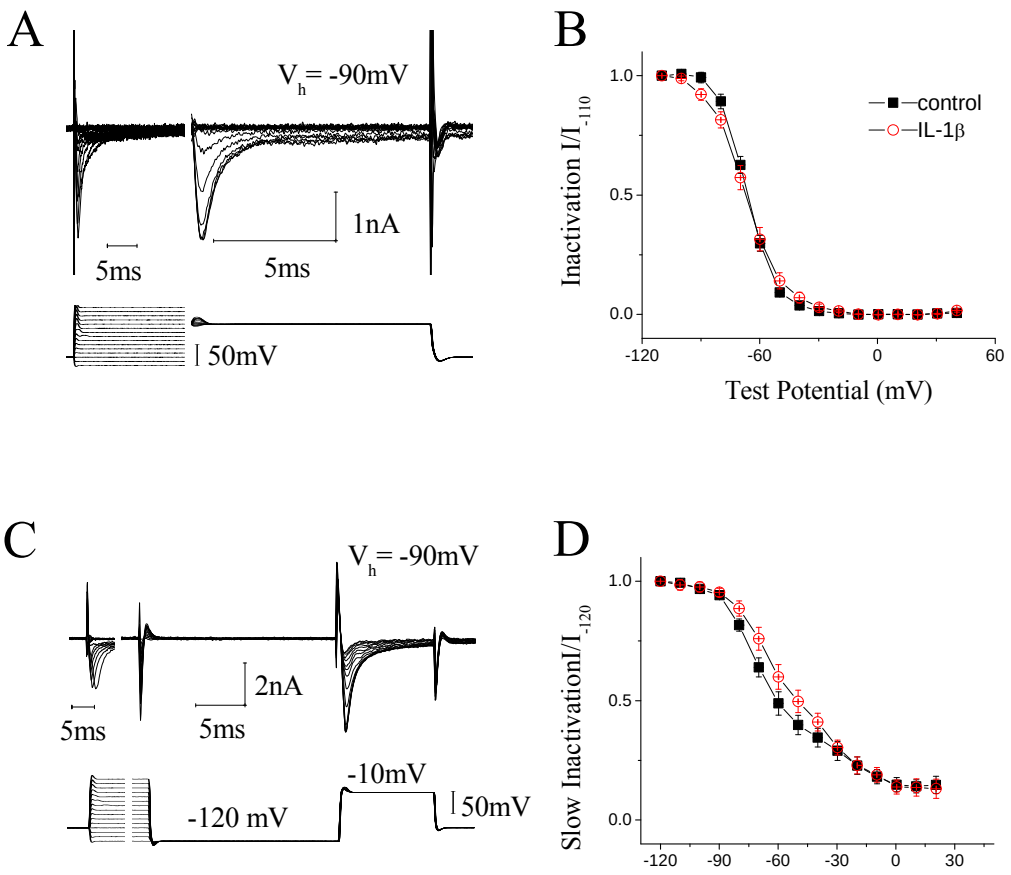
A
V_h = -90mV
1nA
5ms
5ms
50mV
B
Inactivation I/I_-110
1.0
0.5
0.0
-120
-60
0
60
Test Potential (mV)
control
IL-1β
C
V_h = -90mV
2nA
5ms
5ms
-10mV
-120 mV
50mV
D
Slow InactivationI/I_-120
1.0
0.5
0.0
-120
-90
-60
-30
0
30

***Figure 4-3: Effect of long-term IL-1β exposure on TTX-S $I_{Na}$ kinetics of inactivation in small IB4-positive DRG neurons***

A: Effect of IL-1β exposure on AP width in current-clamp studies. IL-1β exposure resulted in a significant increase in small IB4-positive neuron AP width (1.86 ± 0.12 ms, n=20 vs. 2.52 ± 0.16, n=21; *p<0.01*). Increased AP width might be associated with slowed inactivation.

B: Effect of IL-1β exposure on TTX-S $I_{Na}$ kinetics of inactivation. From $V_h$ = -90 mV, single exponent fits (Chapter 2) of TTX-S $I_{Na}$ decay revealed that IL-1β exposure significantly increased fast inactivation time constants between -40 mV and -10 mV (for $V_{cmd}$ = -30 mV: 0.75 ± 0.14 ms, n=12 vs. 1.87 ± 0.39, n=12; *p<0.05*)

C: Representative traces illustrating slower TTX-S $I_{Na}$ decays in small IB4-positive neurons exposed to IL-1β (red trace; scaled to match control) versus control (black trace).

Error bars indicate means ± SE. Significant difference vs. control * = *p<0.05*, † = *p<0.01*and § = *p<0.001* with unpaired t-test.

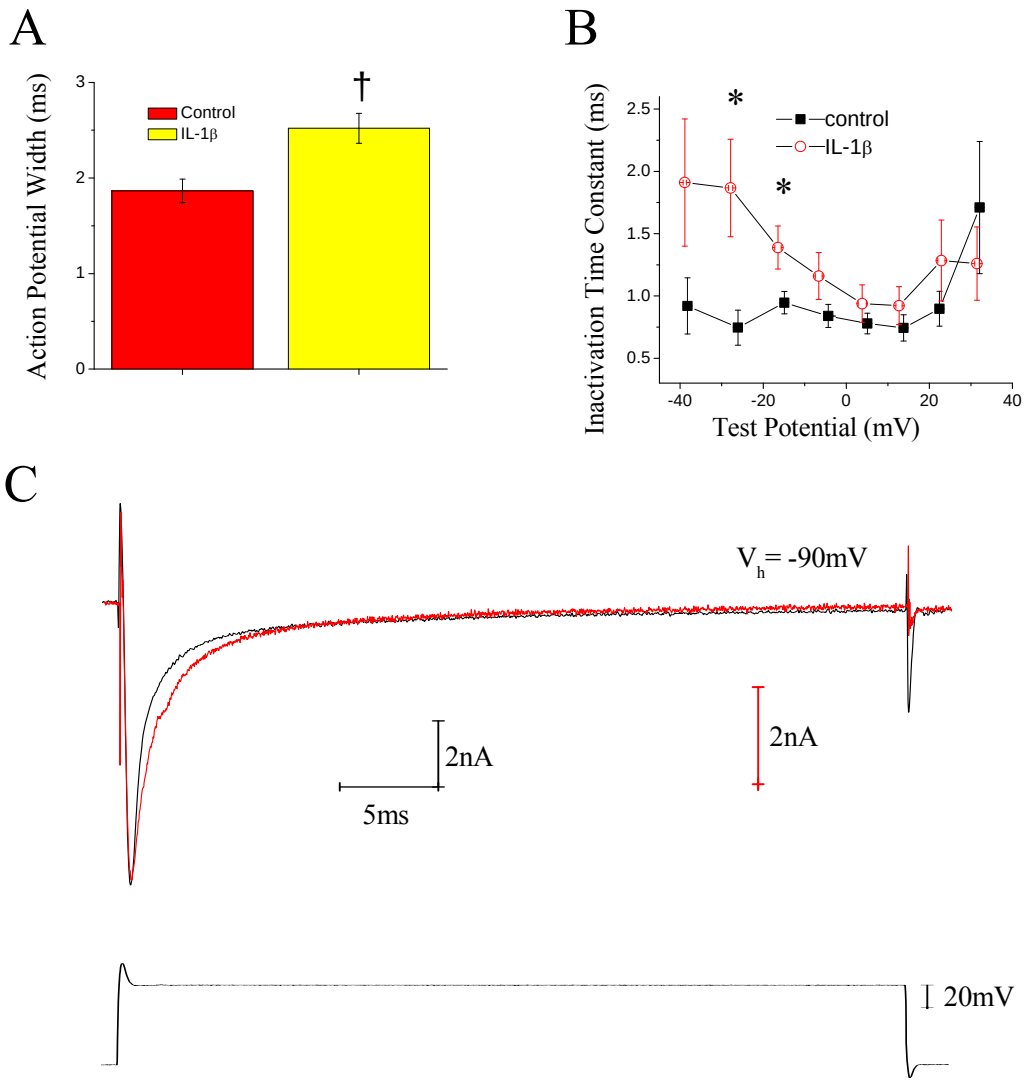
A
Action Potential Width (ms)
Control
IL-1β
†
B
Inactivation Time Constant (ms)
control
IL-1β
*
*
Test Potential (mV)
C
V_h = -90mV
2nA
5ms
2nA
20mV

***Figure 4-4: $I_K$ voltage protocols and the effect of IL-1β on non-inactivating $I_K$ density in IB4-positive DRG neurons***

A: $I_K$ voltage protocols. A family of outward currents recorded at voltages between -60 mV and +60 mV ($V_h$ = -80 mV) after a 500 ms conditioning prepulse to $V_p$ = -120 mV (Ai) or -30 mV (Aii) in the standard NMG-Cl perfusion solution. Digital subtraction (Ai – Aii) revealed the presence of an inactivating current component and is likely attributed to the presence of A-type potassium currents and/or the presence of $I_{K,Ca}$ which may decline as a consequence to the inactivation of calcium conductances (Abdulla and Smith, 2001b).

B: Isolation of non-inactivating $I_K$. In the presence of 5 mM $Mn^{2+}$, a steady-state non-inactivating component could be measured at the end of the stimulation pulse when preceded by $V_p$ = -30 mV and is likely to be delayed-rectifier potassium current (referred to as non-inactivating $I_K$).

C: Effect of IL-1β exposure on non-inactivating $I_K$ density. Control and IL-1β exposed neurons had similar *I-V* plots with no significant difference in peak non-inactivating $I_K$ density ($V_{cmd}$ = +60 mV; +121 ± 17 pA/pF, n=12 vs. +101 ± 21, n=12, respectively; *p>0.05*).

Error bars indicate means ± SE. Significant difference vs. control * = *p<0.05*, † = *p<0.01*and § = *p<0.001* with unpaired t-test. Traces in A and B were not subtracted for leak current.

Ai

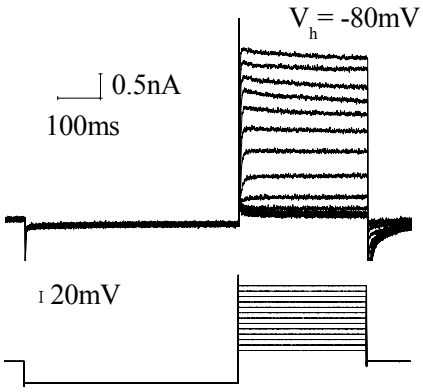


B

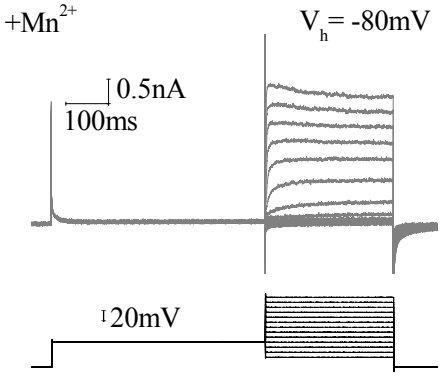


Aii

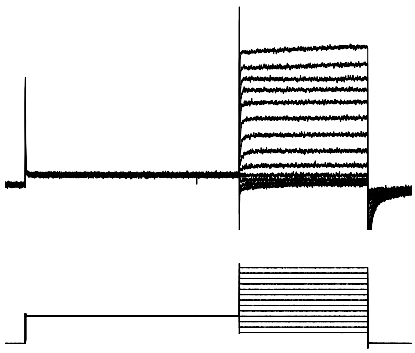

C

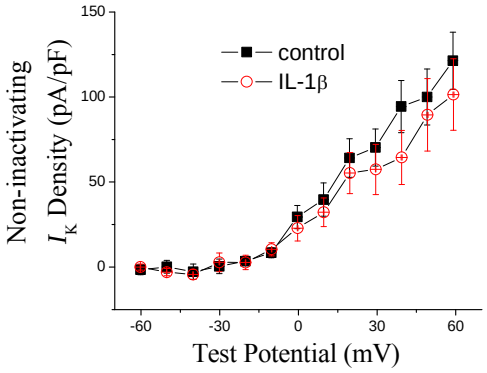


Ai-ii

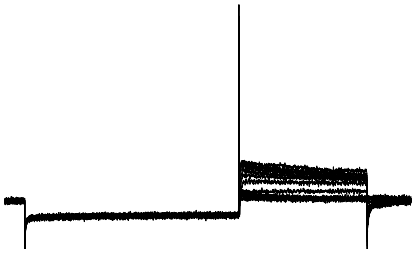

***Figure 4-5: Effect of IL-1β on inactivating $Mn^{2+}$ -resistant $I_K$ density in small IB4-positive DRG neurons***

A: Isolation of inactivating $Mn^{2+}$-R $I_K$. From $V_h$ = -80 mV and in the presence of 5 mM $Mn^{2+}$ (grey traces), digital subtraction of $I_K$ (Ai-Aii) after 500 ms conditioning prepulses to $V_p$ = -120 mV (Ai) and $V_p$ = -30 mV (Aii) revealed the presence of A-type currents. Since A-type currents in DRG neurons may reflect the existence of $I_{Af}$, $I_{As}$ (or $I_D$) and $I_{Aht}$ (Gold et al., 1996b;Everill et al., 1998), in this study they are collectively referred to as inactivating $Mn^{2+}$ -R $I_K$.

B: Effect of IL-1β on inactivating $Mn^{2+}$ -R $I_K$. Control and IL-1β exposed neurons had similar *I-V* plots with no significant difference in peak inactivating $Mn^{2+}$ -R $I_K$ density (+14 ± 7 pA/pF, n=9 vs. +12 ± 7, n=8, respectively; $p>0.05$)

Error bars indicate means ± SE. Significant difference vs. control * = $p<0.05$, † = $p<0.01$and § = $p<0.001$ with unpaired t-test. Traces in A were not subtracted for leak current.

Ai

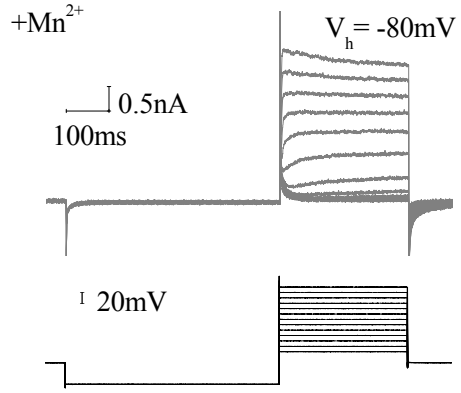
+Mn2+
Vh = -80mV
0.5nA
100ms
20mV

B

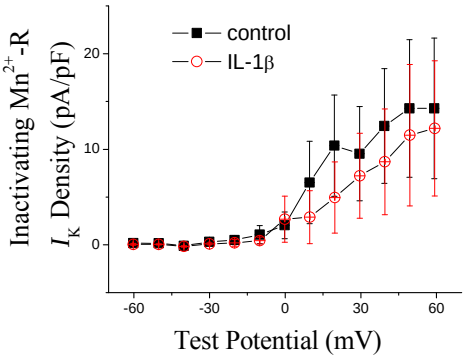
control
IL-1β
Inactivating Mn2+-R
IK Density (pA/pF)
20
10
0
-60
-30
0
30
60
Test Potential (mV)

Aii

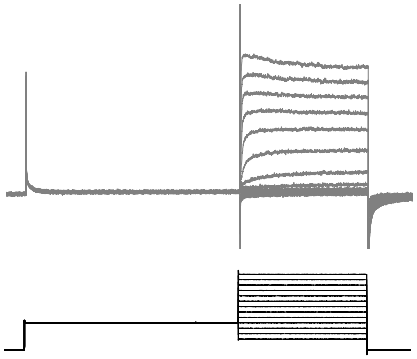

Ai-ii

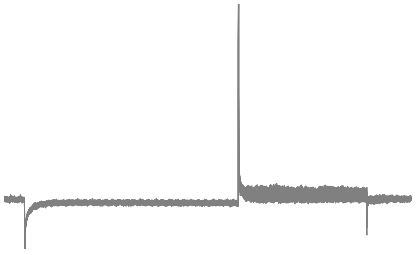

***Figure 4-6: Effect of IL-1β on inactivating $Mn^{2+}$ -sensitive $I_K$ density in small IB4-positive DRG neurons***

A: Isolation of inactivating $Mn^{2+}$ -S $I_K$. From $V_h$ = -80 mV and after a 500 ms conditioning prepulse to $V_p$ = -120 mV, digital subtraction of outward current (Ai-Aii) remaining in the presence of 5mM $Mn^{2+}$ (Ai; grey traces) from total outward current (Aii; black traces) yielded inactivating $Mn^{2+}$ -S $I_K$. Also, notice the rising- and declining- phases in the *I-V* plot (B) between $V_{cmd}$ = -20 and + 20 mV which likely corresponds to the augmentation of $K_{Ca}$ currents in response to onset and offset of $Ca^{2+}$ influx through voltage-gated calcium channels (VGCCs).

B: Effect of IL-1β inactivating $Mn^{2+}$ -S $I_K$. As depicted in the *I-V* plots, IL-1β exposure significantly suppressed inactivating $Mn^{2+}$ -S $I_K$ current densities (peak inactivating $Mn^{2+}$ -S $I_K$ density: from +73 ± 7 pA/pF, n=11 to +42 ± 7, n=10; $p<0.05$).

C: Representative traces illustrating suppressed peak inactivating $Mn^{2+}$ -S $I_K$ ($V_{cmd}$ = + 60 mV) in small IB4-positive neurons exposed to IL-1β (red trace) versus control (black trace).

Error bars indicate means ± SE. Significant difference vs. control * = $p<0.05$, † = $p<0.01$and § = $p<0.001$ with unpaired t-test. Traces in A were not subtracted for leak current.

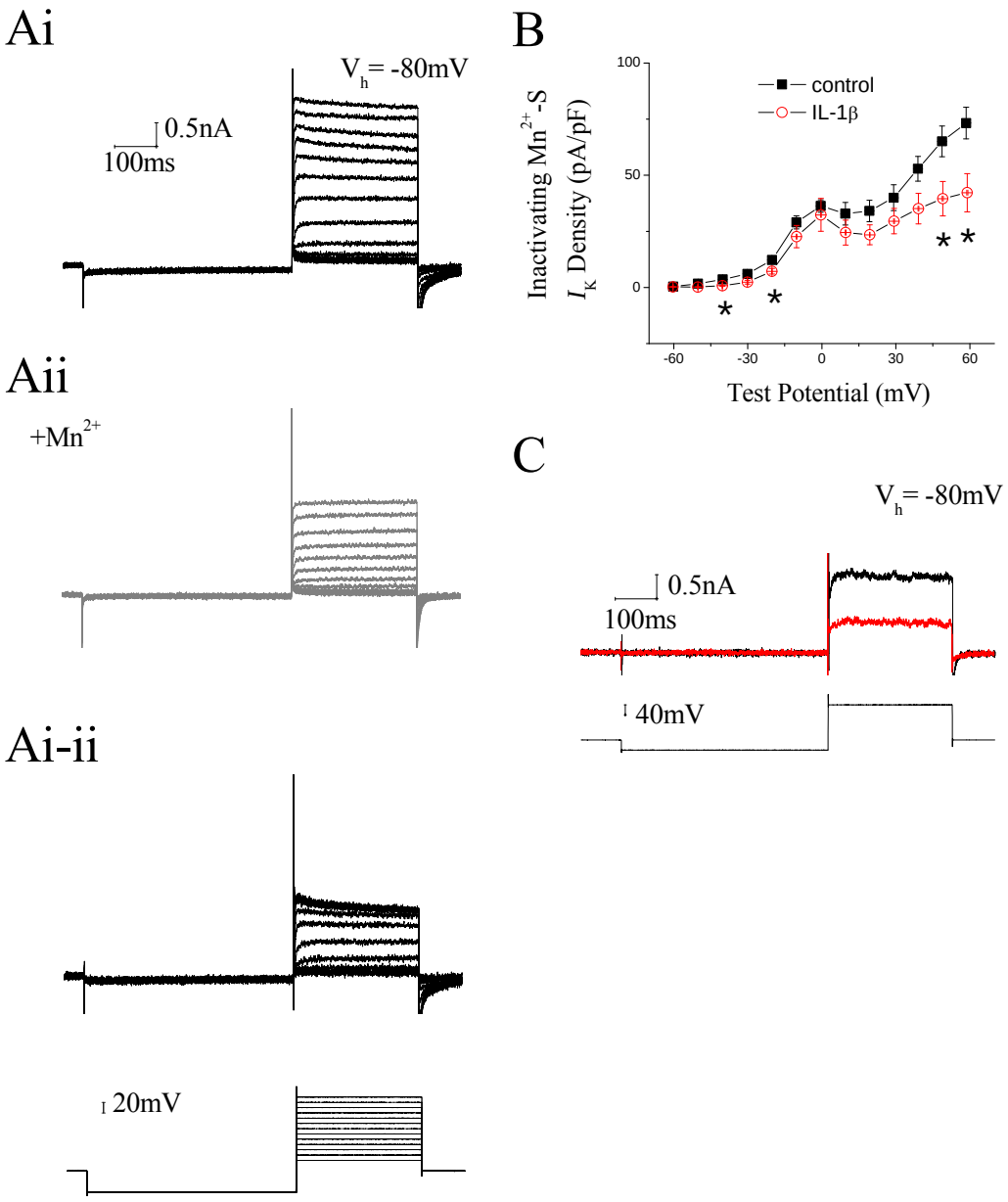
Ai
V_h = -80mV
0.5nA
100ms
Aii
+Mn2+
Ai-ii
20mV
B
Inactivating Mn2+-S
I_K Density (pA/pF)
control
IL-1β
Test Potential (mV)
C
V_h = -80mV
0.5nA
100ms
40mV

***Figure 4-7: Effect of IL-1β on $I_{Ba}$ density and sensitivity to shifts in holding potential in small IB4-positive DRG neurons***

A: $I_{Ba}$ protocol ($V_h$ = -100 mV). $Ba^{2+}$ was substituted for $Ca^{2+}$ as the charge carrier (Chapter 2) and currents ($I_{Ba}$) were evoked in small IB4-positive neurons using a series of 150 ms depolarizing voltage commands from $V_h$ = -100 mV.

B: Effect of IL-1β on $I_{Ba}$ density ($V_h$ = -100 mV). *I-V* plots for control and IL-1β treated small IB4-positive neurons were nearly superimposed and IL-1β had no significant effect on high voltage-activated $I_{Ba}$ (HVA-$I_{Ba}$) peak densities ($V_{cmd}$ = -10 mV; -114 ± 14 pA/pF, n=13 vs. -119 ± 18, n=14; *p>0.05*).

C: $I_{Ba}$ protocol ($V_h$ = -60 mV). Same protocol described in A except $V_h$ = -60 mV.

D: Effect of IL-1β on $I_{Ba}$ density ($V_h$ = -60 mV). There were no clear differences between *I-V* plots for control and IL-1β treated small IB4-positive neurons. Further, IL-1β had no significant effect on peak HVA- $I_{Ba}$ density ($V_{cmd}$ = -10 mV; -14 ± 3 pA/pF, n=11 vs. -19 ± 3, n=14; *p>0.05*).

E: Effect of IL-1β on sensitivity to a shift in holding potential. IL-1β had no significant effect on the (sensitivity) percent decrease in peak HVA-$I_{Ba}$ density (89.1 ± 2.3%, n=11 vs. 82.3 ± 3.6, n=14; *p>0.05*).

Error bars indicate means ± SE. Significant difference vs. control * = *p<0.05*, † = *p<0.01*and § = *p<0.001* with unpaired t-test. Traces in A and C were not subtracted for leak current.

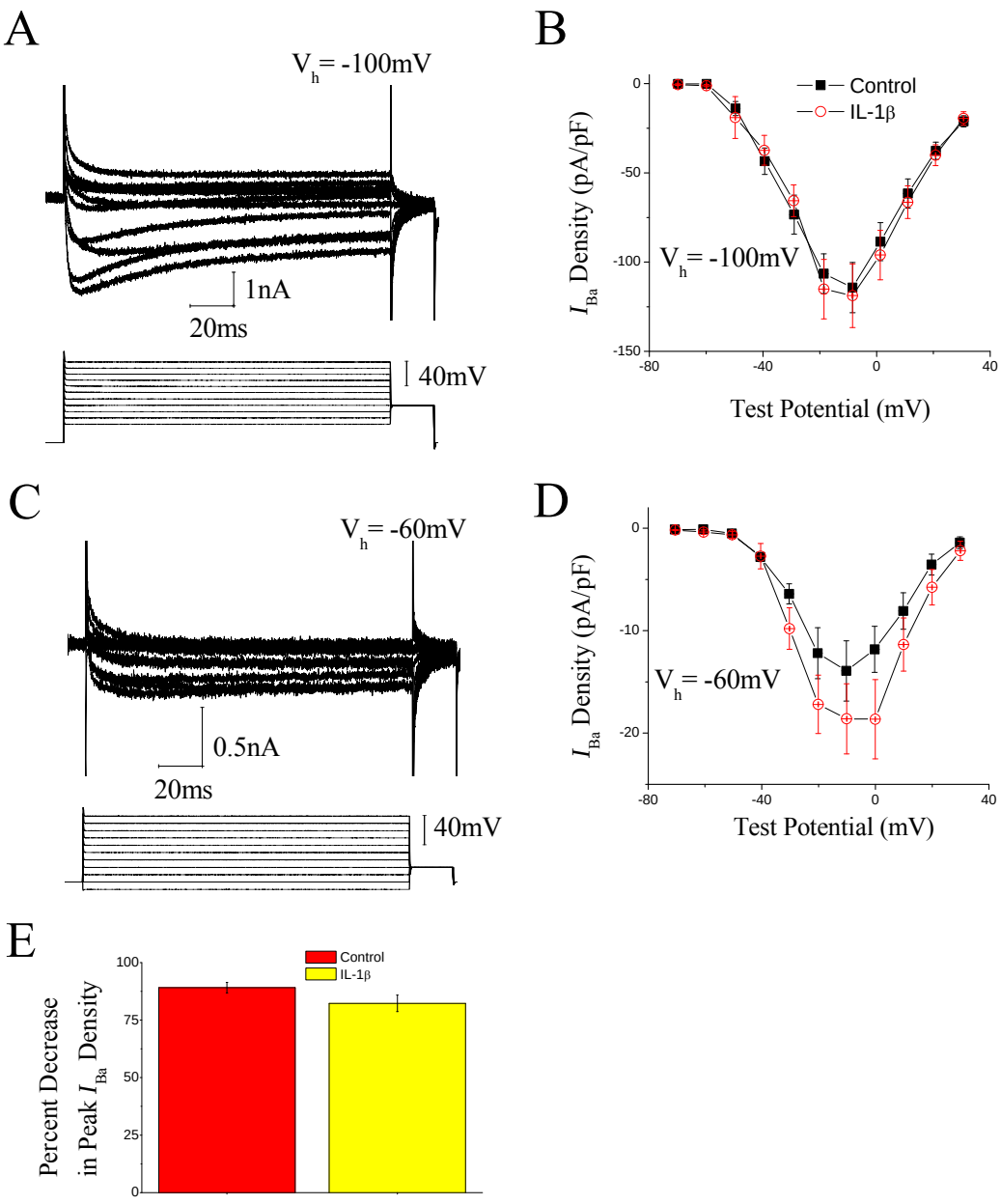
A
V_h = -100mV
1nA
20ms
40mV
B
Control
IL-1β
I_Ba Density (pA/pF)
V_h = -100mV
Test Potential (mV)
C
V_h = -60mV
0.5nA
20ms
40mV
D
I_Ba Density (pA/pF)
V_h = -60mV
Test Potential (mV)
E
Control
IL-1β
Percent Decrease in Peak I_Ba Density

***Figure 4-8: Effect of IL-1β on $I_{Ba}$ voltage dependence of inactivation in small IB4-positive DRG neurons***

A: Voltage dependency of HVA-$I_{Ba}$ inactivation protocol. To more directly examine the possibility that long-term IL-1β affects the voltage dependency of HVA-$I_{Ba}$ inactivation, the fraction of current available at $V_{cmd}$ = -10 mV was determined in response to a series of 3.5 s incremental prepulses.

B: Effect of IL-1β exposure on voltage dependency of HVA-$I_{Ba}$ inactivation. Consistent with the results from sensitivity to shift in $V_h$, single Boltzmann function fitting (Chapter 2) of normalized ($I/I_{-110}$) curves for the voltage dependence of inactivation revealed that IL-1β had no significant effect on the values for $V_{1/2}$ of inactivation (control: -57.1 ± 10.5 mV, n=8 vs. IL-1β: -54.0 ± 11.1, n=6; $p>0.05$) or slope factor (control: 28.8 ± 4.4 mV, n=8 vs. IL-1β: 36.7 ± 7.8, n=6; $p>0.05$; also see Table 4-1).

Error bars indicate means ± SE. Significant difference vs. control * = $p<0.05$, † = $p<0.01$and § = $p<0.001$ with unpaired t-test. Traces in A were not subtracted for leak current.

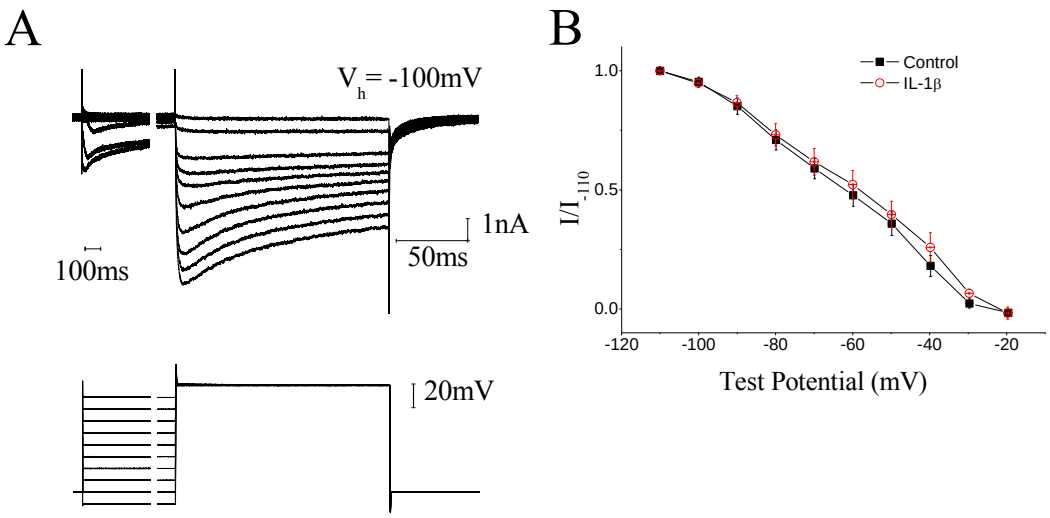
A
V_h = -100mV
1nA
50ms
100ms
20mV
B
Control
IL-1β
1.0
0.5
0.0
I/I_-110
-120
-100
-80
-60
-40
-20
Test Potential (mV)

***Table 4-1: Summary of single Boltzmann function parameters in control versus IL-1β treated small IB4-positive DRG neurons***

Significant difference vs. control * = $p<0.05$, † = $p<0.01$and § = $p<0.001$ with unpaired t-test.

| **Parameter** | **Small $IB_4$ +ve Neurons Control Value ± s.e.m. (n)** | **Small $IB_4$ +ve Neurons IL-1β Value ± s.e.m. (n)** |
|---|---|---|
| $I_{Na}$ activation $V_{1/2}$ (mV) | -35.6 ± 1.8 (12) | -35.3 ± 1.5 (12) |
| $I_{Na}$ activation slope factor (mV) | 3.0 ± 0.5 (12) | 4.2 ± 0.9 (12) |
| $I_{Na}$ steady-state fast inactivation $V_{1/2}$ (mV) | -66.5 ± 1.1 (12) | -68.1± 2.3 (12) |
| $I_{Na}$ steady-state fast inactivation slope factor (mV) | 6.9 ± 0.5 (12) | 9.1 ± 1.4 (12) |
| $I_{Na}$ steady-state slow inactivation $V_{1/2}$ (mV) | -64.2 ± 3.2 (11) | -57.7 ± 3.6 (11) |
| $I_{Na}$ steady-state slow inactivation slope factor (mV) | 16.7 ± 2.0 (11) | 15.9 ± 1.6 (11) |
| $I_{Ba}$ inactivation $V_{1/2}$ (mV) | -57.1 ± 10.5 mV (n=8) | -54.0 ± 11.1 (n=6) |
| $I_{Ba}$ slope factor (mV) | 28.8 ± 4.4 mV (n=8) | 36.7 ± 7.8 (n=6) |

***Table 4-2: Summary of significant findings***

1. Inactivating $Mn^{2+}$ -S $I_K$ currents in my study likely correspond to $K_{Ca}$ currents.
2. Abdulla and Smith (2002).
3. Sarantopoulos et al. (2007).
4. Abdulla and Smith (2001b)

| **Parameter** | **Effect of IL-1β** | **Change consistent with nerve injury studies?** |
|---|---|---|
| **TTX-S $I_{Na}$** density | No change | |
| **TTX-S $I_{Na}$** voltage dependency of activation | No change | |
| **TTX-S $I_{Na}$** voltage dependence of inactivation | No change | |
| **TTX-S $I_{Na}$** kinetics of inactivation | Slower | Yes[2] |
| $I_K$ density | Decreased (inactivating $Mn^{2+}$ -S $I_K$ [1]) | Yes[3,4] |
| $I_{Ba}$ density | No change | |
| $I_{Ba}$ voltage dependence of inactivation | No change | |

### *4.3 References*


1. Abdulla FA, Smith PA (2001a) Axotomy- and autotomy-induced changes in the excitability of rat dorsal root ganglion neurons. J Neurophysiol 85: 630-643.

2. Abdulla FA, Smith PA (2002) Changes in Na(+) channel currents of rat dorsal root ganglion neurons following axotomy and axotomy-induced autotomy. J Neurophysiol 88: 2518-2529.

3. Abdulla FA, Smith PA (2001b) Axotomy- and Autotomy-Induced Changes in Ca2+and K+ Channel Currents of Rat Dorsal Root Ganglion Neurons. J Neurophysiol 85: 644-658.

4. Acheson A, Conover JC, Fandl JP, DeChiara TM, Russell M, Thadani A, Squinto SP, Yancopoulos GD, Lindsay RM (1995) A BDNF autocrine loop in adult sensory neurons prevents cell death. Nature 374: 450-453.

5. Aguayo LG, Weight FF, White G (1991) TTX-sensitive action potentials and excitability of adult rat sensory neurons cultured in serum- and exogenous nerve growth factor-free medium. Neurosci Lett 121: 88-92.

6. Aguayo LG, White G (1992) Effects of nerve growth factor on TTX- and capsaicin-sensitivity in adult rat sensory neurons. Brain Res 570: 61-67.

7. Akins PT, McCleskey EW (1993) Characterization of potassium currents in adult rat sensory neurons and modulation by opioids and cyclic AMP. Neuroscience 56: 759-769.

8. Appel E, Kolman O, Kazimirsky G, Blumberg PM, Brodie C (1997) Regulation of GDNF expression in cultured astrocytes by inflammatory stimuli. Neuroreport 8: 3309-3312.

9. Baccei ML, Kocsis JD (2000) Voltage-Gated Calcium Currents in Axotomized Adult Rat Cutaneous Afferent Neurons. J Neurophysiol 83: 2227-2238.

10. Bahia PK, Suzuki R, Benton DC, Jowett AJ, Chen MX, Trezise DJ, Dickenson AH, Moss GW (2005) A functional role for small-conductance calcium-activated potassium channels in sensory pathways including nociceptive processes. J Neurosci 25: 3489-3498.

11. Bennett DLH, Michael GJ, Ramachandran N, Munson JB, Averill S, Yan Q, McMahon SB, Priestley JV (1998) A distinct subgroup of small DRG cells express GDNF receptor components and GDNF is protective for these neurons after nerve injury. J Neurosci 18: 3059-3072.

12. Binshtok AM, Wang H, Zimmermann K, Amaya F, Vardeh D, Shi L, Brenner GJ, Ji RR, Bean BP, Woolf CJ, Samad TA (2008) Nociceptors are interleukin-1beta sensors. J Neurosci 28: 14062-14073.

13. Black JA, Liu S, Tanaka M, Cummins TR, Waxman SG (2004) Changes in the expression of tetrodotoxin-sensitive sodium channels within dorsal root ganglia neurons in inflammatory pain. Pain 108: 237-247.

14. Caffrey JM, Eng DL, Black JA, Waxman SG, Kocsis JD (1992) Three types of sodium channels in adult rat dorsal root ganglion neurons. Brain Research 592: 283-297.

15. Catacuzzeno L, Fioretti B, Pietrobon D, Franciolini F (2008) The differential expression of low-threshold K+ currents generates distinct firing patterns in different subtypes of adult mouse trigeminal ganglion neurones. J Physiol 586: 5101-5118.

16. Chae KS, Dryer SE (2005) The p38 mitogen-activated protein kinase pathway negatively regulates Ca2+-activated K+ channel trafficking in developing parasympathetic neurons. J Neurochem 94: 367-379.

17. Cummins TR, Aglieco F, Renganathan M, Herzog RI, Dib-Hajj SD, Waxman SG (2001) Nav1.3 sodium channels: rapid repriming and slow closed-state inactivation display quantitative differences after expression

in a mammalian cell line and in spinal sensory neurons. J Neurosci 21: 5952-5961.

18. Cummins TR, Dib-Hajj SD, Waxman SG (2004) Electrophysiological properties of mutant Nav1.7 sodium channels in a painful inherited neuropathy. J Neurosci 24: 8232-8236.

19. Cummins TR, Sheets PL, Waxman SG (2007) The roles of sodium channels in nociception: Implications for mechanisms of pain. Pain 131: 243-257.

20. Cummins TR, Waxman SG (1997) Downregulation of Tetrodotoxin-Resistant Sodium Currents and Upregulation of a Rapidly Repriming Tetrodotoxin-Sensitive Sodium Current in Small Spinal Sensory Neurons after Nerve Injury. J Neurosci 17: 3503-3514.

21. Cusdin FS, Nietlispach D, Maman J, Dale TJ, Powell AJ, Clare JJ, Jackson AP (2010) The sodium channel {beta}3-subunit induces multiphasic gating in NaV1.3 and affects fast inactivation via distinct intracellular regions. J Biol Chem 285: 33404-33412.

22. Dib-Hajj SD, Black JA, Cummins TR, Kenney AM, Kocsis JD, Waxman SG (1998) Rescue of alpha -SNS Sodium Channel Expression in Small

Dorsal Root Ganglion Neurons After Axotomy by Nerve Growth Factor In Vivo. J Neurophysiol 79: 2668-2676.

23. Dib-Hajj SD, Fjell J, Cummins TR, Zheng Z, Fried K, LaMotte R, Black JA, Waxman SG (1999) Plasticity of sodium channel expression in DRG neurons in the chronic constriction injury model of neuropathic pain. Pain 83: 591-600.

24. Djouhri L, Bleazard L, Lawson SN (1998) Association of somatic action potential shape with sensory receptive properties in guinea-pig dorsal root ganglion neurones. J Physiol 513 ( Pt 3): 857-872.

25. Djouhri L, Fang X, Okuse K, Wood JN, Berry CM, Lawson SN (2003) The TTX-Resistant Sodium Channel Nav1.8 (SNS/PN3): Expression and Correlation with Membrane Properties in Rat Nociceptive Primary Afferent Neurons. The Journal of Physiology 550: 739-752.

26. England S, Bevan S, Docherty RJ (1996) PGE2 modulates the tetrodotoxin-resistant sodium current in neonatal rat dorsal root ganglion neurones via the cyclic AMP-protein kinase A cascade. The Journal of Physiology 495: 429-440.

27. Everill B, Kocsis JD (1999) Reduction in Potassium Currents in Identified Cutaneous Afferent Dorsal Root Ganglion Neurons After Axotomy. J Neurophysiol 82: 700-708.

28. Everill B, Rizzo MA, Kocsis JD (1998) Morphologically Identified Cutaneous Afferent DRG Neurons Express Three Different Potassium Currents in Varying Proportions. J Neurophysiol 79: 1814-1824.

29. Fang X, Djouhri L, Black JA, Dib-Hajj SD, Waxman SG, Lawson SN (2002) The Presence and Role of the Tetrodotoxin-Resistant Sodium Channel Nav1.9 (NaN) in Nociceptive Primary Afferent Neurons. J Neurosci 22: 7425-7433.

30. Fang X, Djouhri L, McMullan S, Berry C, Waxman SG, Okuse K, Lawson SN (2006) Intense Isolectin-B4 Binding in Rat Dorsal Root Ganglion Neurons Distinguishes C-Fiber Nociceptors with Broad Action Potentials and High Nav1.9 Expression. J Neurosci 26: 7281-7292.

31. Fazan R, Jr., Whiteis CA, Chapleau MW, Abboud FM, Bielefeldt K (2001) Slow inactivation of sodium currents in the rat nodose neurons. Auton Neurosci 87: 209-216.

32. Fjell J, Cummins TR, Dib-Hajj SD, Fried K, Black JA, Waxman SG (1999) Differential role of GDNF and NGF in the maintenance of two

TTX-resistant sodium channels in adult DRG neurons. Brain Res Mol Brain Res 67: 267-282.

33. Ford CP, Wong KV, Lu VB, Posse dC, Smith PA (2008) Differential neurotrophic regulation of sodium and calcium channels in an adult sympathetic neuron. J Neurophysiol 99: 1319-1332.

34. Fox AP, Nowycky MC, Tsien RW (1987) Kinetic and pharmacological properties distinguishing three types of calcium currents in chick sensory neurones. J Physiol 394: 149-172.

35. Fuchs A, Lirk P, Stucky C, Abram SE, Hogan QH (2005) Painful nerve injury decreases resting cytosolic calcium concentrations in sensory neurons of rats. Anesthesiology 102: 1217-1225.

36. Fuchs A, Rigaud M, Hogan QH (2007a) Painful nerve injury shortens the intracellular Ca2+ signal in axotomized sensory neurons of rats. Anesthesiology 107: 106-116.

37. Fuchs A, Rigaud M, Sarantopoulos CD, Filip P, Hogan QH (2007b) Contribution of calcium channel subtypes to the intracellular calcium signal in sensory neurons: the effect of injury. Anesthesiology 107: 117-127.

38. Funakoshi M, Sonoda Y, Tago K, Tominaga S, Kasahara T (2001) Differential involvement of p38 mitogen-activated protein kinase and phosphatidyl inositol 3-kinase in the IL-1-mediated NF-kappa B and AP-1 activation. Int Immunopharmacol 1: 595-604.

39. Gold MS, Levine JD, Correa AM (1998) Modulation of TTX-R INa by PKC and PKA and their role in PGE2-induced sensitization of rat sensory neurons in vitro. J Neurosci 18: 10345-10355.

40. Gold MS, Reichling DB, Shuster MJ, Levine JD (1996a) Hyperalgesic agents increase a tetrodotoxin-resistant Na+ current in nociceptors. Proc Natl Acad Sci U S A 93: 1108-1112.

41. Gold MS, Shuster MJ, Levine JD (1996b) Characterization of six voltage-gated K+ currents in adult rat sensory neurons. J Neurophysiol 75: 2629-2646.

42. Gold MS, Shuster MJ, Levine JD (1996c) Role of a Ca(2+)-dependent slow afterhyperpolarization in prostaglandin E2-induced sensitization of cultured rat sensory neurons. Neurosci Lett 205: 161-164.

43. Gold MS, Weinreich D, Kim CS, Wang R, Treanor J, Porreca F, Lai J (2003) Redistribution of Na(V)1.8 in uninjured axons enables neuropathic pain. J Neurosci 23: 158-166.

44. Hogan QH, McCallum JB, Sarantopoulos C, Aason M, Mynlieff M, Kwok WM, Bosnjak ZJ (2000) Painful neuropathy decreases membrane calcium current in mammalian primary afferent neurons. Pain 86: 43-53.

45. Hu H, Shao LR, Chavoshy S, Gu N, Trieb M, Behrens R, Laake P, Pongs O, Knaus HG, Ottersen OP, Storm JF (2001) Presynaptic Ca2+-activated K+ channels in glutamatergic hippocampal terminals and their role in spike repolarization and regulation of transmitter release. J Neurosci 21: 9585-9597.

46. Jagodic MM, Pathirathna S, Nelson MT, Mancuso S, Joksovic PM, Rosenberg ER, Bayliss DA, Jevtovic-Todorovic V, Todorovic SM (2007) Cell-Specific Alterations of T-Type Calcium Current in Painful Diabetic Neuropathy Enhance Excitability of Sensory Neurons. J Neurosci 27: 3305-3316.

47. Kim DS, Choi JO, Rim HD, Cho HJ (2002) Downregulation of voltage-gated potassium channel [alpha] gene expression in dorsal root ganglia following chronic constriction injury of the rat sciatic nerve. Molecular Brain Research 105: 146-152.

48. Kostyuk PG, Veselovsky NS, Tsyndrenko AY (1981) Ionic currents in the somatic membrane of rat dorsal root ganglion neurons-I. Sodium currents. Neuroscience 6: 2423-2430.

49. Lai J, Porreca F, Hunter JC, Gold MS (2004) Voltage-gated sodium channels and hyperalgesia. Annu Rev Pharmacol Toxicol 44: 371-397.

50. Lei S, Dryden WF, Smith PA (1997) Regulation of N- and L-Type Ca2+ Channels in Adult Frog Sympathetic Ganglion B Cells by Nerve Growth Factor In Vitro and In Vivo. J Neurophysiol 78: 3359-3370.

51. Li W, Gao SB, Lv CX, Wu Y, Guo ZH, Ding JP, Xu T (2007) Characterization of voltage-and Ca2+-activated K+ channels in rat dorsal root ganglion neurons. J Cell Physiol 212: 348-357.

52. Liu L, Yang TM, Liedtke W, Simon SA (2006) Chronic IL-1beta signaling potentiates voltage-dependent sodium currents in trigeminal nociceptive neurons. J Neurophysiol 95: 1478-1490.

53. Lossin C, Wang DW, Rhodes TH, Vanoye CG, George AL, Jr. (2002) Molecular basis of an inherited epilepsy. Neuron 34: 877-884.

54. Lu SG, Gold MS (2008) Inflammation-induced increase in evoked calcium transients in subpopulations of rat dorsal root ganglion neurons. Neuroscience 153: 279-288.

55. Lu SG, Zhang X, Gold MS (2006) Intracellular calcium regulation among subpopulations of rat dorsal root ganglion neurons. The Journal of Physiology 577: 169-190.

56. Maier JA, Hla T, Maciag T (1990) Cyclooxygenase is an immediate-early gene induced by interleukin-1 in human endothelial cells. J Biol Chem 265: 10805-10808.

57. Martin-Caraballo M, Dryer SE (2002) Glial Cell Line-Derived Neurotrophic Factor and Target-Dependent Regulation of Large-Conductance KCa Channels in Developing Chick Lumbar Motoneurons. J Neurosci 22: 10201-10208.

58. Mayer ML, Sugiyama K (1988) A modulatory action of divalent cations on transient outward current in cultured rat sensory neurones. J Physiol 396: 417-433.

59. McFarlane S, Cooper E (1991) Kinetics and voltage dependence of A-type currents on neonatal rat sensory neurons. J Neurophysiol 66: 1380-1391.

60. Meech RW, Standen NB (1975) Potassium activation in Helix aspersa neurones under voltage clamp: a component mediated by calcium influx. J Physiol 249: 211-239.

61. Meera P, Wallner M, Toro L (2000) A neuronal +¦ subunit (KCNMB4) makes the large conductance, voltage- and Ca2+-activated K+ channel resistant to charybdotoxin and iberiotoxin. Proceedings of the National Academy of Sciences of the United States of America 97: 5562-5567.

62. Molliver DC, Wright DE, Leitner ML, Parsadanian AS, Doster K, Wen D, Yan Q, Snider WD (1997) IB4-binding DRG neurons switch from NGF to GDNF dependence in early postnatal life. Neuron 19: 849-861.

63. Momin A, Cadiou H, Mason A, McNaughton PA (2008) Role of the hyperpolarization-activated current Ih in somatosensory neurons. J Physiol 586: 5911-5929.

64. Morgan K, Stevens EB, Shah B, Cox PJ, Dixon AK, Lee K, Pinnock RD, Hughes J, Richardson PJ, Mizuguchi K, Jackson AP (2000) beta 3: an additional auxiliary subunit of the voltage-sensitive sodium channel that modulates channel gating with distinct kinetics. Proc Natl Acad Sci U S A 97: 2308-2313.

65. Motagally MA, Lukewich MK, Chisholm SP, Neshat S, Lomax AE (2009) Tumour necrosis factor +¦ activates nuclear factor +¦B signalling to reduce N-type voltage-gated Ca2+ current in postganglionic sympathetic neurons. The Journal of Physiology 587: 2623-2634.

66. Nelson MT, Joksovic PM, Perez-Reyes E, Todorovic SM (2005) The endogenous redox agent L-cysteine induces T-type Ca2+ channel-dependent sensitization of a novel subpopulation of rat peripheral nociceptors. J Neurosci 25: 8766-8775.

67. Ninomiya-Tsuji J, Kishimoto K, Hiyama A, Inoue J, Cao Z, Matsumoto K (1999) The kinase TAK1 can activate the NIK-I kappaB as well as the MAP kinase cascade in the IL-1 signalling pathway. Nature 398: 252-256.

68. Nishimune H, Sanes JR, Carlson SS (2004) A synaptic laminin-calcium channel interaction organizes active zones in motor nerve terminals. Nature 432: 580-587.

69. Ogata N, Tatebayashi H (1993) Kinetic analysis of two types of Na+ channels in rat dorsal root ganglia. J Physiol 466: 9-37.

70. Oyelese AA, Rizzo MA, Waxman SG, Kocsis JD (1997) Differential effects of NGF and BDNF on axotomy-induced changes in GABA(A)-receptor-mediated conductance and sodium currents in cutaneous afferent neurons. J Neurophysiol 78: 31-42.

71. Passmore GM (2005) Dorsal root ganglion neurones in culture: a model system for identifying novel analgesic targets? J Pharmacol Toxicol Methods 51: 201-208.

72. Pearce RJ, Duchen MR (1994) Differential expression of membrane currents in dissociated mouse primary sensory neurons. Neuroscience 63: 1041-1056.

73. Qu Y, Curtis R, Lawson D, Gilbride K, Ge P, DiStefano PS, Silos-Santiago I, Catterall WA, Scheuer T (2001) Differential Modulation of Sodium Channel Gating and Persistent Sodium Currents by the [beta]1, [beta]2, and [beta]3 Subunits. Molecular and Cellular Neuroscience 18: 570-580.

74. Rizzo MA, Kocsis JD, Waxman SG (1995) Selective loss of slow and enhancement of fast Na+currents in cutaneous afferent dorsal root ganglion neurones following axotomy. Neurobiology of Disease 2: 87-96.

75. Robinson DR, McNaughton PA, Evans ML, Hicks GA (2004) Characterization of the primary spinal afferent innervation of the mouse colon using retrograde labelling. Neurogastroenterology & Motility 16: 113-124.

76. Rogers JC, Qu Y, Tanada TN, Scheuer T, Catterall WA (1996) Molecular determinants of high affinity binding of alpha-scorpion toxin and sea anemone toxin in the S3-S4 extracellular loop in domain IV of the Na+ channel alpha subunit. J Biol Chem 271: 15950-15962.

77. Roux J, Kawakatsu H, Gartland B, Pespeni M, Sheppard D, Matthay MA, Canessa CM, Pittet JF (2005) Interleukin-1beta decreases expression of the epithelial sodium channel alpha-subunit in alveolar epithelial cells via a p38 MAPK-dependent signaling pathway. J Biol Chem 280: 18579-18589.

78. Rush AM, Cummins TR, Waxman SG (2007) Multiple sodium channels and their roles in electrogenesis within dorsal root ganglion neurons. J Physiol 579: 1-14.

79. Rusin KI, Moises HC (1995) mu-Opioid receptor activation reduces multiple components of high-threshold calcium current in rat sensory neurons. J Neurosci 15: 4315-4327.

80. Rycroft BK, Vikman KS, Christie MJ (2007) Inflammation reduces the contribution of N-type calcium channels to primary afferent synaptic transmission onto NK1 receptor-positive lamina I neurons in the rat dorsal horn. J Physiol 580: 883-894.

81. Saavedra A, Baltazar G, Duarte EP (2007) Interleukin-1[beta] mediates GDNF up-regulation upon dopaminergic injury in ventral midbrain cell cultures. Neurobiology of Disease 25: 92-104.

82. Safieh-Garabedian B, Poole S, Allchorne A, Winter J, Woolf CJ (1995) Contribution of interleukin-1 beta to the inflammation-induced increase in nerve growth factor levels and inflammatory hyperalgesia. Br J Pharmacol 115: 1265-1275.

83. Sarantopoulos CD, McCallum JB, Rigaud M, Fuchs A, Kwok WM, Hogan QH (2007) Opposing effects of spinal nerve ligation on calcium-activated potassium currents in axotomized and adjacent mammalian primary afferent neurons. Brain Res 1132: 84-99.

84. Scholz A, Gruss M, Vogel W (1998) Properties and functions of calcium-activated K+ channels in small neurones of rat dorsal root ganglion studied in a thin slice preparation. J Physiol 513 ( Pt 1): 55-69.

85. Scroggs RS, Fox AP (1992) Calcium current variation between acutely isolated adult rat dorsal root ganglion neurons of different size. J Physiol 445: 639-658.

86. Shah BS, Stevens EB, Gonzalez MI, Bramwell S, Pinnock RD, Lee K, Dixon AK (2000) beta3, a novel auxiliary subunit for the voltage-gated sodium channel, is expressed preferentially in sensory neurons and is upregulated in the chronic constriction injury model of neuropathic pain. Eur J Neurosci 12: 3985-3990.

87. Shipston MJ, Duncan RR, Clark AG, Antoni FA, Tian L (1999) Molecular components of large conductance calcium-activated potassium (BK) channels in mouse pituitary corticotropes. Mol Endocrinol 13: 1728-1737.

88. Snape A, Pittaway JF, Baker MD (2009) Excitability parameters and sensitivity to anemone toxin ATX-II in rat small diameter primary sensory neurones discriminated by Griffonia simplicifolia Isolectin-IB4. The Journal of Physiology.

89. Stansfeld CE, Marsh SJ, Halliwell JV, Brown DA (1986) 4-Aminopyridine and dendrotoxin induce repetitive firing in rat visceral sensory neurones by blocking a slowly inactivating outward current. Neurosci Lett 64: 299-304.

90. Takahashi N, Kikuchi S, Dai Y, Kobayashi K, Fukuoka T, Noguchi K (2003) Expression of auxiliary [beta] subunits of sodium channels in primary afferent neurons and the effect of nerve injury. Neuroscience 121: 441-450.

91. Takeda M, Kitagawa J, Takahashi M, Matsumoto S (2008) Activation of interleukin-1beta receptor suppresses the voltage-gated potassium currents in the small-diameter trigeminal ganglion neurons following peripheral inflammation. Pain 139: 594-602.

92. Takeda M, Kitagawa J, Nasu M, Takahashi M, Iwata K, Matsumoto S (2010) Glial cell line-derived neurotrophic factor acutely modulates the excitability of rat small-diameter trigeminal ganglion neurons innervating facial skin. Brain, Behavior, and Immunity 24: 72-82.

93. Tanabe K, Nishimura K, Dohi S, Kozawa O (2009) Mechanisms of interleukin-1beta-induced GDNF release from rat glioma cells. Brain Res 1274: 11-20.

94. Thompson SH (1977) Three pharmacologically distinct potassium channels in molluscan neurones. The Journal of Physiology 265: 465-488.

95. Todorovic SM, Jevtovic-Todorovic V (2006) The role of T-type calcium channels in peripheral and central pain processing. CNS Neurol Disord Drug Targets 5: 639-653.

96. Vydyanathan A, Wu ZZ, Chen SR, Pan HL (2005) A-type voltage-gated K+ currents influence firing properties of isolectin B4-positive but not isolectin B4-negative primary sensory neurons. J Neurophysiol 93: 3401-3409.

97. Wang H, Woolf CJ (2005) Pain TRPs. Neuron 46: 9-12.

98. Waxman SG, Cummins TR, Dib-Hajj SD, Black JA (2000) Voltage-gated sodium channels and the molecular pathogenesis of pain: a review. J Rehabil Res Dev 37: 517-528.

99. Waxman SG, Kocsis JD, Black JA (1994) Type III sodium channel mRNA is expressed in embryonic but not adult spinal sensory neurons, and is reexpressed following axotomy. J Neurophysiol 72: 466-470.

100. Widmer HlnA, Rowe ICM, Shipston MJ (2003) Conditional protein phosphorylation regulates BK channel activity in rat cerebellar Purkinje neurons. The Journal of Physiology 552: 379-391.

101. Woodall AJ, Richards MA, Turner DJ, Fitzgerald EM (2008) Growth factors differentially regulate neuronal Cav channels via ERK-dependent signalling. Cell Calcium 43: 562-575.

102. Wu ZZ, Chen SR, Pan HL (2004) Differential sensitivity of N- and P/Q-type Ca2+ channel currents to a mu opioid in isolectin B4-positive and -negative dorsal root ganglion neurons. J Pharmacol Exp Ther 311: 939-947.

103. Yang F, Feng L, Zheng F, Johnson SW, Du J, Shen L, Wu CP, Lu B (2001) GDNF acutely modulates excitability and A-type K(+) channels in midbrain dopaminergic neurons. Nat Neurosci 4: 1071-1078.

104. Yoshida S, Matsuda Y, Samejima A (1978) Tetrodotoxin-resistant sodium and calcium components of action potentials in dorsal root ganglion cells of the adult mouse. J Neurophysiol 41: 1096-1106.

105. Yoshida S, Matsumoto S (2005) Effects of +¦-Dendrotoxin on K+ Currents and Action Potentials in Tetrodotoxin-Resistant Adult Rat Trigeminal Ganglion Neurons. J Pharmacol Exp Ther 314: 437-445.

106. Zhang XL, Mok LP, Katz EJ, Gold MS (2010) BKCa currents are enriched in a subpopulation of adult rat cutaneous nociceptive dorsal root ganglion neurons. Eur J Neurosci 31: 450-462.

107. Zhou C, Ye HH, Wang SQ, Chai Z (2006) Interleukin-1[beta] regulation of N-type Ca2+ channels in cortical neurons. Neuroscience Letters 403: 181-185.

108. Zur KB, Oh Y, Waxman SG, Black JA (1995) Differential up-regulation of sodium channel [alpha]- and [beta]1-subunit mRNAs in cultured embryonic DRG neurons following exposure to NGF. Molecular Brain Research 30: 97-105.

# CHAPTER 5

## Long-term IL-1β Exposure:

## Effects On Ionic Currents In Medium-sized DRG Neurons

## *5.1 Results*

Because IL-1β also affected increased the excitability of medium DRG neurons, I analyzed the changes in various ionic conductances that might explain these changes.

### *5.1.1 Sodium currents* ($I_{Na}$) *in medium DRG neurons*

Similar to cultured small-sized IB4-positive DRG neurons, all (20/20) medium neurons recorded had TTX-S $I_{Na}$ and no measurable TTX-R $I_{Na}$ (Figure 5-1Ai – Aii). Interestingly, the *I-V* plot for IL-1β treated medium neurons is visibly smaller in current density at voltage commands between -10 mV and +20 mV (unpaired t-test, $0.05<p\leq0.1$; Figure 5-1B). However, peak TTX-S $I_{Na}$ occurred at $V_{cmd}$ = -20 mV for control neurons (-261 ± 48 pA/pF; n=9), whereas, peak current density occurred at -30 mV for neurons exposed to IL-1β (-176 ± 44 pA/pF; n=11). Consistent with this finding, single Boltzmann function fitting of the curves for the voltage dependence of activation revealed that the average voltage midpoint ($V_{1/2}$) was significantly shifted leftward (hyperpolarizing shift in TTX-S $I_{Na}$ activation) after long-term IL-1β exposure (-32.5 ± 2.6 mV (n=9) vs. -41.4 ± 2.2 mV (n=11); unpaired t-test, $p<0.05$; Figure 5-1C and 5-1D, also see Table 5-1).

When experiments permitted, the voltage dependence of TTX-S $I_{Na}$ inactivation was also investigated using identical voltage protocols described for small IB4-positive neurons (Figures 5-2A and 5-2C). In contrast to activation, IL-1β exposure produced no shifts in the curves for steady-state fast and slow

inactivation (Figures 5-2B and 5-2D, respectively). Unlike small IB4-positive neurons, single exponential fits of TTX-S $I_{Na}$ decay in medium neurons revealed no differences in the kinetics for fast inactivation in response to IL-1β treatment (Figure 5-3A).

*5.1.2 Potassium currents* ($I_K$) *in medium DRG neurons*

As described for small IB4-positive neurons, medium neuron $K^+$ currents were divided into three basic components: non-inactivating (Figure 5-3B), inactivating $Mn^{2+}$ -resistant ($Mn^{2+}$ -R; Figure 5-4A) and $Mn^{2+}$ -sensitive ($Mn^{2+}$ -S; Figure 5-5A) $I_K$. Further, in some neurons, it was not possible to isolate all three $K^+$ current components and, therefore, sampling varied between experiments.

All (9/9) control and (16/16) IL-1β treated medium neurons had non-inactivating $I_K$. In contrast to small-sized IB4-positive neurons, *I-V* plots revealed that non-inactivating $I_K$ densities are substantially smaller following exposure to long-term IL-1β (Figure 5-3C) with significant reductions at command voltages -20 mV to +60 mV (for example, $V_{cmd}$ = +60 mV: +169 ± 25 pA/pF (n=9) vs. +62 ± 10 pA/pF (n=16); unpaired t-test, $p<0.001$; also see Figure 5-3D).

90% (9/10) of control and 94% (15/16) of IL-1β treated medium neurons had measurable inactivating $Mn^{2+}$ -R $I_K$ (Fisher's exact-test, $p>0.05$). Similar to non-inactivating $I_K$, there was a significant reduction in inactivating $Mn^{2+}$ -R $I_K$ density ($V_{cmd}$ = +60 mV; control: +31 ± 9 pA/pF (n=10) vs. IL-1β: +13 ± 4 pA/pF (n=16); unpaired t-test, $p<0.05$; Figure 5-4B and 5-4C).

Last, all (12/12) control and (16/16) IL-1β treated medium neurons had inactivating $Mn^{2+}$-S $I_K$. However, *I-V* plots revealed that current densities, at command voltages -40 mV to +60 mV, were significantly suppressed in response to long-term IL-1β exposure (for example, $V_{cmd}$ = +60 mV: control: +98 ± 16 pA/pF (n=12) vs. IL-1β: +51 ± 10 pA/pF (n=16); unpaired t-test, $p<0.05$; Figure 5-5B and 5-5C). Also in Figure 5-5B, IL-1β exposure reduced the appearance of rising-and declining- phases in the 'n'- shaped *I-V* density plot, at command voltages between -30 mV and + 10 mV. As discussed in Chapter 4, this response indicates the presence of $K_{Ca}$ current and likely corresponds to the onset and offset of $Ca^{2+}$ influx through voltage-gated calcium channels (VGCCs). Therefore, the absence of such phases suggests that IL-1β exposure additionally suppressed $Ca^{2+}$ current in medium neurons (see below).

*5.1.3 Calcium currents* ($I_{Ba}$) *in medium DRG neurons*

In a similar manner to small IB4-positive neurons where $Ba^{2+}$ was used as the charge carrier (Figures 5-6A and 5-6C), the possible effects of IL-1β on $I_{Ba}$ in medium neurons were investigated. By contrast with findings in small IB4-positive neurons where $I_{Ba}$ was unchanged (Figures 4-7 and 4-8), *I-V* plots ($V_h$ = -100 mV) revealed that long-term IL-1β treatment significantly increased medium neuron $I_{Ba}$ densities at command voltages between -40 mV and -10 mV (unpaired t-test, $p<0.01$ for both data points; Figure 5-6B). Further, HVA-$I_{Ba}$ peak current density (recorded at $V_{cmd}$ = -10 mV) in presence of IL-1β (-154 ± 12 pA/pF, n=14) tended to be larger than that recorded in control cultures (-107 ± 22 pA/pF, n=9;

unpaired t-test, $0.05<p\leq0.1$; Figure 5-6B). The presence of low voltage-activated $I_{Ba}$ (LVA-$I_{Ba}$) can be determined with small depolarizing commands to -50 mV which generate a shoulder on *I-V* plots at voltages between -60 mV and -30 mV (Abdulla and Smith, 2001b;Scroggs and Fox, 1992). Since shoulders on *I-V* plots ($V_h$ = -100 mV) were absent in both control and IL-1β treated medium neurons and no significant differences in $I_{Ba}$ density were found at $V_{cmd}$ = -50 mV, LVA-$I_{Ba}$ was not further studied. By default, most of the $I_{Ba}$ described in medium neurons in long-term cell culture is expected to be HVA-$I_{Ba}$.

The effect of 100 pM IL-1β on inactivation was also examined. Opposite to the effect of $V_h$ = -100 mV and suggestive of differences in inactivation, the HVA-$I_{Ba}$ density ($V_{cmd}$ = -10 mV) remaining at $V_h$ = -60mV, was significantly larger in control than in IL-1β treated medium neurons (-58 ± 6 pA/pF, n=10 vs. -38 ± 4, n=11; unpaired t-test, $p<0.01$; Figure 5-6D). Further, relative to control neurons, IL-1β exposure appeared to enhance the sensitivity of HVA-$I_{Ba}$ to holding potential (Figure 5-6B vs. 5-6D). Therefore, sensitivity to a shift in holding potential was calculated as the percent decrease in peak HVA-$I_{Ba}$ density upon depolarization (from $V_h$ = -100 mV to -60 mV; Figure 5-6E). As expected, IL-1β exposure significantly (unpaired t-test, $p<0.01$) enhanced the percent decrease in peak HVA-$I_{Ba}$ density in medium neurons from 20.3 ± 15.5% (n=8) to IL-1β 73.7 ± 3.6% (n=10).

To more directly examine the possibility that long-term IL-1β affects voltage dependency of HVA $I_{Ba}$ inactivation, the fraction of current available was determined in response to a series of 3.5 s incremental prepulses (Figure 5-7A).

Consistent with enhanced sensitivity to holding potential and increased inactivation, single Boltzmann function fitting of curves for the voltage dependence of inactivation revealed that the voltage midpoints ($V_{1/2}$) had a tendency toward a leftward shift (hyperpolarizing shift in HVA-$I_{Ba}$ inactivation) after long-term IL-1β exposure (control: -59 ± 5 mV, n=6 vs. IL-1β: -78.8 ± 5.9, n=13; unpaired t-test, $0.05<p\leq0.1$; Figure 5-7B and Table 5-1). Fitting of inactivation curves also indicated that medium neurons exposed to IL-1β had a significantly increased slope factor (control: 10.7 ± 1.1 mV, n=6 vs. IL-1β: 17.8 ± 1.4, n=13; unpaired t-test, $p<0.01$; also see Table 5-1) which is further suggestive of an enhanced sensitivity to voltage. These results are surprising given that IL-1β appeared to increase HVA-$I_{Ba}$ density (Figure 5-6B), while also increasing inactivation (Figure 5-7B).

### *5.1.4 Hyperpolarization-activated cation current* ($I_H$) *in medium DRG neurons*

Voltage sag reflects the activation of hyperpolarization-activated cation current ($I_H$; Mayer and Westbrook, 1983; Scroggs et al., 1994). As described in Chapter 3, medium neurons were the only neuron subpopulation not to exhibit a decline in the magnitude of voltage sag after long-term IL-1β exposure (Figure 3-8C). Since attenuation of voltage sag and, possible, reductions in $I_H$ are not expected to be consistent with sensory neuron hyperexcitability after peripheral nerve injury (Abdulla and Smith, 2001b;Yao et al., 2003), the effect of long-term IL-1β exposure on DRG neuron $I_H$ was restricted to medium neurons.

As described in Methods (Chapter 2), $V_h$ = -50 mV and $I_H$ was elicited by a series of hyperpolarizing voltage commands (from -60 mV to -130 mV) that were also incremental in duration (from 4.25 s to 2.5 s; Figure 5-8B). This voltage protocol was designed to maximize capture of steady-state $I_H$ activation, yet provide stable cellular voltage-clamp recordings. Similar to that reported by Abdulla and Smith (2001b), the inward current consisted of an initial instantaneous current ($I_{INST}$), followed by slower inward relaxation ($I_H$) that became larger and that developed more rapidly at more negative voltages (Figure 5-8C inset). The $I_H$ blocker, ZD7288 (100 μM), blocked both voltage sag (in current-clamp mode) and $I_H$ (Figures 5-8A and 5-8Bii). All (21/21) medium neurons recorded had measurable $I_H$ and *I-V* plots revealed that IL-1β exposure had a tendency to increase $I_H$ densities in medium neurons (Figure 5-8C). Interestingly, this tendency occurred at voltage commands between -60 mV and -90 mV (unpaired t-test, $0.05<p\leq0.1$; Figure 5-8D) and not at more hyperpolarized commands.

To explore the possibility that difference in $I_H$ densities are a consequence of alterations to $I_H$ kinetics of activation, traces were fitted with the sum of two exponential functions as previously described by Kouranova and colleagues (2008). Since some individual $I_H$ traces (< -80 pA, in particular $V_{cmd}$ = -60mV for all DRG neurons) were better fit by a single exponential function, they were omitted from kinetic analysis. As depicted in Figures 5-8E and 5-8F, values of fast ($\tau_{fast}$) and slow ($\tau_{slow}$) time constants were voltage dependent, becoming faster toward negative voltages in both control and medium neurons exposed to IL-1β.

However, both fast and slow time constants became significantly faster in IL-1β treated cell cultures over a command voltage range that overlapped with the greatest differences in $I_H$ densities (unpaired t-test, $p<0.01$ and $p<0.05$, respectively; Figures 5-8E and 5-8F).

Since shifts in the voltage dependence of $I_H$ activation may also explain differences in $I_H$ densities, the effect of IL-1β on steady-state activation was examined. As described by Kouranova and colleagues (2008), the conductance ratio, $G/G_{-130}$, was calculated from tail current ($I_{H,Tail}$) amplitudes measured 100 – 200 ms after repolarization (Figure 5-8G, inset) and *G-V* relationships for $I_H$ steady-state activation were then plotted (Figure 5-8G). The *G-V* plots, however, are nearly superimposed and single Boltzmann function fitting of the steady-state $I_H$ activation curves revealed that IL-1β had no significant effect on the values for voltage midpoints ($V_{1/2}$) of activation (control: -70.7 ± 2.7 mV (n=9) vs. IL-1β: -65.9 ± 5.1 mV (n=10); unpaired t-test, $p>0.05$; also see Table 5-1).

## *5.2 Discussion*

### *5.2.1 $I_{Na}$ in medium DRG neurons*

#### *5.2.1.1 Characterization of $I_{Na}$ in medium neurons*

In a similar manner to small IB4-positive neurons, medium neurons in long-term culture had TTX-S $I_{Na}$, but no measureable TTX-R $I_{Na}$. Although this observation is in general agreement with the established view that TTX-S $I_{Na}$ is the primary contributor to total $I_{Na}$ in larger-sized sensory neurons (Caffrey et al., 1992;Rizzo et al., 1994;Abdulla and Smith, 2002), the complete absence suggests

that long-term cell cultures did not support the functional expression of TTX-R sodium channels. As discussed in Chapters 3 and 4, this deficiency likely relates to the maintenance of DRG cell cultures in the absence of serum and exogenously added neurotrophins, such as NGF and GDNF (Dib-Hajj et al., 1998a;Fjell et al., 1999;Ford et al., 2008;Aguayo et al., 1991). Therefore, similar to small IB4-positive neurons, it is possible that interpretations made on medium neuron $I_{Na}$ are limited by the lack of TTX-R $I_{Na}$.

TTX-S $I_{Na}$ in control medium diameter neurons had the typical characteristics found in other DRG neuron studies. For instance, rapid activation within a couple of hundred microseconds, thresholds of activation between -50 to -40 mV and maximal amplitudes between -20 to -10 mV (Caffrey et al., 1992;Abdulla and Smith, 2002;Lai et al., 2004;Aguayo et al., 1991;Kostyuk et al., 1981;Ogata and Tatebayashi, 1993). As opposed to the slower inactivation kinetics (~ 10 ms at -40 mV) of TTX-R $I_{Na}$, TTX-S $I_{Na}$ in long-term cultured medium neurons displayed inactivation kinetics (~ 1.5 ms at -40 mV) that are consistent with the well established rapid inactivation of TTX-S $I_{Na}$ (Ogata and Tatebayashi, 1993;Caffrey et al., 1992;Kostyuk et al., 1981). Voltage midpoints (~ -60 mV) for TTX-S $I_{Na}$ fast inactivation are in agreement with findings from Ogata and Tatebayashi (1993), however, there appears to be substantial variability in the literature where others have found more negative voltage midpoints (~ -85 mV) for fast inactivation (Kostyuk et al., 1981;Caffrey et al., 1992). In consistencies are most likely attributed to the use of fluoride in electrode solutions (Kostyuk et al., 1981) which is known to affect TTX-S $I_{Na}$ fast inactivation (Ogata

and Tatebayashi, 1993) and was, therefore, avoided in my study. Last, the voltage midpoint (~ -60 mV) for slow inactivation was similar to fast inactivation, but not clearly more negative which is the case for TTX-R $I_{Na}$ (Fazan, Jr. et al., 2001;Rush et al., 2007b).

*5.2.1.2 Comparisons between TTX-S $I_{Na}$ in small IB4-positive versus medium neurons*

Since it is possible that medium and small IB4-positive neurons express different functional sodium channels that give rise to biophysically distinct TTX-S $I_{Na}$ (Lai et al., 2004;Cummins et al., 2007;Rush et al., 2007b;Herzog et al., 2003;Abdulla and Smith, 2002), a preliminary comparison is made here. TTX-S $I_{Na}$ in these two DRG neuron subtypes both activated rapidly and had nearly identical voltage dependencies (voltage midpoints within 5 mV of each other) for activation and inactivation. In contrast to investigations in adult rat DRG by Caffrey and colleagues (1992) where a slower inactivating (~ 6 ms at -40 mV) TTX-S $I_{Na}$ was found to be preferentially distributed in larger diameter neurons, no TTX-S $I_{Na}$ matching these kinetics were recorded in long-term cultured control medium or small IB4-positive neurons. This finding might be suggestive of an additional phenotypic switch or the loss of a DRG subpopulation in long-term culturing conditions (Aguayo et al., 1991), however, the literature concerning the distribution of biophysically distinct TTX-S $I_{Na}$ appears to be variable. For instance, Abdulla and Smith (2002) also reported a slower TTX-S $I_{Na}$ in acutely isolated DRG neurons, but this current was restricted to a subpopulation of small, rather than large, neurons. Since I only measured sodium currents in medium and

small IB4-positive neurons which became hyperexcitable after long-term IL-1β exposure, the existence of a 'slow' TTX-S $I_{Na}$ may have been found in a subpopulation of DRG neurons not investigated here.

Despite the similarities between TTX-S $I_{Na}$ found in medium and small IB4-positive, it cannot be stated conclusively that they are identical. For instance TTX-S sodium channel isoforms expressed in DRG neurons have other distinct biophysical properties (Rush et al., 2007b;Cummins et al., 2007;Herzog et al., 2003), such as rapid repriming ($Na_V1.6$) versus slow onset of closed-state inactivation ($Na_V1.7$), which cannot be determined with the protocols used in my study. Interpretations are further complicated by the known differential distribution of the auxiliary β–subunits and, possibly, other associated proteins among DRG neuron subtypes which can profoundly affect the behaviour of individual sodium channel isoforms (Pertin et al., 2005;Takahashi et al., 2003;Cummins et al., 2007;Rush et al., 2006b).

Last, the effects of IL-1β on TTX-S $I_{Na}$ in medium (discussed below) and small IB4-positive neurons (Chapter 4) are distinct and, therefore, suggest that the underlying channel isoforms are different. However, such straightforward interpretations are complicated by differences in the responsiveness of medium and small IB4-positive neurons to other mediators, such as BDNF and GDNF, respectively (Chapter 1) which may have been generated in response to long-term IL-1β exposure (Tanabe et al., 2009;Purmessur et al., 2008;Appel et al., 1997;Saavedra et al., 2007).

*5.2.1.3 Effect of long-term IL-1β exposure on TTX-S $I_{Na}$ in medium neurons*

The principal finding in this part of the investigation is that TTX-S $I_{Na}$ activated at more hyperpolarized potentials after long-term exposure to IL-1β and is characterized by a significant leftward shift in the voltage midpoint for voltage dependency of activation (Figure 5-1C and 5-1D). As discussed in Chapter 4, there is considerable variability in literature regarding the sodium currents and/or corresponding sodium channel subtypes after nerve injury and few have described the potential effects of nerve injury on the voltage dependency of TTX-S $I_{Na}$. This is surprising given that TTX-S $I_{Na}$ currents are the major contributor to AP upstroke in larger sensory neurons (Caffrey et al., 1992) and that myelinated primary afferents are known to be a substantial source of ectopic, spontaneous discharge after peripheral nerve injury (Devor, 2009). Sodium current activation at more negative voltages would be expected to decrease AP threshold and, therefore, facilitate spontaneous firing in injured neurons. However, Cummins and Waxman (1997) reported that voltage dependency of activation for TTX-S $I_{Na}$ in small nociceptive neurons was unchanged in response to sciatic nerve ligation and section, instead, the conductance exhibited more rapid repriming which is thought to maintain high frequency firing. Rapid repriming is not likely to account for all aberrant activity related to sodium currents after nerve injury, since Everill and colleagues (2001) found that rapidly repriming TTX-S sodium conductances were unchanged in large sensory neurons using the same nerve injury model.

As discussed in Chapter 4, the presence of a rapidly repriming TTX-S $I_{Na}$ after long-term IL-1β exposure was not determined in my study, and, therefore, cannot be dismissed. However, as the voltage dependence of activation was unchanged after nerve injury, alternative or additional changes to TTX-S $I_{Na}$ may have occurred in my study. For example, nerve injury is also known to alter the expression of auxiliary β subunits, including the upregulation of the β3 subunit in small DRG neurons (Takahashi et al., 2003;Shah et al., 2000) which can produce a hyperpolarizing shift in the activation threshold for particular TTX-R sodium channel isoforms (PN3) in heterologous expression systems (Shah et al., 2000). In relation to TTX-S sodium channel isoforms, however, β3 has been reported to produce a depolarizing shift in the voltage dependence for activation of $Na_V1.3$ in heterologous expression systems (Cusdin et al., 2010). Such a shift is opposite to the effect of IL-1β exposure on medium neuron TTX-S $I_{Na}$ in my study and, therefore, suggests that other possibilities exist. This may include, the yet to be determined, downregulation of the β3 subunit in DRG cell cultures exposed to IL-1β.

Alternatively, sodium channel upregulation may not involve changes in the expression of subunits or accessory proteins, but, rather, a direct modulation of channel function. For instance, many inflammatory mediators, including $PGE_2$, modulate sensory neuron TTX-R $I_{Na}$ through activation of PKC and/or PKA which can produce hyperpolarizing shifts in voltage midpoints of activation, as well as, inactivation (England et al., 1996;Gold et al., 1996a;Gold et al., 1998). Interestingly, England and colleagues (1996) reported that hyperpolarizing shifts

in TTX-R $I_{Na}$ activation curves in response to $PGE_2$ were frequently accompanied by decreases in peak conductance and, in this way, resembles the tendencies toward reduced TTX-S $I_{Na}$ densities in medium DRG neurons after long-term IL-1β in my study. Consistent with this, exposure to IL-1β has also been previously reported to reduce voltage-gated sodium currents in retinal ganglion cells (Diem et al., 2003) and trigeminal nociceptive neurons (Liu et al., 2006).

The effects of inflammatory mediators on TTX-S $I_{Na}$ has not been extensively studied, however, a reduction in sodium current seem at odds with sensory neuron hyperexcitability and by the finding that acute IL-1β can also potentiate TTX-S $I_{Na}$ in nociceptive neurons (Binshtok et al., 2008). The contradiction in the actions of IL-1β on sodium currents may relate to variables such as the source of neurons (DRG vs. trigeminal ganglion), sodium channel isoform or the duration of exposure (5 minutes vs. 24 hours). Interestingly, the downregulation of epithelial sodium channels in human middle ear epithelial cells in response to a 24 hour exposure to IL-1β involved the extracellular signal regulated kinase (ERK) 1/2. Further, activation of ERK1/2 has been reported to directly phosphorylate specific residues within intracellular loop 1 (L1) of the $Na_V1.7$ sodium channel and, thereby, regulates gating properties, including channel activation at more hyperpolarized potentials (Stamboulian et al., 2010). In this way, IL-1β modulation of TTX-S $I_{Na}$ may still support DRG neuron hyperexcitability, despite potential decreases in peak sodium current. Taken together, it is possible that modulation of medium neuron TTX-S $I_{Na}$ in response to long-term IL-1β exposure could involve the secondary production of particular

pro-inflammatory molecules, such as $PGE_2$ (Maier et al., 1990), and/or involve specific intracellular signalling molecules, such as ERK1/2. Their involvement in my study, however, remains to be elucidated.

*5.2.1.4 Functional implications of TTX-S $I_{Na}$ regulation in medium neurons in response to long-term IL-1β exposure*

Since the activation of sodium channels is a major contributor to AP upstroke, a hyperpolarizing shift in the voltage dependence for activation of TTX-S $I_{Na}$, in response to IL-1β exposure, likely corresponds to the reduction in medium neuron rheobase observed under current-clamp evaluation and, therefore, contributes to hyperexcitability (Chapter 3). In support, hyperpolarizing shifts in the activation of the TTX-S sodium channels, such as $Na_V1.7$, either by ERK1/2 phosphorylation (Stamboulian et al., 2010) or gain of function mutations (Cummins et al., 2004), are associated with sensory neuron hyperexcitability and pain hypersensitivity. Since upregulation of $Na_V1.7$ can generate large ramp currents near RMP which are thought to amplify small membrane depolarizations in sensory neurons and, therefore, decrease AP threshold (Cummins et al., 2004), it would be interesting to examine this phenomenon in future studies.

While upregulation of $Na_V1.7$ may have occurred in response to long-term IL-1β exposure, the slow-repriming characteristics of this sodium channel suggests a limited role in repetitive firing (Cummins et al., 2007). Coupled to this, $Na_V1.7$ upregulation in cell types (sympathetic ganglion neurons) that lack the TTX-R sodium channel, $Na_V1.8$, has been reported to produce membrane depolarization and reduce excitability (Rush et al., 2006a). Since these alterations

were not found in my current-clamp study, the effect of IL-1β exposure on medium neuron excitability is not likely to be limited to $Na_V1.7$ upregulation. Alternatively, long-term IL-1β exposure may be associated with the upregulation of the embryonic sodium channel, $Na_V1.3$, which is also known to generate ramp currents, as well as, rapidly reprime and support high frequency discharge after nerve injury (Cummins et al., 2007;Cummins and Waxman, 1997;Rush et al., 2007a;Cummins et al., 2001). Therefore, in addition to the possible effect on ramp currents, it would be worthwhile to examine the effect of long-term IL-1β exposure on the repriming of TTX-S $I_{Na}$ in medium DRG neurons.

Medium neurons also had an increase in the maximal rate of depolarization in response to IL-1β exposure. Since differences in rates of sensory neuron depolarization are attributed to the differential kinetic properties and/or relative densities of TTX-R and TTX-S $I_{Na}$ in sensory neurons (Djouhri et al., 1998), the lack of TTX-R $I_{Na}$ with no clear differences in peak TTX-S $I_{Na}$ density in my study precludes such straightforward explanations. Since there appeared to be no effect on the kinetics of TTX-S $I_{Na}$ (representative traces appear similar in Figure 5-1D), there remains the possibility that IL-1β exerted effects on factors (other conductances) additional to TTX-S $I_{Na}$ (discussed below). Last, the effects of IL-1β exposure on additional currents in medium neurons may also account for increased AP height, since the difference between RMP and AP height (~ 47 mV; see Table 3-2) is beyond the predicted equilibrium potential for sodium current ($E_{Na}$ = ~ -40 mV). Future studies could use computer modeling to test this possibility.

### *5.2.2 $I_K$ in medium DRG neurons*

#### *5.2.2.1 Isolation of potassium currents in medium neurons*

As described in Chapter 4, the complexity and variability of potassium currents in DRG neurons (Akins and McCleskey, 1993;Gold et al., 1996b;Zhang et al., 2010) posed several challenges in the examination of $K_V$ and $K_{Ca}$ currents in my study. For example, in Figure 5-3B, some slowly inactivating current still remained after a -30 mV prepulse and suggests that inactivating A-type currents were not always clearly isolated from non-inactivating $I_K$ (delayed rectifier) currents. Similar to small IB4-positive neurons, this likely reflected the presence of the slowly and incompletely inactivating, dendrotoxin-sensitive current ($I_D$) (Stansfeld et al., 1986;Everill et al., 1998) or, possibly, the slow ($I_{As}$) A-type potassium currents identified in medium diameter DRG neurons by Gold and colleagues (1996b). Another limitation, was the use of 5 mM $Mn^{2+}$ to block calcium-dependent components of potassium conductances which could interfere with the activation and/or inactivation of A-type currents in cultured rat DRG neurons (Mayer and Sugiyama, 1988) and, ultimately, the measurements of $Mn^{2+}$ -resistant ($Mn^{2+}$-R) and –sensitive ($Mn^{2+}$-S) inactivating $I_K$ components in my study. Taken together, the numerous potassium conductances in sensory neurons, where some have over-lapping properties, are difficult to study by any one means and ideally require a combination of pharmacological, biophysical and molecular approaches (Zhang et al., 2010;Gold et al., 1996b;Everill et al., 1998;Sarantopoulos et al., 2007). Despite the potential limitations in the methodology used in my study, experiments were designed to survey families of

potassium currents and assess their possible contributions to medium neuron hyperexcitability in response to long-term IL-1β exposure. Similar to small IB4-positive neurons, changes in any one of, or combination of, the three potassium currents studied in response to IL-1β exposure would, therefore, justify a more specialized approach in future studies.

*5.2.2.2 Comparisons between $I_K$ in small IB4-positive versus medium DRG neurons*

In contrast to small and/ or IB4-positive sensory neurons, detailed information on $K_V$ and $K_{Ca}$ currents in medium diameter sensory neurons is, for the most part, unavailable. However, acutely isolated small and/or IB4-positive DRG neurons are known to be enriched with $BK_{Ca}$ and, possibly, $SK_{Ca}$ currents, relative to medium DRG neurons (Gold et al., 1996c;Zhang et al., 2010;Sarantopoulos et al., 2007). In contrast, control medium neurons in long-term cell culture appeared to have slightly greater densities of inactivating $Mn^{2+}$ -sensitive ($Mn^{2+}$-S) $I_K$ than small IB4-positive neurons (Figures 4-6B vs. 5-5B). As discussed below this discrepancy may be related to a higher density of voltage-gated calcium channels (VGCCs) in medium neurons or a shift in the phenotype of small IB4-positive neurons in long-term cell culture (Chapter 4). In general agreement with the literature (Chapter 1), however, A-type potassium currents were present in both small IB4-positive and medium neurons in long-term cell culture (Gold et al., 1996b;Villiere and McLachlan, 1996). Given the diversity of potassium channel subunits and splice variants found in the DRG (Zhang et al., 2010;Yang et al., 2004;Ishikawa et al., 1999;Winkelman et al., 2005), it is likely

that the $K_V$ and $K_{Ca}$ currents found in small IB4-positive and medium neurons are not biophysically and/or pharmacologically identical between these two DRG neuron subtypes. This is supported by findings from Gold and colleagues (1996b) on the differential distribution of several distinct $K_V$ currents among DRG neuron subpopulations and may also be the case for the differential regulation of $I_K$ between medium (discussed below) and small IB4-positive neurons in response to long-term IL-1β exposure.

*5.2.2.3 Effect of long-term IL-1β exposure on potassium currents in medium neurons*

The major finding in this part of the investigation is that non-inactivating $I_K$, as well as, inactivating $Mn^{2+}$ -R and $Mn^{2+}$ -S $I_K$ densities in medium neurons were all significantly reduced in response to long-term IL-1β exposure. This finding is similar to the observed changes in $K_V$ and $K_{Ca}$ currents/channels in medium diameter sensory neurons observed after nerve injury (Abdulla and Smith, 2001b;Sarantopoulos et al., 2007;Boettger et al., 2002), as well as, studies that likely included medium sensory neurons or myelinated primary afferents (Kim et al., 2002;Everill and Kocsis, 1999;Ishikawa et al., 1999;Yang et al., 2004). In contrast to small IB4-positive neurons (Chapter 4), it is, therefore, possible that IL-1β has an extensive role in modulating potassium currents in medium diameter DRG neurons after nerve injury.

Reductions in $K_V$ currents are consistent with the finding that acute IL-1β application on acutely isolated, trigeminal ganglion neurons suppressed $K_V$ currents, including A-type current (Takeda et al., 2008). Further, Takeda and

colleagues (2008) reported that the suppression of $K_V$ currents was receptor dependent and, therefore, likely involves protein kinase C (PKC) and/or p38 mitogen-activated protein kinase (p38 MAPK) signalling pathways which have been previously implicated in the modulation of $I_{Na}$ (Binshtok et al., 2008;Liu et al., 2006). In support, site directed mutagenesis has revealed PKC phosphorylation sites in $K_V1.4$ and $K_V4.3$ channels that are required for the suppression of A-type currents by endothelin (Hagiwara et al., 2003).

Alternatively, suppression of $K_V$ currents in response to long-term IL-1β exposure could be secondary to the generation of $PGE_2$ (Maier et al., 1990) or neurotrophins (Purmessur et al., 2008). For instance, the production of $PGE_2$ was necessary for the inhibition of non-inactivating $I_K$ by tumor necrosis factor-α (TNF-α) in DRG neurons (Liu et al., 2008). The suppression of delayed-rectifier $I_K$ in DRG neurons through the activation of the p75 neurotrophin receptor ($p75^{NTR}$) with BDNF (Zhang et al., 2008) is another possibility, since the expression of p75 neurotrophin receptor ($p75^{NTR}$) is in most DRG neurons (Wright and Snider, 1995), including medium to large diameter neurons that co-express the TrkB receptor (Zhang et al., 2008;Mu et al., 1993). Taken together, it appears that there are multiple ways that non-inactivating $I_K$, as well as, inactivating $Mn^{2+}$ -R $I_K$ could be suppressed in medium neurons exposed to IL-1β and future studies could delineate the signalling pathway(s) or mediator(s) critical for these alterations.

The reduction in inactivating $Mn^{2+}$ -S $I_K$ density in medium neurons is, possibly, related to a suppression in VGCC current, since there appeared to be

substantial inactivation of $I_{Ba}$ in response to long-term IL-1β exposure (Figures 5-6D and 5-6E; discussed below). In support, the control inactivating $Mn^{2+}$ -S $I_K$ *I-V* density plot had rising- and declining- phases which are associated with the respective onset and offset of $Ca^{2+}$ entry through VGCCs, whereas, these phases were absent in medium neurons exposed to IL-1β (Figure 5-5B). This contrasts the change found for small IB4-positive neurons (Chapter 4), but may be in agreement with findings from Abdulla and Smith (2001b), where suppression of $K_{Ca}$ current, after axotomy nerve injury, was secondary to a decrease in $Ca^{2+}$ current. On the other hand, since $K_{Ca}$ currents are also sensitive to intracellular $Ca^{2+}$ ($[Ca^{2+}]_i$) handling (Scholz et al., 1998;Gold et al., 1996c), it is possible that suppression of $K_{Ca}$ currents in medium neurons is secondary to alterations in mechanisms that regulate $[Ca^{2+}]_i$ in DRG neurons (Lu et al., 2006). Consistent with this possibility, reductions in resting $[Ca^{2+}]_i$ and evoked $Ca^{2+}$ transients in subpopulations of injured DRG neurons, that likely included medium neurons in my study, were observed after nerve injury (Fuchs et al., 2005;Fuchs et al., 2007). As discussed in Chapter 4, it is interesting that chronic inflammation was reported to have the opposite effect in cutaneous DRG neurons (Lu and Gold, 2008). Future studies should determine if suppression of inactivating $Mn^{2+}$ -S $I_K$ density in medium neurons exposed to IL-1β is secondary to a reduction in $Ca^{2+}$, either by changes in $Ca^{2+}$ influx through VGCCs or $[Ca^{2+}]_i$ handling.

As described in Chapter 4, it is known that $K_{Ca}$ currents can be downregulated by prostaglandins and the adenosine 3',5' –cyclic monophosphate (cAMP) second messenger cascade (Gold et al., 1996c;Shipston et al.,

1999;Widmer et al., 2003), therefore, IL-1β could have suppressed inactivating $Mn^{2+}$ -S $I_K$ in medium neurons secondary to the production of $PGE_2$ (Maier et al., 1990). Since IL-1β signalling is known to involve p38 MAPK (Funakoshi et al., 2001;Roux et al., 2005;Tanabe et al., 2009;Binshtok et al., 2008), long-term IL-1β exposure may have directly reduced trafficking of $K_{Ca}$ subunits to the membrane, as has been described in chick ciliary ganglion neurons (Chae and Dryer, 2005). Last, it was recently determined that rat DRG contain all 4 regulatory β−subunits for $BK_{Ca}$ channels (Zhang et al., 2010), therefore, IL-1β could have influenced $K_{Ca}$ function through interactions with β-subunits in a similar manner proposed for sodium channels (discussed above; also see Chapter 4).

*5.2.2.4 Functional implications of $I_K$ suppression in medium neurons in response to long-term IL-1β exposure*

The suppression of all three $I_K$ components in medium neurons exposed to IL-1β likely included delayed rectifier, A-type and $K_{Ca}$ currents. Given the diverse roles of $K_V$ and $K_{Ca}$ currents in the regulation of AP shape and membrane excitability, their suppression is expected to underlie several of the changes observed in my current-clamp investigation (Chapter 3). Since many A-type currents are considered low threshold and fast activating, they are thought to function in the clamping of membrane potential near RMP, thereby, preventing the membrane potential from reaching AP threshold (Catacuzzeno et al., 2008;Vydyanathan et al., 2005). Consistent with this physiological function, a reduction in inactivating $Mn^{2+}$ -R $I_K$ density in response to long-term IL-1β

exposure likely corresponds to the reduction in medium neuron rheobase and, possibly, the increase in the maximal rate of depolarization observed under current-clamp evaluation, and, therefore, contributes to hyperexcitability (Chapter 3). This finding is in agreement with several investigations involving inhibition of A-type currents with blockers, such as 4-AP, or downregulation with $K_V$ channel α-subunit targeted small interfering RNA (siRNA) (Catacuzzeno et al., 2008;Yoshida and Matsumoto, 2005;Glazebrook et al., 2002;Chi and Nicol, 2007;Vydyanathan et al., 2005).

From studies involving the suppression of A-type currents, it is also known these currents are involved in regulating repetitive firing and, therefore, the suppression of inactivating $Mn^{2+}$ -R $I_K$ density is expected to contribute to increased firing frequencies and AP number in medium neurons exposed to IL-1β. Further, A-type currents can be subdivided into components that have distinct biophysical properties which likely extend to distinct roles in the regulation of membrane excitability (Catacuzzeno et al., 2008;Gold et al., 1996b;Stansfeld et al., 1986). For instance, dendrotoxin-sensitive A-type currents ($I_D$) are slowly inactivating and are thought to be involved in AP firing adaptation, whereas, 4-AP –sensitive (>0.1 mM; Chapter 1) A-type currents ($I_A$) are rapidly inactivating and are thought to be involved AP firing latency (Catacuzzeno et al., 2008;Stansfeld et al., 1986;Vydyanathan et al., 2005). These differences may explain why firing frequencies increased, while AP cumulative latencies were unaffected in medium exposed to IL-1β. Therefore, future studies, employing more extensive pharmacological and biophysical protocols, could examine the contribution of A-

type current components to medium neuron hyperexcitability. However, due to the diversity of $K_V$ channel subunits expressed in sensory neurons, an array of overlapping biophysical and pharmacological properties exist and, therefore, it would also be ideal to test properties, determined empirically, in computer models (Glazebrook et al., 2002;Catacuzzeno et al., 2008).

The decrease in AHP amplitude and duration in medium neurons in response to long-term IL-1β exposure (Chapter 3) is consistent with the suppression of fast afterhyperpolarization ($AHP_{fast}$). Since $BK_{Ca}$ channels are known to underlie $AHP_{fast}$ (Scholz et al., 1998), my current-clamp findings suggest suppression of inactivating $Mn^{2+}$ -S $I_K$ involved a reduction in $BK_{Ca}$ current density and similar alterations have been previously reported when $BK_{Ca}$ channels are blocked with iberiotoxin or charybdotoxin (Scholz et al., 1998;Li et al., 2007). As discussed in Chapter 4, AHP duration was only assessed for ~80 ms following AP generation and it is likely that changes in slower AHP components, if present, were not detected in my study. Further, inhibition of $AHP_{slow}$ with apamin (Gold et al., 1996c), suggests involvement of $SK_{Ca}$ channels and, therefore, $SK_{Ca}$ current could also represent a component of inactivating $Mn^{2+}$ -S $I_K$ which was suppressed in response to long-term IL-1β exposure.

In addition to the suppression of A-type currents, it is possible that suppression of inactivating $Mn^{2+}$ -S $I_K$ resulted in enhancement of repetitive discharge in medium neurons exposed to IL-1β. In support, experiments involving the use of iberiotoxin or apamin to, respectively, block either $BK_{Ca}$ or $SK_{Ca}$ channels, demonstrate inhibition of AHP which shortens the refractory period and

enhances repetitive discharge (Gold et al., 1996c;Scholz et al., 1998;Li et al., 2007). However, since the functional roles of $K_{Ca}$ channels in medium DRG neurons are less certain than in small sensory neurons (Gold et al., 1996c;Bahia et al., 2005;Zhang et al., 2010;Li et al., 2007), future studies should incorporate appropriate pharmacological protocols in order to confirm the presence and assess changes in specific $K_{Ca}$ currents in response to long-term IL-1β exposure.

Last, despite suppression of inactivating $Mn^{2+}$ -S $I_K$ and non-inactivating $I_K$ , it is surprising that medium neuron AP width was unaffected in response to long-term IL-1β exposure. This is inconsistent with findings where the blocking of $BK_{Ca}$ with iberiotoxin or the non-selective blocking of delayed rectifier currents with TEA, resulted in the broadening of APs in DRG neurons (Li et al., 2007;Scholz et al., 1998;Yoshida and Matsumoto, 2005;Villiere and McLachlan, 1996). Further, since delayed-rectifier $I_K$ is generally thought to be involved in AP repolarization (Gold et al., 1996b), the absence of a clear increase in AP width in medium neurons exposed to IL-1β, makes the functional contribution of non-inactivating $I_K$ suppression uncertain. This apparent paradox may be attributed to a concurrent decrease in $Ca^{2+}$ influx which may also influence AP width (Yoshida et al., 1978) in subsets of sensory neurons (discussed below).

### *5.2.3 Calcium currents ($I_{Ba}$) in medium DRG neurons*

#### *5.2.3.1 Characterization of $I_{Ba}$ in medium neurons in long-term cell culture*

As discussed in Chapter 4, the presence of low voltage-activated $I_{Ba}$ (LVA-$I_{Ba}$) can be determined with small depolarizing commands to -50 mV

which generate a shoulder on *I-V* plots at voltages between -60 mV and -30 mV (Abdulla and Smith, 2001b;Scroggs and Fox, 1992). The absence of prominent shoulders on *I-V* plots ($V_h$ = -100 mV), suggests that LVA calcium channels were not a substantial contributor to total calcium current in medium neurons in long-term cell culture. Further, since IL-1β exposure had no clear effect on $I_{Ba}$ density in response to weak depolarizations ($V_{cmd}$ = -50 mV), LVA calcium currents are not likely to contribute medium neuron hyperexcitability.

The majority of inward current recorded in control medium is expected to be high voltage-activated $I_{Ba}$ (HVA-$I_{Ba}$) which is in partial agreement with the literature. For instance, many studies have described a subpopulation of medium-sized DRG neurons with relatively larger LVA calcium current amplitudes than other subpopulations (Abdulla and Smith, 2001b;Pearce and Duchen, 1994;Lu et al., 2006;Scroggs and Fox, 1992;Hogan et al., 2000) and likely correspond to afterdepolarizing potential (ADP; Chapter 3) neurons in current-clamp configuration (White et al., 1989). Although the possibility remains that this sensory neurons subpopulation was simply missed, it is more likely that functional LVA calcium channels, if present after acute isolation, were not supported in defined medium cell cultures in the absence of exogenously applied neurotrophins. In support, Aguayo and colleagues (1991) also reported the absence of LVA calcium currents under similar cell culturing conditions and, therefore, might be evidence of a phenotypic shift in medium neurons in long-term cell culture. The loss of LVA calcium currents is consistent with the absence

of ADP neurons in my current-clamp investigation (Chapter 3) and may have precluded further effects of IL-1β on medium neuron excitability.

Last, although DRG neurons are known to express a full complement of voltage-gated calcium channel subtypes (Wu et al., 2004;Fox et al., 1987;Scroggs and Fox, 1992;Rusin and Moises, 1995), their pharmacological separation and biophysical characterization is beyond the scope of my study. Rather, a preliminary comparison on HVA-$I_{Ba}$ from control medium neurons in long-term cell culture is made with that from acutely isolated medium neurons. Consistent with the literature, HVA-$I_{Ba}$ activated at ~ -50 mV ($V_h$ = -100 mV) with peak current densities (~ 100 pA/pF) at ~ -10 mV (Abdulla and Smith, 2001b;Hogan et al., 2000). Furthermore, HVA-$I_{Ba}$ *I-V* plots ($V_h$ = -100 mV) in control medium neurons were comparable to *I-V* plots in small IB4-positive neurons in long-term cell cultures (Figures 5-6B and 4-7B, respectively), however, there may be differences in calcium current subtype composition underlying HVA calcium current between these two sensory neuron subpopulations (Abdulla and Smith, 2001b;Scroggs and Fox, 1992).

*5.2.3.2 Effect of long-term IL-1β exposure on HVA-$I_{Ba}$ in medium neurons*

The major finding in this part of the investigation is that there was significant suppression of peak HVA-$I_{Ba}$ density at a holding potential (-60 mV) reflective of RMP in medium neurons exposed to IL-1β. This finding appears to be consistent with the literature where HVA calcium currents are decreased after nerve injury (Abdulla and Smith, 2001b;Baccei and Kocsis, 2000;Hogan et al., 2000). Although the effect of IL-1β on HVA-$I_{Ba}$ is also in agreement with regard

to the involvement of increased inactivation (Abdulla and Smith, 2001b;Baccei and Kocsis, 2000), a major difference is the surprisingly significant increase in HVA-$I_{Ba}$ density when medium neurons are hyperpolarized to a holding potential of -100 mV to achieve near maximal channel availability. The most straightforward explanation for this paradox between increased HVA-$I_{Ba}$ density and inactivation involves an increase in the functional expression of HVA calcium channels that undergo inactivation at $V_h$ = -60 mV (N-type VGCCs) (Fox et al., 1987), thereby, increasing their proportion relative to L-type VGCCs which undergo minimal inactivation at the same holding potential. In support, BDNF which is potentially produced and released in response to IL-1β (Purmessur et al., 2008), has previously been reported to increase the expression of N and P/Q-type, but not L-type, VGCCs in the somata of hippocampal neurons in culture (Baldelli et al., 2000), as well as, increase the relative contribution of N and P/Q-type channels to presynaptic release in hippocampus (Baldelli et al., 2002). Given the known responsiveness of medium diameter DRG neurons to BDNF (Wright and Snider, 1995), perhaps a similar relatively selective upregulation of HVA calcium channel subtypes occurred in response to long-term IL-1β exposure. Future studies should examine this possibility through the inclusion of pharmacological protocols which would allow for the determination of relative contributions of HVA calcium channel subtypes to total HVA-$I_{Ba}$ (Abdulla and Smith, 2001b).

Last, since inactivation of VGCCs is not strictly voltage-dependent and can depend upon the amount of current, as well as, the accumulation of intracellular $Ca^{2+}$ at the vicinity of the channel (calcium-dependent inactivation)

(Jones and Marks, 1989;Chad and Eckert, 1984), it is possible that these additional factors may contribute to altered HVA calcium channel function in medium neurons exposed to IL-1β. For instance, given that chronic inflammation suppresses $[Ca^{2+}]i$ regulatory mechanisms in medium diameter DRG neurons (Lu and Gold, 2008), it is conceivable that IL-1β could have the same effect, thereby, resulting in increased accumulation of $[Ca^{2+}]i$ upon HVA calcium channel activation and a concurrent augmentation of calcium-dependent inactivation. Calcium-dependent inactivation, however, was not likely to play a significant role in my investigation of HVA-$I_{Ba}$, since this process is relatively selective for $Ca^{2+}$, inactivation of HVA-$I_{Ba}$ ($V_h$ = -100 mV vs. -60 mV) occurred with minimal channel activation and 10 mM EGTA was used in the internal solution to buffer $[Ca^{2+}]i$ (Fox et al., 1987). However, alterations in medium neuron $[Ca^{2+}]i$ handling in response to long-term IL-1β exposure could have impacted my current-clamp investigation and, therefore, future studies should explore this possibility.

*5.2.3.3 Functional implications for the suppression of HVA-$I_{Ba}$ in medium neurons in response to long-term IL-1β exposure*

Although upregulation of HVA-$I_{Ba}$ was apparent at more hyperpolarized voltages, suppression of HVA-$I_{Ba}$ at a holding potential of -60 mV suggests calcium entry through VGCCs was diminished at physiological voltages in medium neurons exposed to IL-1β. This, in turn, may have contributed to the suppression of $K_{Ca}$ currents and is evidenced by the reduction in the 'n'- shaped appearance of the *I-V* density plot for $Mn^{2+}$-S $I_K$ (Figure 5-5B). Since $I_K$ densities

were measured at $V_h$ = -80 mV, the suppression of $I_{Ca}$ density would not be as apparent, however, it would still be less in medium neurons exposed to IL-1β (for control: 88% of peak $I_{Ca}$ density = ~ -94.6 pA/pF vs. for IL-1β: 57% of peak $I_{Ca}$ density = ~ -87.8 pA/pF). Future studies, should determine if attenuation of $K_{Ca}$ current is truly secondary to suppression in $I_{Ca}$ and could be examined with biophysical protocols (Abdulla and Smith, 2001b) which measure $Mn^{2+}$ -S $I_K$ at holding potentials that counteract the difference in $I_{Ca}$ density between control and medium neurons exposed to IL-1β.

Last, since AP shape in DRG neurons is partly determined by calcium (Yoshida et al., 1978;Matsuda et al., 1978;Villiere and McLachlan, 1996), a reduction in $I_{Ca}$ would be expected to be involved in alterations (or lack thereof) to APs in medium neurons exposed to IL-1β. For instance, given the association of $Ca^{2+}$ in APs with humps on the descending phase and, therefore, AP width, a reduction in $I_{Ca}$ may have counter-balanced the propensity toward AP broadening as a result of an overall decrease in $I_K$. Furthermore, since $I_{Ca}$ has the most positive equilibrium potential, it is thought to contribute substantially to AP peak amplitude , yet its reduction, suggests that $I_{Ca}$ is unlikely to result in the increased AP height in medium neurons exposed to IL-1β. Since specific interpretations are likely complicated by interactions between $I_{Ca}$ and other conductances, future studies should include computer modelling to determine if the changes in $I_{Ca}$ fit with changes observed for other conductances.

### *5.2.4 $I_H$ in medium DRG neurons*

#### *5.2.4.1 Characterization of $I_H$ in medium neurons*

$I_H$ properties in control long-term cultured medium neurons were close to those reported for acutely isolated medium to large–sized DRG neurons. For instance, $I_H$ densities (~ -12 pA/pF at -110 mV) in my study were between values reported in large (~ -33 pA/pF) and small (~ -3 pA/pF) DRG neurons (Kouranova et al., 2008). In contrast medium neuron $I_H$ densities in long-term culture were larger than those in acutely isolated DRG neurons of similar size (Tu et al., 2004;Yao et al., 2003). Since comparable recording solutions were used, the discrepancy may simply be related to recovery of HCN channels after DRG neuron isolation in long-term cell cultures. The value for the voltage midpoint ($V_{1/2}$) for $I_H$ activation was -70.7 mV and was similar to the values (-73 to -74 mV) previously obtained for medium diameter neurons (Cardenas et al., 1999;Yao et al., 2003). However, my $V_{1/2}$ value is more positive than those reported in other sensory neuron studies and may relate to the absence of ATP in their recording pipettes (Kouranova et al., 2008) or the duration of protocols used to activate $I_H$ (Kouranova et al., 2008;Momin et al., 2008;Orio et al., 2009), both of which are known to influence $V_{1/2}$ (Yao et al., 2003;Ulens and Tytgat, 2001;Raes et al., 1997).

Consistent with several other findings the kinetics for $I_H$ activation in my study were voltage dependent and could be described by a double exponential (Yao et al., 2003;Tu et al., 2004;Kouranova et al., 2008). Further, $\tau_{fast}$ and $\tau_{slow}$ were intermediate to values found in acutely isolated medium and large DRG

neurons (Tu et al., 2004; Momin et al., 2008; Kouranova et al., 2008). Long-term cultured medium diameter neuron biophysical properties were also intermediate between values reported for HCN1 and HCN2 or possibly HCN3channels in recombinant systems (Ulens and Tytgat, 2001;Stieber et al., 2005) and are, therefore, consistent with the known expression of $I_H$ channel isoforms HCN1, HCN2 and HCN3, but not the kinetically slower HCN4 isoform in DRG neurons (Tu et al., 2004;Kouranova et al., 2008;Chaplan et al., 2003;Momin et al., 2008).

*5.2.4.2 Effect of long-term IL-1β exposure on $I_H$ in medium neurons*

The major finding in this part of the investigation is that the rates of $I_H$ activation became significantly faster after long-term exposure to IL-1β (Figures 5-8E and 5-8F). These differences primarily occurred over a physiologically relevant voltage range (-90 mV to -70 mV) and were concurrent with a tendency towards increased $I_H$ density, but not with a shift in voltage dependency of activation. The effects of nerve injury on $I_H$ are variable (Yao et al., 2003;Abdulla and Smith, 2001b;Chaplan et al., 2003), however, changes in $I_H$ properties described in my study are similar to the upregulation of $I_H$ after chronic compression of the DRG (CCD)(Yao et al., 2003). One notable and puzzling exception, is that $I_H$ densities were not clearly increased in the presence of IL-1β at more negative (-130 mV) command voltages. A possible explanation is that IL-1β exposure altered the relative proportion of HCN channel isoforms expressed on medium neuron membranes towards channels with faster opening kinetics (HCN1 homomers) rather than an increase in the total number of functional HCN channels. Similar changes have been reported for sodium currents and their

respective channel isoforms in injured DRG (Gold et al., 2003;Cummins and Waxman, 1997;Dib-Hajj et al., 1998b;Waxman et al., 1994).

Alternatively, $PGE_2$ dependent increases in adenosine 3',5' –cyclic monophosphate (cAMP) have been reported in sensory neuron cultures (Hingtgen et al., 1995) and may have modified $I_H$. cAMP can directly bind to a cyclic-nucleotide domain in the C-terminal of the HCN channel (DiFrancesco and Tortora, 1991) and has been reported to accelerate the opening of HCN2 channels (Wainger et al., 2001), as well as, enhancing $I_H$ through altering the voltage dependence of activation (Ingram and Williams, 1996). Although I did not observe a change in the voltage dependence of activation for $I_H$ in response to long-term IL-1β exposure, this may be attributed to an inability to achieve steady-state activation with shorter (<10 s) duration command voltages (Ulens and Tytgat, 2001) and, therefore, modulation of cAMP responsive HCN2 channels cannot be ruled out. Last, auxiliary subunits have been reported for the HCN channel family and change in their expression alters $I_H$ properties (Yu et al., 2001) and the responsiveness of HCN channels to cAMP (Zolles et al., 2009).

*5.2.4.3 Functional implications of $I_H$ upregulation in medium neurons*

The upregulation of $I_H$ after nerve injury or in the presence of inflammatory mediators is associated with sensory neuron hyperexcitability and the development of pain-related behaviours (Jiang et al., 2008;Yao et al., 2003;Chaplan et al., 2003;Momin et al., 2008;Cho et al., 2009). HCN channels have unique or 'funny' biophysical properties such that they are active at RMP and their tonic activation is the equivalent of a constant current injection which

opposes membrane hyperpolarization, leading to subthreshold membrane oscillations and repetitive firing (Momin et al., 2008;Pape, 1996;Brown et al., 1979;DiFrancesco, 2001). Therefore, the upregulation of $I_H$ in medium neurons exposed to long-term IL-1β may account some of the changes seen in current-clamp investigations. For instance, the changes in $I_H$ activation kinetics and densities occurred at physiologically relevant membrane hyperpolarizations, thus, changes in $I_H$ may have contributed to the significant decrease in AHP duration at 50% repolarization. Further, the relatively slow activation kinetics of $I_H$ would explain why changes were not observed earlier at 25% repolarization. Shortening of AHP duration may have, in turn, generated higher AP firing frequencies and the increased the number of APs generated in response to sustained current commands. These observations are consistent with the upregulation or downregulation of $I_H$ with $PGE_2$ or clonidine and the increase or decrease in the rate of repetitive discharge, respectively (Momin et al., 2008;Yagi and Sumino, 1998). However, Momin and colleagues (2008) reported that upregulation of $I_H$ with $PGE_2$ was not associated with a change in AP threshold or AP rates of depolarization or repolarization, suggesting that other ionic mechanisms, such as $I_{Na}$, have a role in the determination of these AP parameters in their study, as well, as in mine. Also, $I_H$ upregulation in response to long-term IL-1β exposure did not involve a depolarizing shift in the voltage dependence of $I_H$ activation and this may explain why RMP was unchanged. In support, Yao and colleagues (2003) also reported upregulation of $I_H$ after nerve injury in the absence of a shift in the

voltage dependence of activation and this was concurrent with no difference in mean RMP values.

Upregulation of $I_H$, however, is well known to be associated with primary afferent spontaneous activity (Jiang et al., 2008;Yao et al., 2003;Chaplan et al., 2003). Since long-term IL-1β exposure was not concurrent with the development of spontaneous activity, this suggests upregulation of $I_H$ in my study did not have a profound impact on medium neuron electrical activity. However, the absence of T-type current and their contribution to subthreshold membrane oscillations and low threshold AP firing (White et al., 1989;Todorovic and Jevtovic-Todorovic, 2006) may have limited the ability of $I_H$ to generate spontaneous activity. Regulation of $I_H$ is also associated with changes to voltage sag (Abdulla and Smith, 2001b;Abdulla and Smith, 2001a;Scroggs et al., 1994;Mayer and Westbrook, 1983), and, therefore, the absence of an alteration to the magnitude of voltage sag in my current clamp studies represents another contradiction to the upregulation of $I_H$. However, the major change in the presence of IL-1β was the increased rate of $I_H$ activation along with subtle changes to current density. This might simply be interpreted as changes to $I_H$ density were insufficient to influence the overall magnitude in changes to membrane potentials in larger DRG neurons with relatively low input resistances. In contrast, the $I_H$ rates of activation were nearly doubled at maximal physiological membrane hyperpolarizations (~ -90mV; Figure 5-8E) in the presence of IL-1β and was paralleled to a ~50% decrease in the membrane time constant (Table 3-2), thereby, suggesting that $I_H$ upregulation

did impact medium neuron electrical behaviour upon membrane hyperpolarization.

### *5.2.5 Conclusion on the effects of IL-1β exposure on ionic currents in medium DRG neurons*

The effects of short-term (minutes to hours) IL-1β application on sodium, calcium and potassium conductances have been previously described in various *in vitro* preparations, including small, nociceptive sensory neurons of the DRG and trigeminal ganglia. My study expands on these findings by examining the effects of long-term IL-1β exposure on sensory neuron excitability and its relation to changes in sensory neurons observed after nerve injury. In Chapter 3, I not only confirmed that IL-1β enhances DRG neuron excitability after short-term applications, but further demonstrated hyperexcitability in medium and small IB4-positive sensory neuron subpopulations after 5 to 6 days exposure. I interpret these findings to be the *in vitro* equivalent to the enduring increase in primary afferent excitability reported after nerve injury and, therefore, would expand the recognized role of IL-1β in acute inflammatory pain to neuropathic pain. To further establish this possibility, I hypothesized that long-term IL-1β exposure would alter ionic currents in a manner consistent with sensory neuron hyperexcitability.

In this chapter, the major findings in medium DRG neurons exposed to IL-1β (Table 5-2) and were as follows: 1) hyperpolarizing shifts in TTX-S $I_{Na}$ activation; 2) suppression of $K_{Ca}$, A-type and delayed-rectifier potassium current

densities; 3) suppression of HVA-$I_{Ba}$, and hence HVA-$I_{Ca}$, current densities; 4) increased HVA-$I_{Ba}$ inactivation; and 5) an increase in the rates of activation for $I_H$. These changes are in good agreement with the broad spectrum of alterations observed after nerve injury (Sarantopoulos et al., 2007;Abdulla and Smith, 2001b;Yao et al., 2003;Everill and Kocsis, 1999;Hogan et al., 2000;Baccei and Kocsis, 2000;Yang et al., 2004) and, therefore, suggests that IL-1β plays a substantial role in the generation of hyperexcitability in injured medium diameter sensory neurons.

Consistent with my current-clamp findings (Table 3-5), the effects of IL-1β on ionic currents reported here are more extensive than in small IB4-positive neurons. There are at least a couple possibilities for differences:

1. Phenotypic shift, as a consequence of serum and exogenous neurotrophin – free cell culturing conditions, likely precluded potential effects of IL-1β on additional ionic conductances intrinsically important to small IB4-positive neuron electrogenesis. This included the loss of TTX-R $I_{Na}$ and the minimal support of A-type potassium currents which are both known to be enriched in acutely isolated small IB4-positive sensory neurons (Fang et al., 2006;Vydyanathan et al., 2005;Fjell et al., 1999) and modulated by short-term IL-1β applications (Takeda et al., 2008;Binshtok et al., 2008).

2. Alternatively, the effects of IL-1β may have been secondary to the production of other mediators which may, in turn, selectivity affect medium neurons. For instance, medium diameter neurons predominantly express TrkB receptors (Mu et al., 1993;Wright and Snider, 1995), while small IB4-positive neurons express

GDNF receptor components (Molliver et al., 1997;Airaksinen and Saarma, 2002;Bennett et al., 1998), therefore, the possible production and release of BDNF (Purmessur et al., 2008) in response to IL-1β would be expected to exert greater effects in medium neurons.

Although the changes reported here are substantial when compared to small IB4-positive neurons, limitations in my experimental approach may have under estimated the importance of IL-1β to the generation of medium diameter neuron hyperexcitability after nerve injury. For instance, phenotypic shift may have occurred in medium neurons in long-term cell culture and is evidenced by the absence of LVA-$I_{Ba}$. Since LVA or T-type currents have unique biophysical properties that lower AP thresholds and facilitate repetitive firing (Zamponi et al., 2009;Todorovic and Jevtovic-Todorovic, 2006), their potential upregulation in response to IL-1β exposure would be expected to further enhance medium sensory neuron excitability. Another limitation in my study is that the biophysical and pharmacological protocols used were not sufficient to monitor all changes produced by IL-1β. For example, I did not assess rapid repriming of TTX-S $I_{Na}$ or the relative contributions of VGCC subtypes to total HVA-$I_{Ba}$ current.

Despite limitations, the changes described here for medium neurons relate well to increased excitability (Table 3-5) and to pain mechanisms. For instance, the hyperpolarizing shift in of TTX-S $I_{Na}$ voltage dependence of activation, as well as, the suppression of A-type current densities would be expected to decrease rheobase. Reductions in $K_{Ca}$ current densities and increased rates of $I_H$ activation would be expected to lead to decreased AHP amplitude and duration which,

coupled to the suppression of A-type currents, would enhance repetitive discharge. Although the physiological relevance of these alterations in the cell bodies of medium neurons is uncertain, it is possible that IL-1β produces similar changes at peripheral nerve terminals, leading to a decrease in AP firing threshold and, therefore, produce hypersensitivity. It is also important to consider that medium diameter sensory correspond to Aδ–fibres (Harper and Lawson, 1985;Villiere and McLachlan, 1996) which are known to transmit either nociceptive or non-nociceptive information to the dorsal horn of the spinal cord (Rose et al., 1986;Koerber et al., 1988). Therefore, increased excitability in response to IL-1β release after nerve injury might explain hyperalgesia, as well as, allodynia. Finally, it would be necessary to model the observed changes and examine their applicability to the generation of medium sensory neuron hyperexcitability in response to long-term IL-1β exposure.

***Figure 5-1: $I_{Na}$ in long-term cell culture and the effect of IL-1β on TTX-sensitive $I_{Na}$ activation in medium DRG neurons***

A: All medium neuron $I_{Na}$ in long-term cell culture was TTX-S $I_{Na}$. Total $I_{Na}$ (black traces) was recorded from DRG neurons using a series of 40 ms depolarizing voltage commands from $V_h$ = -90 mV (Ai). Neurons were then treated with 300 nM TTX (grey traces) to isolate TTX-S $I_{Na}$ from TTX-R $I_{Na}$ (Aii) and digital subtraction (Ai-ii) revealed that all measurable current was TTX-S $I_{Na}$.

B: Effect of IL-1β exposure on TTX-S $I_{Na}$ density. The *I-V* plot for IL-1β treated medium neurons is visibly smaller in TTX-S $I_{Na}$ density at voltage commands between -10 mV and +20 mV ($0.05<p\leq0.1$). However, peak TTX-S $I_{Na}$ occurred at $V_{cmd}$ = -20 mV for control neurons (-261 ± 48 pA/pF; n=9), whereas, peak current density occurred at -30 mV for neurons exposed to IL-1β (-176 ± 44 pA/pF; n=11).

C: Effect of IL-1β exposure on TTX-S $I_{Na}$ on voltage dependence of activation. Normalized *I-V* curves were fit with a single Boltzmann function (Chapter 2). IL-1β produced a significant hyperpolarizing shift on values for $V_{1/2}$ (-32.5 ± 2.6 mV, n=9 vs. -41.4 ± 2.2 mV, n=11; $p<0.05$). Slope factor was unaffected (3.6 ± 1.1 mV, n=9 vs. 3.3 ± 0.5, n=11; $p>0.05$).

D: Series of representative traces illustrating that IL-1β exposure (red traces) resulted in the activation of TTX-S $I_{Na}$ at more hyperpolarized potentials than control neurons (black traces). Error bars indicate means ± SE. Significant difference vs. control * = $p<0.05$, † = $p<0.01$ and § = $p<0.001$ with unpaired t-test. Traces in A were not subtracted for leak current.

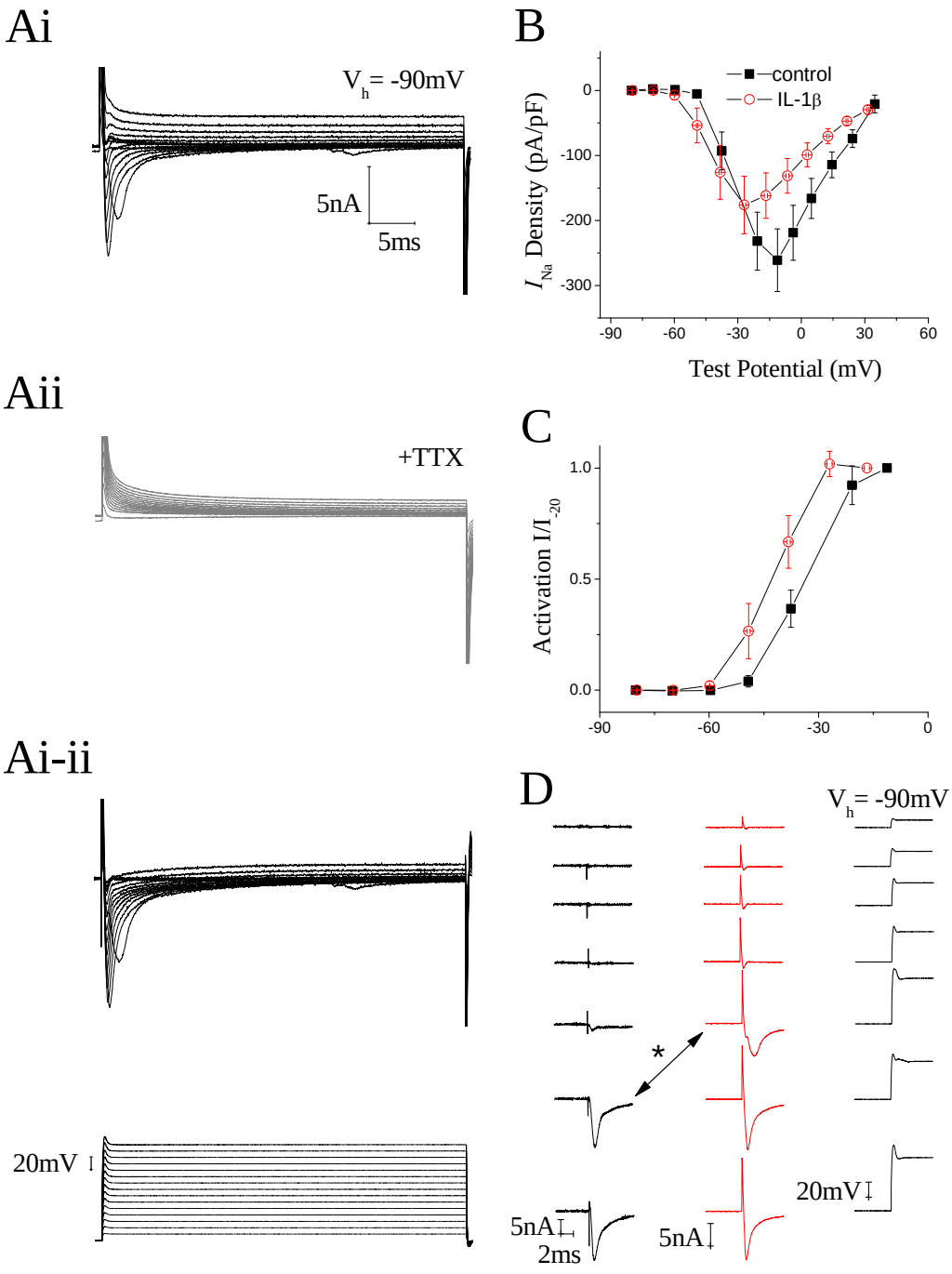
Ai
$V_h$ = -90mV
5nA
5ms
Aii
+TTX
Ai-ii
20mV
B
control
IL-1β
$I_{Na}$ Density (pA/pF)
0
-100
-200
-300
-90
-60
-30
0
30
60
Test Potential (mV)
C
Activation $I/I_{-20}$
1.0
0.5
0.0
-90
-60
-30
0
D
$V_h$ = -90mV
*
5nA
2ms
5nA
20mV

***Figure 5-2: Effect of IL-1β on TTX-sensitive $I_{Na}$ steady-state inactivation and kinetics of inactivation in medium DRG neurons***

A: TTX-S $I_{Na}$ steady-state fast inactivation protocol. From a $V_h$ = -90 mV, 300 ms incremental depolarizing prepulses preceded 10 ms test pulses to -10 mV to determine the fraction of current available.

B: Effect of IL-1β exposure on TTX-S $I_{Na}$ steady-state fast inactivation. Normalized steady-state fast inactivation curves were fit with a single Boltzmann function (Chapter 2). IL-1β had no significant effect on values for $V_{1/2}$ (-61.3 ± 1.9 mV, n=7 vs. -62.0 ± 0.9, n=11; *p>0.05*) or slope factor (7.7 ± 0.8 mV, n=7 vs. 8.8 ± 0.9, n=11; *p>0.05*).

C: TTX-S $I_{Na}$ steady-state slow inactivation protocol. From $V_h$ = -90 mV, 5 s prepulses, followed by 20 ms recovery pulses to -120 mV (to allow recovery from fast inactivation), preceded 10 ms test pulses to -10 mV to determine the fraction of current available.

D: Effect of IL-1β exposure on TTX-S $I_{Na}$ steady-state slow inactivation. Normalized steady-state slow inactivation curves were fit with a single Boltzmann function (Chapter 2). IL-1β had no significant effect on values for $V_{1/2}$ (-62.4 ± 6.1 mV, n=5 vs. -57.8 ± 2.5, n=5; *p>0.05*) or slope factor (13.5 ± 1.9 mV, n=5 vs. 13.6 ± 1.1, n=5; *p>0.05*).

E: Effect of IL-1β exposure on TTX-S $I_{Na}$ kinetics of inactivation. From $V_h$ = -90 mV, single exponent fits of TTX-S $I_{Na}$ decay revealed no differences in the kinetics for fast inactivation in response to IL-1β treatment (for $V_{cmd}$ = -40 mV: 1.53 ± 0.59 ms, n=5 vs. 1.82 ± 0.61, n=11; *p>0.05*)

Error bars indicate means ± SE. Significant difference vs. control * = $p<0.05$, † = $p<0.01$and § = $p<0.001$ with unpaired t-test. Traces in A and C were not subtracted for leak current.

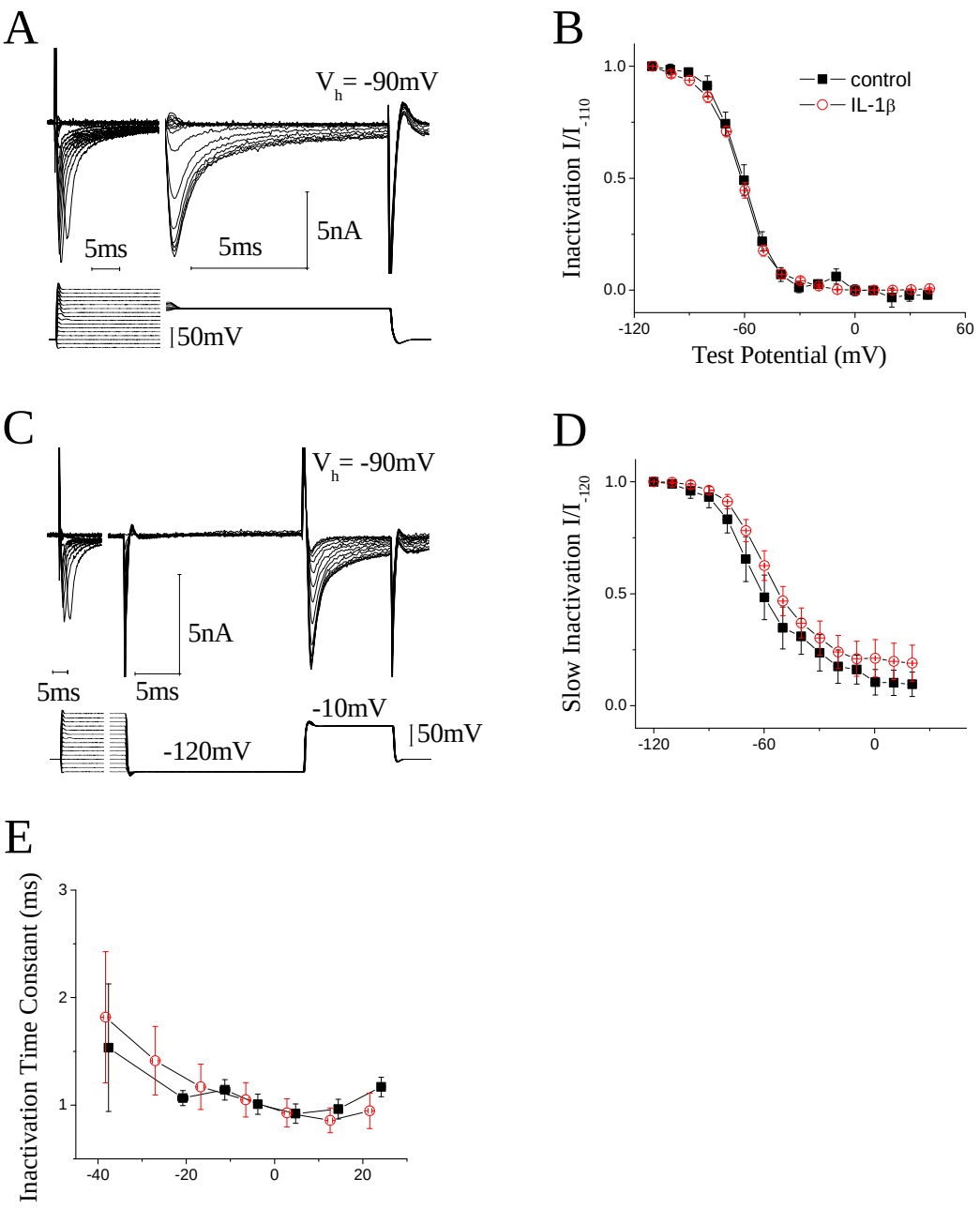
A
$V_h$ = -90mV
5ms
5ms
5nA
|50mV
B
control
IL-1β
Inactivation $I/I_{-110}$
1.0
0.5
0.0
-120
-60
0
60
Test Potential (mV)
C
$V_h$ = -90mV
5nA
5ms
5ms
-10mV
-120mV
|50mV
D
Slow Inactivation $I/I_{-120}$
1.0
0.5
0.0
-120
-60
0
E
Inactivation Time Constant (ms)
3
2
1
-40
-20
0
20

***Figure 5-3: $I_K$ voltage protocols and the effect of IL-1β on non-inactivating $I_K$ density in medium DRG neurons***

A: $I_K$ voltage protocols. A family of outward currents recorded at voltages between -60 mV and +60 mV ($V_h$ = -80 mV) after a 500 ms conditioning prepulse to $V_p$ = -120 mV (Ai) or -30 mV (Aii) in the standard NMG-Cl perfusion solution. Digital subtraction (Ai – Aii) revealed the presence of inactivating current components (A-type and/or $K_{Ca}$ currents).

B: Isolation of non-inactivating $I_K$. In the presence of 5 mM $Mn^{2+}$, a steady-state non-inactivating component could be measured at the end of the stimulation pulse when preceded by $V_p$ = -30 mV and is referred to as non-inactivating $I_K$.

C: Effect of IL-1β exposure on non-inactivating $I_K$ density. *I-V* plots revealed that non-inactivating $I_K$ densities are substantially smaller following exposure to long-term IL-1β with significant reductions at command voltages -20 mV to +60 mV (for example, $V_{cmd}$ = +60 mV: +169 ± 25 pA/pF, n=9 vs. +62 ± 10, n=16; *p<0.001*).

D: Representative traces illustrating suppressed peak non-inactivating $I_K$ ($V_{cmd}$ = + 60 mV) in medium neurons exposed to IL-1β (red trace) versus control (black trace).

Error bars indicate means ± SE. Significant difference vs. control * = *p<0.05*, † = *p<0.01* and § = *p<0.001* with unpaired t-test. Traces in A, B and D were not subtracted for leak current.

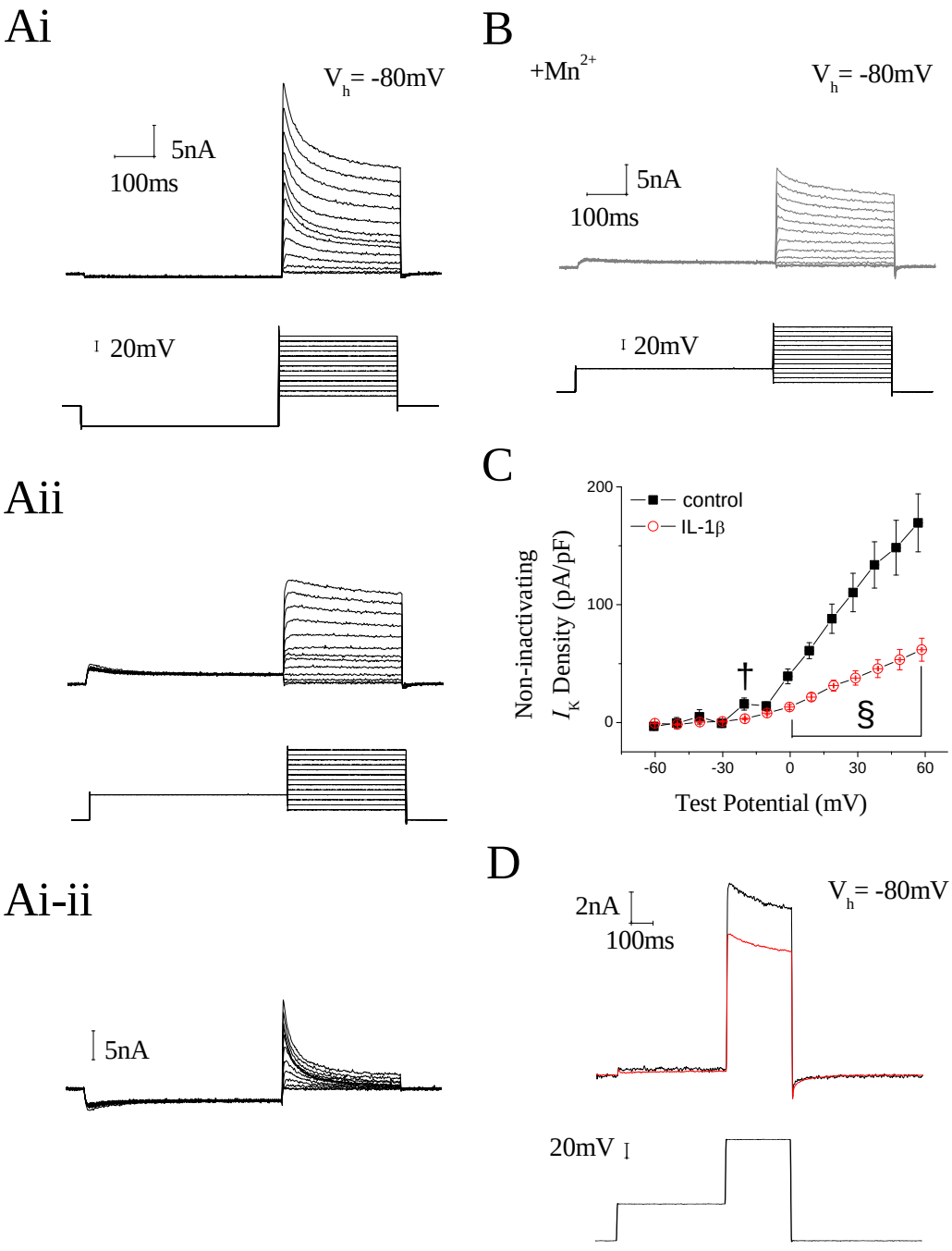
Ai
$V_h$= -80mV
5nA
100ms
20mV
B
+$Mn^{2+}$
$V_h$= -80mV
5nA
100ms
20mV
Aii
C
control
IL-1β
Non-inactivating
$I_K$ Density (pA/pF)
200
100
0
-60
-30
0
30
60
†
§
Test Potential (mV)
Ai-ii
5nA
D
2nA
100ms
$V_h$= -80mV
20mV

***Figure 5-4: Effect of IL-1β on inactivating $Mn^{2+}$ -resistant $I_K$ density in medium DRG neurons***

A: Isolation of inactivating $Mn^{2+}$-R $I_K$. From $V_h$ = -80 mV and in the presence of 5 mM $Mn^{2+}$ (grey traces), digital subtraction of $I_K$ (Ai-Aii) after 500 ms conditioning prepulses to $V_p$ = -120 mV (Ai) and $V_p$ = -30 mV (Aii) revealed the presence of A-type currents which are collectively referred to as inactivating $Mn^{2+}$ -R $I_K$ in this study.

B: Effect of IL-1β on inactivating $Mn^{2+}$-R $I_K$. As indicated in *I-V* plots, IL-1β significantly suppressed peak ($V_{cmd}$ = +60 mV) inactivating $Mn^{2+}$-R $I_K$ density (control: +31 ± 9 pA/pF, n=10 vs. IL-1β: +13 ± 4, n=16; *p<0.05*).

C: Representative traces illustrating suppressed peak inactivating $Mn^{2+}$-R $I_K$ ($V_{cmd}$ = + 60 mV) in medium neurons exposed to IL-1β (red trace) versus control (black trace).

D: Representative traces confirming the block of medium neuron calcium current ($Ba^{2+}$ used as a charge carrier ($I_{Ba}$); black trace) in the presence of 5 mM $Mn^{2+}$ (grey trace). $I_{Ba}$ was evoked using $V_{cmd}$ = -20 mV from $V_h$ = -100 mV.

Error bars indicate means ± SE. Significant difference vs. control * = *p<0.05*, † = *p<0.01*and § = *p<0.001* with unpaired t-test. Traces in A, C and D were not subtracted for leak current.

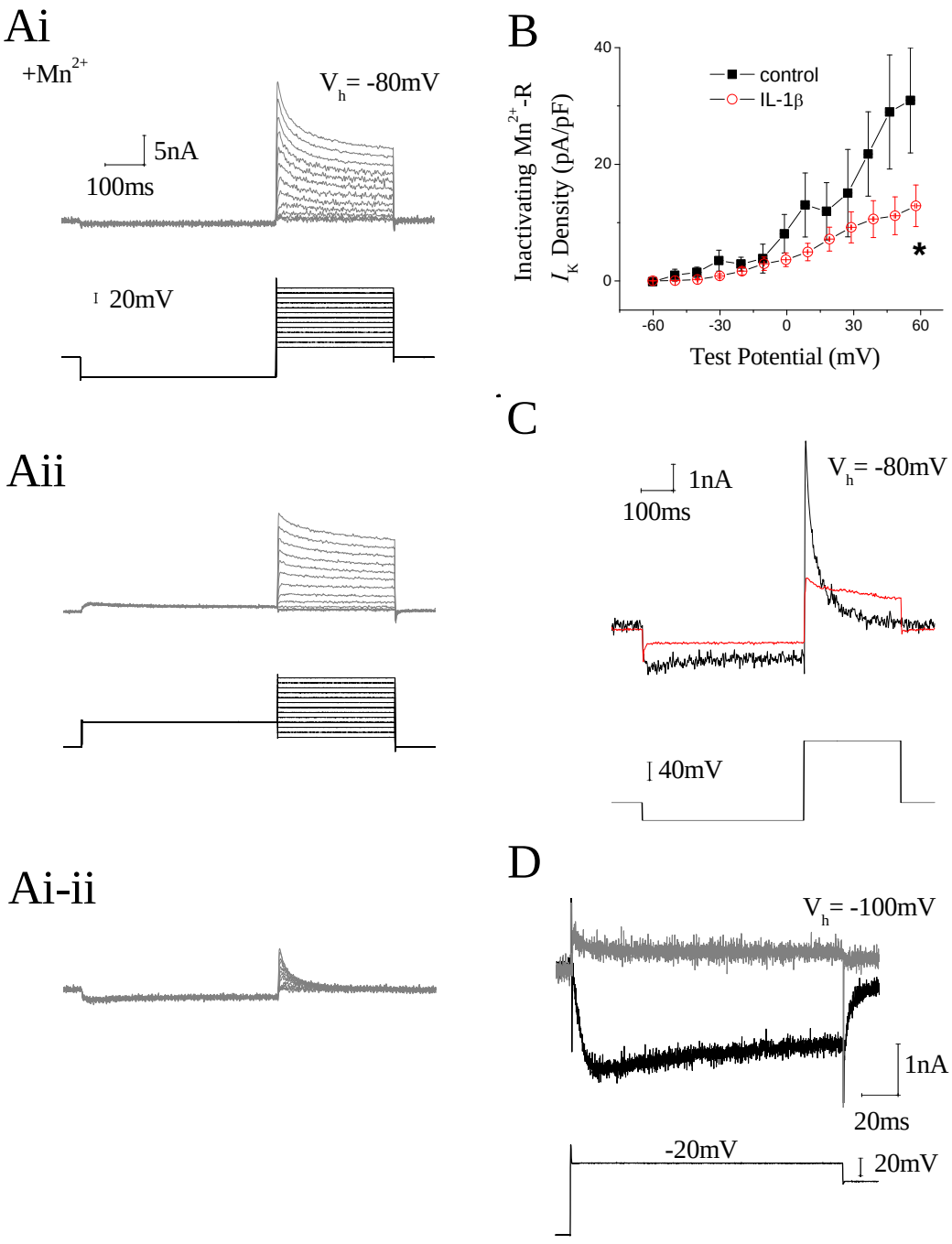
Ai
+Mn2+
Vh= -80mV
5nA
100ms
20mV
Aii
Ai-ii
B
Inactivating Mn2+-R
IK Density (pA/pF)
control
IL-1β
40
20
0
-60
-30
0
30
60
Test Potential (mV)
*
C
1nA
100ms
Vh= -80mV
40mV
D
Vh= -100mV
1nA
20ms
-20mV
20mV

***Figure 5-5: Effect of IL-1β on inactivating $Mn^{2+}$ -sensitive $I_K$ density in medium DRG neurons***

A: Isolation of inactivating $Mn^{2+}$ -S $I_K$. From $V_h$ = -80 mV and after a 500 ms conditioning prepulse to $V_p$ = -120 mV, digital subtraction of outward current (Ai-Aii) remaining in the presence of 5mM $Mn^{2+}$ (Ai; grey traces) from total outward current (Aii; black traces) yielded inactivating $Mn^{2+}$ -S $I_K$. Also, notice the rising- and declining- phases in the control *I-V* plot (B) between $V_{cmd}$ = -30 and +10 mV which are associated with the respective onset and offset of $Ca^{2+}$ entry through activated VGCCs.

B: Effect of IL-1β on inactivating $Mn^{2+}$ -S $I_K$. As depicted in the *I-V* plots, IL-1β exposure significantly suppressed inactivating $Mn^{2+}$ -S $I_K$ current densities (peak inactivating $Mn^{2+}$ -S $I_K$ density ($V_{cmd}$ = +60 mV): from +98 ± 16 pA/pF, n=12 to +51 ± 10, n=16; *p<0.05*). Also, IL-1β exposure reduced the appearance of the rising- and declining- phases in the *I-V* plot and, therefore, suggests that IL-1β exposure additionally suppressed $Ca^{2+}$ current in medium neurons.

C: Representative traces illustrating suppressed peak inactivating $Mn^{2+}$ -S $I_K$ ($V_{cmd}$ = + 60 mV) in medium neurons exposed to IL-1β (red trace) versus control (black trace).

Error bars indicate means ± SE. Significant difference vs. control * = *p<0.05*, † = *p<0.01*and § = *p<0.001* with unpaired t-test. Traces in A and C were not subtracted for leak current.

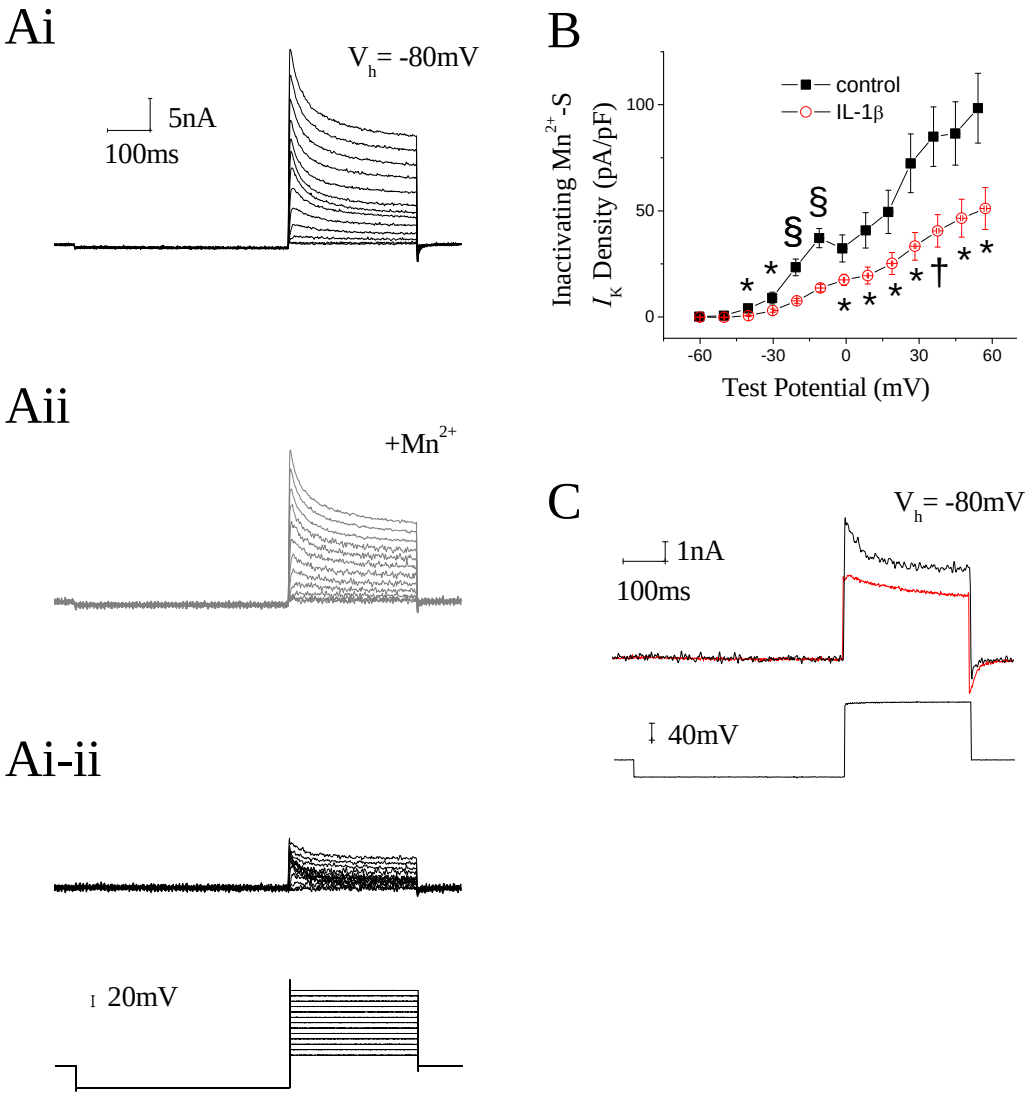
Ai
V_h = -80mV
5nA
100ms
Aii
+Mn2+
Ai-ii
20mV
B
control
IL-1β
Inactivating Mn2+-S
I_K Density (pA/pF)
Test Potential (mV)
100
50
0
-60
-30
0
30
60
§
§
*
*
*
*
*
*
*
*
†
C
V_h = -80mV
1nA
100ms
40mV

***Figure 5-6: Effect of IL-1β on $I_{Ba}$ density and sensitivity to shifts in holding potential in small IB4-positive DRG neurons***

A: $I_{Ba}$ protocol ($V_h$ = -100 mV). $Ba^{2+}$ was substituted for $Ca^{2+}$ as the charge carrier (Chapter 2) and currents ($I_{Ba}$) were evoked in medium neurons using a series of 150 ms depolarizing voltage commands from $V_h$ = -100 mV.

B: Effect of IL-1β on $I_{Ba}$ density ($V_h$ = -100 mV). *I-V* plots revealed that long-term IL-1β treatment significantly increased $I_{Ba}$ densities at command voltages between -40 mV and -10 mV ($p<0.01$for both data points). Further, IL-1b exposure tended to increase HVA-$I_{Ba}$ density ($V_{cmd}$ = -10 mV; -107 ± 22 pA/pF, n=9 vs. -154 ± 12, n=14; $0.05<p\leq0.1$).

C: $I_{Ba}$ protocol ($V_h$ = -60 mV). Same protocol described in A except $V_h$ = -60 mV.

D: Effect of IL-1β on $I_{Ba}$ density ($V_h$ = -60 mV). Opposite to the effect at $V_h$ = -100 mV and suggestive of differences in inactivation, the HVA-$I_{Ba}$ density remaining at $V_h$ = -60 mV, was significantly smaller in neurons exposed to IL-1β ($V_{cmd}$ = -10 mV; -58 ± 6 pA/pF, n=10 vs. -38 ± 4, n=11; $p<0.01$).

E: Effect of IL-1β on sensitivity to a shift in holding potential. IL-1β exposure significantly enhanced (sensitivity) the percent decrease in peak HVA-$I_{Ba}$ density (20.3 ± 15.5%, n=8 vs. 73.7 ± 3.6%; n=10; $p<0.01$).

Error bars indicate means ± SE. Significant difference vs. control * = $p<0.05$, † = $p<0.01$and § = $p<0.001$ with unpaired t-test. Traces in A, C and E were not subtracted for leak current.

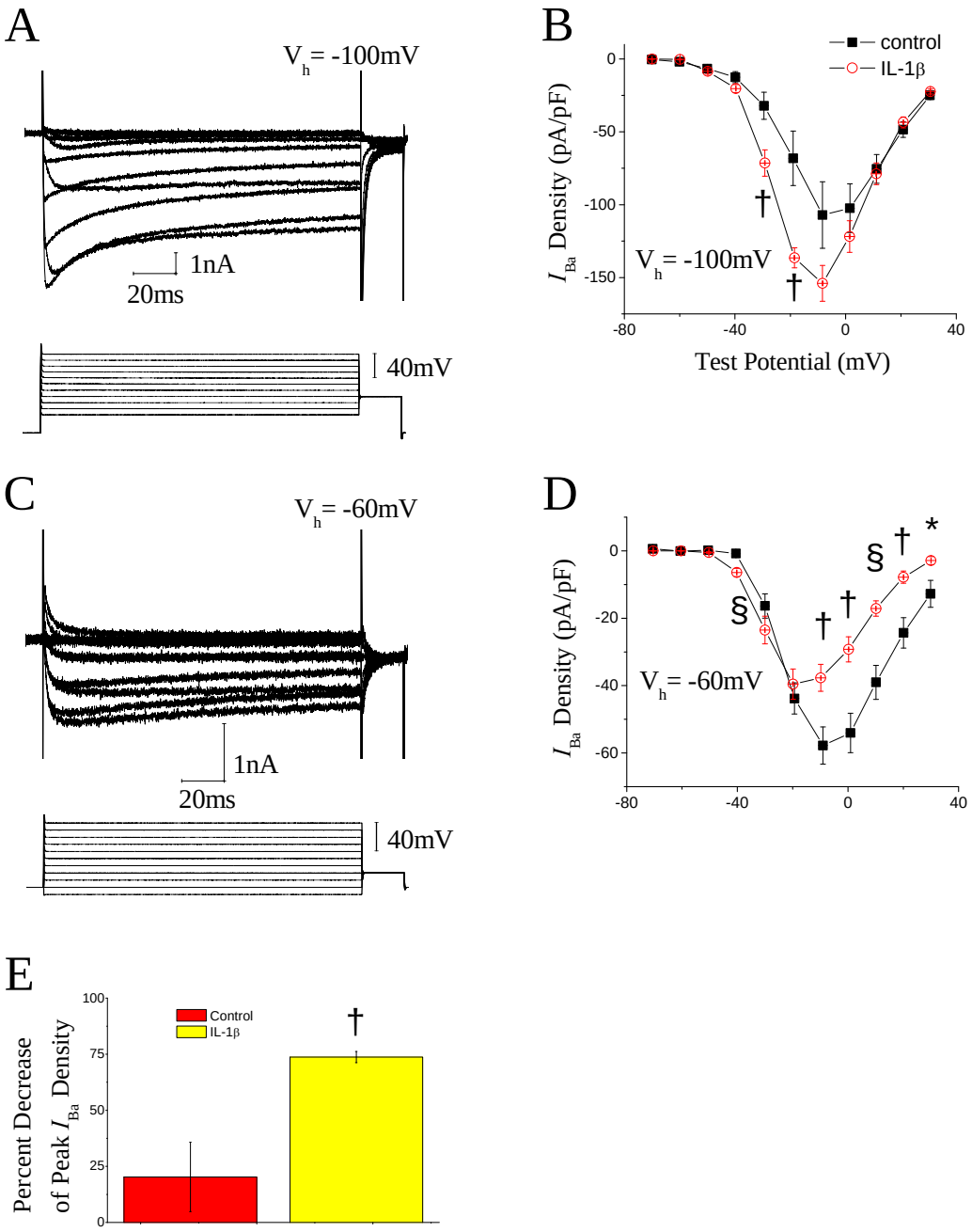
A
$V_h$ = -100mV
1nA
20ms
40mV
B
control
IL-1β
$I_{Ba}$ Density (pA/pF)
$V_h$ = -100mV
Test Potential (mV)
C
$V_h$ = -60mV
1nA
20ms
40mV
D
$I_{Ba}$ Density (pA/pF)
$V_h$ = -60mV
E
Percent Decrease of Peak $I_{Ba}$ Density
Control
IL-1β

***Figure 5-7: Effect of IL-1β on $I_{Ba}$ voltage dependence of inactivation in medium DRG neurons***

A: Voltage dependency of HVA-$I_{Ba}$ inactivation protocol. To more directly examine the possibility that long-term IL-1β affects the voltage dependency of HVA-$I_{Ba}$ inactivation, the fraction of current available at $V_{cmd}$ = -10 mV was determined in response to a series of 3.5 s incremental prepulses.

B: Effect of IL-1β exposure on voltage dependency of HVA-$I_{Ba}$ inactivation. Consistent with enhanced sensitivity to holding potential and increased inactivation, single Boltzmann function fitting of curves for the voltage dependence of inactivation revealed that the values for voltage midpoints ($V_{1/2}$) had a tendency toward a leftward shift (hyperpolarizing shift in HVA-$I_{Ba}$ inactivation) after long-term IL-1β exposure (-59.0 ± 5.0 mV, n=6 vs. -78.8 ± 5.9, n=13; $0.05<p\leq0.1$; Table 5-1). Single Boltzmann function fitting of inactivation curves also indicated that medium neurons exposed to IL-1β had a significantly increased slope factor (10.7 ± 1.1 mV, n=6 vs. 17.8 ± 1.4, n=13; $p<0.01$; also see Table 5-1) which is further suggestive of an enhanced sensitivity to voltage.

Error bars indicate means ± SE. Significant difference vs. control * = $p<0.05$, † = $p<0.01$and § = $p<0.001$ with unpaired t-test. Traces in A were not subtracted for leak current.

A

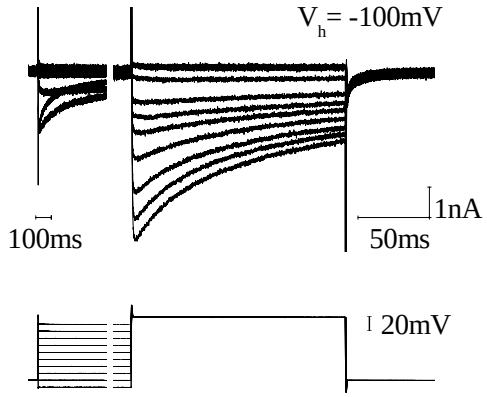
V_h = -100mV
100ms
1nA
50ms
20mV

B

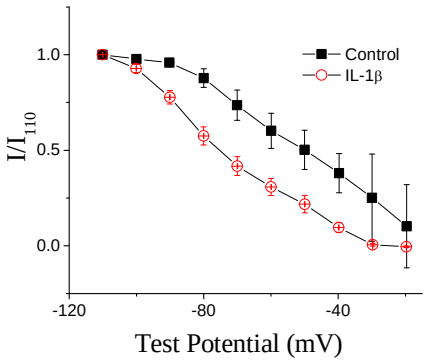
Control
IL-1β
I/I110
1.0
0.5
0.0
-120
-80
-40
Test Potential (mV)

***Figure 5-8: Effect of IL-1β on $I_H$ in medium DRG neurons***

A: Representative traces (current-clamp configuration) illustrating time-dependent changes or voltage sag (Chapter 3) in medium neuron membrane response to hyperpolarizing current (black trace). The $I_H$ blocker ZD7288 (100 μM) blocked voltage sag (grey trace).

B: Isolation of $I_H$. As described in Methods (Chapter 2), $V_h$ = -50 mV and $I_H$ (Bi) was elicited by a series of hyperpolarizing voltage commands (from -60 mV to -130 mV) that were also incremental in duration (from 4.25 s to 2.5 s). This voltage protocol was designed to maximize capture of steady-state $I_H$ activation, yet provide stable cellular voltage-clamp recordings. The presence of $I_H$ could be confirmed with block by ZD7288 (100 μM; Bii).

C: Effect of IL-1β on $I_H$ density. The inward current consisted of an initial instantaneous current ($I_{INST}$), followed by slower inward relaxation ($I_H$) that became larger and that developed more rapidly at more negative voltages (inset). *I-V* plots revealed that IL-1β exposure had a tendency to increase $I_H$ densities at voltage commands between -60 mV and -90 mV ($0.05<p\leq0.1$) and not at more hyperpolarized commands.

D: Representative traces illustrating that neurons exposed to IL-1β (red trace) appeared to have larger $I_H$ currents ($V_{cmd}$ = -80 mV) than control (black trace).

E and F: Effect of IL-1β on $I_H$ kinetics of activation. The time course for the activation of $I_H$ was fit with the sum of two exponential functions (Chapter 2). Fast ($\tau_{fast}$; E) and slow ($\tau_{slow}$; F) time constants for $I_H$ activation became significantly faster in neurons exposed to IL-1β over a command voltage range

that overlapped with the greatest differences in $I_H$ densities ($V_{cmd}$ = -70 mV $\tau_{fast}$; control: 570.5 ± 92.0 ms, n=5 vs. IL-1β: 294.0 ± 45.1, n=11; *p<0.01*and $\tau_{slow}$; control: 4592.3 ± 1114.4 ms, n=5 vs. IL-1β: 1800.4 ± 421.9, n=11; *p<0.05*).

G: Effect of IL-1β on the voltage dependency of steady-state activation. The conductance ratio, $G/G_{-130}$, was calculated from tail current ($I_{H,Tail}$) amplitudes measured 100 – 200 ms after repolarization (inset). The *G-V* plots, however, are nearly superimposed and single Boltzmann function fitting of the steady-state $I_H$ activation curves revealed that IL-1β had no significant effect on the values for voltage midpoints ($V_{1/2}$) of activation (control: -70.7 ± 2.7 mV, n=9 vs. IL-1β: -65.9 ± 5.1 mV, n=10; *p>0.05*; also see Table 5-1).

Error bars indicate means ± SE. Significant difference vs. control * = *p<0.05*, † = *p<0.01*and § = *p<0.001* with unpaired t-test. Traces in A were not subtracted for leak current.

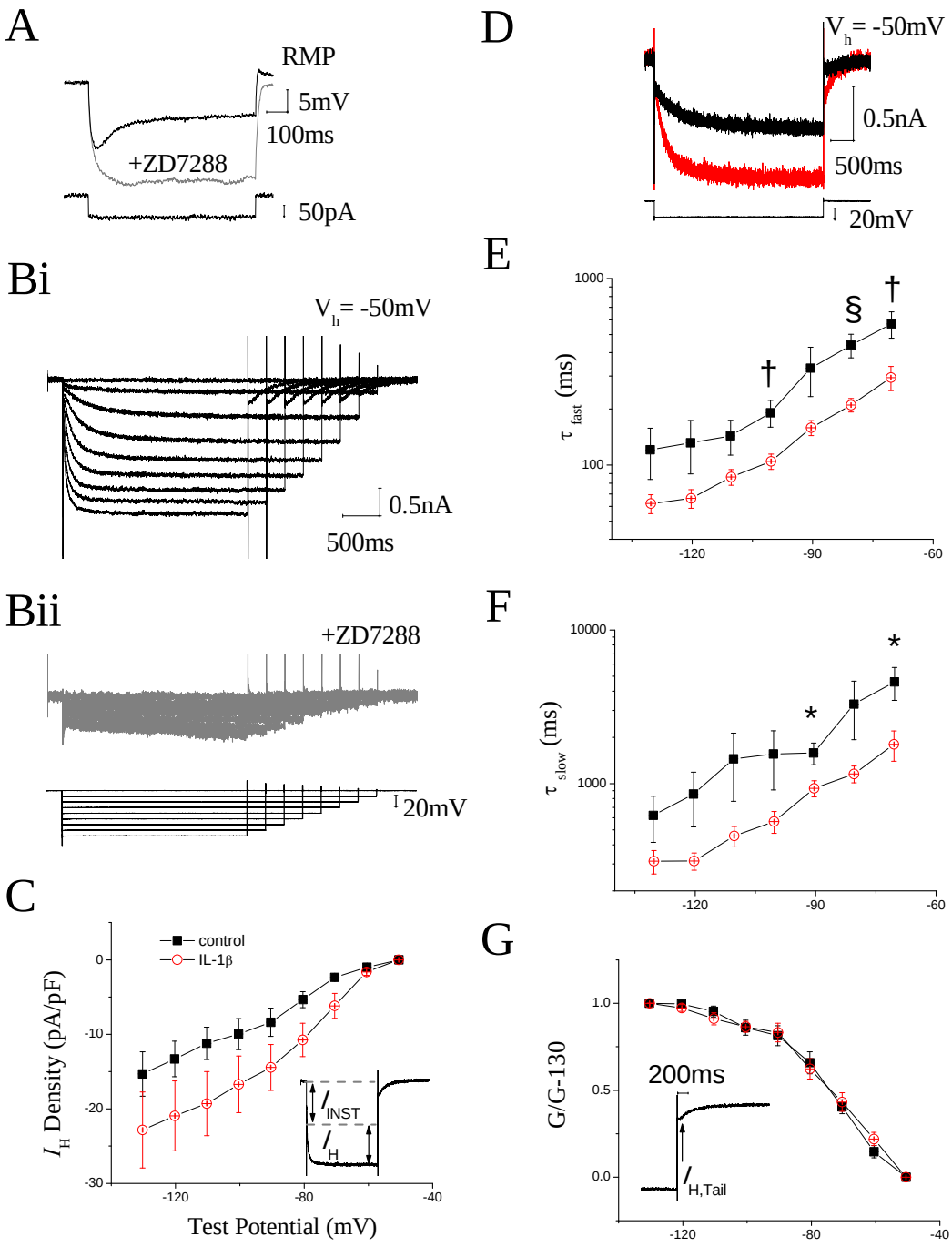
A
RMP
5mV
100ms
+ZD7288
50pA
Bi
V_h = -50mV
0.5nA
500ms
Bii
+ZD7288
20mV
C
control
IL-1β
I_H Density (pA/pF)
0
-10
-20
-30
-120
-80
-40
I_INST
I_H
Test Potential (mV)
D
V_h = -50mV
0.5nA
500ms
20mV
E
τ fast (ms)
1000
100
-120
-90
-60
§
†
†
F
τ slow (ms)
10000
1000
-120
-90
-60
*
*
G
G/G-130
1.0
0.5
0.0
200ms
I_H,Tail
-120
-80
-40

***Table 5-1: Summary of single Boltzmann function parameters in control versus IL-1β treated medium DRG neurons***

Significant difference vs. control * = $p<0.05$, † = $p<0.01$ and § = $p<0.001$ with unpaired t-test.

| **Parameter** | **Medium Neurons**<br>**Control**<br>**Value ± s.e.m. (n)** | **Medium Neurons**<br>**IL-1β**<br>**Value ± s.e.m. (n)** |
|---|---|---|
| $I_{Na}$ activation $V_{1/2}$ (mV) | -32.5 ± 2.6 mV (n=9) | -41.4 ± 2.2 mV (n=11)* |
| $I_{Na}$ activation slope factor (mV) | 3.6 ± 1.1 mV (n=9) | 3.3 ± 0.5 (n=11) |
| $I_{Na}$ steady-state fast inactivation $V_{1/2}$ (mV) | -61.3 ± 1.9 mV (n=7) | -62.0 ± 0.9 (n=11) |
| $I_{Na}$ steady-state fast inactivation slope factor (mV) | 7.7 ± 0.8 mV (n=7) | 8.8 ± 0.9 (n=11) |
| $I_{Na}$ steady-state slow inactivation $V_{1/2}$ (mV) | -62.4 ± 6.1 mV (n=5) | -57.8 ± 2.5 (n=5) |
| $I_{Na}$ steady-state slow inactivation slope factor (mV) | 13.5 ± 1.9 mV (n=5) | 13.6 ± 1.1 (n=5) |
| $I_{Ba}$ inactivation $V_{1/2}$ (mV) | -59.0 ± 5.0 mV (n=6) | -78.8 ± 5.9 (n=13) |
| $I_{Ba}$ slope factor (mV) | 10.7 ± 1.1 mV (n=6) | 17.8 ± 1.4 (n=13)† |
| $I_{H}$ steady-state activation $V_{1/2}$ (mV) | -70.7 ± 2.7 mV (n=9) | -65.9 ± 5.1 mV (n=10) |
| $I_{H}$ slope factor (mV) | 12.2 ± 1.6 mV (n=9) | 10.7 ± 1.7 (n=10) |

***Table 5-2: Summary of significant findings***

*References:*

1. Non-inactivating $I_K$ in my study likely corresponds to delayed-rectifier $I_K$.
2. Inactivating $Mn^{2+}$ -R $I_K$ likely corresponds to A-type currents.
3. Inactivating $Mn^{2+}$ -S $I_K$ likely corresponds to $K_{Ca}$ currents.
4. Cummins and Waxman (1997).
5. Abdulla and Smith (2001b).
6. Sarantopoulos et al. (2007).
7. Everill and Kocsis (1999).
8. Yang et al. (2004).
9. Baccei and Kocsis (2000).
10. Hogan et al. (2000).
11. Yao et al. (2003).

| Parameter | Effect of IL-1β | Change consistent with nerve injury studies? |
|---|---|---|
| **TTX-S $I_{Na}$** density | No change | |
| **TTX-S $I_{Na}$** voltage dependency of activation | Hyperpolarizing shift | No[4] |
| **TTX-S $I_{Na}$** voltage dependence of inactivation | No change | |
| **TTX-S $I_{Na}$** kinetics of inactivation | No change | |
| **$I_K$** density | Decreased (non-inactivating $I_K$[1]; inactivating $Mn^{2+}$-$R^2$ and $Mn^{2+}$-S $I_K$[3]) | Yes[5,6,7,8] |
| **HVA-$I_{Ba}$** density | Increased ($V_h$ = -100 mV); Decreased ($V_h$ = -60 mV) | *Yes (decrease only)*[5,9,10] |
| **HVA-$I_{Ba}$** voltage dependence of inactivation | Increased sensitivity to $V_h$ (slope factor and % decrease of peak current) | Yes[5,9] |
| **$I_H$** density | No change | |
| **$I_H$** kinetics of activation | Faster | Yes[11] |
| **$I_H$** voltage dependence of activation | No change | |

### *5.3 References*


1. Abdulla FA, Smith PA (2001a) Axotomy- and autotomy-induced changes in the excitability of rat dorsal root ganglion neurons. J Neurophysiol 85: 630-643.

2. Abdulla FA, Smith PA (2002) Changes in Na(+) channel currents of rat dorsal root ganglion neurons following axotomy and axotomy-induced autotomy. J Neurophysiol 88: 2518-2529.

3. Abdulla FA, Smith PA (2001b) Axotomy- and Autotomy-Induced Changes in Ca2+and K+ Channel Currents of Rat Dorsal Root Ganglion Neurons. J Neurophysiol 85: 644-658.

4. Aguayo LG, Weight FF, White G (1991) TTX-sensitive action potentials and excitability of adult rat sensory neurons cultured in serum- and exogenous nerve growth factor-free medium. Neurosci Lett 121: 88-92.

5. Airaksinen MS, Saarma M (2002) The GDNF family: Signalling, biological functions and therapeutic value. Nat Rev Neurosci 3: 383-394.

6. Akins PT, McCleskey EW (1993) Characterization of potassium currents in adult rat sensory neurons and modulation by opioids and cyclic AMP. Neuroscience 56: 759-769.

7. Appel E, Kolman O, Kazimirsky G, Blumberg PM, Brodie C (1997) Regulation of GDNF expression in cultured astrocytes by inflammatory stimuli. Neuroreport 8: 3309-3312.

8. Baccei ML, Kocsis JD (2000) Voltage-Gated Calcium Currents in Axotomized Adult Rat Cutaneous Afferent Neurons. J Neurophysiol 83: 2227-2238.

9. Bahia PK, Suzuki R, Benton DC, Jowett AJ, Chen MX, Trezise DJ, Dickenson AH, Moss GW (2005) A functional role for small-conductance calcium-activated potassium channels in sensory pathways including nociceptive processes. J Neurosci 25: 3489-3498.

10. Baldelli P, Forni PE, Carbone E (2000) BDNF, NT-3 and NGF induce distinct new Ca2+ channel synthesis in developing hippocampal neurons. Eur J Neurosci 12: 4017-4032.

11. Baldelli P, Novara M, Carabelli V, Hernandez-Guijo JM, Carbone E (2002) BDNF up-regulates evoked GABAergic transmission in developing hippocampus by potentiating presynaptic N- and P/Q-type Ca2+ channels signalling. Eur J Neurosci 16: 2297-2310.

12. Bennett DLH, Michael GJ, Ramachandran N, Munson JB, Averill S, Yan Q, McMahon SB, Priestley JV (1998) A distinct subgroup of small DRG

cells express GDNF receptor components and GDNF is protective for these neurons after nerve injury. J Neurosci 18: 3059-3072.

13. Binshtok AM, Wang H, Zimmermann K, Amaya F, Vardeh D, Shi L, Brenner GJ, Ji RR, Bean BP, Woolf CJ, Samad TA (2008) Nociceptors are interleukin-1beta sensors. J Neurosci 28: 14062-14073.

14. Boettger MK, Till S, Chen MX, Anand U, Otto WR, Plumpton C, Trezise DJ, Tate SN, Bountra C, Coward K, Birch R, Anand P (2002) Calcium-activated potassium channel SK1- and IK1-like immunoreactivity in injured human sensory neurones and its regulation by neurotrophic factors. Brain 125: 252-263.

15. Brown H, DiFrancesco D, Noble S (1979) Cardiac pacemaker oscillation and its modulation by autonomic transmitters. J Exp Biol 81: 175-204.

16. Caffrey JM, Eng DL, Black JA, Waxman SG, Kocsis JD (1992) Three types of sodium channels in adult rat dorsal root ganglion neurons. Brain Research 592: 283-297.

17. Cardenas CG, Mar LP, Vysokanov AV, Arnold PB, Cardenas LM, Surmeier DJ, Scroggs RS (1999) Serotonergic modulation of hyperpolarization-activated current in acutely isolated rat dorsal root ganglion neurons. J Physiol 518 ( Pt 2): 507-523.

18. Catacuzzeno L, Fioretti B, Pietrobon D, Franciolini F (2008) The differential expression of low-threshold K+ currents generates distinct firing patterns in different subtypes of adult mouse trigeminal ganglion neurones. J Physiol 586: 5101-5118.

19. Chad JE, Eckert R (1984) Calcium domains associated with individual channels can account for anomalous voltage relations of CA-dependent responses. Biophys J 45: 993-999.

20. Chae KS, Dryer SE (2005) The p38 mitogen-activated protein kinase pathway negatively regulates Ca2+-activated K+ channel trafficking in developing parasympathetic neurons. J Neurochem 94: 367-379.

21. Chaplan SR, Guo HQ, Lee DH, Luo L, Liu C, Kuei C, Velumian AA, Butler MP, Brown SM, Dubin AE (2003) Neuronal hyperpolarization-activated pacemaker channels drive neuropathic pain. J Neurosci 23: 1169-1178.

22. Chi XX, Nicol GD (2007) Manipulation of the potassium channel Kv1.1 and its effect on neuronal excitability in rat sensory neurons. J Neurophysiol 98: 2683-2692.

23. Cho HJ, Staikopoulos V, Furness JB, Jennings EA (2009) Inflammation-induced increase in hyperpolarization-activated, cyclic nucleotide-gated

channel protein in trigeminal ganglion neurons and the effect of buprenorphine. Neuroscience 162: 453-461.

24. Cummins TR, Aglieco F, Renganathan M, Herzog RI, Dib-Hajj SD, Waxman SG (2001) Nav1.3 sodium channels: rapid repriming and slow closed-state inactivation display quantitative differences after expression in a mammalian cell line and in spinal sensory neurons. J Neurosci 21: 5952-5961.

25. Cummins TR, Dib-Hajj SD, Waxman SG (2004) Electrophysiological properties of mutant Nav1.7 sodium channels in a painful inherited neuropathy. J Neurosci 24: 8232-8236.

26. Cummins TR, Sheets PL, Waxman SG (2007) The roles of sodium channels in nociception: Implications for mechanisms of pain. Pain 131: 243-257.

27. Cummins TR, Waxman SG (1997) Downregulation of Tetrodotoxin-Resistant Sodium Currents and Upregulation of a Rapidly Repriming Tetrodotoxin-Sensitive Sodium Current in Small Spinal Sensory Neurons after Nerve Injury. J Neurosci 17: 3503-3514.

28. Cusdin FS, Nietlispach D, Maman J, Dale TJ, Powell AJ, Clare JJ, Jackson AP (2010) The sodium channel {beta}3-subunit induces

multiphasic gating in NaV1.3 and affects fast inactivation via distinct intracellular regions. J Biol Chem 285: 33404-33412.

29. Devor M (2009) Ectopic discharge in Abeta afferents as a source of neuropathic pain. Exp Brain Res 196: 115-128.

30. Dib-Hajj SD, Black JA, Cummins TR, Kenney AM, Kocsis JD, Waxman SG (1998a) Rescue of alpha -SNS Sodium Channel Expression in Small Dorsal Root Ganglion Neurons After Axotomy by Nerve Growth Factor In Vivo. J Neurophysiol 79: 2668-2676.

31. Dib-Hajj SD, Tyrrell L, Black JA, Waxman SG (1998b) NaN, a novel voltage-gated Na channel, is expressed preferentially in peripheral sensory neurons and down-regulated after axotomy. Proceedings of the National Academy of Sciences of the United States of America 95: 8963-8968.

32. Diem R, Hobom M, Grotsch P, Kramer B, Bahr M (2003) Interleukin-1 beta protects neurons via the interleukin-1 (IL-1) receptor-mediated Akt pathway and by IL-1 receptor-independent decrease of transmembrane currents in vivo. Mol Cell Neurosci 22: 487-500.

33. DiFrancesco D, Tortora P (1991) Direct activation of cardiac pacemaker channels by intracellular cyclic AMP. Nature 351: 145-147.

34. DiFrancesco D (2001) Serious workings of the funny current. Progress in Biophysics and Molecular Biology 90: 13-25.

35. Djouhri L, Bleazard L, Lawson SN (1998) Association of somatic action potential shape with sensory receptive properties in guinea-pig dorsal root ganglion neurones. J Physiol 513 ( Pt 3): 857-872.

36. England S, Bevan S, Docherty RJ (1996) PGE2 modulates the tetrodotoxin-resistant sodium current in neonatal rat dorsal root ganglion neurones via the cyclic AMP-protein kinase A cascade. The Journal of Physiology 495: 429-440.

37. Everill B, Kocsis JD (1999) Reduction in Potassium Currents in Identified Cutaneous Afferent Dorsal Root Ganglion Neurons After Axotomy. J Neurophysiol 82: 700-708.

38. Everill B, Rizzo MA, Kocsis JD (1998) Morphologically Identified Cutaneous Afferent DRG Neurons Express Three Different Potassium Currents in Varying Proportions. J Neurophysiol 79: 1814-1824.

39. Fang X, Djouhri L, McMullan S, Berry C, Waxman SG, Okuse K, Lawson SN (2006) Intense Isolectin-B4 Binding in Rat Dorsal Root Ganglion Neurons Distinguishes C-Fiber Nociceptors with Broad Action Potentials and High Nav1.9 Expression. J Neurosci 26: 7281-7292.

40. Fazan R, Jr., Whiteis CA, Chapleau MW, Abboud FM, Bielefeldt K (2001) Slow inactivation of sodium currents in the rat nodose neurons. Auton Neurosci 87: 209-216.

41. Fjell J, Cummins TR, Dib-Hajj SD, Fried K, Black JA, Waxman SG (1999) Differential role of GDNF and NGF in the maintenance of two TTX-resistant sodium channels in adult DRG neurons. Brain Res Mol Brain Res 67: 267-282.

42. Ford CP, Wong KV, Lu VB, Posse dC, Smith PA (2008) Differential neurotrophic regulation of sodium and calcium channels in an adult sympathetic neuron. J Neurophysiol 99: 1319-1332.

43. Fox AP, Nowycky MC, Tsien RW (1987) Kinetic and pharmacological properties distinguishing three types of calcium currents in chick sensory neurones. J Physiol 394: 149-172.

44. Fuchs A, Lirk P, Stucky C, Abram SE, Hogan QH (2005) Painful nerve injury decreases resting cytosolic calcium concentrations in sensory neurons of rats. Anesthesiology 102: 1217-1225.

45. Fuchs A, Rigaud M, Hogan QH (2007) Painful nerve injury shortens the intracellular Ca2+ signal in axotomized sensory neurons of rats. Anesthesiology 107: 106-116.

46. Funakoshi M, Sonoda Y, Tago K, Tominaga S, Kasahara T (2001) Differential involvement of p38 mitogen-activated protein kinase and phosphatidyl inositol 3-kinase in the IL-1-mediated NF-kappa B and AP-1 activation. Int Immunopharmacol 1: 595-604.

47. Glazebrook PA, Ramirez AN, Schild JH, Shieh CC, Doan T, Wible BA, Kunze DL (2002) Potassium channels Kv1.1, Kv1.2 and Kv1.6 influence excitability of rat visceral sensory neurons. The Journal of Physiology 541: 467-482.

48. Gold MS, Levine JD, Correa AM (1998) Modulation of TTX-R INa by PKC and PKA and their role in PGE2-induced sensitization of rat sensory neurons in vitro. J Neurosci 18: 10345-10355.

49. Gold MS, Reichling DB, Shuster MJ, Levine JD (1996a) Hyperalgesic agents increase a tetrodotoxin-resistant Na+ current in nociceptors. Proc Natl Acad Sci U S A 93: 1108-1112.

50. Gold MS, Shuster MJ, Levine JD (1996b) Characterization of six voltage-gated K+ currents in adult rat sensory neurons. J Neurophysiol 75: 2629-2646.

51. Gold MS, Shuster MJ, Levine JD (1996c) Role of a Ca(2+)-dependent slow afterhyperpolarization in prostaglandin E2-induced sensitization of cultured rat sensory neurons. Neurosci Lett 205: 161-164.

52. Gold MS, Weinreich D, Kim CS, Wang R, Treanor J, Porreca F, Lai J (2003) Redistribution of Na(V)1.8 in uninjured axons enables neuropathic pain. J Neurosci 23: 158-166.

53. Hagiwara K, Nunoki K, Ishii K, Abe T, Yanagisawa T (2003) Differential inhibition of hjkhj transient outward currents of Kv1.4 and Kv4.3 by endothelin. Biochemical and Biophysical Research Communications 310: 634-640.

54. Harper AA, Lawson SN (1985) Conduction velocity is related to morphological cell type in rat dorsal root ganglion neurones. J Physiol 359: 31-46.

55. Herzog RI, Cummins TR, Ghassemi F, Dib-Hajj SD, Waxman SG (2003) Distinct repriming and closed-state inactivation kinetics of Nav1.6 and Nav1.7 sodium channels in mouse spinal sensory neurons. The Journal of Physiology 551: 741-750.

56. Hingtgen CM, Waite KJ, Vasko MR (1995) Prostaglandins facilitate peptide release from rat sensory neurons by activating the adenosine 3',5'-cyclic monophosphate transduction cascade. J Neurosci 15: 5411-5419.

57. Hogan QH, McCallum JB, Sarantopoulos C, Aason M, Mynlieff M, Kwok WM, Bosnjak ZJ (2000) Painful neuropathy decreases membrane calcium current in mammalian primary afferent neurons. Pain 86: 43-53.

58. Ingram SL, Williams JT (1996) Modulation of the hyperpolarization-activated current (Ih) by cyclic nucleotides in guinea-pig primary afferent neurons. J Physiol 492 ( Pt 1): 97-106.

59. Ishikawa K, Tanaka M, Black JA, Waxman SG (1999) Changes in expression of voltage-gated potassium channels in dorsal root ganglion neurons following axotomy. Muscle Nerve 22: 502-507.

60. Jiang YQ, Xing GG, Wang SL, Tu HY, Chi YN, Li J, Liu FY, Han JS, Wan Y (2008) Axonal accumulation of hyperpolarization-activated cyclic nucleotide-gated cation channels contributes to mechanical allodynia after peripheral nerve injury in rat. Pain 137: 495-506.

61. Jones SW, Marks TN (1989) Calcium currents in bullfrog sympathetic neurons. II. Inactivation. J Gen Physiol 94: 169-182.

62. Kim DS, Choi JO, Rim HD, Cho HJ (2002) Downregulation of voltage-gated potassium channel [alpha] gene expression in dorsal root ganglia following chronic constriction injury of the rat sciatic nerve. Molecular Brain Research 105: 146-152.

63. Koerber HR, Druzinsky RE, Mendell LM (1988) Properties of somata of spinal dorsal root ganglion cells differ according to peripheral receptor innervated. J Neurophysiol 60: 1584-1596.

64. Kostyuk PG, Veselovsky NS, Tsyndrenko AY (1981) Ionic currents in the somatic membrane of rat dorsal root ganglion neurons-I. Sodium currents. Neuroscience 6: 2423-2430.

65. Kouranova EV, Strassle BW, Ring RH, Bowlby MR, Vasilyev DV (2008) Hyperpolarization-activated cyclic nucleotide-gated channel mRNA and protein expression in large versus small diameter dorsal root ganglion neurons: correlation with hyperpolarization-activated current gating. Neuroscience 153: 1008-1019.

66. Lai J, Porreca F, Hunter JC, Gold MS (2004) Voltage-gated sodium channels and hyperalgesia. Annu Rev Pharmacol Toxicol 44: 371-397.

67. Li W, Gao SB, Lv CX, Wu Y, Guo ZH, Ding JP, Xu T (2007) Characterization of voltage-and Ca2+-activated K+ channels in rat dorsal root ganglion neurons. J Cell Physiol 212: 348-357.

68. Liu BG, Dobretsov M, Stimers JR, Zhang JM (2008) Tumor Necrosis Factor-alpha Suppresses Activation of Sustained Potassium Currents in Rat Small Diameter Sensory Neurons. Open Pain J 1: 1.

69. Liu L, Yang TM, Liedtke W, Simon SA (2006) Chronic IL-1beta signaling potentiates voltage-dependent sodium currents in trigeminal nociceptive neurons. J Neurophysiol 95: 1478-1490.

70. Lu SG, Gold MS (2008) Inflammation-induced increase in evoked calcium transients in subpopulations of rat dorsal root ganglion neurons. Neuroscience 153: 279-288.

71. Lu SG, Zhang X, Gold MS (2006) Intracellular calcium regulation among subpopulations of rat dorsal root ganglion neurons. The Journal of Physiology 577: 169-190.

72. Maier JA, Hla T, Maciag T (1990) Cyclooxygenase is an immediate-early gene induced by interleukin-1 in human endothelial cells. J Biol Chem 265: 10805-10808.

73. Matsuda Y, Yoshida S, Yonezawa T (1978) Tetrodotoxin sensitivity and Ca component of action potentials of mouse dorsal root ganglion cells cultured in vitro. Brain Res 154: 69-82.

74. Mayer ML, Sugiyama K (1988) A modulatory action of divalent cations on transient outward current in cultured rat sensory neurones. J Physiol 396: 417-433.

75. Mayer ML, Westbrook GL (1983) A voltage-clamp analysis of inward (anomalous) rectification in mouse spinal sensory ganglion neurones. J Physiol 340: 19-45.

76. Molliver DC, Wright DE, Leitner ML, Parsadanian AS, Doster K, Wen D, Yan Q, Snider WD (1997) IB4-binding DRG neurons switch from NGF to GDNF dependence in early postnatal life. Neuron 19: 849-861.

77. Momin A, Cadiou H, Mason A, McNaughton PA (2008) Role of the hyperpolarization-activated current Ih in somatosensory neurons. J Physiol 586: 5911-5929.

78. Mu X, Silos-Santiago I, Carroll SL, Snider WD (1993) Neurotrophin receptor genes are expressed in distinct patterns in developing dorsal root ganglia. J Neurosci 13: 4029-4041.

79. Ogata N, Tatebayashi H (1993) Kinetic analysis of two types of Na+ channels in rat dorsal root ganglia. J Physiol 466: 9-37.

80. Orio P, Madrid R, de la PE, Parra A, Meseguer V, Bayliss DA, Belmonte C, Viana F (2009) Characteristics and physiological role of hyperpolarization activated currents in mouse cold thermoreceptors. J Physiol 587: 1961-1976.

81. Pape HC (1996) Queer current and pacemaker: the hyperpolarization-activated cation current in neurons. Annu Rev Physiol 58: 299-327.

82. Pearce RJ, Duchen MR (1994) Differential expression of membrane currents in dissociated mouse primary sensory neurons. Neuroscience 63: 1041-1056.

83. Pertin M, Ji RR, Berta T, Powell AJ, Karchewski L, Tate SN, Isom LL, Woolf CJ, Gilliard N, Spahn DR, Decosterd I (2005) Upregulation of the Voltage-Gated Sodium Channel {beta}2 Subunit in Neuropathic Pain Models: Characterization of Expression in Injured and Non-Injured Primary Sensory Neurons. J Neurosci 25: 10970-10980.

84. Purmessur D, Freemont AJ, Hoyland JA (2008) Expression and regulation of neurotrophins in the nondegenerate and degenerate human intervertebral disc. Arthritis Res Ther 10: R99.

85. Raes A, Wang Z, van den Berg RJ, Goethals M, Van d, V, van Bogaert PP (1997) Effect of cAMP and ATP on the hyperpolarization-activated current in mouse dorsal root ganglion neurons. Pflugers Arch 434: 543-550.

86. Rizzo MA, Kocsis JD, Waxman SG (1994) Slow sodium conductances of dorsal root ganglion neurons: intraneuronal homogeneity and interneuronal heterogeneity. J Neurophysiol 72: 2796-2815.

87. Rose RD, Koerber HR, Sedivec MJ, Mendell LM (1986) Somal action potential duration differs in identified primary afferents. Neurosci Lett 63: 259-264.

88. Roux J, Kawakatsu H, Gartland B, Pespeni M, Sheppard D, Matthay MA, Canessa CM, Pittet JF (2005) Interleukin-1beta decreases expression of the epithelial sodium channel alpha-subunit in alveolar epithelial cells via a p38 MAPK-dependent signaling pathway. J Biol Chem 280: 18579-18589.

89. Rush AM, Cummins TR, Waxman SG (2007a) Multiple sodium channels and their roles in electrogenesis within dorsal root ganglion neurons. J Physiol 579: 1-14.

90. Rush AM, Cummins TR, Waxman SG (2007b) Multiple sodium channels and their roles in electrogenesis within dorsal root ganglion neurons. J Physiol 579: 1-14.

91. Rush AM, Dib-Hajj SD, Liu S, Cummins TR, Black JA, Waxman SG (2006a) A single sodium channel mutation produces hyper- or hypoexcitability in different types of neurons. Proc Natl Acad Sci U S A 103: 8245-8250.

92. Rush AM, Wittmack EK, Tyrrell L, Black JA, Dib-Hajj SD, Waxman SG (2006b) Differential modulation of sodium channel Na(v)1.6 by two members of the fibroblast growth factor homologous factor 2 subfamily. Eur J Neurosci 23: 2551-2562.

93. Rusin KI, Moises HC (1995) mu-Opioid receptor activation reduces multiple components of high-threshold calcium current in rat sensory neurons. J Neurosci 15: 4315-4327.

94. Saavedra A, Baltazar G, Duarte EP (2007) Interleukin-1[beta] mediates GDNF up-regulation upon dopaminergic injury in ventral midbrain cell cultures. Neurobiology of Disease 25: 92-104.

95. Sarantopoulos CD, McCallum JB, Rigaud M, Fuchs A, Kwok WM, Hogan QH (2007) Opposing effects of spinal nerve ligation on calcium-

activated potassium currents in axotomized and adjacent mammalian primary afferent neurons. Brain Res 1132: 84-99.

96. Scholz A, Gruss M, Vogel W (1998) Properties and functions of calcium-activated K+ channels in small neurones of rat dorsal root ganglion studied in a thin slice preparation. J Physiol 513 ( Pt 1): 55-69.

97. Scroggs RS, Fox AP (1992) Calcium current variation between acutely isolated adult rat dorsal root ganglion neurons of different size. J Physiol 445: 639-658.

98. Scroggs RS, Todorovic SM, Anderson EG, Fox AP (1994) Variation in IH, IIR, and ILEAK between acutely isolated adult rat dorsal root ganglion neurons of different size. J Neurophysiol 71: 271-279.

99. Shah BS, Stevens EB, Gonzalez MI, Bramwell S, Pinnock RD, Lee K, Dixon AK (2000) beta3, a novel auxiliary subunit for the voltage-gated sodium channel, is expressed preferentially in sensory neurons and is upregulated in the chronic constriction injury model of neuropathic pain. Eur J Neurosci 12: 3985-3990.

100. Shipston MJ, Duncan RR, Clark AG, Antoni FA, Tian L (1999) Molecular components of large conductance calcium-activated potassium (BK) channels in mouse pituitary corticotropes. Mol Endocrinol 13: 1728-1737.

101. Stamboulian S, Choi JS, Ahn HS, Chang YW, Tyrrell L, Black JA, Waxman SG, Dib-Hajj SD (2010) ERK1/2 Mitogen-Activated Protein Kinase Phosphorylates Sodium Channel Nav1.7 and Alters Its Gating Properties. J Neurosci 30: 1637-1647.

102. Stansfeld CE, Marsh SJ, Halliwell JV, Brown DA (1986) 4-Aminopyridine and dendrotoxin induce repetitive firing in rat visceral sensory neurones by blocking a slowly inactivating outward current. Neurosci Lett 64: 299-304.

103. Stieber J, Stockl G, Herrmann S, Hassfurth B, Hofmann F (2005) Functional expression of the human HCN3 channel. J Biol Chem 280: 34635-34643.

104. Takahashi N, Kikuchi S, Dai Y, Kobayashi K, Fukuoka T, Noguchi K (2003) Expression of auxiliary [beta] subunits of sodium channels in primary afferent neurons and the effect of nerve injury. Neuroscience 121: 441-450.

105. Takeda M, Kitagawa J, Takahashi M, Matsumoto S (2008) Activation of interleukin-1beta receptor suppresses the voltage-gated potassium currents in the small-diameter trigeminal ganglion neurons following peripheral inflammation. Pain 139: 594-602.

106. Tanabe K, Nishimura K, Dohi S, Kozawa O (2009) Mechanisms of interleukin-1beta-induced GDNF release from rat glioma cells. Brain Res 1274: 11-20.

107. Todorovic SM, Jevtovic-Todorovic V (2006) The role of T-type calcium channels in peripheral and central pain processing. CNS Neurol Disord Drug Targets 5: 639-653.

108. Tu H, Deng L, Sun Q, Yao L, Han JS, Wan Y (2004) Hyperpolarization-activated, cyclic nucleotide-gated cation channels: roles in the differential electrophysiological properties of rat primary afferent neurons. J Neurosci Res 76: 713-722.

109. Ulens C, Tytgat J (2001) Functional heteromerization of HCN1 and HCN2 pacemaker channels. J Biol Chem 276: 6069-6072.

110. Villiere V, McLachlan EM (1996) Electrophysiological properties of neurons in intact rat dorsal root ganglia classified by conduction velocity and action potential duration. J Neurophysiol 76: 1924-1941.

111. Vydyanathan A, Wu ZZ, Chen SR, Pan HL (2005) A-type voltage-gated K+ currents influence firing properties of isolectin B4-positive but not isolectin B4-negative primary sensory neurons. J Neurophysiol 93: 3401-3409.

112. Wainger BJ, DeGennaro M, Santoro B, Siegelbaum SA, Tibbs GR (2001) Molecular mechanism of cAMP modulation of HCN pacemaker channels. Nature 411: 805-810.

113. Waxman SG, Kocsis JD, Black JA (1994) Type III sodium channel mRNA is expressed in embryonic but not adult spinal sensory neurons, and is reexpressed following axotomy. J Neurophysiol 72: 466-470.

114. White G, Lovinger DM, Weight FF (1989) Transient low-threshold Ca2+ current triggers burst firing through an afterdepolarizing potential in an adult mammalian neuron. Proc Natl Acad Sci U S A 86: 6802-6806.

115. Widmer HlnA, Rowe ICM, Shipston MJ (2003) Conditional protein phosphorylation regulates BK channel activity in rat cerebellar Purkinje neurons. The Journal of Physiology 552: 379-391.

116. Winkelman DLB, Beck CL, Ypey DL, O'Leary ME (2005) Inhibition of the A-type K<sup>+</sup> channels of dorsal root ganglion neurons by the long-duration anesthetic butamben. J Pharmacol Exp Ther 314: 1177-1186.

117. Wright DE, Snider WD (1995) Neurotrophin receptor mRNA expression defines distinct populations of neurons in rat dorsal root ganglia. J Comp Neurol 351: 329-338.

118. Wu ZZ, Chen SR, Pan HL (2004) Differential sensitivity of N- and P/Q-type Ca2+ channel currents to a mu opioid in isolectin B4-positive and -negative dorsal root ganglion neurons. J Pharmacol Exp Ther 311: 939-947.

119. Yagi J, Sumino R (1998) Inhibition of a hyperpolarization-activated current by clonidine in rat dorsal root ganglion neurons. J Neurophysiol 80: 1094-1104.

120. Yang E-K, Takimoto K, Hayashi Y, De Groat WC, Yoshimura N (2004) Altered expression of potassium channel subunit mRNA and [alpha]-dendrotoxin sensitivity of potassium currents in rat dorsal root ganglion neurons after axotomy. Neuroscience 123: 867-874.

121. Yao H, Donnelly DF, Ma C, LaMotte RH (2003) Upregulation of the hyperpolarization-activated cation current after chronic compression of the dorsal root ganglion. J Neurosci 23: 2069-2074.

122. Yoshida S, Matsuda Y, Samejima A (1978) Tetrodotoxin-resistant sodium and calcium components of action potentials in dorsal root ganglion cells of the adult mouse. J Neurophysiol 41: 1096-1106.

123. Yoshida S, Matsumoto S (2005) Effects of +¦-Dendrotoxin on K+ Currents and Action Potentials in Tetrodotoxin-Resistant Adult Rat Trigeminal Ganglion Neurons. J Pharmacol Exp Ther 314: 437-445.

124. Yu H, Wu J, Potapova I, Wymore RT, Holmes B, Zuckerman J, Pan Z, Wang H, Shi W, Robinson RB, El Maghrabi MR, Benjamin W, Dixon J, McKinnon D, Cohen IS, Wymore R (2001) MinK-Related Peptide 1 : A {beta} Subunit for the HCN Ion Channel Subunit Family Enhances Expression and Speeds Activation. Circ Res 88: e84-e87.

125. Zamponi GW, Lewis RJ, Todorovic SM, Arneric SP, Snutch TP (2009) Role of voltage-gated calcium channels in ascending pain pathways. Brain Research Reviews 60: 84-89.

126. Zhang XL, Mok LP, Katz EJ, Gold MS (2010) BKCa currents are enriched in a subpopulation of adult rat cutaneous nociceptive dorsal root ganglion neurons. Eur J Neurosci 31: 450-462.

127. Zhang YH, Chi XX, Nicol GD (2008) Brain-derived neurotrophic factor enhances the excitability of rat sensory neurons through activation of the p75 neurotrophin receptor and the sphingomyelin pathway. J Physiol 586: 3113-3127.

128. Zolles G, Wenzel D, Bildl W, Schulte U, Hofmann A, Muller CS, Thumfart JO, Vlachos A, Deller T, Pfeifer A, Fleischmann BK, Roeper J, Fakler B, Klocker N (2009) Association with the auxiliary subunit PEX5R/Trip8b controls responsiveness of HCN channels to cAMP and adrenergic stimulation. Neuron 62: 814-825.

# CHAPTER 6

General Discussion and Final Conclusions

My thesis work is a thorough examination of the effects of long-term IL-1β exposure on DRG neuron electrical membrane properties in cell culture. Since it is known that IL-1β can directly excite sensory neurons and can have sustained release after peripheral nerve injury, I have hypothesized that IL-1β promotes an enduring increase in the excitability of primary afferent neurons. This change may underlie mechanisms involved in the establishment of chronic, intractable neuropathic pain. Therefore, by examining the effects of long-term IL-1β exposure on sensory neuron excitability and identifying its mechanism of action, we can better understand the etiological basis for neuropathic pain, as well as, identifiy potenial pharmacological targets for treatment.

The major findings from my thesis work are as follows:

1. Increases in DRG neuron excitability are evident with acute applications of IL-1β, as well as, after long-term IL-1β exposure.

2. Increases in cell excitability after long-term IL-1β exposure are possibly limited to specific DRG neuron subpopulations.

3. Some, but not all, effects of IL-1β are receptor (IL-1RI) mediated.

4. Finally, changes in DRG neuron ionic currents are consistent with hyperexcitability.

### *6.1 DRG Cell Cultures: "Studying Pain in a Dish"*

#### *6.1.1 Why use DRG cell cultures?*

The use of DRG neurons in cell culture provides a suitable model to study the effects of pain mediators. For instance, DRG cell culturing allowed me to

assess changes in response to IL-1β without the possible interference from other systems *in vivo*, such as interactions with autonomic nerves (Devor et al., 1994). Further, neuronal cell enrichment (Lindsay, 1988) was aimed at minimizing indirect effects mediated via the action of IL-1β on non-neuronal cells. Since increased excitability after nerve injury is not limited to a particular sensory neuron subpopulation, the existence of four readily identifiable DRG neuron subtypes in cell culture allowed me to individually assess the effect of long-term IL-1β exposure. Last, DRG cell cultures allowed me to examine the effects of IL-1β at a predetermined concentration and duration in order to emulate its release after peripheral nerve injury.

### *6.1.2 Possible limitations*

Two important considerations must be discussed regarding DRG cell cultures in my study. First, neurotrophin-free defined medium likely affected the observed phenotypes of DRG neuron and this may have precluded potential effects of IL-1β. This is exemplified by the loss of TTX-R $I_{Na}$ and the narrower than expected APs of small IB4-positive and –negative neurons. Since TTX-R $I_{Na}$ is a major contributor to AP electrogenesis in small neurons and is known to be directly upregulated by IL-1β, phenotypic alteration likely contributed to the negative finding for small IB4-negative neurons and, relative to medium neurons, a modest effect in small IB4-positive neurons. As mentioned in previous chapters, the decision to use defined medium without exogenously added neurotrophins was based primarily on stabilizing ambient IL-1β at low (≤ 5pM) levels in long-

term DRG cell cultures so that I could achieve a clear difference when adding 100 pM IL-1β. Despite this, it is important to consider the following:

1. IL-1β still produced hyperexcitability in small IB4-positive neurons despite loss of TTX-R $I_{Na}$ and, therefore, other ionic currents are likely important.

2. Neurotrophin receptor signalling pathways that converge upon IL-1β receptor pathways, such as MAPKs, might also preclude effects of IL-1β.

3. Last, since multiple trophic factors are likely required for the maintenance of phenotype among the DRG neuron subpopulations identified in my study, how does one avoid a biased approach by the use of only well recognized neurotrophins, such as NGF and/or GDNF?

Another limitation is the presence of non-neuronal cells in DRG cell cultures and their known expression of IL-1RI (Copray et al., 2001). Therefore, IL-1β exposure could result in the production and release of inflammatory mediators from non-neuronal cells which would, in turn, introduce indirect effects of IL-1β on DRG neurons. As described in Methods (Chapter 2), neuronal enrichment procedures were established to minimize the growth of non-neuronal cells in my cultures. Despite these efforts, non-neuronal cells, which likely included Schwann cells and fibroblasts (Lindsay, 1988), existed and increased in number with culture duration. However, since non-neuronal cells, such as Schwann cells, can be a source of IL-1β (Sommer and Kress, 2004;Watkins and Maier, 1999), it is interesting that their increased presence was not concurrent with an increase in ambient IL-1β levels (Figure 2-3). Coupled to this, given that my DRG cultures were low in cell density, when qualitatively compared to non-

enriched cell cultures (Figure 2-2), it is possible that non-neuronal cells do not represent a significant source for the production of IL-1β or other yet to be defined inflammatory mediators. Consistent with this hypothesis, the possible production and release of neurotrophins, such as NGF and GDNF (Safieh-Garabedian et al., 1995;Tanabe et al., 2009;Appel et al., 1997;Lindholm et al., 1987), in response to long-term IL-1β exposure did not reach sufficient levels to promote the re-emergence of TTX-R $I_{Na}$ in small neurons. Thus, although there is no direct evidence, these observations all suggest that indirect effects of IL-1β, associated with the presence of non-neuronal cells, were minimal.

Taken together, given these two limitations, I have to exercise caution in interpreting my thesis findings as 'selective' and 'direct' effects of long-term IL-1β exposure on DRG neurons. An avenue of opportunity might be the use of microwells to culture single DRG neurons (Lindsay, 1988) where the direct effect of long-term IL-1β exposure on a given neuron would be possible to examine. With cellular sources of inflammatory mediators limited to a single neuron, there would also be the potential to add neurotrophins without a concurrent instability in ambient IL-1β levels. Single DRG neuron cultures would, therefore, permit a more stringent re-examination of the apparent selective effect of IL-1β exposure towards small IB4-positive versus -negative neurons while retaining nociceptor phenotypes in cell culture.

### *6.2 IL-1β Promotes an Enduring Increase in Sensory Neuron Excitability*

The effects of short-term (minutes to hours) IL-1β application on sensory neuron electrical membrane properties have been previously described in various *in vitro* preparations, including small, nociceptive sensory neurons of the DRG and trigeminal ganglia (Binshtok et al., 2008;Takeda et al., 2008a;Takeda et al., 2008b;Liu et al., 2006). My study expands on these findings by examining the effects of long-term IL-1β exposure on sensory neuron excitability and its relation to changes in sensory neurons observed after nerve injury. In the previous chapters, I not only confirmed that IL-1β enhances DRG neuron excitability after short-term (1 min.) applications, but further demonstrated hyperexcitability in medium and small IB4-positive sensory neuron subpopulations after 5 to 6 days exposure. I interpret these findings to be the *in vitro* equivalent to the enduring increase in primary afferent excitability reported after nerve injury and, therefore, would expand the recognized role of IL-1β in acute inflammatory pain to neuropathic pain. Last, the identification of receptor mediated effects and several contributing ionic mechanisms, suggests my findings have relevance to the treatment of neuropathic pain.

#### *6.2.1 Effects of IL-1β are possibly limited to specific sensory neuron subpopulations*

The effects of long-term IL-1β exposure were DRG neuron subpopulation specific. Similar to nerve injury and acute IL-1β application, long-term IL-1β exposure produced several changes in medium and small IB4-positive neurons

which were consistent with hyperexcitability. In contrast, large neurons responded in an opposite manner (hypoexcitable), whereas, small IB4-negative neurons were devoid of any measurable response. Since *in vivo* and *in vitro* nerve injury studies report hyperexcitability in small, nociceptive and large, non-nociceptive sensory neurons subpopulations, the hypoexcitability of large neurons in IL-1β exposed cultures suggests that IL-1β has a restricted role in the generation of increased excitability in injured sensory neurons. This is further supported by the lack of response from small IB4-negative neurons.

This finding is surprising, given that most sensory neurons express the IL-1β receptor, IL-1RI (Liu et al., 2006;Copray et al., 2001), and, therefore, I expected changes in the electrical behaviour of sensory neurons to be more or less consistent among DRG neuron subpopulations. There are at least three possibilities for differences:

1. As already discussed above, phenotypic shift in long-term cell cultures may have precluded changes consistent with hyperexcitability in small IB4-negative neurons exposed to IL-1β and neurotrophin supplemented single DRG neuron cultures might present an opportunity to re-examine this possibility.

2. Alternatively, sensory neuron subpopulations are known to have variability in the contribution of ionic currents that underlie AP generation. For instance, acutely isolated small diameter IB4-positive DRG neurons are known to be enriched with $BK_{Ca}$ and A-type currents (Zhang et al., 2010;Vydyanathan et al., 2005), while larger-sized sensory neurons are enriched with $I_H$ currents (Abdulla and Smith, 2001b;Scroggs et al., 1994). Therefore, the effect of IL-1β exposure

may be predetermined by the complement of ion channels functionally expressed in a given sensory neuron subpopulation. Future studies, could use computer models to determine if hyperexcitability, in response to long-term IL-1β exposure, was determined by modulation of 'enriched' ionic currents known to be associated with medium or small IB4-positive neurons.

3. Last, the effects of IL-1β may have been secondary to the production of other mediators which may, in turn, selectivity affect only certain sensory neuron subpopulations. For instance, medium diameter neurons predominantly express TrkB receptors, while remaining DRG neuron subpopulations primarily express other neurotrophin receptors, including TrkA in small IB4- negative neurons and TrkC in large neurons (Mu et al., 1993;Wright and Snider, 1995;Snider and Wright, 1996;Bennett et al., 1996). Therefore, if hyperexcitability was achieved secondarily to the production of a given neurotrophin, such as BDNF, then this effect would be expected to be greatest in medium neurons. Since BDNF recombinant binding proteins have proven efficacy in attenuating effects of BDNF in organotypic spinal cord slice cultures (Lu et al., 2009), future studies could involve similar experiments in long-term DRG cell cultures exposed to IL-1β to examine if effects were secondary to the production of BDNF.

Despite the need for further characterization, if the effects of long-term IL-1β are genuinely sensory neuron specific, the following conclusions can be made. First, the clear hypoexcitability demonstrated in large DRG neurons exposed to IL-1β, would suggest other inflammatory mediators or other processes may be required for the hyperexcitability observed in large primary afferent fibres after

peripheral nerve injury. Second, the unresponsiveness of small IB4-negative neurons in response to IL-1β exposure would suggest that functional distinctions between small IB4-positive and -negative neurons extend to the ability to detect the prolonged presence of IL-1β after peripheral nerve injury and, perhaps, to relevance in neuropathic pain. Alternatively, small IB4-negative neurons may respond to other inflammatory mediators released after peripheral nerve injury similar to that proposed for large DRG neurons.

### *6.2.2 Some, but not all, effects of IL-1β are receptor (IL-1RI) mediated*

IL-1Ra co-application antagonized or mitigated several of the hyperexcitable features associated with long-term IL-1β exposure, including the shortening of AHP duration in medium neurons, the broadening of APs in small IB4-positive neurons and the enhancements of repetitive discharge in both DRG neuron subpopulations (Chapter 3). These effects on DRG neuron electrical behaviour are concluded to be receptor-mediated, suggesting that the clinically available human recombinant IL-1Ra, Kineret® (Anakinra, Amgen Inc., Thousand Oaks, CA, USA), might have therapeutic potential after peripheral nerve injury in a manner similar to its currently effective use in the management of rheumatoid arthritis (Braddock and Quinn, 2004). In support, it was recently reported that IL-1Ra administered subcutaneously with osmotic micropumps could attenuate mechanical allodynia, autotomy, as well as, spontaneous ectopic activity after spinal nerve injury (Gabay et al., 2010).

However, IL-1Ra was unable to attenuate the effect of IL-1β on rheobase in medium neuron and suggest limits to the use of IL-1RI antagonists in peripheral nerve injury. This finding may be attributed to the possibility that IL-1β has biological activity independent of IL-1RI signalling which has been reported *in vivo*, as well as, in cell culture (Humphreys and Grencis, 2009;Herseth et al., 2009;Andre et al., 2006;Diem et al., 2003). IL-1RI independent effects would, therefore, provide a rationale basis for the continued development of therapeutic approaches targeting the production and/or release of IL-1β, such as caspase-1 or matrix metalloprotease inhibitors (Figure 6-1) (Allan et al., 2005;Kawasaki et al., 2008). Furthermore, IL-1RI independent effects would suggest novel therapeutic targets likely exist for IL-1β actions in nerve injury and await discovery.

### *6.2.3 Changes in DRG neuron ionic currents are consistent with increased excitability*

Many of the major findings in medium and small IB4-positive DRG neurons exposed to IL-1β (Tables 4-2 and 5-2), such as a decrease in the rate of decay for TTX-S $I_{Na}$ in small IB4-positive neurons, increase in the rates of activation for $I_H$ in medium neurons and suppression of $K_{Ca}$ currents in both sensory neuron subpopulations are in good agreement with the broad spectrum of alterations observed after nerve injury (Sarantopoulos et al., 2007;Abdulla and Smith, 2001b;Yao et al., 2003;Everill and Kocsis, 1999;Hogan et al., 2000;Baccei and Kocsis, 2000;Yang et al., 2004). However, consistent with my current-clamp

findings (Table 3-5), the effects of IL-1β on ionic currents reported in my thesis work are more extensive in medium neurons than in small IB4-positive neurons. As discussed above differences are likely attributed to phenotypic shift or the effects of IL-1β may have been secondary to the production of other mediators which may, in turn, selectivity affect medium neurons.

Although the observed changes in ionic currents are consistent with hyperexcitability in medium and small IB4-positive DRG neurons, limitations in my experimental approach may have under estimated the importance of IL-1β. For instance, phenotypic shift in long-term cell culture resulting in losses of TTX-R $I_{Na}$ or T-type calcium currents would have precluded potential upregulation in response to IL-1β exposure and further increases in sensory neuron excitability. Another limitation in my study is that the biophysical and pharmacological protocols used were not sufficient to monitor other possible changes produced by IL-1β, such as rapid repriming of TTX-S $I_{Na}$ or the relative contributions of VGCC subtypes to total HVA-$I_{Ba}$ current. Therefore, additional ionic mechanisms may underlie sensory neuron excitability in response to long-term IL-1β exposure.

Despite limitations, the changes described in Chapters 4 and 5 for small IB4-positive and medium neurons, respectively, relate well to increased excitability (Table 3-5). For instance, the hyperpolarizing shift in of TTX-S $I_{Na}$ voltage dependence of activation, as well as, the suppression of A-type current densities would be expected to decrease rheobase in medium neurons. While reductions in $K_{Ca}$ current densities would be expected to suppress components of

the AHP and, therefore, enhance repetitive discharge in both DRG neuron subpopulations.

Finally, it would be interesting to model the observed changes and examine their applicability to the generation of medium and small IB4-positive sensory neuron hyperexcitability in response to long-term IL-1β exposure. This approach may identify key regulators of hyperexcitablity in injured sensory neurons and, therefore, point to future therapies targeting specific ion channels. For instance, the upregulation of $I_H$ in my study, as well as, the demonstrated efficacy of $I_H$ blockade in the alleviation of mechanical allodynia after nerve injury (Chaplan et al., 2003;Lee et al., 2005), might shift the spotlight from sodium channels to HCN channels as a novel therapeutic target for neuropathic pain.

### *6.3 Contribution to Neuropathic Pain Mechanisms*

#### *6.3.1 Relevance to primary afferents*

APs elicited at sensory nerve terminals are thought to bypass the DRG en route to the spinal cord, and, therefore, the contribution of electrical activity within DRG cell bodies to sensory transmission remains uncertain (Amir and Devor, 2003;Passmore, 2005). In my investigation, there are at least three main reasons to study DRG cell body electrical activity:

1. It is technically possible, through whole-cell current and voltage-clamp recordings, to, respectively, study excitability and follow through with an

investigation of contributing ionic mechanisms (Abdulla and Smith, 2001a;Abdulla and Smith, 2002;Abdulla and Smith, 2001b).

2. Ion channels expressed in the somatic membrane are also expressed in the nerve terminals and, hence, can be used as a cellular model of the nerve terminals (Villiere and McLachlan, 1996;Gold et al., 1996).

3) Last, after nerve injury, ectopic primary afferent discharge has been traced to the DRG (Wall and Devor, 1983;Kajander et al., 1992).

Given the above, alterations in the electrical membrane properties of DRG neuron cell bodies exposed to IL-1β may be reflective of changes produced at peripheral and/or central primary afferent nerve terminals. For instance, the hyperpolarizing shift in of TTX-S $I_{Na}$ voltage dependence of activation, as well as, the suppression of A-type current densities found in medium neurons exposed to IL-1β would be expected to decrease AP firing threshold at peripheral nerve terminals and, therefore, produce hypersensitivity. It is also important to consider that medium diameter sensory neurons normally associate with Aδ-fibres (Harper and Lawson, 1985;Villiere and McLachlan, 1996) which are known to transmit either nociceptive or non-nociceptive information to the dorsal horn of the spinal cord (Rose et al., 1986;Koerber et al., 1988). Therefore, increased excitability in response to IL-1β release after nerve injury might explain hyperalgesia, as well as, allodynia. As for changes in small IB4-positive neurons exposed to IL-1β, it is possible that the decrease in the rate of TTX-S $I_{Na}$ and suppression of $K_{Ca}$ current densities would produce similar changes at central nerve terminals, leading to sustained membrane depolarization and increased $Ca^{2+}$ entry and, therefore,

increased neurotransmitter release for this functionally distinct class of nociceptors.

The absence of spontaneous activity in medium and small IB4-positive neuron cell bodies, suggests that the effect of long-term IL-1β exposure on electrical membrane properties in these two sensory neurons subpopulations were not sufficient to generate ectopic discharge, at least under the conditions of my experiments. This is interesting, since spontaneous activity can originate in injured DRG *in vivo* (Wall and Devor, 1983) or *ex vivo* (Study and Kral, 1996) and in response to acute applications of IL-1β *in vitro* (Binshtok et al., 2008). Furthermore, the observation that exposure of large DRG neurons to IL-1β reduces their excitability, is in direct contrast to the well documented finding that most ectopic activity after peripheral nerve injury is generated in large diameter, fast conducting Aβ primary afferents (Devor, 2009). There are, however, several possibilities for this deviation from the literature in my thesis work. One explanation could be that the functional expression of a particular ion channel or cell signalling molecule, crucial to spontaneous activity, is down-regulated in long-term DRG cell cultures. For instance, the absence of T-type calcium currents and their contribution to subthreshold membrane oscillations and AP discharge may have precluded this finding in my DRG cell cultures (Jagodic et al., 2008;Liu et al., 2001). Again, it would be useful to re-examine the effects of long-term IL-1β exposure in single neuron cultures where sensory neuron phenotypes could be better maintained through appropriate neurotrophin supplementation. This strategy would be particularly valuable in the case for large DRG neurons, where

phenotype shift and/or support in long-term cell culture is suspected to have played a role in their hypoexcitable response to IL-1β exposure.

Alternatively, the concentration of IL-1β used by Binshtok and colleagues (2008) was six-fold greater than the concentration added to my DRG cell cultures and, therefore, spontaneous activity may be a concentration dependent effect of IL-1β. Further, the reported levels of IL-1β after injury are variable (pM to nM range) and likely depends on the type of injury and/or the tissue used for analysis (Kawasaki et al., 2008;Xie et al., 2006;Dinarello, 2005).Therefore, it would be interesting to re-examine the effects of IL-1β at higher concentrations known to produce spontaneous activity in acutely isolated DRG neurons.

Last, Abdulla and Smith (2001) reported a lack of spontaneous activity in injured DRG neurons *in vitro* and attributed their discrepancy to a lack of features inherent of dissociated neurons which exist *in vivo*. This could include trophic support from intact DRG and/or from target tissues. Further, injured DRG neurons *in vivo* may be subject to chemical cross-excitation (Amir and Devor, 1996) and ongoing effects of secreted mediators such as, noradrenaline (McLachlan et al., 1993). These limitations of an *in vitro* study may also be the case in my thesis work rather than a limited role for IL-1β. In support, an *in vivo* study reported that the IL-1β receptor antagonist, IL-1Ra, suppressed spontaneous primary afferent activity after nerve injury (Gabay et al., 2010) and, therefore, IL-1β is likely to play role in spontaneous ectopic discharge observed *in vivo*.

*6.3.2 Relevance to central sensitization*

Although my thesis work has demonstrated that long-term IL-1β exposure can promote an enduring increase in the excitability of sensory neurons that may reflect peripheral hypersensitivity sensitivity, as well as, increased drive at central terminals, it is unclear whether these events contribute to establishment and/or maintenance of neuropathic pain. With regard to the establishment of neuropathic pain, multiple mechanisms have been described to increase excitability and decrease inhibition. It may be possible that enhanced discharge into the spinal cord from Aδ– and non-peptidergic C–fibres (medium and small IB4-positive DRG neurons, respectively) induces temporal summation of synaptic responses which can enhance synaptic strength (Latremoliere and Woolf, 2009). Coupled to this, enhanced discharge might increase local release of ATP which could activate microglia in the superficial dorsal horn (Scholz and Woolf, 2007;Ulmann et al., 2008). This is interesting since nociceptive Aδ– and non-peptidergic C-fibres have distinct terminations in lamina I (LI) and dorsally within inner lamina II (LIIid), respectively, which may, in turn, promote regional specific changes (Bradbury et al., 1998;Traub et al., 1989;Ribeiro-da-Silva and Cuello, 1995;Light and Perl, 1979). For instance, BDNF release from activated microglia in LI has been reported to be involved in the collapse of the transanionic gradient and the attenuation of GABA mediated inhibition (Coull et al., 2005;Prescott et al., 2006), while BDNF release enhanced NMDA receptor mediated excitatory post synaptic currents (epscs) in LII dorsal horn neurons (Garraway et al., 2003). The net effect is a decrease in inhibitory synapses and an increase in excitatory synapses.

Several other pro-inflammatory substances could also be released in the spinal cord in response to increased primary afferent discharge after nerve injury, including IL-1β itself (Scholz and Woolf, 2007). It is interesting that the prolonged exposure of organotypic cultures of rat spinal cord to IL-1β produces relatively modest changes (Gustafson-Vickers et al., 2008), when compared to BDNF (Lu et al., 2007), that are consistent with increased superficial dorsal horn excitability.

After nerve injury it is also possible that Aδ– and non-peptidergic C – fibres undergo phenotypic shift and begin to express neurotrophins and neuropetides, thereby, reinforcing several mechanisms involved in central sensitization, including an increase in the synaptic efficacy of their synaptic input into the spinal cord (Scholz and Woolf, 2007). For instance, under normal circumstances, BDNF mRNA and protein is expressed in nociceptive peptidergic sensory neurons (Michael et al., 1997), however, BDNF becomes upregulated in large-diameter DRG neurons and is concurrent with increased anterograde transport to the dorsal horn after sciatic axotomy (Tonra et al., 1998). Another example of phenotypic switch pertains to substance P (SP). Some nerve injuries (Baranowski et al., 1993) result in a reversed pattern where large, rather than small, sensory neurons begin to express (Noguchi et al., 1994;Noguchi et al., 1995) and become responsive to SP (Abdulla et al., 2001). Coupled to this, IL-1β has been reported to increase SP content and release in DRG neurons (Inoue et al., 1999;Skoff et al., 2009). It is not known from these studies if the production of SP is DRG neuron subpopulation specific or if the same would apply for

BDNF. Therefore, the possibility remains that IL-1β could promote the novel expression of neurotrophins and neuropeptides in medium and small IB4-positive neurons. Future studies could examine this possibility in DRG cell cultures exposed to IL-1β.

The functional role of changes found for large and small IB4-negative DRG neurons exposed to IL-1β is less certain. As stated above nerve injury has been reported to increase excitability in small nociceptive, as well as, large non-nociceptive primary afferent neurons and, therefore, absence of hyperexcitability in response to IL-1β exposure in these two sensory neuron subpopulations may reflect constraints of long-term cell culture in neurotrophin free- and serum-defined medium. However, it is thought that small IB4-positive and negative neurons have different functional roles in pain physiology (Fang et al., 2006;Fjell et al., 1999;Stucky and Lewin, 1999;Snider and McMahon, 1998) and, therefore, this may extend to the ability to respond to prolonged IL-1β release after nerve injury. Interestingly, it was determined through following transneural transport of genetically expressed lectin tracer in non-peptidergic nociceptors that these neurons are involved in circuits with strong projections to limbic and motor areas (Braz et al., 2005). Therefore, their increased excitability in response to prolonged IL-1β exposure after peripheral nerve injury may reflect the strong emotional components (Mogil, 2009), as well as, sensori-motor behaviours (Chudler and Dong, 1995) associated with chronic pain states.

Finally, although it can be appreciated that prolonged release of IL-1β after peripheral nerve is likely important in the establishment of central

sensitization, it is unclear what role this would have in the maintenance of central mechanisms. Part of this uncertainty is that it is simply not known to what extent primary afferents contribute once central pain mechanisms are in place (Devor, 2009). For primary afferents to have an ongoing contribution to central sensitization and, possibly, neuropathic pain, it would be expected that primary afferents would continue to be hyperexcitable after nerve regeneration is complete and the inflammatory response is restored to a basal state. To test this possibility, future studies could involve the removal of IL-1β after long-term exposure in cell cultures and re-examine electrical membrane properties in DRG neuron subpopulations.

### *6.3.3 Relevance to neuropathic pain management*

The identification of IL-1β receptor mediated effects and several contributing ionic mechanisms, suggests my findings have relevance to the treatment of neuropathic pain. As stated above, this may involve targeting the production, release or actions of IL-1β (Figure 6-1). The finding that IL-1Ra can reverse mechanical allodynia after peripheral nerve injury (Gabay et al., 2010), suggests that targeting IL-1β may have utility beyond use as a prophylactic in peri-operative care. Since IL-1β production is involved in nerve degeneration, as well as, nerve regeneration (Temporin et al., 2008b;Temporin et al., 2008a;Horie et al., 1997), more studies will likely need to be conducted to determine if interruption of IL-1β has undesirable consequences on recovery after nerve injury. Other opportunities may include the targeting of ionic mechanisms that are

likely important in the generation of hyperexcitability in sensory neurons exposed to IL-1β, such as $I_H$. However, since HCN channels are expressed in a variety of tissues, including the heart (DiFrancesco, 2001), future studies would have to investigate the therapeutic index of such therapies.

Last, neuropathic pain may not arise from an obvious site of injury or inflammation and it is characteristically resistant to the actions of NSAIDs (Arner and Meyerson, 1988;Argoff et al., 2006). Since IL-1β is a pro-inflammatory cytokine, this might also suggest that targeting IL-1β would have limited use beyond recovery from nerve injury. However, there is evidence that IL-1β is also upregulated in the spinal cord after nerve injury (Kawasaki et al., 2008), including potential release from astrocytes which are considered to be involved in the maintenance of central sensitization (Zhuang et al., 2005;Zhuang et al., 2006) and, possibly, neuropathic pain. Therefore, therapies targeting IL-1β may have applicability in the early, as well as, the later stages of neuropathic pain.

### *6.4 Conclusions*

My findings on the effect of long-term IL-1β exposure on DRG neuron electrical membrane properties are intriguing in the following ways:

1. Hyperexcitability in medium DRG neurons exposed to IL-1β likely includes mixed populations of neurons corresponding to nociceptive and non-nociceptive primary afferent fibres and, therefore, has relevance to hyperalgesia and allodynia, respectively.

2. The responsiveness of small IB4-positive DRG neurons, but not IB4-negative, to prolonged IL-1β exposure is consistent with the suggestion that small, IB4-negative afferents are involved in inflammatory pain, while small, IB4-positive afferents are involved neuropathic pain.

3. The identification of receptor mediated effects and several contributing ionic mechanisms, suggests my findings have relevance to the treatment of neuropathic pain.

4. Last, IL-1β can contribute to hyperexcitability independent of IL-1RI signalling and this should be taken into account when targeting IL-1β, or more specifically IL-1RI, in the management of neuropathic pain.

There is no definitive answer as to the evolutionary function of neuropathic pain, however, it may be possible that clinical advances have brought survival beyond a point of damage that a mortal body is meant to sustain. Therefore, just as it has been a moral obligation to prolong life, a moral obligation now exists to improve the quality of prolonged life. To this end, an association between enduring increases in primary afferent activity after peripheral nerve injury and neuropathic pain has been established, however, the role of inflammatory mediators in this process is unclear. The findings in my thesis work expand the recognized role of IL-1β in acute inflammatory pain to neuropathic pain. By examining the effects of long-term IL-1β exposure on sensory neuron excitability and identifying its mechanism of action, we can better understand the etiological basis for neuropathic pain, as well as, identifiy potenial pharmacological targets for treatment.

***Figure 6-1: Regulation of IL-1β production and release presents several targets for therapeutic intervention***

A diagram illustrating the regulation of expression of the gene encoding IL-1β, the cellular release of IL-1β and its biological activity is shown. It is therefore possible to:

1) Inhibition of the gene encoding IL-1β transcription anti-inflammatory molecules, such as IL-10 and annexin-1.
2) Prevent the processing of pro-IL-1b to its mature, active form by the inhibition of caspase-1.
3) Block the release of IL-1β with a novel family of cytokine-release inhibitory drugs (CRIDs).
4) Bind IL-1β with IL-1trap (an IL-1 antibody) or soluble IL-1RII (sIL-iRII).
5) Compete for binding to IL-1RI with IL-1Ra (anakinra).
6) Inhibit downstream signalling cascades, such as p38 MAPK.
7) Inhibit downstream enzymes involved in the secondary production of inflammatory mediators, such as COX-2 and the production of $PGE_2$.

Adapted from Allan et al. (2005).

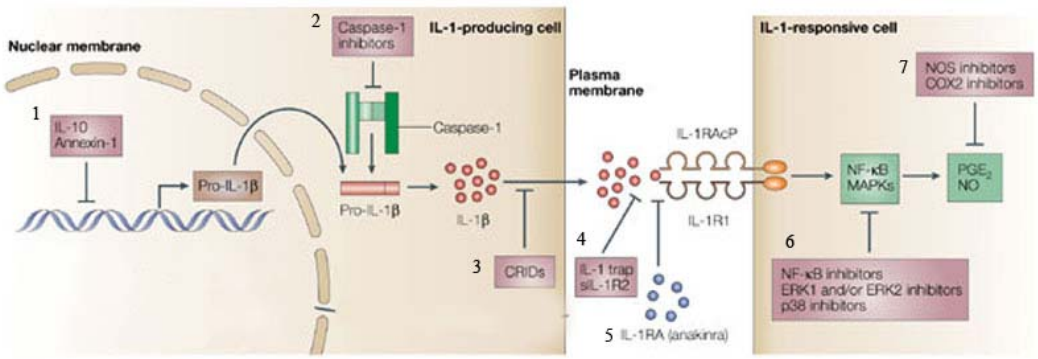
Nuclear membrane
IL-1-producing cell
2
Caspase-1 inhibitors
1
IL-10
Annexin-1
Pro-IL-1β
Caspase-1
Pro-IL-1β
IL-1β
3
CRIDs
Plasma membrane
IL-1RAcP
IL-1R1
4
IL-1 trap
sIL-1R2
5 IL-1RA (anakinra)
IL-1-responsive cell
7
NOS inhibitors
COX2 inhibitors
NF-κB
MAPKs
PGE2
NO
6
NF-κB inhibitors
ERK1 and/or ERK2 inhibitors
p38 inhibitors

***Figure 6-2: Summary diagram of the effects of long-term IL-1β exposure on DRG neurons***

This diagram shows the primary afferent fibre with both peripheral and central terminals, the associated cell body and the dorsal horn of the spinal cord.

1. Following peripheral nerve injury, the release of IL-1β can be sustained for several days to weeks.

2. In cell culture, long-term IL-1β exposure increased the excitability of medium and small IB4-positive DRG neuron cell bodies. I interpret these findings to be the *in vitro* equivalent of the enduring increase in primary afferent excitability reported after peripheral nerve injury.

3. The hyperpolarizing shift in TTX-S $I_{Na}$ voltage dependence of activation, as well as, the suppression of A-type current densities in medium neurons exposed to IL-1β would be expected to decrease AP firing threshold at peripheral nerve terminals and, therefore, produce hypersensitivity.

4. The decrease in the rate of TTX-S $I_{Na}$ and suppression of $K_{Ca}$ current densities in small IB4-positive neurons exposed to IL-1β would be expected to produce similar changes at central nerve terminals, leading to sustained membrane depolarization and increased $Ca^{2+}$ entry and, therefore, increased neurotransmitter release.

5. These effects would be expected to contribute to the development of central sensitization and, possibly, neuropathic pain.

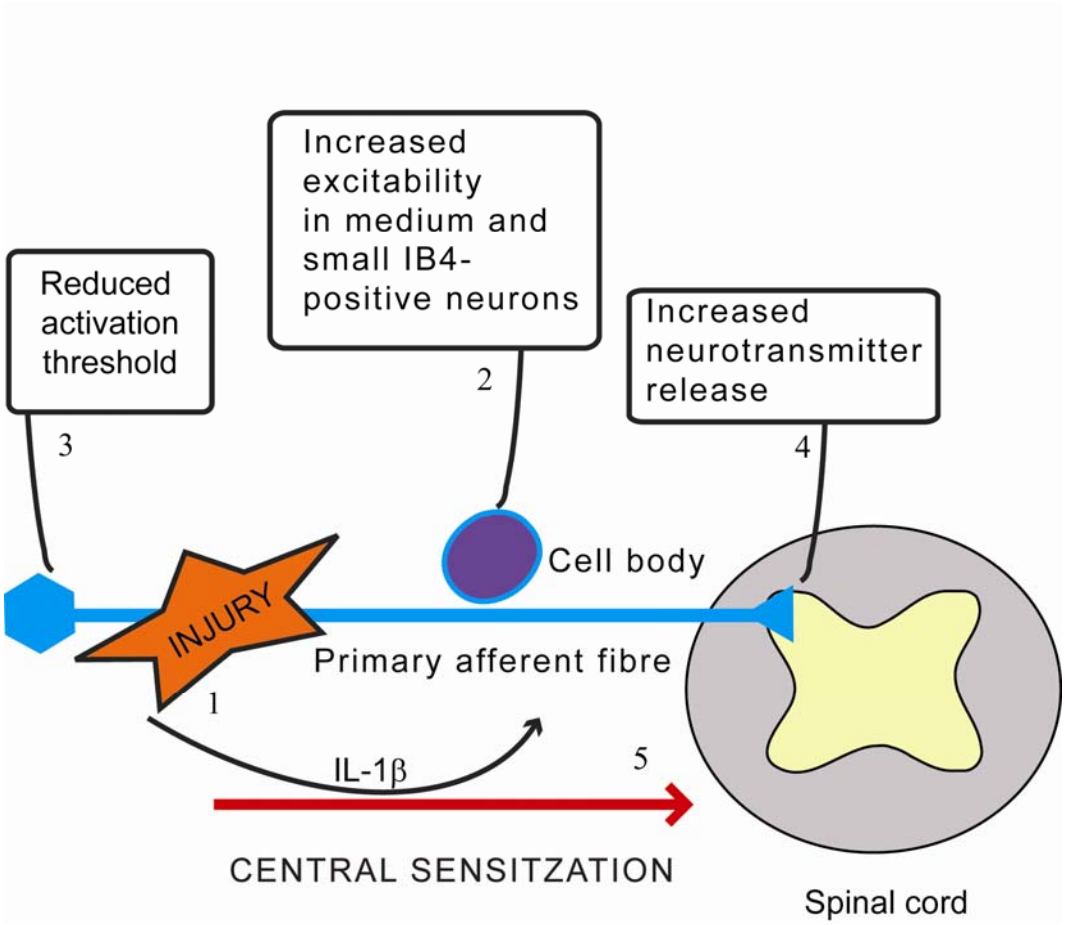
Increased excitability in medium and small IB4-positive neurons
Reduced activation threshold
Increased neurotransmitter release
2
3
4
Cell body
INJURY
Primary afferent fibre
1
IL-1β
5
CENTRAL SENSITZATION
Spinal cord

### *6.5 References*


1. Abdulla FA, Smith PA (2001a) Axotomy- and autotomy-induced changes in the excitability of rat dorsal root ganglion neurons. J Neurophysiol 85: 630-643.

2. Abdulla FA, Smith PA (2002) Changes in Na(+) channel currents of rat dorsal root ganglion neurons following axotomy and axotomy-induced autotomy. J Neurophysiol 88: 2518-2529.

3. Abdulla FA, Stebbing MJ, Smith PA (2001) Effects of substance P on excitability and ionic currents of normal and axotomized rat dorsal root ganglion neurons. Eur J Neurosci 13: 545-552.

4. Abdulla FA, Smith PA (2001b) Axotomy- and Autotomy-Induced Changes in Ca2+and K+ Channel Currents of Rat Dorsal Root Ganglion Neurons. J Neurophysiol 85: 644-658.

5. Allan SM, Tyrrell PJ, Rothwell NJ (2005) Interleukin-1 and neuronal injury. Nat Rev Immunol 5: 629-640.

6. Amir R, Devor M (1996) Chemically mediated cross-excitation in rat dorsal root ganglia. J Neurosci 16: 4733-4741.

7. Amir R, Devor M (2003) Electrical Excitability of the Soma of Sensory Neurons Is Required for Spike Invasion of the Soma, but Not for Through-Conduction. Biophysical Journal 84: 2181-2191.

8. Andre R, Moggs JG, Kimber I, Rothwell NJ, Pinteaux E (2006) Gene regulation by IL-1beta independent of IL-1R1 in the mouse brain. Glia 53: 477-483.

9. Appel E, Kolman O, Kazimirsky G, Blumberg PM, Brodie C (1997) Regulation of GDNF expression in cultured astrocytes by inflammatory stimuli. Neuroreport 8: 3309-3312.

10. Argoff CE, Backonja MM, Belgrade MJ, Bennett GJ, Clark MR, Cole BE, Fishbain DA, Irving GA, McCarberg BH, McLean MJ (2006) Consensus guidelines: treatment planning and options. Diabetic peripheral neuropathic pain. Mayo Clin Proc 81: S12-S25.

11. Arner S, Meyerson BA (1988) Lack of analgesic effect of opioids on neuropathic and idiopathic forms of pain. Pain 33: 11-23.

12. Baccei ML, Kocsis JD (2000) Voltage-Gated Calcium Currents in Axotomized Adult Rat Cutaneous Afferent Neurons. J Neurophysiol 83: 2227-2238.

13. Baranowski AP, Priestley JV, McMahon S (1993) Substance P in cutaneous primary sensory neurons--a comparison of models of nerve injury that allow varying degrees of regeneration. Neuroscience 55: 1025-1036.

14. Bennett DL, Averill S, Clary DO, Priestley JV, McMahon SB (1996) Postnatal changes in the expression of the trkA high-affinity NGF receptor in primary sensory neurons. Eur J Neurosci 8: 2204-2208.

15. Binshtok AM, Wang H, Zimmermann K, Amaya F, Vardeh D, Shi L, Brenner GJ, Ji RR, Bean BP, Woolf CJ, Samad TA (2008) Nociceptors are interleukin-1beta sensors. J Neurosci 28: 14062-14073.

16. Bradbury EJ, Burnstock G, McMahon SB (1998) The expression of P2X3 purinoreceptors in sensory neurons: effects of axotomy and glial-derived neurotrophic factor. Mol Cell Neurosci 12: 256-268.

17. Braddock M, Quinn A (2004) Targeting IL-1 in inflammatory disease: new opportunities for therapeutic intervention. Nat Rev Drug Discov 3: 330-339.

18. Braz JM, Nassar MA, Wood JN, Basbaum AI (2005) Parallel "pain" pathways arise from subpopulations of primary afferent nociceptor. Neuron 47: 787-793.

19. Chaplan SR, Guo HQ, Lee DH, Luo L, Liu C, Kuei C, Velumian AA, Butler MP, Brown SM, Dubin AE (2003) Neuronal hyperpolarization-activated pacemaker channels drive neuropathic pain. J Neurosci 23: 1169-1178.

20. Chudler EH, Dong WK (1995) The role of the basal ganglia in nociception and pain. Pain 60: 3-38.

21. Copray JC, Mantingh I, Brouwer N, Biber K, Kust BM, Liem RS, Huitinga I, Tilders FJ, Van Dam AM, Boddeke HW (2001) Expression of interleukin-1 beta in rat dorsal root ganglia. J Neuroimmunol 118: 203-211.

22. Coull JA, Beggs S, Boudreau D, Boivin D, Tsuda M, Inoue K, Gravel C, Salter MW, De Koninck Y (2005) BDNF from microglia causes the shift in neuronal anion gradient underlying neuropathic pain. Nature 438: 1017-1021.

23. Devor M (2009) Ectopic discharge in Abeta afferents as a source of neuropathic pain. Exp Brain Res 196: 115-128.

24. Devor M, Janig W, Michaelis M (1994) Modulation of activity in dorsal root ganglion neurons by sympathetic activation in nerve-injured rats. J Neurophysiol 71: 38-47.

25. Diem R, Hobom M, Grotsch P, Kramer B, Bahr M (2003) Interleukin-1 beta protects neurons via the interleukin-1 (IL-1) receptor-mediated Akt pathway and by IL-1 receptor-independent decrease of transmembrane currents in vivo. Mol Cell Neurosci 22: 487-500.

26. DiFrancesco D (2001) Serious workings of the funny current. Progress in Biophysics and Molecular Biology 90: 13-25.

27. Dinarello CA (2005) Interleukin-1beta. Crit Care Med 33: S460-S462.

28. Everill B, Kocsis JD (1999) Reduction in Potassium Currents in Identified Cutaneous Afferent Dorsal Root Ganglion Neurons After Axotomy. J Neurophysiol 82: 700-708.

29. Fang X, Djouhri L, McMullan S, Berry C, Waxman SG, Okuse K, Lawson SN (2006) Intense Isolectin-B4 Binding in Rat Dorsal Root Ganglion Neurons Distinguishes C-Fiber Nociceptors with Broad Action Potentials and High Nav1.9 Expression. J Neurosci 26: 7281-7292.

30. Fjell J, Cummins TR, Dib-Hajj SD, Fried K, Black JA, Waxman SG (1999) Differential role of GDNF and NGF in the maintenance of two TTX-resistant sodium channels in adult DRG neurons. Brain Res Mol Brain Res 67: 267-282.

31. Gabay E, Wolf G, Shavit Y, Yirmiya R, Tal M (2010) Chronic blockade of interleukin-1 (IL-1) prevents and attenuates neuropathic pain behavior and spontaneous ectopic neuronal activity following nerve injury. Eur J Pain.

32. Garraway SM, Petruska JC, Mendell LM (2003) BDNF sensitizes the response of lamina II neurons to high threshold primary afferent inputs. Eur J Neurosci 18: 2467-2476.

33. Gold MS, Dastmalchi S, Levine JD (1996) Co-expression of nociceptor properties in dorsal root ganglion neurons from the adult rat in vitro. Neuroscience 71: 265-275.

34. Gustafson-Vickers SL, Lu VB, Lai AY, Todd KG, Ballanyi K, Smith PA (2008) Long-term actions of interleukin-1beta on delay and tonic firing neurons in rat superficial dorsal horn and their relevance to central sensitization. Mol Pain 4: 63.

35. Harper AA, Lawson SN (1985) Conduction velocity is related to morphological cell type in rat dorsal root ganglion neurones. J Physiol 359: 31-46.

36. Herseth JI, Refsnes M, Lag M, Schwarze PE (2009) Role of IL-1 beta and COX2 in silica-induced IL-6 release and loss of pneumocytes in co-cultures. Toxicol In Vitro 23: 1342-1353.

37. Hogan QH, McCallum JB, Sarantopoulos C, Aason M, Mynlieff M, Kwok WM, Bosnjak ZJ (2000) Painful neuropathy decreases membrane calcium current in mammalian primary afferent neurons. Pain 86: 43-53.

38. Horie H, Sakai I, Akahori Y, Kadoya T (1997) IL-1 beta enhances neurite regeneration from transected-nerve terminals of adult rat DRG. Neuroreport 8: 1955-1959.

39. Humphreys NE, Grencis RK (2009) IL-1-dependent, IL-1R1-independent resistance to gastrointestinal nematodes. Eur J Immunol 39: 1036-1045.

40. Inoue A, Ikoma K, Morioka N, Kumagai K, Hashimoto T, Hide I, Nakata Y (1999) Interleukin-1beta induces substance P release from primary afferent neurons through the cyclooxygenase-2 system. J Neurochem 73: 2206-2213.

41. Jagodic MM, Pathirathna S, Joksovic PM, Lee W, Nelson MT, Naik AK, Su P, Jevtovic-Todorovic V, Todorovic SM (2008) Upregulation of the T-Type Calcium Current in Small Rat Sensory Neurons After Chronic Constrictive Injury of the Sciatic Nerve. J Neurophysiol 99: 3151-3156.

42. Kajander KC, Wakisaka S, Bennett GJ (1992) Spontaneous discharge originates in the dorsal root ganglion at the onset of a painful peripheral neuropathy in the rat. Neurosci Lett 138: 225-228.

43. Kawasaki Y, Xu ZZ, Wang X, Park JY, Zhuang ZY, Tan PH, Gao YJ, Roy K, Corfas G, Lo EH, Ji RR (2008) Distinct roles of matrix metalloproteases in the early- and late-phase development of neuropathic pain. Nat Med 14: 331-336.

44. Koerber HR, Druzinsky RE, Mendell LM (1988) Properties of somata of spinal dorsal root ganglion cells differ according to peripheral receptor innervated. J Neurophysiol 60: 1584-1596.

45. Latremoliere A, Woolf CJ (2009) Central sensitization: a generator of pain hypersensitivity by central neural plasticity. J Pain 10: 895-926.

46. Lee DH, Chang L, Sorkin LS, Chaplan SR (2005) Hyperpolarization-Activated, Cation-Nonselective, Cyclic Nucleotide-Modulated Channel Blockade Alleviates Mechanical Allodynia and Suppresses Ectopic Discharge in Spinal Nerve Ligated Rats. The Journal of Pain 6: 417-424.

47. Light AR, Perl ER (1979) Spinal termination of functionally identified primary afferent neurons with slowly conducting myelinated fibers. J Comp Neurol 186: 133-150.

48. Lindholm D, Heumann R, Meyer M, Thoenen H (1987) Interleukin-1 regulates synthesis of nerve growth factor in non-neuronal cells of rat sciatic nerve. Nature 330: 658-659.

49. Lindsay RM (1988) Nerve growth factors (NGF, BDNF) enhance axonal regeneration but are not required for survival of adult sensory neurons. J Neurosci 8: 2394-2405.

50. Liu L, Yang TM, Liedtke W, Simon SA (2006) Chronic IL-1beta signaling potentiates voltage-dependent sodium currents in trigeminal nociceptive neurons. J Neurophysiol 95: 1478-1490.

51. Liu XZ, Zhou JL, Chung KS, Chung JM (2001) Ion channels associated with the ectopic discharges generated after segmental spinal nerve injury in the rat. Brain Research 900: 119-127.

52. Lu VB, Ballanyi K, Colmers WF, Smith PA (2007) Neuron type-specific effects of brain-derived neurotrophic factor in rat superficial dorsal horn and their relevance to 'central sensitization'. J Physiol 584: 543-563.

53. Lu VB, Biggs JE, Stebbing MJ, Balasubramanyan S, Todd KG, Lai AY, Colmers WF, Dawbarn D, Ballanyi K, Smith PA (2009) Brain-derived neurotrophic factor drives the changes in excitatory synaptic transmission

in the rat superficial dorsal horn that follow sciatic nerve injury. J Physiol 587: 1013-1032.

54. McLachlan EM, Janig W, Devor M, Michaelis M (1993) Peripheral nerve injury triggers noradrenergic sprouting within dorsal root ganglia. Nature 363: 543-546.

55. Michael GJ, Averill S, Nitkunan A, Rattray M, Bennett DL, Yan Q, Priestley JV (1997) Nerve growth factor treatment increases brain-derived neurotrophic factor selectively in TrkA-expressing dorsal root ganglion cells and in their central terminations within the spinal cord. J Neurosci 17: 8476-8490.

56. Mogil JS (2009) Animal models of pain: progress and challenges. Nat Rev Neurosci 10: 283-294.

57. Mu X, Silos-Santiago I, Carroll SL, Snider WD (1993) Neurotrophin receptor genes are expressed in distinct patterns in developing dorsal root ganglia. J Neurosci 13: 4029-4041.

58. Noguchi K, Dubner R, De Leon M, Senba E, Ruda MA (1994) Axotomy induces preprotachykinin gene expression in a subpopulation of dorsal root ganglion neurons. J Neurosci Res 37: 596-603.

59. Noguchi K, Kawai Y, Fukuoka T, Senba E, Miki K (1995) Substance P induced by peripheral nerve injury in primary afferent sensory neurons and its effect on dorsal column nucleus neurons. J Neurosci 15: 7633-7643.

60. Passmore GM (2005) Dorsal root ganglion neurones in culture: a model system for identifying novel analgesic targets? J Pharmacol Toxicol Methods 51: 201-208.

61. Prescott SA, Sejnowski TJ, De Koninck Y (2006) Reduction of anion reversal potential subverts the inhibitory control of firing rate in spinal lamina I neurons: towards a biophysical basis for neuropathic pain. Mol Pain 2: 32.

62. Ribeiro-da-Silva A, Cuello AC (1995) Organization of peptidergic neurons in the dorsal horn of the spinal cord: anatomical and functional correlates. Prog Brain Res 104: 41-59.

63. Rose RD, Koerber HR, Sedivec MJ, Mendell LM (1986) Somal action potential duration differs in identified primary afferents. Neurosci Lett 63: 259-264.

64. Safieh-Garabedian B, Poole S, Allchorne A, Winter J, Woolf CJ (1995) Contribution of interleukin-1 beta to the inflammation-induced increase in

nerve growth factor levels and inflammatory hyperalgesia. Br J Pharmacol 115: 1265-1275.

65. Sarantopoulos CD, McCallum JB, Rigaud M, Fuchs A, Kwok WM, Hogan QH (2007) Opposing effects of spinal nerve ligation on calcium-activated potassium currents in axotomized and adjacent mammalian primary afferent neurons. Brain Res 1132: 84-99.

66. Scholz J, Woolf CJ (2007) The neuropathic pain triad: neurons, immune cells and glia. Nat Neurosci 10: 1361-1368.

67. Scroggs RS, Todorovic SM, Anderson EG, Fox AP (1994) Variation in IH, IIR, and ILEAK between acutely isolated adult rat dorsal root ganglion neurons of different size. J Neurophysiol 71: 271-279.

68. Skoff AM, Zhao C, Adler JE (2009) Interleukin-1[alpha] regulates substance P expression and release in adult sensory neurons. Experimental Neurology 217: 395-400.

69. Snider WD, Wright DE (1996) Neurotrophins cause a new sensation. Neuron 16: 229-232.

70. Snider WD, McMahon SB (1998) Tackling Pain at the Source: New Ideas about Nociceptors. Neuron 20: 629-632.

71. Sommer C, Kress M (2004) Recent findings on how proinflammatory cytokines cause pain: peripheral mechanisms in inflammatory and neuropathic hyperalgesia. Neurosci Lett 361: 184-187.

72. Stucky CL, Lewin GR (1999) Isolectin B(4)-positive and -negative nociceptors are functionally distinct. J Neurosci 19: 6497-6505.

73. Study RE, Kral MG (1996) Spontaneous action potential activity in isolated dorsal root ganglion neurons from rats with a painful neuropathy. Pain 65: 235-242.

74. Takeda M, Kitagawa J, Takahashi M, Matsumoto S (2008a) Activation of interleukin-1beta receptor suppresses the voltage-gated potassium currents in the small-diameter trigeminal ganglion neurons following peripheral inflammation. Pain 139: 594-602.

75. Takeda M, Takahashi M, Matsumoto S (2008b) Contribution of activated interleukin receptors in trigeminal ganglion neurons to hyperalgesia via satellite glial interleukin-1beta paracrine mechanism. Brain Behav Immun 22: 1016-1023.

76. Tanabe K, Nishimura K, Dohi S, Kozawa O (2009) Mechanisms of interleukin-1beta-induced GDNF release from rat glioma cells. Brain Res 1274: 11-20.

77. Temporin K, Tanaka H, Kuroda Y, Okada K, Yachi K, Moritomo H, Murase T, Yoshikawa H (2008a) IL-1[beta] promotes neurite outgrowth by deactivating RhoA via p38 MAPK pathway. Biochemical and Biophysical Research Communications 365: 375-380.

78. Temporin K, Tanaka H, Kuroda Y, Okada K, Yachi K, Moritomo H, Murase T, Yoshikawa H (2008b) Interleukin-1 beta promotes sensory nerve regeneration after sciatic nerve injury. Neuroscience Letters 440: 130-133.

79. Tonra JR, Curtis R, Wong V, Cliffer KD, Park JS, Timmes A, Nguyen T, Lindsay RM, Acheson A, DiStefano PS (1998) Axotomy upregulates the anterograde transport and expression of brain-derived neurotrophic factor by sensory neurons. J Neurosci 18: 4374-4383.

80. Traub RJ, Solodkin A, Ruda MA (1989) Calcitonin gene-related peptide immunoreactivity in the cat lumbosacral spinal cord and the effects of multiple dorsal rhizotomies. J Comp Neurol 287: 225-237.

81. Ulmann L, Hatcher JP, Hughes JP, Chaumont S, Green PJ, Conquet F, Buell GN, Reeve AJ, Chessell IP, Rassendren F (2008) Up-regulation of P2X4 receptors in spinal microglia after peripheral nerve injury mediates BDNF release and neuropathic pain. J Neurosci 28: 11263-11268.

82. Villiere V, McLachlan EM (1996) Electrophysiological properties of neurons in intact rat dorsal root ganglia classified by conduction velocity and action potential duration. J Neurophysiol 76: 1924-1941.

83. Vydyanathan A, Wu ZZ, Chen SR, Pan HL (2005) A-type voltage-gated K+ currents influence firing properties of isolectin B4-positive but not isolectin B4-negative primary sensory neurons. J Neurophysiol 93: 3401-3409.

84. Wall PD, Devor M (1983) Sensory afferent impulses originate from dorsal root ganglia as well as from the periphery in normal and nerve injured rats. Pain 17: 321-339.

85. Watkins LR, Maier SF (1999) Implications of immune-to-brain communication for sickness and pain. Proc Natl Acad Sci U S A 96: 7710-7713.

86. Wright DE, Snider WD (1995) Neurotrophin receptor mRNA expression defines distinct populations of neurons in rat dorsal root ganglia. J Comp Neurol 351: 329-338.

87. Xie WR, Deng H, Li H, Bowen TL, Strong JA, Zhang JM (2006) Robust increase of cutaneous sensitivity, cytokine production and sympathetic

sprouting in rats with localized inflammatory irritation of the spinal ganglia. Neuroscience 142: 809-822.

88. Yang E-K, Takimoto K, Hayashi Y, De Groat WC, Yoshimura N (2004) Altered expression of potassium channel subunit mRNA and [alpha]-dendrotoxin sensitivity of potassium currents in rat dorsal root ganglion neurons after axotomy. Neuroscience 123: 867-874.

89. Yao H, Donnelly DF, Ma C, LaMotte RH (2003) Upregulation of the hyperpolarization-activated cation current after chronic compression of the dorsal root ganglion. J Neurosci 23: 2069-2074.

90. Zhang XL, Mok LP, Katz EJ, Gold MS (2010) BKCa currents are enriched in a subpopulation of adult rat cutaneous nociceptive dorsal root ganglion neurons. Eur J Neurosci 31: 450-462.

91. Zhuang ZY, Gerner P, Woolf CJ, Ji RR (2005) ERK is sequentially activated in neurons, microglia, and astrocytes by spinal nerve ligation and contributes to mechanical allodynia in this neuropathic pain model. Pain 114: 149-159.

92. Zhuang ZY, Wen YR, Zhang DR, Borsello T, Bonny C, Strichartz GR, Decosterd I, Ji RR (2006) A peptide c-Jun N-terminal kinase (JNK) inhibitor blocks mechanical allodynia after spinal nerve ligation:

respective roles of JNK activation in primary sensory neurons and spinal astrocytes for neuropathic pain development and maintenance. J Neurosci 26: 3551-3560.